AD-A181 433 CRITERIA FOR ASPHALT-RUBBER CONCRETE IN CIVIL AIRPORT PAVEMENTS VOLUME 2..(U) TEXAS TRANSPORTATION INST COLLEGE STATION D H HOYT ET AL. MAR 87 RF-4982-2 1/3

UNCLASSIFIED DOT/FAA/PM-86/39-VOL-2 DTFA01-83-C-30076 F/G 13/3 NL

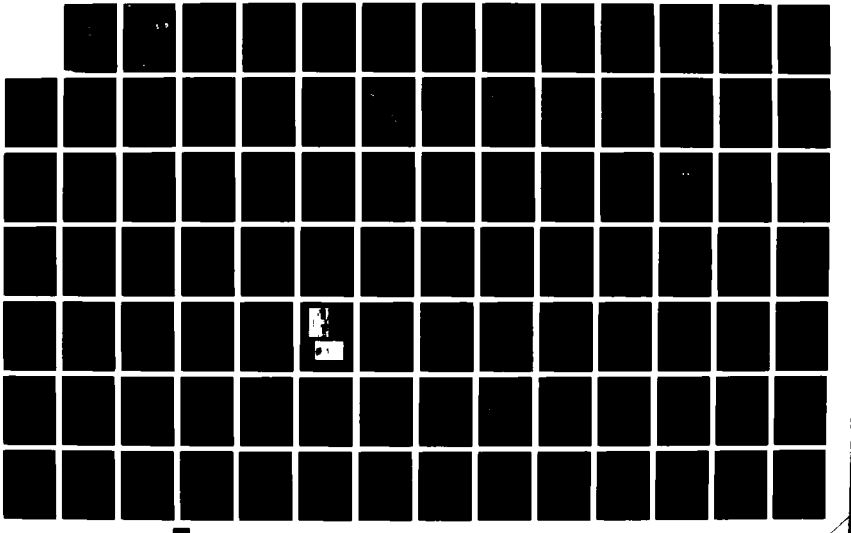

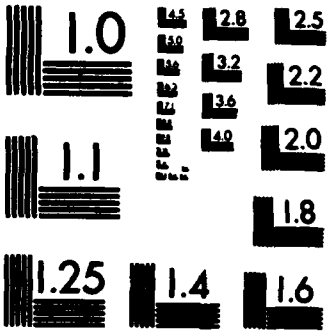

MICROCOPY RESOLUTION TEST CHART
NATIONAL BUREAU OF STANDARDS-1963-A

DOT/FAA/PM-86/39,II
Program Engineering
and Maintenance Service
Washington, D.C. 20591

Criteria for Asphalt-Rubber Concrete in Civil Airport Pavements

Vol. II—Evaluation of Asphalt-Rubber Concrete

Denise M. Hoyt
Robert L. Lytton
Freddy L. Roberts

Texas Transportation Institute
Texas A&M University
College Station, Texas

March 1987

Final Report

U.S. Department of Transportation
Federal Aviation Administration

Technical Report Documentation Page

1. Report No.	2. Government Accession No.	3. Recipient's Catalog No.
DOT/FAA/PM-86/39, II	ADA181433	

4. Title and Subtitle
Criteria for Asphalt-Rubber Concrete in Civil Airport Pavements: Evaluation of Asphalt-Rubber Concrete

5. Report Date
March, 1987

6. Performing Organization Code

7. Author(s)
Denise M. Hoyt, Robert L. Lytton, Freddy L. Roberts

8. Performing Organization Report No.
RF 4982-2

9. Performing Organization Name and Address
Texas Transportation Institute
Texas A&M University
College Station, Texas

10. Work Unit No. (TRAIS)

11. Contract or Grant No.
DTFA 01-83-C-30076

12. Sponsoring Agency Name and Address
U.S. Department of Transportation
Federal Aviation Administration
800 Independence Avenue, S. W.
Washington, D.C. 20591

13. Type of Report and Period Covered
Final September 1983 March 1987

14. Sponsoring Agency Code
APM-700

15. Supplementary Notes

16. Abstract

Asphalt-rubber concrete and an asphalt concrete control were tested in the laboratory and materials characterizations were generated, including Marshall Stability, resilient modulus, fatigue and fracture properties, creep compliance, and permanent deformation properties. The characterization parameters and an airport runway model for a municipal airport were input into the modified ILLIPAVE computer program for analysis of rutting and cracking damage and the relative lives of the materials in each of four climatic zones. An economic evaluation was then performed comparing the costs and service lives of each material in each zone.

A cracking index of 0.2 was chosen as a comparative level. The asphalt-rubber concrete passed the entire design period of 20 years for all climatic zones without reaching this comparison level. The asphalt concrete reached this level in 10 years or more. A rut depth of 0.7 inches was chosen as the critical rutting level. For all four climatic zones, the asphalt concrete control reached the critical rutting level before the asphalt-rubber concrete; but both materials reached the critical level within the 20-year design period. Rutting was chosen as the expected critical failure mode for both materials in all zones.

An equivalent uniform annual cost per square yard over the life of the pavement for the construction cost of each pavement was determined. The material with the least equivalent uniform annual cost was selected as the most cost-effective. Only in the dry-no freeze zone was the asphalt concrete more cost-effective than the asphalt-rubber concrete. In the other three zones, the low or medium (optimum) binder content asphalt-rubber concrete was the most cost-effective material.

17. Key Words	18. Distribution Statement
Asphalt-rubber concrete, materials characterization, modified ILLIPAVE, rutting, cracking	No restrictions. This document is available to the public through the National Technical Information Service, 5285 Port Royal Road, Springfield, Virginia 22161.

19. Security Classif. (of this report)	20. Security Classif. (of this page)	21. No. of Pages	22. Price
Unclassified	Unclassified	239	

Form DOT F 1700.7 (8-72) Reproduction of completed page authorized

METRIC CONVERSION FACTORS

Approximate Conversions to Metric Measures

Symbol	When You Know	Multiply by	To Find	Symbol
		LENGTH		
in	inches	*2.5	centimeters	cm
ft	feet	30	centimeters	cm
yd	yards	0.9	meters	m
mi	miles	1.6	kilometers	km
		AREA		
in^2	square inches	6.5	square centimeters	cm^2
ft^2	square feet	0.09	square meters	m^2
yd^2	square yards	0.8	square meters	m^2
mi^2	square miles	2.6	square kilometers	km^2
	acres	0.4	hectares	ha
		MASS (weight)		
oz	ounces	28	grams	g
lb	pounds	0.45	kilograms	kg
	short tons (2000 lb)	0.9	tonnes	t
		VOLUME		
tsp	teaspoons	5	milliliters	ml
Tbsp	tablespoons	15	milliliters	ml
fl oz	fluid ounces	30	milliliters	ml
c	cups	0.24	liters	l
pt	pints	0.47	liters	l
qt	quarts	0.95	liters	l
gal	gallons	3.8	liters	l
ft^3	cubic feet	0.03	cubic meters	m^3
yd^3	cubic yards	0.76	cubic meters	m^3
		TEMPERATURE (exact)		
°F	Fahrenheit temperature	5/9 (after subtracting 32)	Celsius temperature	°C

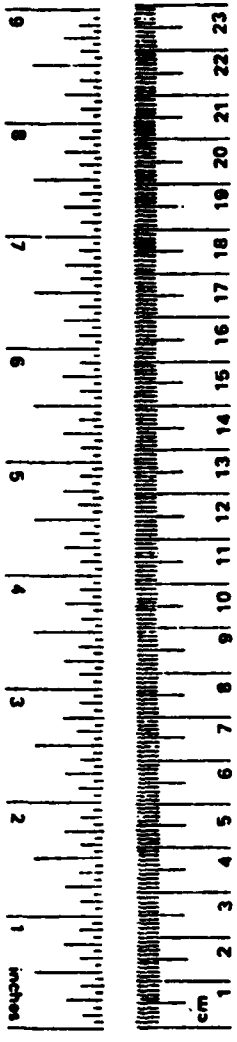

*1 in = 2.54 (exactly). For other exact conversions and more detailed tables, see NBS Misc. Publ. 286, Units of Weights and Measures, Price $2.25, SD Catalog No. C13.10:286.

Approximate Conversions from Metric Measures

Symbol	When You Know	Multiply by	To Find	Symbol
		LENGTH		
mm	millimeters	0.04	inches	in
cm	centimeters	0.4	inches	in
m	meters	3.3	feet	ft
m	meters	1.1	yards	yd
km	kilometers	0.6	miles	mi
		AREA		
cm^2	square centimeters	0.16	square inches	in^2
m^2	square meters	1.2	square yards	yd^2
km^2	square kilometers	0.4	square miles	mi^2
ha	hectares (10,000 m^2)	2.5	acres	
		MASS (weight)		
g	grams	0.035	ounces	oz
kg	kilograms	2.2	pounds	lb
t	tonnes (1000 kg)	1.1	short tons	
		VOLUME		
ml	milliliters	0.03	fluid ounces	fl oz
l	liters	2.1	pints	pt
l	liters	1.06	quarts	qt
l	liters	0.26	gallons	gal
m^3	cubic meters	35	cubic feet	ft^3
m^3	cubic meters	1.3	cubic yards	yd^3
		TEMPERATURE (exact)		
°C	Celsius temperature	9/5 (then add 32)	Fahrenheit temperature	°F

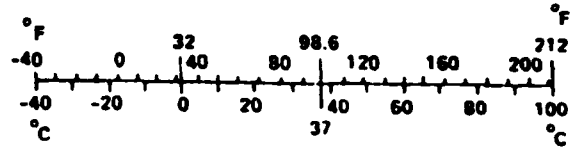

ACKNOWLEDGEMENTS

The authors extend appreciation to Dr. Aston McLaughlin of the FAA who served as the contract technical representative and who met with project personnel on several occasions to discuss project progress. His comments were always helpful and incisive and his assistance with decisions involving certain elements of the research helped immeasurably.

Mr. Robert A. Benko of the Great Lakes Region of the FAA is to be thanked for sharing his experience and valuable data on the construction of Wexford County Airport, Cadillac, Michigan. This project included a rubberized bituminous surface course constructed with unvulcanized synthetic rubber in liquid latex form. While the rubberized bituminous material is quite different from the asphalt-rubber material produced from scrap rubber, the construction experience was useful for the recommendations made in this report on construction guidelines.

We want to extend our thanks to two consultants who provided valuable literature and special help in preparing the specifications for field preparation of asphalt-rubber materials: Dr. Rudy Jimenez and Ray Pavlovich. Thanks also is due to Dr. Scott Shuler and Cindy Adams who coordinated their work with ours so that the most effective use of available research funds could be realized.

PREFACE

This report is the result of a project sponsored by the Federal Aviation Administration, U.S. Department of Transportation, and conducted by the Texas Transportation Institute (TTI) of Texas A&M University.

This is the second of two reports on contract number DTFA 01-83-C-30076 "Criteria for Asphalt-Rubber Concrete in Civil Airport Pavements" and it includes the testing and material characterization of an asphalt-rubber concrete and an asphalt concrete control, a performance evaluation, and an economic evaluation of the cost-effectiveness of the two materials.

TABLE OF CONTENTS

Section Page

LIST OF TABLES

LIST OF FIGURES

CHAPTER I. INTRODUCTION

The introductory chapter in the first volume of this report gives some historical background on the development and use of asphalt-rubber in highway pavements.

That introduction highlighted the interest that has been shown by the engineering community in the use of asphalt-rubber since it was developed by Charles H. McDonald, Consulting Engineer, Phoenix, Arizona beginning in the 1960's. It also suggested some of the areas in which there are additional needs for information concerning field performance, relationships between laboratory-developed properties and performance, design techniques, specifications and tests for compliance and construction practices.

Airport pavements are special cases that have not been treated widely in the literature and they pose special problems for the asphalt-rubber mixes because of the high tire pressures and multiple loads that are applied.

OBJECTIVES

The primary objectives of the research in this project are to:

1. Develop processes for preparing asphalt-rubber binders in the laboratory that have properties similar to those produced in the field.
2. Modify the FAA laboratory asphalt concrete mixture design procedure for use with these asphalt-rubber binders.
3. Determine the engineering properties of typical asphalt-rubber concrete materials.
4. Perform a cost-effectiveness analysis to determine if these materials should be considered as alternatives in future designs.
5. Develop model specifications and construction procedures for the use of these materials in the field.

SCOPE OF VOLUME 1

The first volume of this report DOT/FAA/PM-86/39, entitled "Criteria for Asphalt-Rubber Concrete in Civil Airport Pavements: Mixture Design", addressed Objectives One and Two and the model specifications in Objective Five. Specifically, that volume included the development of the laboratory procedure for preparing asphalt-rubber for use in mixture design, the development of the mixture design procedure, and the guide specifications for field production of the asphalt-rubber binders.

SCOPE OF THIS VOLUME

This volume is concerned with the remaining Objectives, numbers Three and Four, and the construction procedures in Objective Five. Specifically, this volume includes the laboratory tests for materials characterization of asphalt rubber in stability, modulus, fatigue, fracture, creep, and permanent deformation; the prediction of the performance of airport pavements under a variety of climatic conditions; the comparison of costs of asphalt concrete and asphalt-rubber concrete over their predicted performance lives; and the production and construction procedures which should be used with asphalt-rubber concrete to achieve a uniformly high quality pavement which performs well under aircraft traffic. The production and construction procedures are included as Appendix A and the remaining appendixes record the data on material properties, aircraft, and tire contact pressures that were used in this report.

CHAPTER II. LABORATORY EVALUATION OF ASPHALT-RUBBER CONCRETE

This chapter presents the results of a testing program to determine the materials characteristics of asphalt-rubber concrete with low, medium, and high binder contents and a commonly used asphalt concrete with an AC-10 asphalt cement binder. These properties are used in predicting the relative performance of airport pavements constructed with these materials, which are, in turn, used in a cost-effectiveness analysis of these materials.

The materials properties and the tests that are used to determine them are presented in this chapter. The materials properties include:

1. Stability (Marshall Stability)
2. Modulus (Indirect Tension Loading)
3. Fatigue (Beam Fatigue Loading)
4. Fracture ("Overlay" Test)
5. Creep Compliance (Creep Test)
6. Permanent Deformation (Repeated Load Test)

Each of the tests will be described followed by typical results of the testing of each of the four mixes that are considered.

OVERALL TESTING OBJECTIVES

The tests on each of the four mixes were made to determine the properties of asphalt-rubber concrete and asphalt concrete at a variety of temperatures and typical loading rates so as to allow the prediction of the performance of a typical airport pavement in four different climatic zones: (1) wet-freeze, (2) wet-no freeze, (3) dry-freeze, and (4) dry-no freeze. More will be explained about these climatic zones in the chapter on performance prediction. The computer program used in the analysis is capable of taking into account the seasonal changes of temperature and material properties that occur during the life of the pavement. Also, by determining the stiffness of each of the four mixes at different temperatures, it is possible to determine the temperature-susceptibility of each mix; i.e., those mixes which change modulus the

most will be the most adversely affected by temperature changes in the field.

All samples of asphalt-rubber concrete that were used for testing were prepared in accordance with the modifications to the Asphalt Institute's MS-2 manual procedures that were recommended in Volume 1, except that a compaction temperature of 375°F (191°C) was found to be too high to compact the beam specimens used for fatigue and overlay testing. The asphalt-rubber concrete material at 375°F (191°C) moved too much under the compactor to be well-compacted. Therefore, a lower compaction temperature (325°F, or 163°C) was used for all specimens prepared in the mix design and materials characterization in this portion of the study. The asphalt concrete samples were prepared in accordance with the MS-2 manual procedures as they are.

The sample preparation and testing were done with one primary objective in view: to permit a realistic comparison of asphalt-rubber concrete with ordinary asphalt concrete performance and cost-effectiveness when they are used in airport pavements.

SELECTION OF MATERIALS FOR TESTING

Aggregate

A mixture of crushed limestone and field sand was chosen for the aggregate, as these materials generally produce a high quality mix which performs well in both test and field conditions. A maximum particle size of 1/2" (100 percent passing the 1/2 in. sieve; some retained on the 3/8 in. sieve) was chosen. ASTM C125 defines the maximum size of coarse aggregate as the smallest sieve opening through which the entire sample passes (Ref 1). The aggregates were blended to meet the 1977 FAA aggregate grading specification for pavements with a bituminous surface course and designed to accommodate aircraft with gross weights of 60,000 pounds (27,000 kg) or more, or with tire pressures of 100 psi (690 kPa) or more (Ref 2). This grading band is similar to the 1983 ASTM specification grading band for bituminous paving mixtures and 3/8"

nominal maximum size of aggregate (100 percent passing the 1/2 in. sieve; some retained on the 3/8 in. sieve) which is commonly used for highway pavements carrying heavy truck traffic (Ref 3). ASTM grading requirements are based upon nominal maximum size which allows for a small percentage (usually about 5%) of the sample weight to be retained on that sieve (Ref 1). The percents of material passing through standard sieve sizes for the FAA and the ASTM specifications are shown in Table 1.

The middle of the FAA grading band was chosen as the target for the combined aggregate grading. The band and the mid-band gradation are shown in Figure 1.

The limestone and the field sand were obtained from White's Mines in Brownwood, Texas. The limestone was obtained from the producer in four different sizes and the material was weighed from each batch of material as shown in Table 2. The limestone dust had to be sieved before use because it contained too high a percentage of fines (material passing the #200 sieve) to meet the grading specifications. The field sand was sieved through the #8 sieve before use to remove sticks and organic debris and to break up large clods.

Two sieving methods were used to produce a final aggregate blend. For the initial testing which was described in Volume 1 of this report, small hand shakers were used and only the limestone dust was sieved, as described above. However, this was found to be a very time-consuming process and was not satisfactory for the production of the samples needed for the material characterization and testing described in this volume. A sieve method in which all of the limestone and field sand materials were sieved through large sieves on a Gillson mechanical shaker was therefore adopted. The combined aggregate was then produced by weight from the resulting sized material. Both sieving and weighing methods met the mid-band of the FAA grading specification, and are shown in Figure 2.

Asphalt Concrete Control Mix

The material chosen for the control was an AC-10 Lab Standard (American Petrofina was used). A Marshall mix design was performed and

TABLE 1. 1977 FAA Aggregate Grading Band for Bituminous Surface Course with 1/2" (12.5 mm) Maximum Particle Size.*

	% passing (by weight)	
Sieve Size	FAA Specification	ASTM Specification
1/2 in. (12.5mm)	100	100
3/8 in. (9.5mm)	79-93	90-100
#4 (4.75mm)	59-73	55-85
#8 (2.36mm)	46-60	32-67
#16 (1.18mm)	34-48	---
#30 (600μm)	24-38	---
#50 (300μm)	15-27	7-23
#100 (150μm)	8-18	---
#200 (75μm)	3-6	2-10

*For aircraft weighing 60,000 pounds or more or with tire pressures of 100 psi or more; compared with the 1983 ASTM aggregate grading band for bituminous paving mixtures with 3/8" (9.5 mm) nominal maximum size of aggregate.

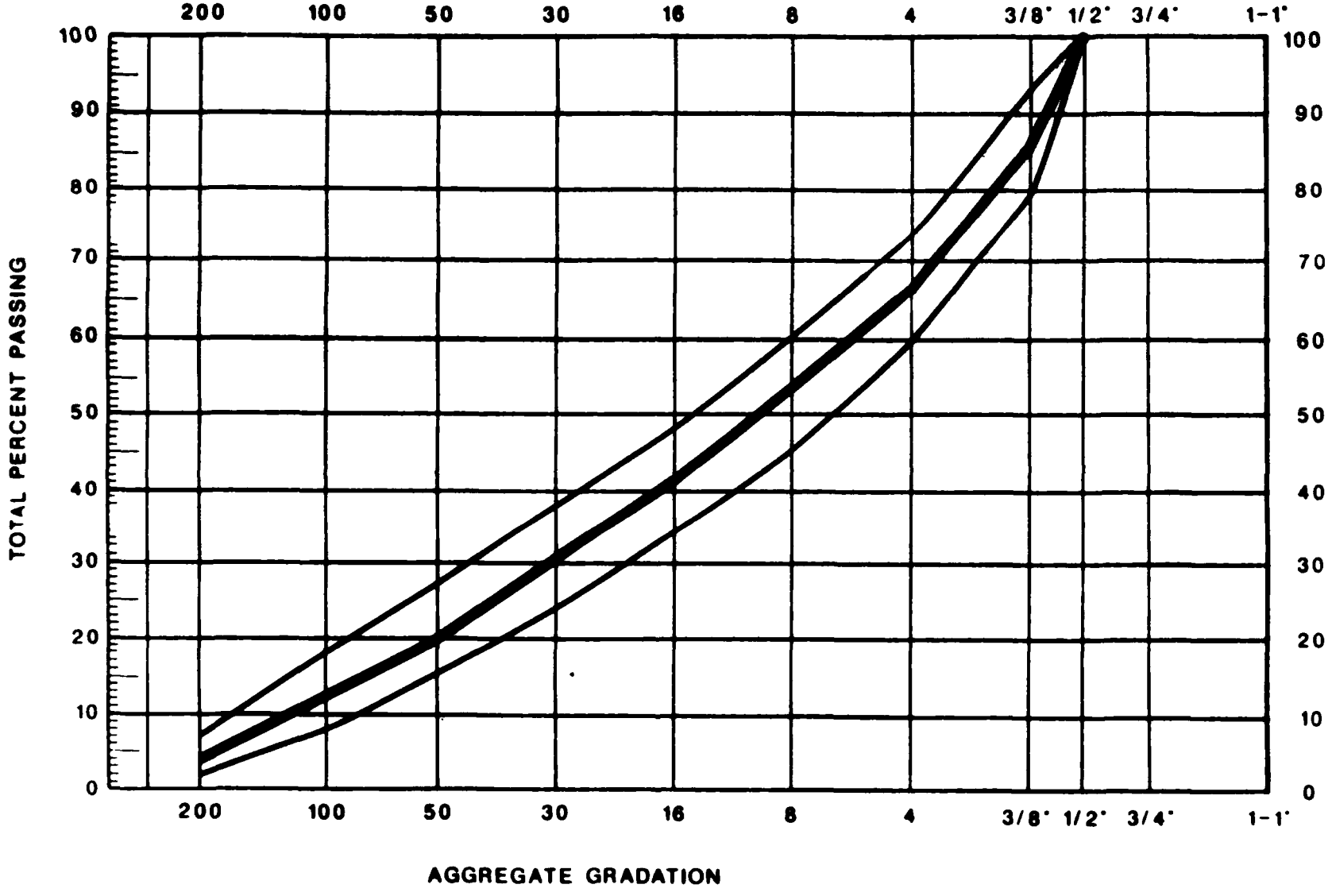

Figure 1. 1977 FAA Specification Aggregate Grading Band for 1/2-Inch Maximum Particle Size; Mid-Band Gradation is Shown.

TABLE 2. Weight Percentages Used From Each Type of Aggregate Obtained From the Producer.

Material/Size	% Used
-1/2", +3/8" only, limestone	13.5
3/8" grade limestone, as supplied by producer	12.9
1/4" grade limestone, as supplied by producer	17.2
Brownwood field sand	17.2
Limestone dust (crusher supply), as supplied by producer then broken down by the following sieves:	
Sieve Size	
#8	1.8
#16	12.5
#30	9.8
#50	8.1
#100	0.0
#200	5.2
passing #200	1.8

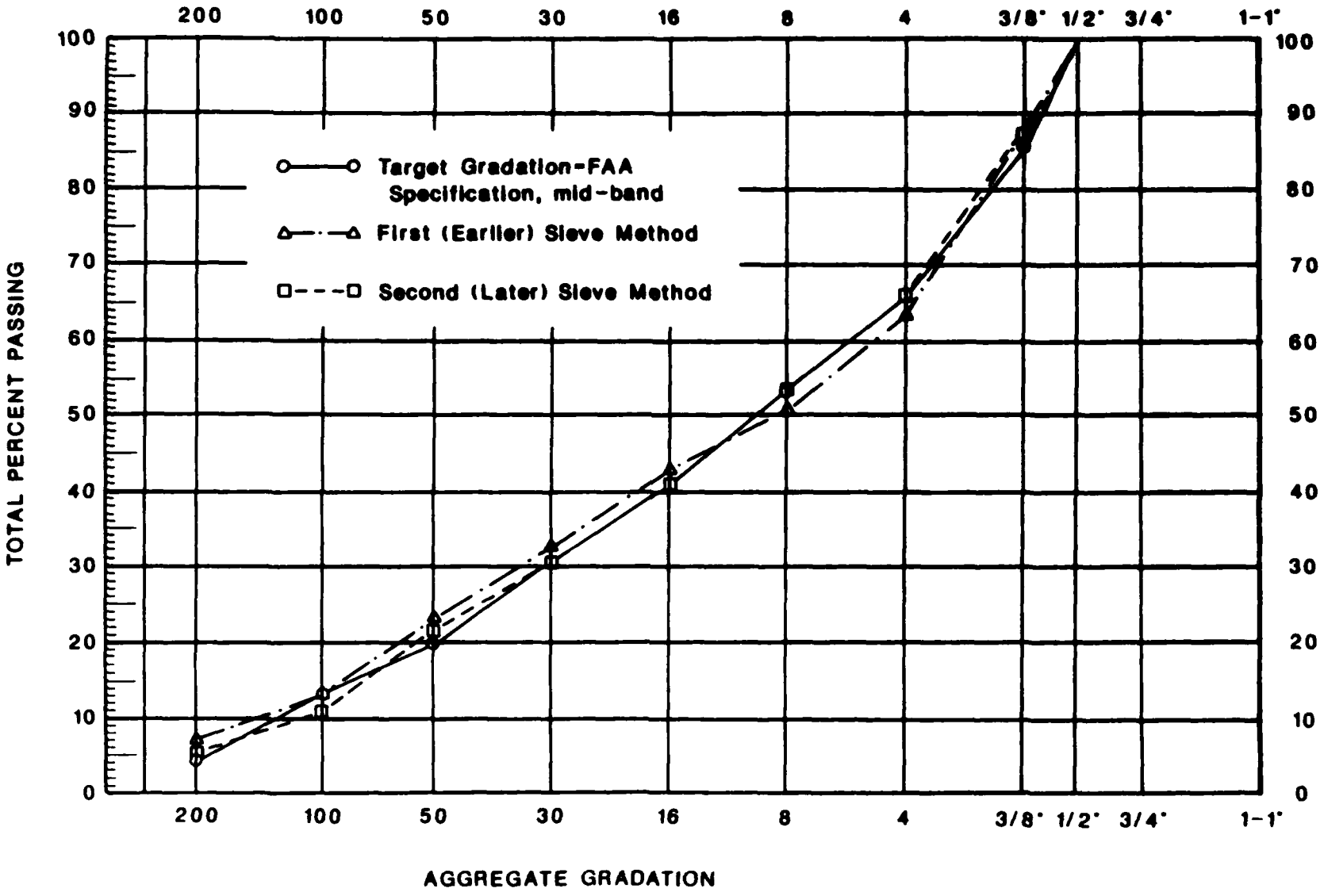

Figure 2. Aggregate Blends Resulting from Two Sieve Methods and FAA Specification Aggregate Gradation (Mid-Band).

the results are plotted in Figure 3. The optimum binder content was chosen as follows:

Property	% Binder
Unit Weight	5.30%
Marshall Stability	4.82%
% Air Voids	4.41%
Optimum	4.84%
Use	4.8%

The target air voids content was 4%, the median of the air void range specified in the Marshall mix design method (Ref 4).

The Marshall mix design method, in the May 1985 addendum to MS-2 (Ref 4) which updates Figure III-5 on VMA, prescribes a minimum VMA of about 15.5% for a nominal maximum particle size of 3/8 in. MS-2 describes the nominal maximum particle size as "the largest sieve size listed in the applicable specification upon which any material is permitted to be retained" (Ref 4: p. 32), which was 3/8 in. for the aggregate gradation specification used in this study. The FAA specification for a Bituminous Surface Course (Ref 2) prescribes a minimum VMA of 15% for the same aggregate gradation, described as a 1/2 in. maximum particle size (100 percent passing the 1/2 in. sieve) by FAA. However, Figure 3 in this report shows that the VMA of the asphalt concrete mix at 4.8% binder content is around 13%. The mix meets the other criteria described in MS-2, and therefore the mix was accepted with a 4.8% binder content in spite of the low VMA. Studies have been reported (Ref 5) which indicate that a minimum VMA in mix design will not guarantee good pavement performance, and that minimum VMA requirements can eliminate some aggregates from use which have acceptable service records. Some studies (Ref 5) have indicated that a minimum VMA limit under 12% is a more appropriate specification limit. Because of the questionable value of the current minimum VMA standards and because the limestone aggregate used in this research had previously been used in many successful mixes,

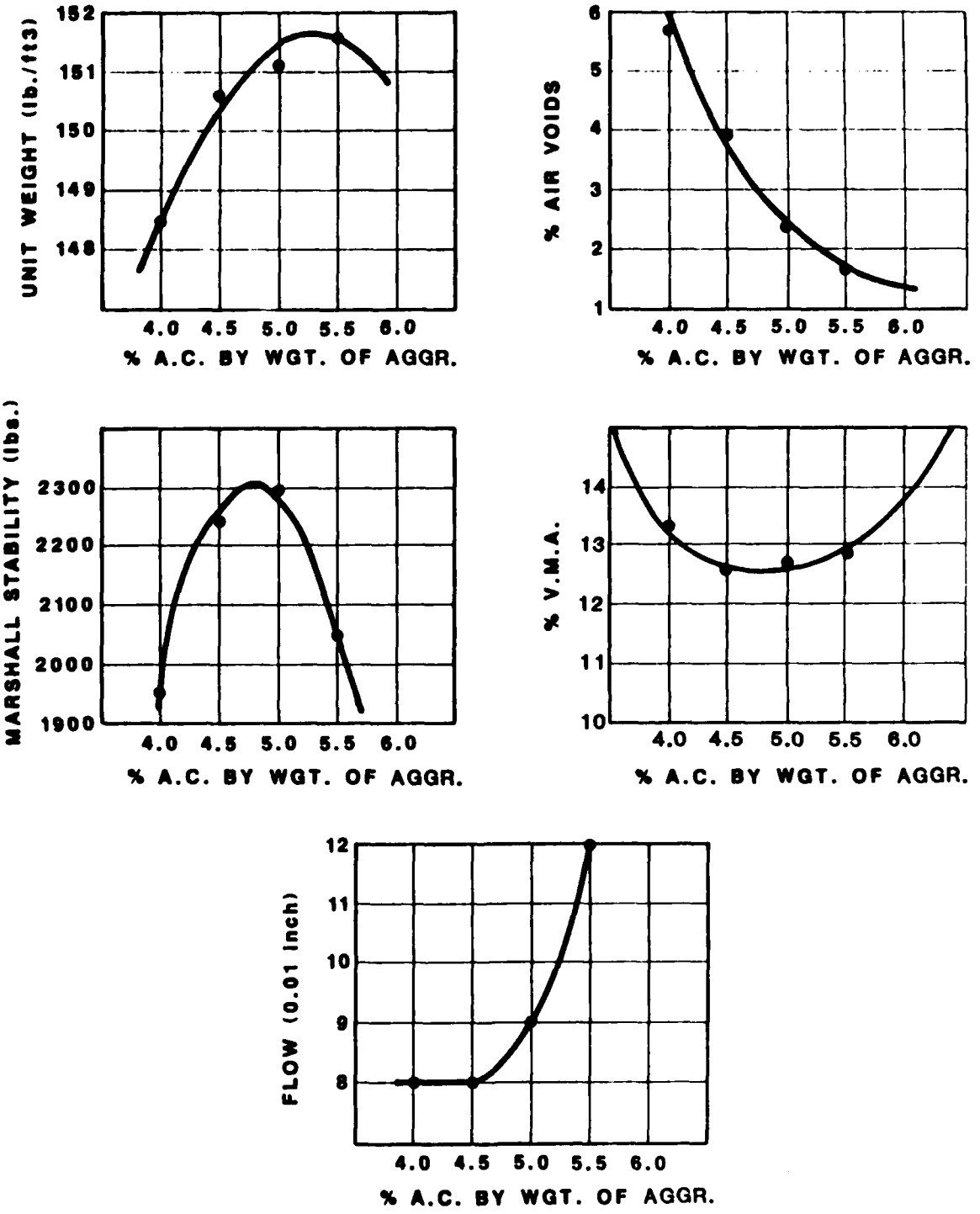

Figure 3. Test Property Curves for the Marshall Method Mix Design for the AC-10 Asphalt Concrete Control Material.

the VMA of 13% for the asphalt concrete mix with 4.8% binder content was accepted.

Asphalt-Rubber Concrete Mix

The asphalt-rubber binder was obtained from a Texas State Department of Highways and Public Transportation project in Victoria, Texas and shall hereafter be referred to as Victoria asphalt-rubber. The job was being performed by the Arizona Refining Company, who produced the asphalt-rubber material. Victoria asphalt-rubber was a mix of 77% AC-10 asphalt cement with 3% extender oil and 20% rubber which was digested for about two hours. The rubber was a blend of the following types of ambient grind, vulcanized whole tire rubber: Baker CR40 (40%) and C107 (20%), and Genstar C106 (30%) and C112 (10%). The combined rubber gradation is shown in Figure 4. As discussed in Volume 1 of this report, an adjusted aggregate blend must be calculated which accounts for the rubber particles in the mix. The calculated, adjusted aggregate blend for the Victoria asphalt-rubber concrete is shown in Table 3 and is compared with the unadjusted aggregate blend which meets the FAA specification at mid-band. It can be seen from this table that the adjusted blend of the mineral aggregate (aggregate weight, for blend with rubber) was almost the same as the unadjusted aggregate mixture (aggregate weight, for blend without rubber) which did not account for rubber particles acting as aggregate in the mix. The difference between the two aggregate blends was too small to be accurately measured when preparing the aggregate mixture for use in making test specimens. Also, the difference in the two blends was probably smaller than random differences in the aggregates would be. Therefore, it was decided that in this case the same aggregate weights could be used for both the asphalt concrete control and the asphalt-rubber concrete test samples. It must be emphasized here that the aggregate mixture modification which accounts for the rubber particles in the mix must always be checked before this decision can be made.

A modified Marshall mix design was performed using the Victoria asphalt-rubber and the FAA specification mid-band aggregate gradation.

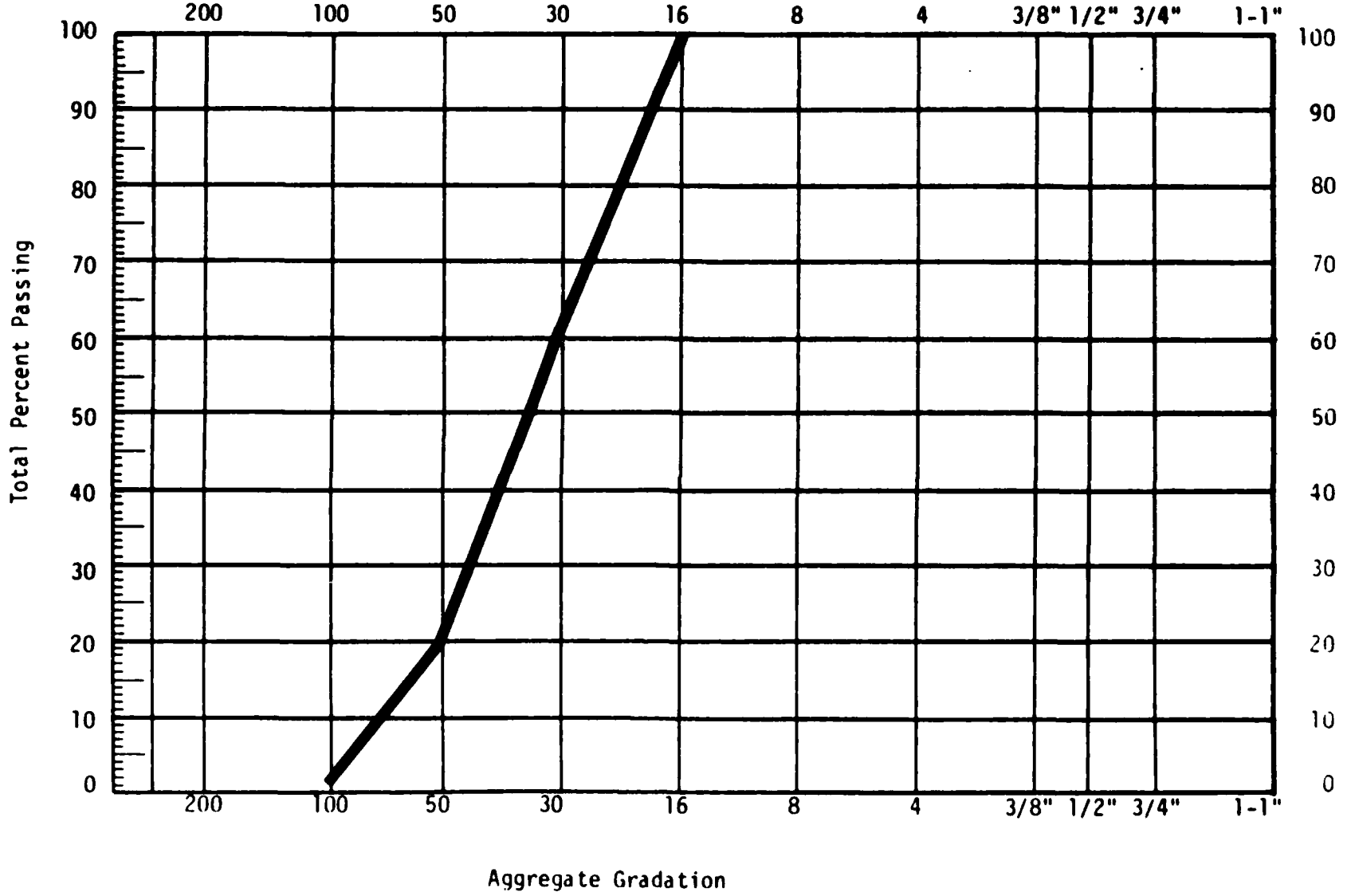

Figure 4. Gradation of the Rubber in the Victoria Asphalt-Rubber Binder.

TABLE 3. Calculation of Modified Aggregate Blend to Account for Rubber Particles in Asphalt-Rubber Concrete Mix.

Mix Weights: aggregate, 1200 g.
asphalt-rubber, 56.76 g.*
rubber only, 11.35 g. (= 20% rubber in asphalt-rubber)
total, aggregate + rubber particles, 1211.35 g.

% PASSING: for blend without rubber** (total aggregate = 1200g)			% PASSING: for blend with rubber (total solids = 1211.35g)				
Size	Aggr.%	Weight(g.)	Rubber%	Weight(g.)	Aggr.%***	Weight(g.)	Rubber+Aggr. Weight(g)**
1/2"	100.0	1200.00	100.0	11.35	100.0	1200.00	1211.35
3/8"	86.0	1032.00	100.0	11.35	85.9	1030.41	1041.76
#4	66.0	792.00	100.0	11.35	65.7	788.14	799.49
#8	53.0	636.00	100.0	11.35	52.6	630.67	642.02
#16	41.0	492.00	100.0	11.35	40.4	485.30	496.65
#30	30.5	366.00	62.5	0.59	30.7	368.87	369.46
#50	20.0	240.00	20.8	2.36	20.0	239.91	242.27
#100	13.0	156.00	1.8	0.20	13.1	157.27	157.48
#200	4.5	54.00	---	0.00	4.5	54.51	54.51

*using 4.73% (by weight of aggregate) Victoria asphalt-rubber
**using aggregate gradation from 1977 FAA specification
***NOTE: this column becomes the new aggregate job mix formula which is used for portioning out the mineral aggregate for the asphalt-rubber concrete mixture.

However, it was quickly realized that the air void contents in these Marshall samples were higher than the air void contents in the asphalt concrete control samples, and that the standard requirement in the Marshall mix design method for three to five percent air voids could not be met. The difficulties experienced by earlier researchers in compacting asphalt-rubber materials in the laboratory was discussed in Volume 1 of this report. Higher air void contents and swelling of samples after extrusion from molds have been experienced previously. This was due possibly to a rebound action of the rubber particles away from the walls of the mold. Because of this, an air void content of 7% was chosen as the optimum for the asphalt-rubber concrete in this mix design, with the realization that the asphalt-rubber concrete might still perform well in the testing phase of the study and that it might compact better in the field. An air void content of 7% was considered to be low enough to avoid the problem of the air voids becoming interconnected within the mix, causing moisture susceptibility. Plots of the mix design results for the Victoria asphalt-rubber concrete are shown in Figure 5. The optimum binder content was chosen as follows:

Property	% Binder
Unit Weight	4.875%
Marshall Stability	4.050%
% Air Voids	5.265%
Optimum	4.730%
Use	4.73%

The mix design data summarized above resulted in optimum binder contents for the two materials (asphalt concrete control and Victoria asphalt-rubber concrete) which were close enough to each other to be considered the same. This was not expected.

Construction guidelines generally specify a $\pm$ 0.5% tolerance on binder content. Therefore, the asphalt-rubber concrete was tested at the optimum binder content and at optimum $\pm$ 0.5%. In the testing program in this study, four mixes were tested as shown below.

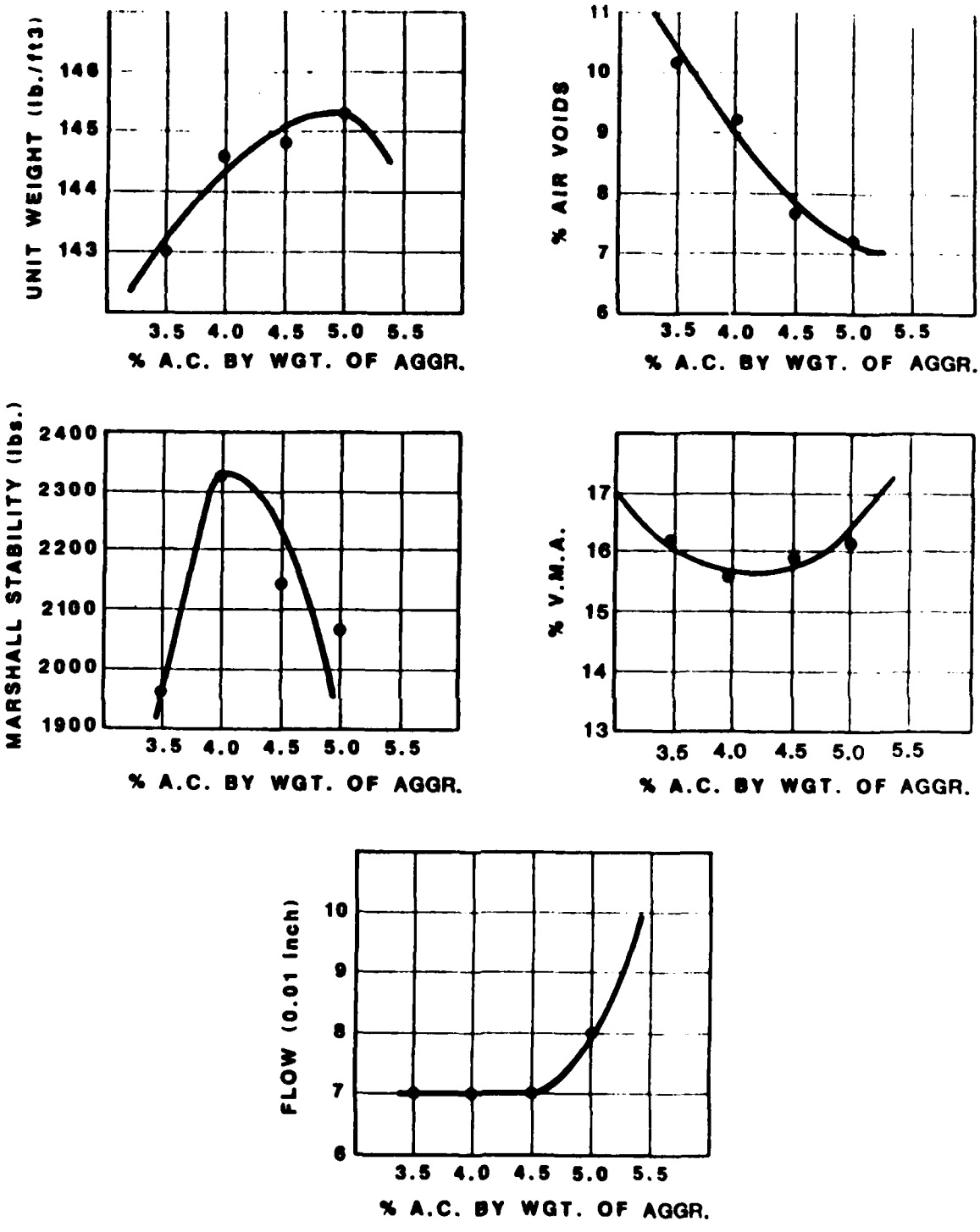

Figure 5. Property Curves for the Marshall Method Mix Design for the Victoria Asphalt-Rubber Concrete Material.

Material	Binder Content	% Asphalt Cement and Extender Oil	% Rubber	% Binder
Control AC-10	Optimum	100	0	4.80
Asphalt-Rubber Concrete	Low (-0.5%)	80	20	4.23
Asphalt-Rubber Concrete	Medium (Optimum)	80	20	4.73
Asphalt-Rubber Concrete	High (+0.5%)	80	20	5.23

DESIGN OF EXPERIMENTS

In order to make a comparison of the performance and life cycle cost of asphalt concrete with asphalt-rubber concrete, a number of laboratory tests were performed to characterize the important properties of each mix. These tests included: Marshall Stability, Resilient Modulus Tests, Beam Fatigue Tests, Crack Propagation Tests with the TTI "Overlay" Tester, Creep Tests, and Repeated Load Tests. The properties determined by these tests are subsequently used in predicting the performance of an airport pavement under a variety of commercial aircraft. The results of these predictions are discussed in Chapter III of this volume. Each of these tests is described in more detail in the following sections.

It is important to determine the material properties over a practical range of stress and temperature conditions and to test a sufficient number of replicates to permit a reliable representation of these properties.

In the resilient modulus tests, three temperatures were used, $33^{o}F$ ($0^{o}C$), $77^{o}F$ ($25^{o}C$), and $104^{o}F$ ($40^{o}C$), for all four materials: the AC-10 control mix, and the low, medium, and high binder content asphalt-rubber concrete. Three replicates were used for each combination of temperature and mix.

Beam fatigue tests were made at three temperatures: $34^{o}F$ ($1^{o}C$), $68^{o}F$ ($20^{o}C$), and $104^{o}F$ ($40^{o}C$) in order to obtain the temperature dependence of the fatigue properties of each mix. Three replicates were used at each

of three initial stress levels, making a total of nine beam tests that were made for each combination of temperature and mix.

The Crack Propagation Tests were made with the Texas Transportation Institute overlay tester which will be described more in detail in a subsequent section. The device is designed to repeatedly open and close a crack of constant width along the bottom edge of a beam sample and is used to measure the fracture properties of the beam material. This test has been found to be more reliable and repeatable than the beam fatigue tests in providing material properties. Tests were made at two temperatures, 34°F (1°C) and 77°F (25°C). Two replications were made on each combination of temperature and mix.

Repeated load tests were also made on cylindrical samples of the same size as the creep tests, i.e., 4 inches (10 cm) in diameter and 8 inches (20 cm) high. The purpose of the test is to determine how permanent, or plastic, deformation is accumulated in a material that is subjected to repeated stresses similar to those which are applied by passing aircraft traffic. The testing procedure is as recommended by the Federal Highway Administration to provide input data for the VESYS programs (Ref 6). The test procedure is described in more detail in a subsequent section. Tests were made at three temperatures, 40°F (4.4°C), 70°F (21.1°C) and 100°F (37.8°C). One sample was tested for each combination of material and temperature.

TESTING PROGRAM AND CHARACTERIZATION OF MATERIALS

Laboratory test results were used for most of the material characterization of the asphalt material comprising the top layer. The material parameters and the tests used to define them are described below.

For the underlying layers, typical materials were selected and the material characterization for these layers was estimated and then held constant for all combinations of surface material, environmental zone, and aircraft traffic. (See the section on Design Data in Chapter III in this report.) This was done to ensure that differences in the resultant

pavement damage could be attributed to differences in the material response of the top (bituminous) layer, which was varied from asphalt concrete through three binder contents of asphalt-rubber concrete.

Marshall Stability

The Marshall stability results from the mix designs were used to obtain a preliminary evaluation of the comparative resistance to deformation of the materials. Marshall stabilities were performed as described in the Marshall mix design method as outlined in MS-2 of the Asphalt Institute (Ref 4).

The maximum stabilities for the two mixes (AC-10 asphalt concrete control and Victoria asphalt-rubber concrete) were approximately equal, but the maximum stability for the AC control material occurred at a higher binder content (4.8%) than that of the asphalt rubber concrete material (4.1%). The shapes of the stability versus binder content curves were similar (as shown in Figure 6), indicating that the stabilities of the two materials were about equally sensitive to changes in the binder content. For the asphalt concrete, a $\pm$ 0.5% range in binder content above and below the point of maximum stability resulted in a stability range of about 2,160 to 2,320 pounds; the same range in binder content about the maximum stability point of asphalt rubber concrete resulted in a stability range of about 2,035 to 2,330 pounds.

The stabilities were well above the minimum stability required for heavy traffic in the Marshall mix design (1,500 pounds), and therefore no difficulty was expected in achieving the minimum stability at the design binder contents.

Resilient Modulus

In this study, resilient moduli were used as input data to the modified ILLIPAVE analysis program (Ref 7, 8, 9). The resilient modulus, defined as the ratio of repeated axial deviator stress to the recoverable axial strain, was measured by a Mark IV device as developed by Schmidt (Ref 10). This device applies a 0.1 second load pulse every three

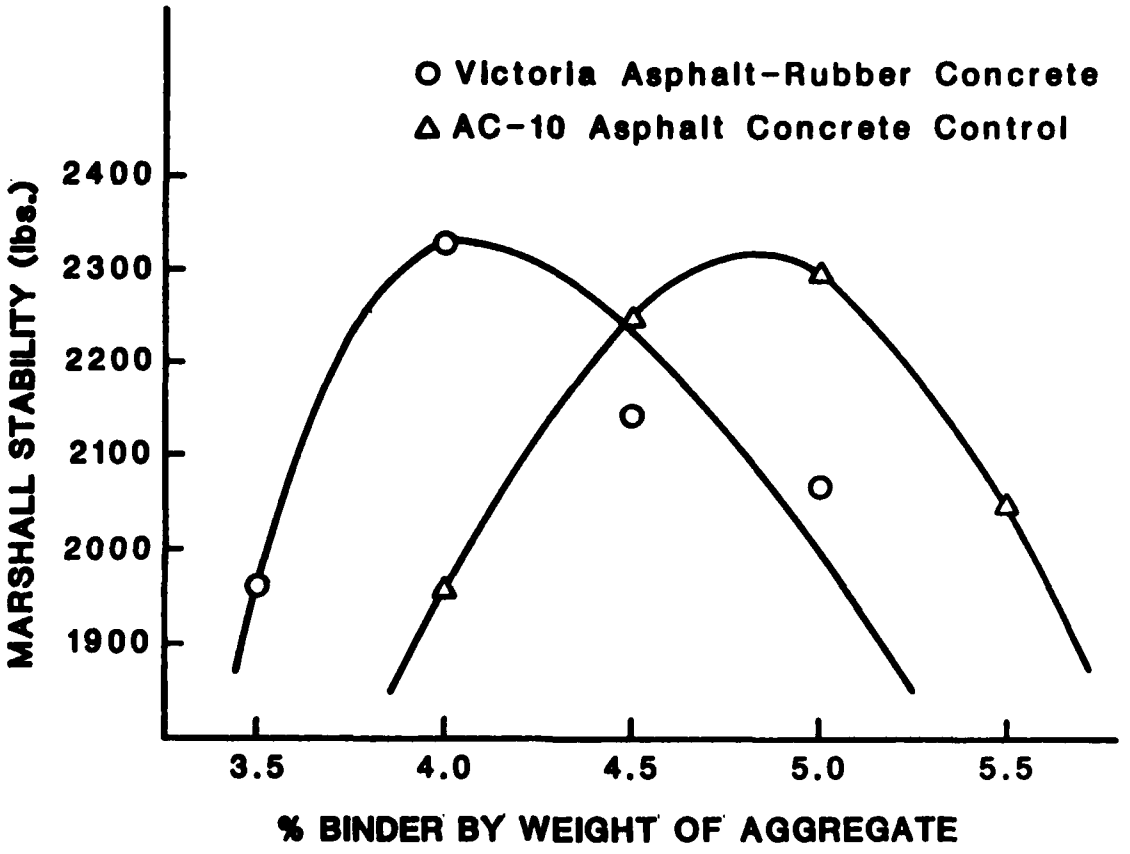

Figure 6. Comparison of Marshall Stabilities of Mixes Used in the Testing Program.

seconds across the vertical diameter of a cylindrical, Marshall type specimen. The resultant deformation (a dynamic test response) across the horizontal diameter is measured by Gould Statham Universal Transducing Cells (UC3's) (Ref 11). Resilient modulus is calculated according to the following formula:

$$M_R = \frac{P(\mu + 0.2734)}{\Delta t} \qquad (1)$$

where P = load (lbs)

μ = Poisson's Ratio for asphalt ≈ 0.35

Δ = change in diameter, or deformation (in.x10-6)

t = sample height (in.)

Curves of resilient modulus (psi) versus temperature (^{o}F) were plotted for each material and are shown in Figure 7. A combined plot of resilient modulus versus temperature, shown in Figure 8, indicated that the asphalt concrete control material had a modulus which was more temperature susceptible than the moduli of the asphalt-rubber materials.

The diametral resilient modulus described above "is often subjected to criticism because of the light load used, the conditions of biaxial stressing and the rigid assumptions which should be closely adhered to, but are not, in order for the cylindrical, diametrically loaded specimen to respond elastically" (Ref 12, p. 182). However, for this study, the resilient modulus was chosen because it is easily obtained at different temperatures; and for purposes of comparison of materials it was felt that the resilient modulus was a sufficient estimate of modulus to be used in the analysis program. In reality, however, for viscoelastic materials like asphalt and rubberized asphalt, the modulus is variable and depends upon load duration and temperature. Creep compliance, which is the inverse of the time-dependent modulus, is commonly used by researchers to describe the variation of modulus with load duration of viscoelastic materials (Ref 13). In this study, creep compliances were calculated and compared for the asphalt materials. (See the section on Creep Testing and Creep Compliances in this report.)

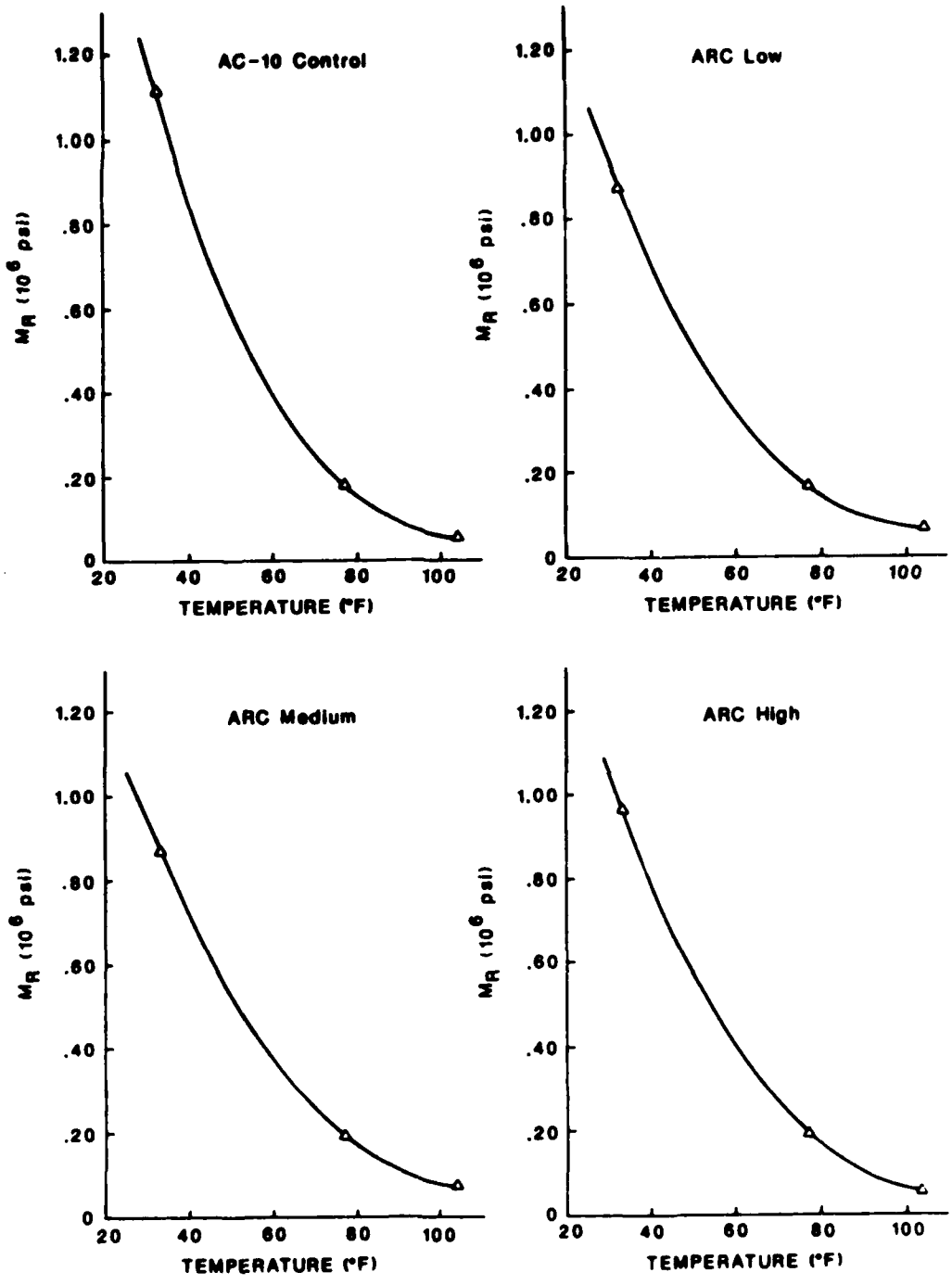

Figure 7. Plots of Resilient Modulus Versus Temperature for Each of the Four Materials in This Study.

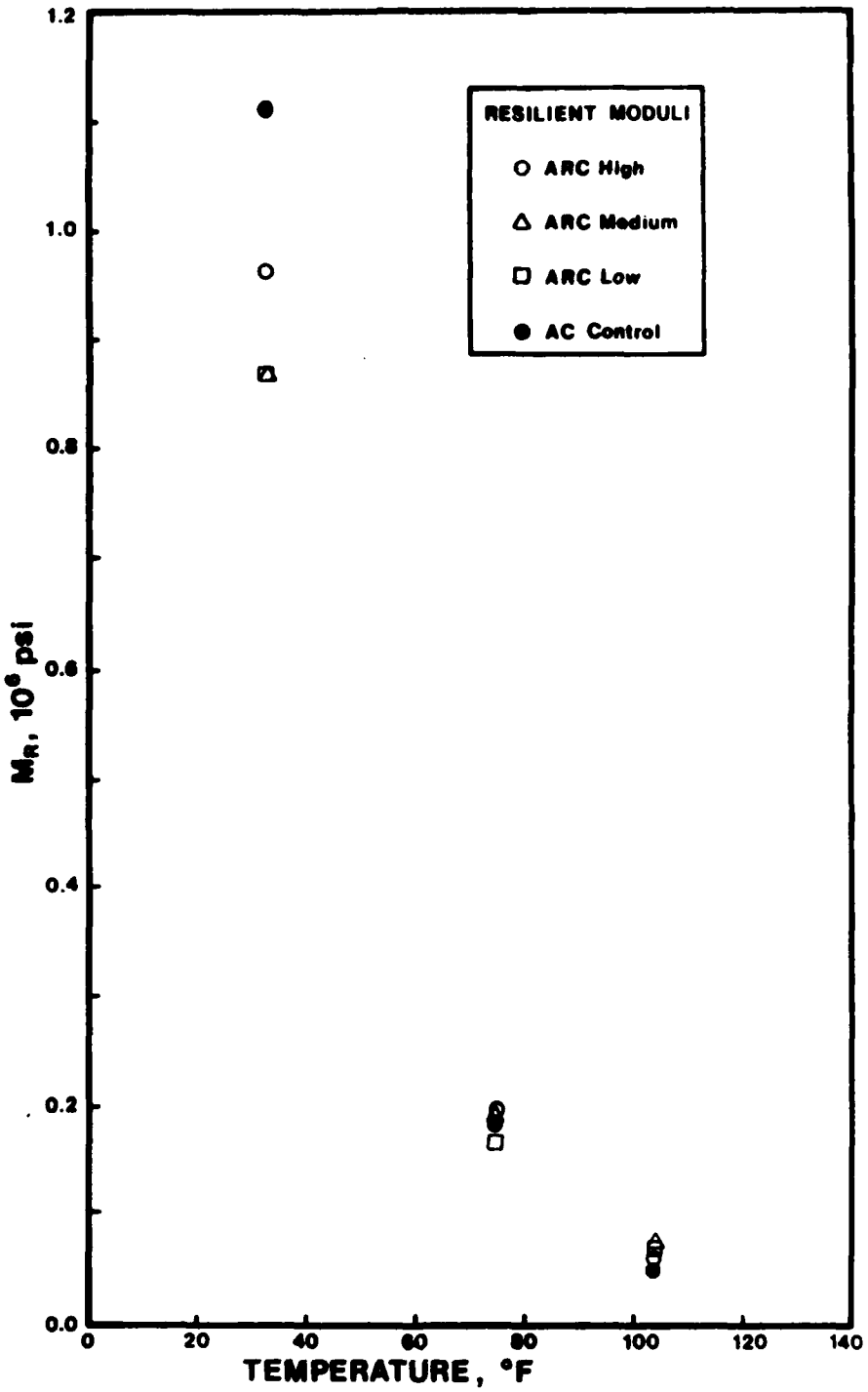

Figure 8. Combined Plot Showing Resilient Modulus Versus Temperature for the Four Materials in This Study.

It is a better approximation of field conditions to use a modulus for the underlying layers which is stress-sensitive and is calculated by the program for each stress condition. The ILLIPAVE program as modified at Texas A&M University and used in this study has this capability (Ref 8). However, primarily to ensure a consistent response of the underlying layers, the moduli were input as constants for those layers. The assumption was made that temperature effects were only felt in the bituminous layer, which was 15.5 inches thick.

Fatigue Testing and Fatigue Parameters

Fatigue is the phenomenon "of repetitive load-induced cracking due to a repeated stress or strain level below the ultimate strength of the material" (Ref 10, p. 282). Fatigue cracking generally is considered to initiate at the bottom of the asphalt layer and then propagate upwards to the pavement surface. Thus, the tensile strain at the bottom of the stiff layer (often the asphalt layer) is chosen as one of the failure criteria in most pavement analyses. Several methods of fatigue testing and analysis can be performed using various types of specimens. The phenomenological regression approach and the fracture mechanics approach were applied to the materials in this study.

The phenomenological regression approach is the most commonly used method for analyzing highway materials (Ref 12). The surface layer is characterized for fatigue using the familiar relation:

$$N_f = K_1 \, (1/\varepsilon_t)^{K2} \qquad (2)$$

where N_f = number of repetitions or load applications to failure

ε_t = tensile strain induced

K_1, K_2 = regression constants

This equation describes a straight line on a plot of cycles to failure versus bending strain, where log K_1 is the intercept of the y-axis (y-axis occurs where log K_1 = 0, or K_1 = 1), and $-K_2$ is the slope of the straight line. The parameters are influenced by such factors as the type

of load, dimensions of the test specimen, loading rate, test type, temperature, and properties of the mix, including air voids, aggregate gradation and type, asphalt content and viscosity, etc. Thus, K_1 and K_2 are not material properties (Ref 12).

This study used beam fatigue tests. These can be performed in either a controlled stress or a controlled strain mode. The type of pavement being simulated in the testing determines which mode of testing is proper (Ref 12). Previous researchers have stated that controlled stress loading is typically experienced by stiff, thick pavements (six inches thick or more). Controlled strain loading is encountered in thin pavements of two inches thick or less (Ref 14; this reference quotes Ref 15). Because airfield pavements are designed for heavy aircraft loads, they would be thick and therefore subject to controlled stress loading. This was the type of loading applied in the beam fatigue tests.

This study followed the procedures for fatigue testing which are described in the VESYS IIM User's Manual (Ref 6). VESYS uses a repeated load flexure device with beam specimens. The third-point loading configuration theoretically applies a constant bending moment over the center 4 inches of a 15 inch long specimen (Ref 6). The deflection up and down is measured at the center of the beam with a Linear Variable Differential Transformer, LVDT, which in these tests was bonded to the specimen with a stiff clay. This study used a device which applied a repeated tension-compression load in the form of a haversine wave for 0.1 second duration with 0.4 second rest periods. A schematic of the device is shown in Figure 9.

Temperature (which affects binder stiffness) and stress level both have a pronounced effect upon fatigue life. Therefore, the temperature around the fatigue devices was controlled and fatigue tests were performed at a variety of temperatures and stress levels. Tests were performed in temperature chambers at 34°F (1°C), 68°F (20°C), and 104°F (40°C). Applied loads were chosen so that some specimens failed at cycle numbers in the thousands, some at cycle numbers in the tens of thousands, and some at cycle numbers in the hundreds of thousands. This was done by a trial-and-error method; but the aim of obtaining a range of data points

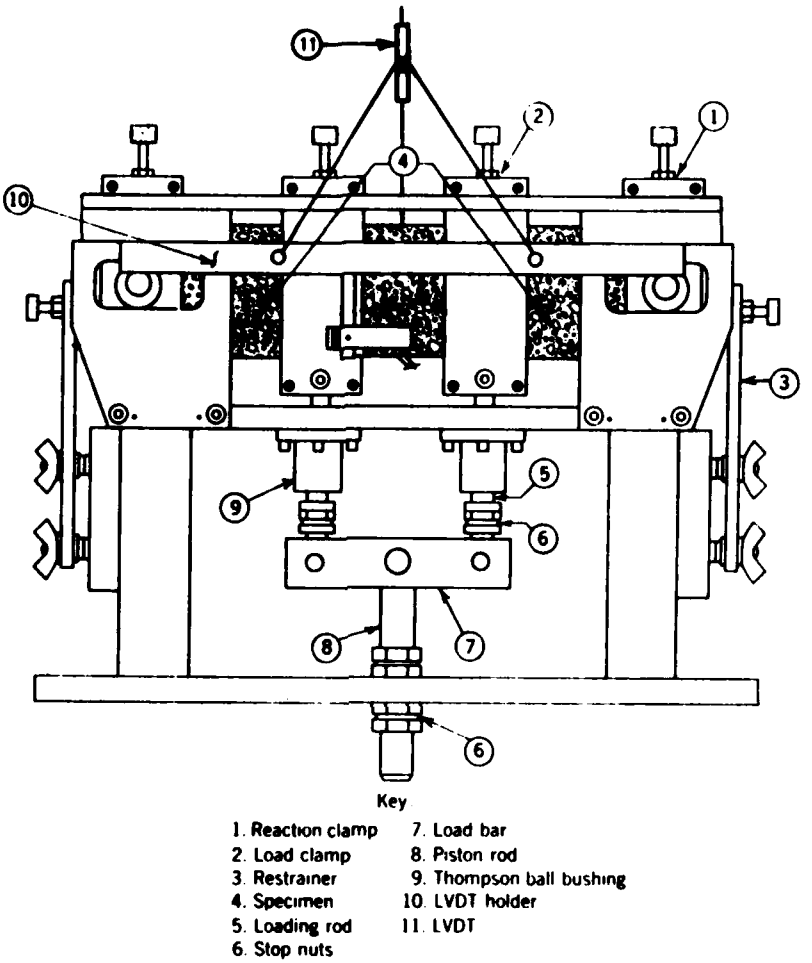

Figure 9. Repeated Flexural Apparatus Used for Beam Fatigue Tests. (Reference 10)

was achieved fairly easily. A strip chart was used to record chart load and chart deformation. This information, along with initial bending strain and the number of cycles to failure, was put into a computer program which calculated the following: load in pounds, deflection in inches, elastic modulus, bending strain, and the parameters K_1 and K_2 with an R-value to estimate the goodness of fit (Figure 10). Initial bending strain was the strain measured in the beam at the beginning of the test, usually at or around 200 cycles. At 200 cycles, it was assumed that the test machine was set up and functioning smoothly and that at this time the initial bending strain could be read without fluctuation introduced by adjusting the equipment setup or by transient responses in the test specimen. The program also plotted initial bending strain, ε_i, versus number of cycles to failure, N_f (Figure 11). On this plot there is one data point for each specimen tested; the data points should plot approximately as a straight line. However, in this research and in all other published fatigue test results there is quite a bit of scatter in the data points. Therefore, a best-fit line is regressed through the data points. The parameters and the R-values which describe the goodness-of-fit of the regression equations calculated from the laboratory tests are summarized in Table 4.

Several researchers have postulated that "a linear relationship exists between K_2 and log K_1, irrespective of mixture properties and test procedures" (Ref 16, p. 40; contains references to Ref 17 and Ref 18). The results from the laboratory tests in this study were therefore plotted to see if this held true for the tests in this study (Figure 12). As can be seen in the plot, a roughly linear relation was confirmed. Kennedy (Ref 16, 17) developed the following linear regression relationship from combining several sets of data:

$$K_2 = 1.350 - 0.252 \log K_1 \quad (R = 0.95;\ s_e = 0.29) \qquad (3)$$

BEAM FATIGUE DATA

PROJECT DESCRIPTION:
TTI RF4982 - ARC-MEDIUM @ 104 F.

TEST DATE 9-23-85

BEAM NUMBER	CHART LOAD	LOAD POUNDS	CHART DEF	DEF IN INCHES	E MODULUS	BENDING STRAIN	CYCLES TO FAILURE
F10M	3	60	3.2	.0266656	11835.4	.0022508	4186
F13M	2	40	7.4	.0123284	17066.2	.0010406	15460
F14M	3	60	6.6	.0219978	14346.8	.0018568	13780
F16M	5	50	6	.009996	26310.5	.0008437	37986
F18M	2	40	7	.011662	18041.5	.0009843	413700
F19M	3.6	72	6	.019998	18937.8	.001688	6769
F20M	3	60	3.6	.0299988	10520.4	.0025322	3071
F22M	2.2	44	5.8	.0096628	23951.6	.0008156	358793
F23M	5	50	5.6	.0093296	28189.8	.0007875	81467

THE REGRESSION EQUATION IS OF THE FORM:
CYCLES TO FAILURE=K1*((1/BENDING STRAIN)^K2)
IN THIS SAMPLE, THE CONSTANTS K1 AND K2 ARE:
K1= 1.04875199046E-5 K2= 3.25894736888

CORRELATION COEFFICIENT R=-.833275432648

THIS EQUATION GIVES THE FOLLOWING RESULTS.

SAMPLE NUMBER	BENDING STRAIN	CYCLES TO FAILURE PREDICTED	CYCLES TO FAILURE ACTUAL
1	.0022508605	4459	4186
2	.0010406482	55096	15460
3	.0018568485	8348	13780
4	.0008437688	109131	37986
5	.0009843969	66035	413700
6	.0016880441	11389	6769
7	.002532218	3038	3071
8	.0008156431	121880	358793
9	.0007875175	136446	81467

Figure 10. Computer Printout of Fatigue Data Analysis and Calculated Fatigue Parameters.

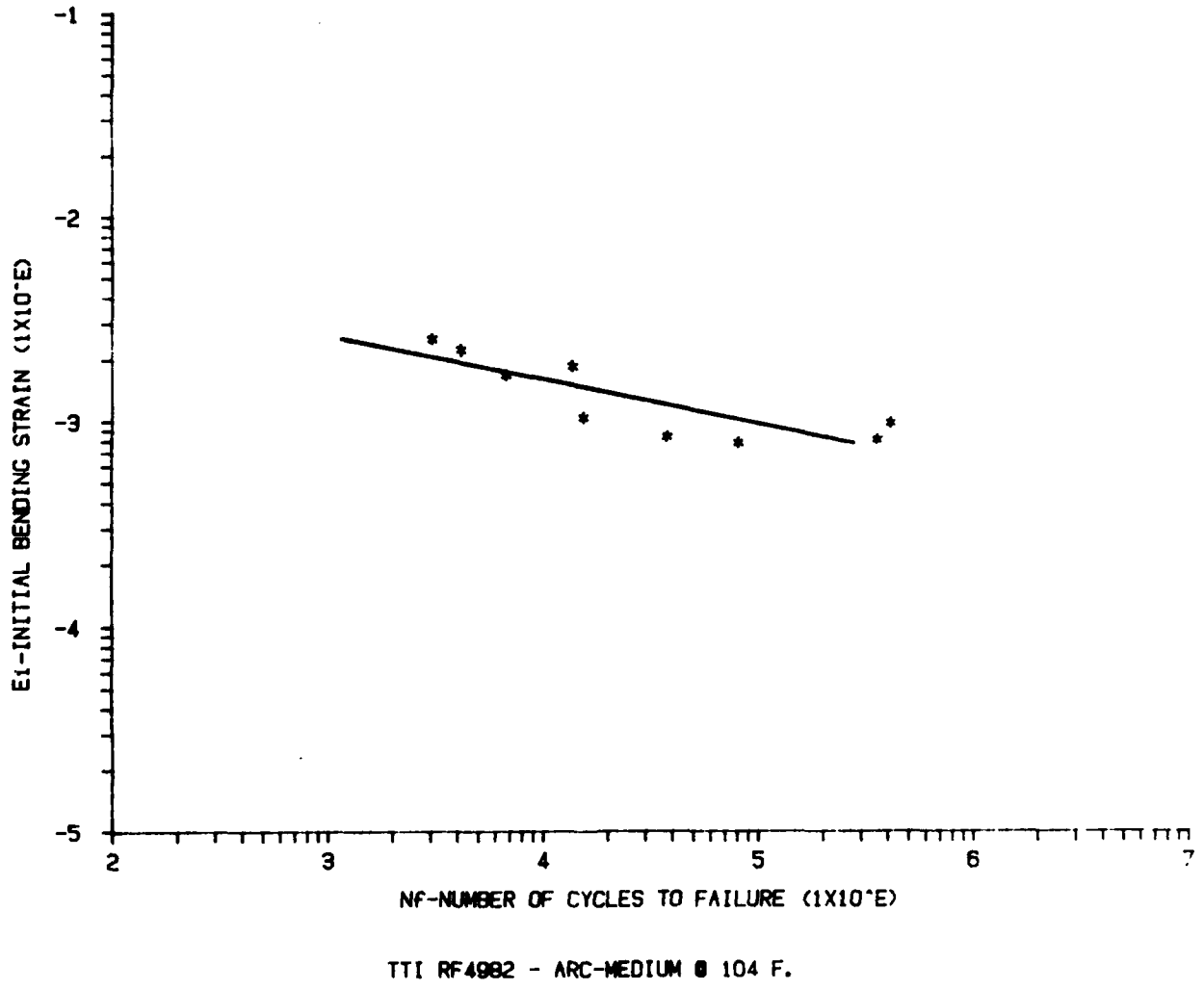

Figure 11. Computer Plot of Laboratory Fatigue Test Results.

TABLE 4. Material Parameters Calculated from Laboratory Fatigue Tests Performed in This Study.

Material	Temperature, °F (°C)	Number of Samples	R	K_1	K_2	$\log K_1$
AC-10 Control	104 (40)	8	-0.89	3.21×10^{-3}	2.35	-2.49
	68 (20)	8	-0.95	9.48×10^{-12}	4.69	-11.02
	34 (1)	7	-0.63	1.43×10^{-6}	2.92	-5.85
ARC-Low	104 (40)	10	-0.96	2.72×10^{-6}	3.38	-5.57
	68 (20)	9	-0.92	1.03×10^{-6}	3.17	-5.99
	34 (1)	7	-0.93	4.47×10^{-12}	4.48	-11.35
ARC-Medium	104 (40)	10	-0.85	2.82×10^{-6}	3.47	-5.55
	68 (20)	9	-0.98	3.16×10^{-5}	2.82	-4.50
	34 (1)	9	-0.86	9.91×10^{-10}	4.04	-9.00
ARC-High	104 (40)	10	-0.91	1.02×10^{-4}	2.95	-3.99
	68 (20)	10	-0.99	4.90×10^{-4}	2.52	-3.31
	34 (1)	8	-0.81	3.82×10^{-7}	3.19	-6.42

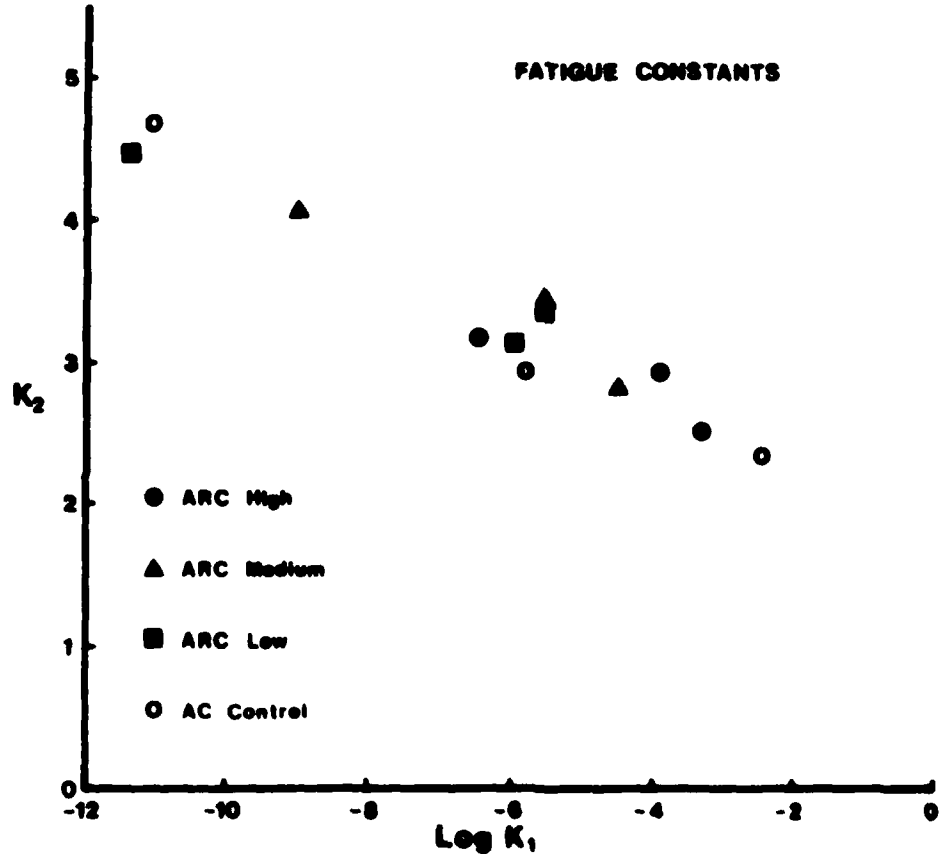

Figure 12. Combined Plot of Fatigue Parameters Calculated from Laboratory Data.

The K_1 values computed from the lab data in this study were used in Kennedy's regression equation to see how well the K_2 values calculated from Kennedy's equation compared with the K_2 values calculated from the lab data. The results and comparisons are tabulated in Table 5.

In order to use the laboratory results in a comparative analysis which was sensitive to the differences due to both material and temperature, a double regression procedure was applied to the lab data, as follows. First, $|\log K_1|$ versus log T (where T indicates temperature in Fahrenheit degrees) was plotted and a linear regression was performed for each of the four materials (asphalt concrete control and three binder contents of asphalt-rubber concrete; see Figure 13). This yielded a set of equations (one for each material) where temperature was the independent variable and K_1 was the dependent variable. Then K_2 versus log K_1 was plotted and a linear regression was performed for each material (see Figure 14). This yielded a set of equations with log K_1 as the independent variable and K_2 as the dependent variable. Using these sets of equations, any temperature could be chosen and the fatigue parameters could be calculated for each material at that temperature. The equations thus derived are shown in Table 6. The fatigue parameters calculated for some of the temperatures used to characterize seasons within the environmental zones are shown in Table 7.

Several researchers have previously shown that the number of cycles to failure experienced by materials in the laboratory is lower than that experienced by materials in the field. Such factors as healing of the pavement between load applications, residual stresses, and variability in the position of the wheel load are not accounted for by the laboratory fatigue relationship (Ref 12). This difference can be adjusted for by applying a multiplier to the laboratory value of K_1. Finn (Ref 19), after looking at field data versus laboratory data from the AASHO Road Test in Illinois, has suggested that a multiplier of 13 applied to the value of K_1 would adjust the lab data to more accurately represent the field fatigue life of asphalt materials. Therefore, a sampling of the computer runs made in this study were rerun with $(K_1)Field = 13*(K_1)Lab$. In general, the result was to divide the calculated cracking index by 13 when the (K_1)Field was used. Therefore, the cracking index for total

TABLE 5. Comparison of the Fatigue Parameter K_2 From Laboratory Tests Conducted in This Study to the Parameter K_2 Calculated From the Regression Equation Developed in Reference 17.

Regression Equation from Reference 17:

$$K_2 = 1.350 - 0.252 \log K_1$$

$$(R = 0.95;\ S_e = 0.29)$$

Material	Temperature, ^oF (^oC)	From Lab Tests, This Study		From Ref 17 Equation,	$\Delta = (K_2)_{lab} - (K_2)_{Ref\ 17}$
		$(K_1)_{lab}$	$(K_2)_{lab}$	$(K_2)_{Ref\ 17}$	
AC-10 Control	104 (40)	3.21×10^{-3}	2.35	1.98	0.37
	68 (20)	9.48×10^{-12}	4.69	4.13	0.56
	34 (1)	1.43×10^{-6}	2.92	2.82	0.10
ARC-Low	104 (40)	2.72×10^{-6}	3.38	2.75	0.63
	68 (20)	1.03×10^{-6}	3.17	2.86	0.31
	34 (1)	4.47×10^{-12}	4.48	4.21	0.27
ARC-Medium	104 (40)	2.82×10^{-6}	3.47	2.75	0.72
	68 (20)	3.16×10^{-5}	2.82	2.48	0.34
	34 (1)	9.91×10^{-10}	4.04	3.62	0.42
ARC-High	104 (40)	1.02×10^{-4}	2.95	2.36	0.59
	68 (20)	4.90×10^{-4}	2.52	2.18	0.33
	34 (1)	3.82×10^{-7}	3.19	2.97	0.23

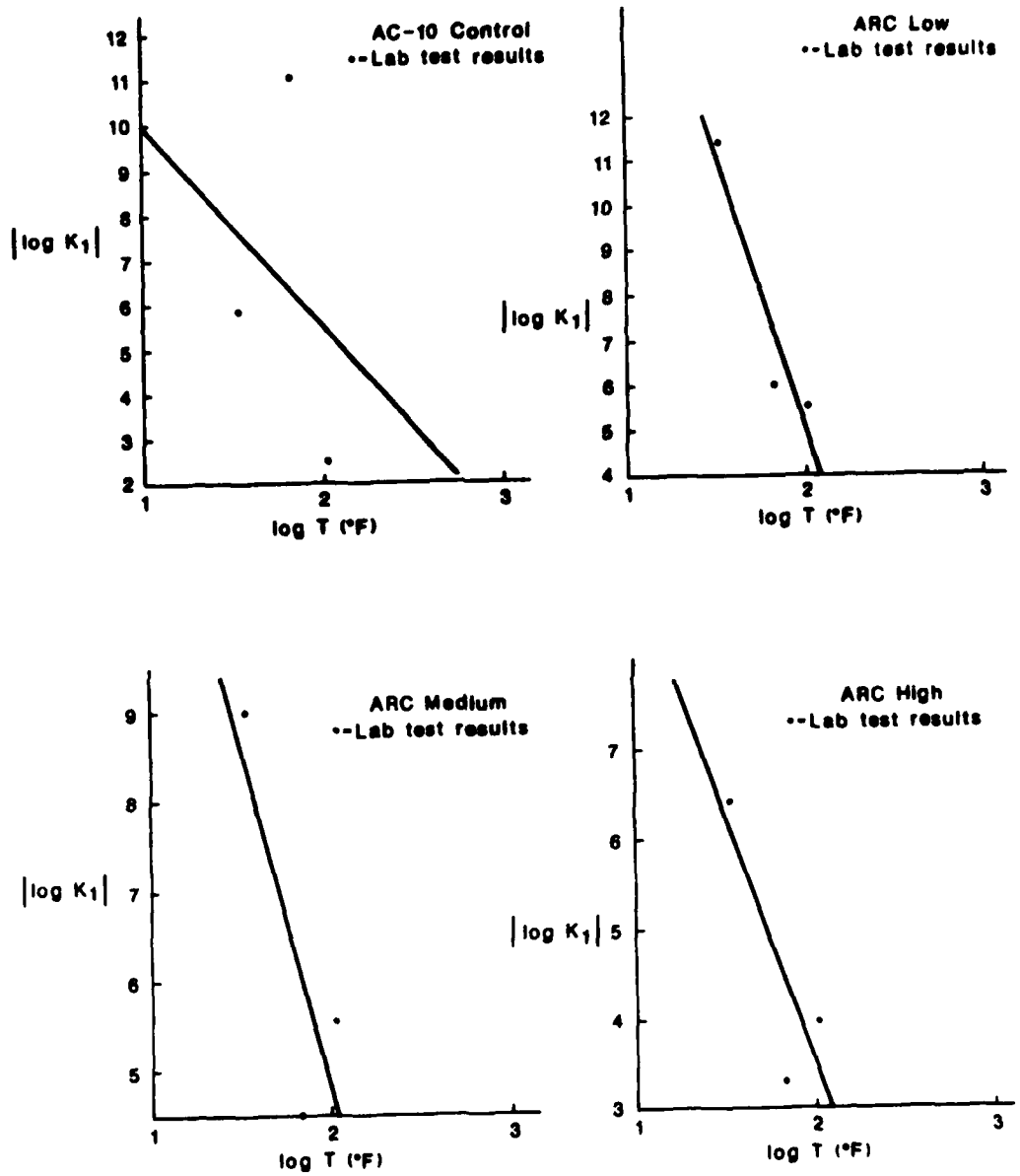

Figure 13. Plots of $|\log K_1|$ Versus Log T Showing Laboratory Data Points and Linear Regressions.

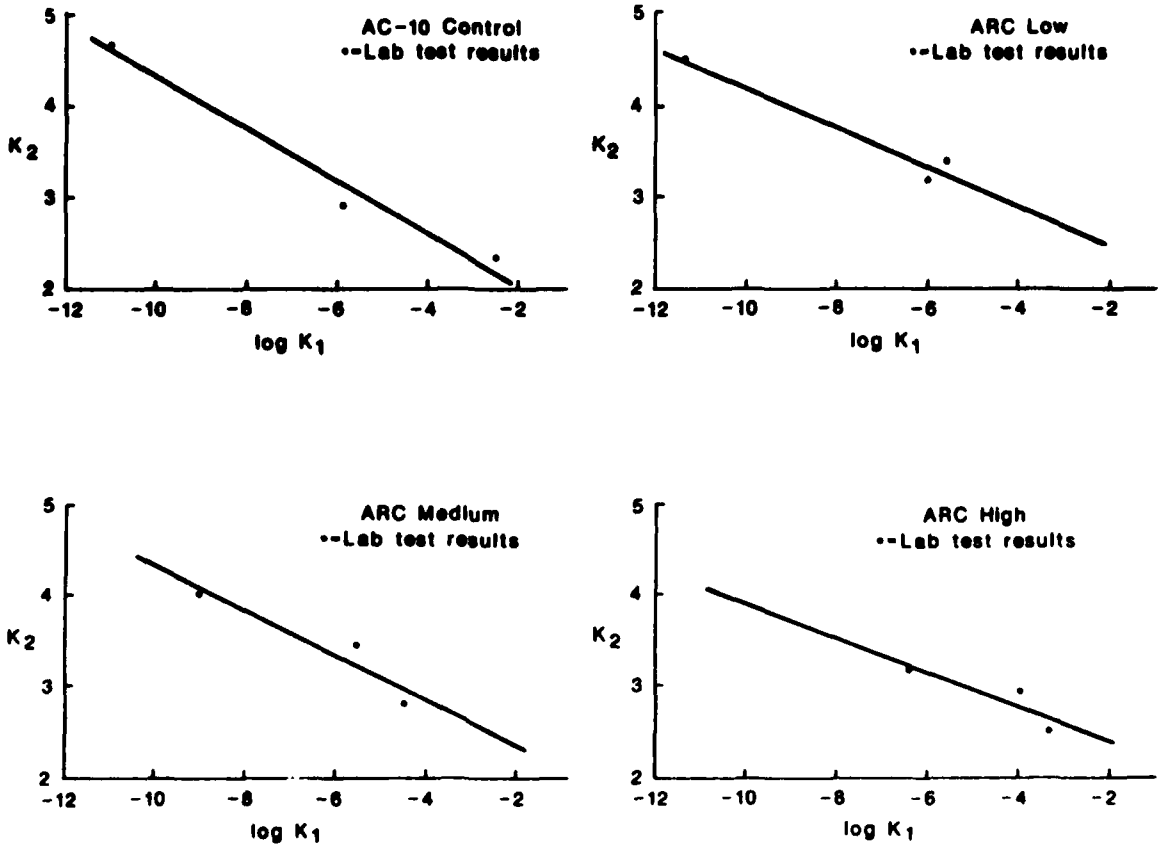

Figure 14. Plots of K_2 Versus Log K_1 Showing Laboratory Data Points and Linear Regressions.

TABLE 6. Regression Equations Generated From Laboratory Data and Used to Predict Fatigue Parameters for Any Temperature (^{o}F).

$|\log K_1|$ vs. $\log T(^{o}F)$

AC-10 Control	$\|\log K_1\| = 14.630 - 4.558 \log T$
ARC-Low	$\|\log K_1\| = 30.034 - 12.488 \log T$
ARC-Medium	$\|\log K_1\| = 20.483 - 7.879 \log T$
ARC-High	$\|\log K_1\| = 14.466 - 5.516 \log T$

K_2 vs. $\log K_1$

AC-10 Control	$K_2 = 1.512 - 0.280 (\log K_1)$
ARC-Low	$K_2 = 2.052 - 0.213 (\log K_1)$
ARC-Medium	$K_2 = 1.900 - 0.243 (\log K_1)$
ARC-High	$K_2 = 2.033 - 0.187 (\log K_1)$

TABLE 7. Fatigue Parameter Values Calculated for Selected Temperatures from Regression Equations Developed for the Materials in This Study.

Material	Temperature °F (°C)	K_1 (not adjusted to field conditions)	K_2	N_f, when $\varepsilon = 10^{-3}$ in/in
AC-10 Control	35 (1.7)	2.56×10^{-8}	3.64	2,130
	50 (10.0)	1.30×10^{-7}	3.43	2,530
	60 (15.6)	2.99×10^{-7}	3.34	3,130
	75 (23.9)	8.26×10^{-7}	3.21	3,520
	90 (32.2)	1.90×10^{-6}	3.11	4,060
	105 (40.6)	3.83×10^{-6}	3.03	4,710
ARC-Low	35 (1.7)	1.77×10^{-11}	4.34	190
	50 (10.0)	1.52×10^{-9}	3.93	940
	60 (15.6)	1.48×10^{-8}	3.72	2,140
	75 (23.9)	2.41×10^{-7}	3.46	5,780
	90 (32.2)	2.35×10^{-6}	3.25	13,200
	105 (40.6)	1.61×10^{-5}	3.07	26,100
ARC-Medium	35 (1.7)	4.81×10^{-9}	3.92	2,770
	50 (10.0)	7.99×10^{-8}	3.62	5,790
	60 (15.6)	3.36×10^{-7}	3.47	8,640
	75 (23.9)	1.95×10^{-6}	3.29	14,500
	90 (32.2)	8.20×10^{-6}	3.13	20,100
	105 (40.6)	2.76×10^{-5}	3.01	29,600
ARC-High	35 (1.7)	1.12×10^{-6}	3.14	2,950
	50 (10.0)	8.03×10^{-6}	2.98	1,990
	60 (15.6)	2.20×10^{-5}	2.90	11,000
	75 (23.9)	7.52×10^{-5}	2.80	18,900
	90 (32.2)	2.06×10^{-4}	2.72	29,800
	105 (40.6)	4.81×10^{-4}	2.65	42,900

combined traffic from each ILLIPAVE run was divided by 13 to give the field estimate of fatigue life. In this report, the designation of field fatigue life is used to describe the calculated cracking index after it has been divided by the adjustment factor of 13.

The adjustment factor of 13 which was derived by Finn to be applied to laboratory values of K_1 may not be accurate for all types of materials. A means has been developed to derive the K_1 adjustment factor for a material from laboratory data which involve the creep, permanent deformation, and healing properties of the material (Ref 20). Additional tests involving healing would need to be performed on the materials in this study to apply this method.

The phenomenological regression approach to fatigue is a somewhat simple approach which has been adopted by many researchers. However, this approach does not consider crack initiation and propagation. This aspect is considered by fracture mechanics methods. The test described in the next section is one of these methods.

Overlay Testing and Fracture Properties

The Texas Transportation Institute "overlay tester" was originally developed to investigate thermal reflection cracking in overlays but its versatility and repeatability have made it a regular part of the laboratory investigation of paving materials. The overlay tester is shown schematically in Figure 15. A beam made of the paving material is fastened to two platens, one fixed and the other movable. The center line of the beam is placed above the joint between the two platens. A force, P, is exerted on the movable platen to open and close a crack in the bottom of the beam. The maximum opening is pre-set and the opening, u, is monitored continuously with a Linear Variable Differential Transformer, LVDT, while, at the same time, the load, P, is measured with a load cell. Repeated opening and closing of the joint drives the crack upward progressively and it eventually reaches the top of the beam, at which time the test is terminated.

The test was devised to simulate the opening and closing of the crack or joint in an old pavement beneath an overlay due to changes in daily

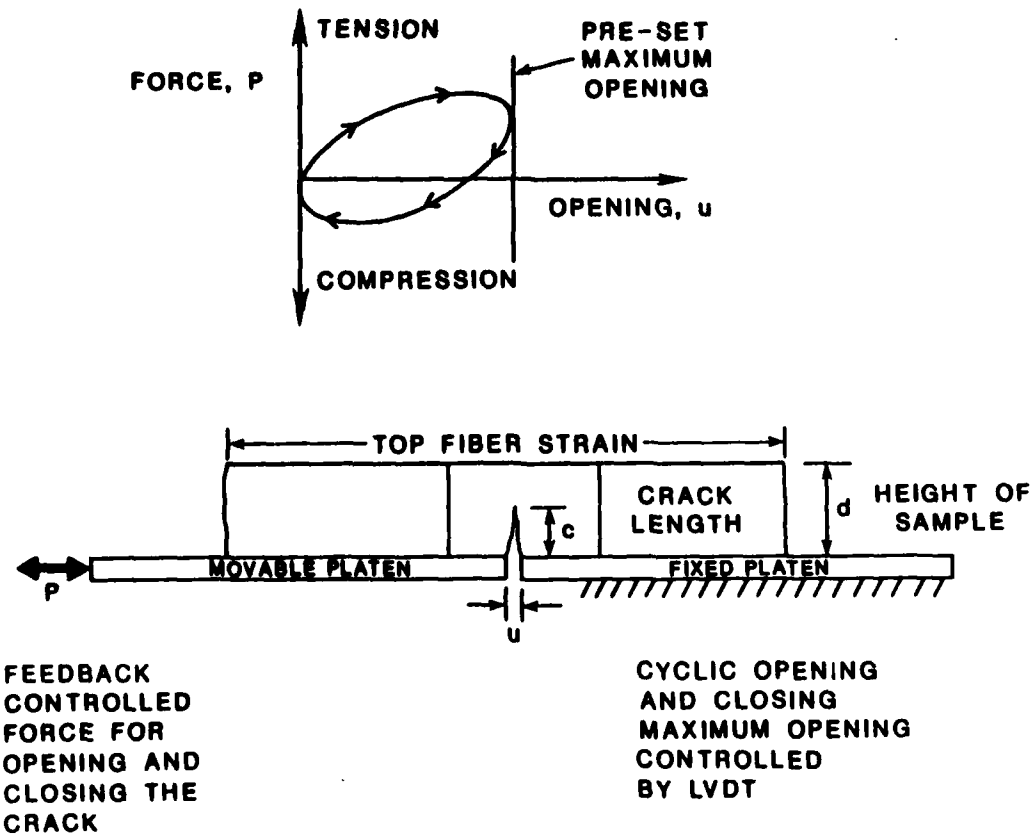

Figure 15. Schematic Diagram of the Texas Transportation Institute Overlay Tester.

temperature. The crack length is observed and measured visually on each side of the beam sample and the average crack length is used to compute the fracture properties of the beam material. The strain in the top fiber is measured with another LVDT principally when a strain relieving layer has been built into the beam so as to determine the extent to which strain has been relieved.

The fracture properties that are measured are the constants A and n that appear in Paris' Law (Ref 21), as follows:

$$\frac{dc}{dN} = A\ (\Delta K)^n \qquad (4)$$

where c = the crack length

N = the number of load cycles

dc/dN = the "crack speed", or the rate of growth of the crack.

ΔK = the change of "stress intensity factor" during the application of the load

A = the fracture coefficient

n = the fracture exponent

The "stress intensity factor" is calculated with an elastic finite element computer program and is taken from a graph of Kd/E_u versus c/d, as shown in Figure 16. Once the crack length ratio, c/d, is known, the value of the change of stress intensity factor, ΔK, during the load cycle can be calculated.

A graph of the "crack speed", dc/dN, versus the change of stress intensity factor, both on a logarithmic scale, shows a straight-line portion with a slope, n, and an intercept, A, as shown in Figure 17.

The measured values of A and n are given in Table 8, along with some of the other test data.

Although these constants are derived empirically from this test, it has been shown theoretically (Ref 22) that the fracture coefficient, A, depends upon the tensile strength and creep compliance of the beam material in tension and that the fracture exponent, n, depends solely upon the slope of the creep compliance curve. This relationship will be shown in a subsequent section of this chapter. Because both A and n

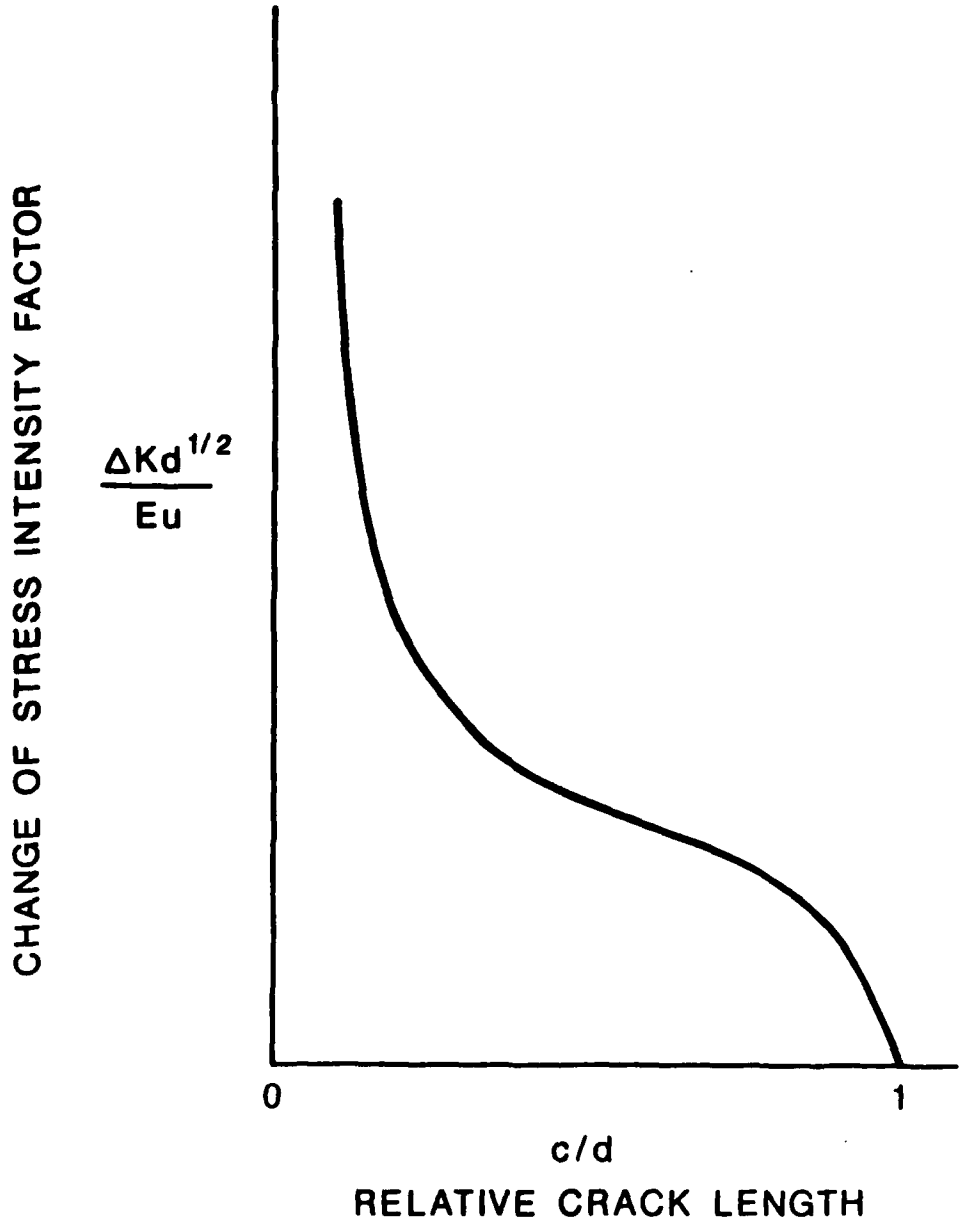

Figure 16. Computed Relation Between Change of Stress Intensity Factor and Crack Length.

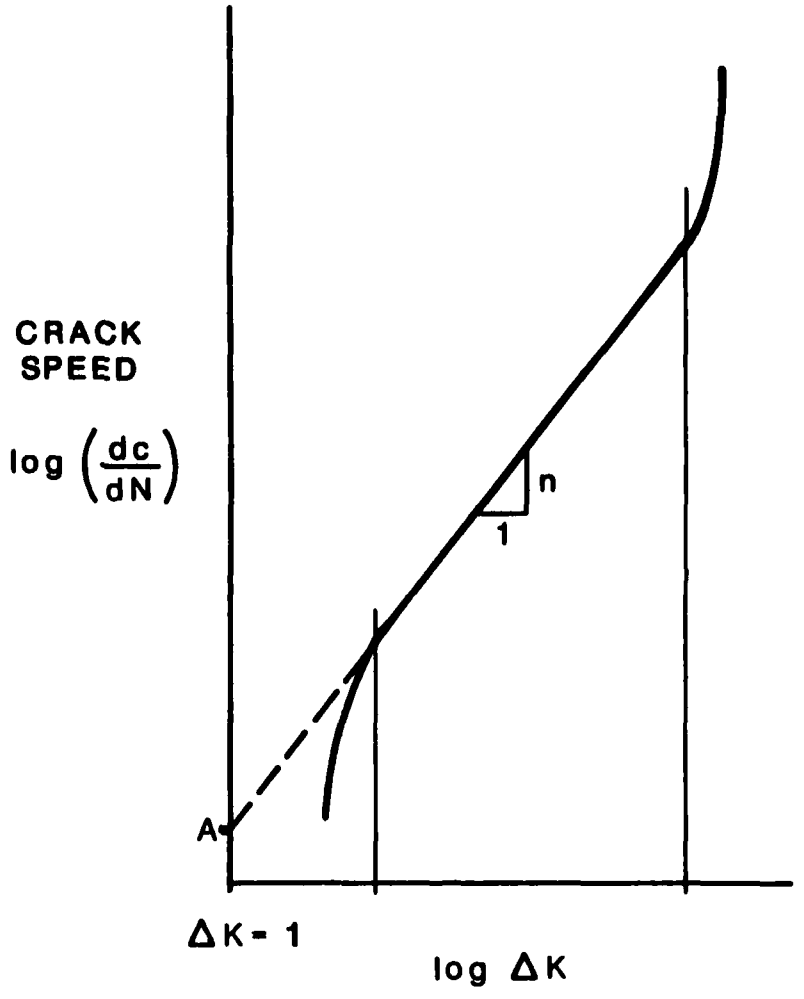

Figure 17. Typical Graph of Crack Speed Versus Change of Stress Intensity Factor.

TABLE 8. Results of Fracture Tests.

Material	Sample No.	Temp. °F (°C)	Crack Opening, in.	Load Cycle Time, sec.	No. of Cycles to Failure	Fracture Properties A	n
AC-10	T1C	34 (1°)	0.02	20	4	0.160×10^{1}	-0.075
(4.73%	T4C	34 (1°)	0.02	20	30	0.363×10^{-3}	0.875
Binder)	T2C	77 (25°)	0.07	10	9	0.292×10^{-4}	1.61
	T3C	77 (25°)	0.05	10	142	0.300×10^{-10}	3.34
ARC-Low	T1L	34 (1°)	0.02	20	400	0.123×10^{4}	-1.47
(4.23%	T3L	34 (1°)	0.02	20	834	0.281×10^{6}	-2.12
Binder)	T4L	77 (25°)	0.05	10	50	0.681×10^{-9}	3.16
	T2L	77 (25°)	0.05	10	7	0.312×10^{-4}	1.56
ARC-Medium	T2M	34 (1°)	0.02	20	1253	0.756×10^{-8}	2.34
(4.73%	T4M	34 (1°)	0.01	20	1084	0.367×10^{3}	-1.26
Binder)	T3M	77 (25°)	0.07	10	4	0.595×10^{-2}	0.836
	T1M	77 (25°)	0.06	10	2	0.677×10^{0}	0.079
ARC-High	T2H	34 (1°)	0.02	20	241	0.977×10^{-8}	1.22
(5.23%	T4H	34 (1°)	0.02	20	470	0.304×10^{6}	-2.11
Binder)	T5H	77 (25°)	0.05	10	410	0.178×10^{-18}	6.67

depend upon the tensile creep compliance of the material in a simple way, it is expected that they are related to each other. This expectation is borne out in fact and illustrated in Figure 18 which is a graph of log10 A versus n.

The most apparent feature of the graph in Figure 18 is that all of the lines are roughly parallel with each other. In fact, the slopes are not equal between materials but are virtually identical for the same material measured at high and low temperatures. The slope of each line is given in Table 9.

It has been found empirically that the sum of n and $\log_{10}$ A, which is called the "Crack Speed Index", is a good indicator of the relative effectiveness of the material in retarding cracking. The lower the Crack Speed Index, the better is the material in reducing cracking. The last column in Table 9 gives average values of the Crack Speed Index.

On the basis of the Crack Speed Index the ranking of the four materials for fracture resistance at low temperatures ($34^{o}F$) from the best to the worst is:

1. ARC-Medium
2. ARC-High
3. AC-10
4. ARC-Low

Because the fourth sample of the high binder content asphalt-rubber concrete proved to be defective, not all of the materials can be ranked for fracture resistance at moderate temperatures ($77^{o}F$). However, of the three that can the ranked, their order, from the best to the worst is:

1. AC-10
2. ARC-Low
3. ARC-Medium

These results indicate that, with respect to fracture resistance, the asphalt-rubber concrete with medium (optimum) binder content performs best at low temperatures ($34^{o}F$) whereas the asphalt concrete performs best at moderate temperatures ($77^{o}F$).

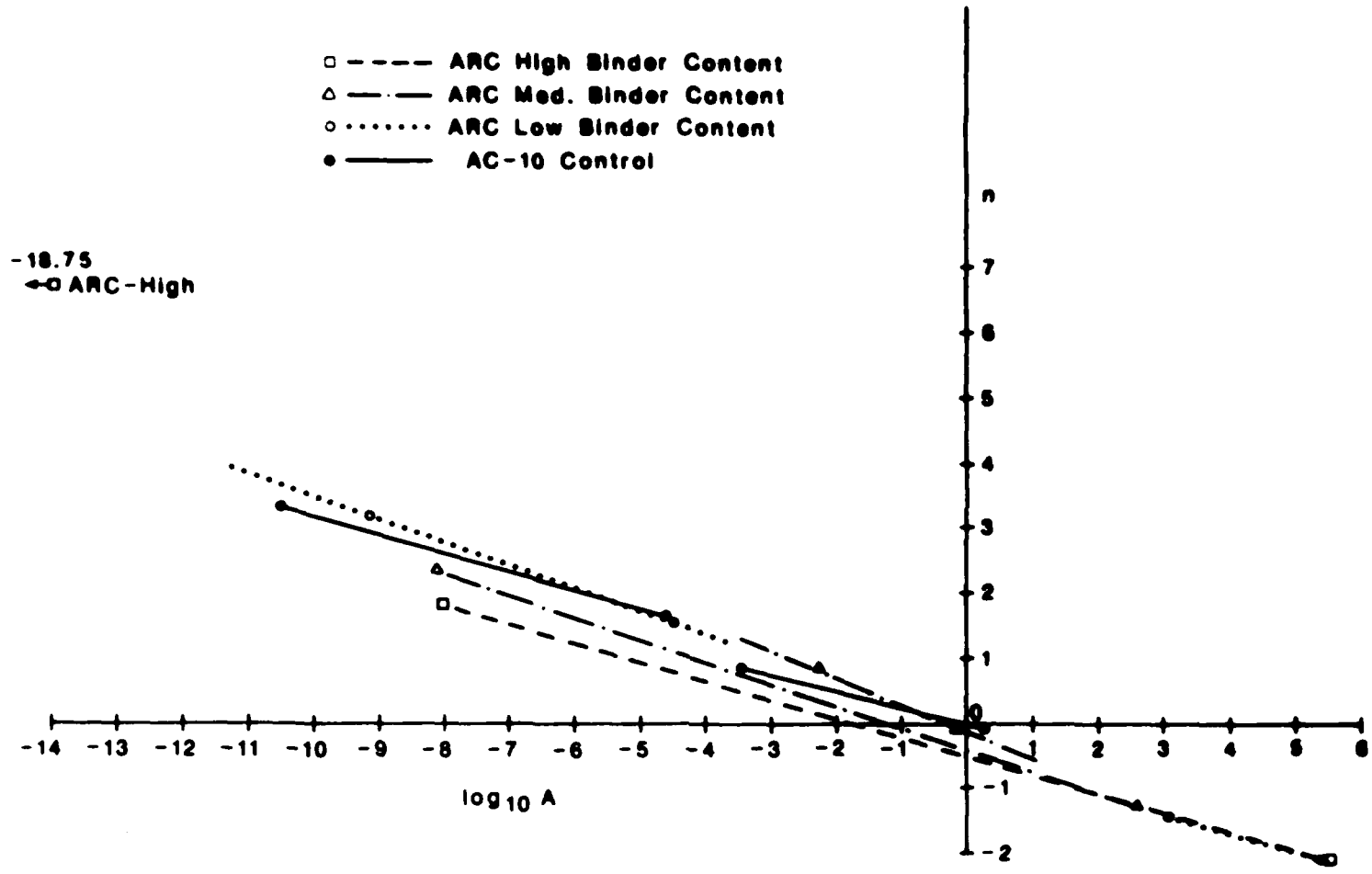

Figure 18. Graph of Log_{10} A Versus n.

TABLE 9. Slopes of the $\log_{10}$ A versus n Graph.

Material	Temperature ^{o}F (^{o}C)	Slope	Crack Speed Index
AC-10	34 (1^{o})	0.261	-1.223
	77 (25^{o})	0.289	-5.054
ARC-Low	34 (1^{o})	0.276	2.474
	77 (25^{o})	0.283	-4.476
ARC-Medium	34 (1^{o})	0.337	-2.288
	77 (25^{o})	0.368	-0.740
ARC-High	34 (1^{o})	0.291	-1.408
	77 (25^{o})	---	---

Creep Testing and Creep Compliances

The creep of asphaltic concrete and asphalt-rubber concrete is not only an important material property in itself, it is also related to and is an indicator of several important properties of these materials including their permanent deformation, temperature susceptibility, and fracture properties. Because a creep test is simple and quick to run at a variety of temperatures, it is useful to run a series of these tests to assist in interpreting the expected performance of pavements built with these materials.

The creep test is made in a temperature chamber on a cylindrical sample that is 4 inches (10.8 cm) in diameter and 8 inches (21.6 cm) high. Collars are clipped around the sample to support two LVDT's which measure the displacement of the middle half of the sample. A schematic and a photograph of a creep sample mounted in the testing equipment are shown in Figure 19.

A stress that is less than half of the expected failure stress of the sample is applied to the top surface of the sample and is held constant for 1000 seconds while the two LVDT's measure the displacement on opposite sides of the sample. The displacement is divided by the distance between the two LVDT collars to give a strain which is recorded at several times during the length of the test. The strain, $\varepsilon(t)$, is divided by the constant applied stress, σ_o, to give the creep compliance, $D(t)$. The results of the creep tests which were made on the four materials are given in Table 10. A plot of some of the typical results is shown on a semi-logarithmic graph in Figure 20.

Averages of the compliances measured at each temperature were fit with a curve of the form

$$D(t) = D_1 \, t^m \qquad (5)$$

with the resulting constants as shown in Table 11. It is apparent from this table that as the temperature increases, the values of D_1 increase and the values of m decrease.

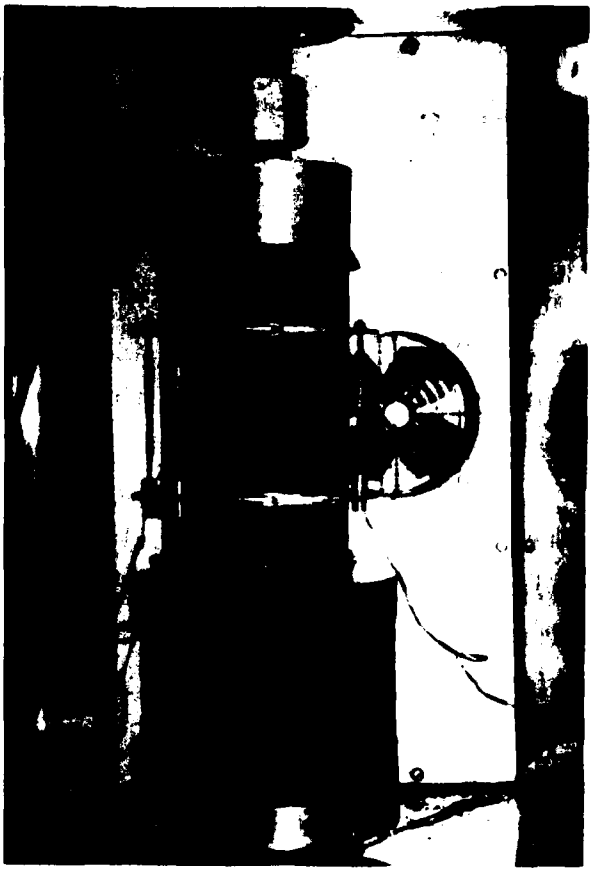

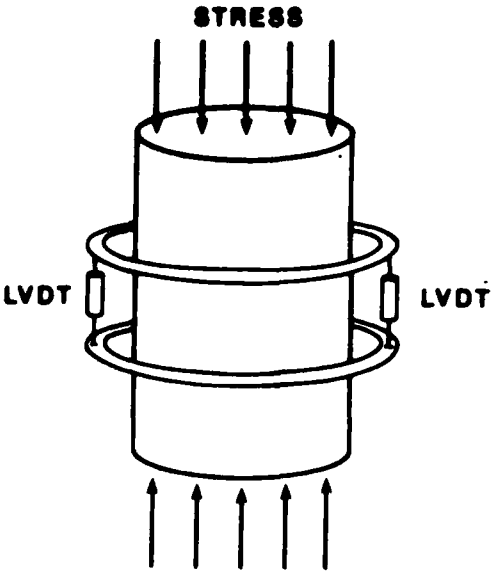

Figure 19. Creep Test Sample with LVDT Measuring Collar and Test Equipment.

TABLE 10. Creep Compliance of Asphalt-Rubber and Asphaltic Concrete Materials.

Mat'l	Sample	Temp. (°F)	Time After Loading (sec) 1.00E-01	1.00E+00	1.00E+01	1.00E+02	1.00E+03
AC10Cont	AC10-3	40	6.88E-07	1.47E-07*	3.44E-06	7.47E-06	1.59E-05
	AC10-5	40	7.50E-07	1.84E-06	3.47E-06	8.59E-06	1.89E-05
	AC10-10	40	5.47E-07	9.84E-07	1.95E-06	4.84E-06	----
	AC10-7	70	3.67E-06	1.02E-05	1.89E-05	2.69E-05	4.04E-05
	AC10-2	70	1.09E-06*	1.13E-05	2.23E-05	2.92E-05	3.90E-05
	AC10-8	70	2.89E-06	8.28E-06	1.53E-05	2.23E-05	3.38E-05
	AC10-1	100	1.46E-05	2.90E-05	3.44E-05	3.96E-05	4.62E-05
	AC10-4	100	1.04E-05	2.27E-05	2.55E-05	2.84E-05	3.44E-05
	AC10-6	100	8.13E-06	1.88E-05	2.56E-05	2.88E-05	3.98E-05
AR-Low	AR1L	40	1.44E-06	2.66E-06	6.50E-06	1.16E-05	1.87E-05
	AR3L	40	8.44E-07	1.78E-06	3.66E-06	6.88E-06	1.33E-05
	AR7L	40	1.88E-07	2.81E-07	6.88E-07	1.45E-06	2.23E-06
	AR2L	70	3.13E-06	8.36E-06	1.56E-05	2.23E-05	2.81E-05
	AR4L	70	3.13E-06	7.81E-06	1.41E-05	2.13E-05	3.01E-05
	AR8L	70	3.13E-06	8.59E-06	1.62E-05	2.58E-05	3.92E-05
	AR5L	100	8.54E-06	1.70E-05	2.38E-05	2.75E-05	3.09E-05
	AR6L	100	7.92E-06	1.49E-05	2.10E-05	2.71E-05	3.37E-05
	AR9L	100	3.44E-06	1.58E-05	2.38E-05	3.15E-05	4.22E-05
AR-Med.	AR2M	40	5.31E-07	1.31E-06	2.98E-06	5.56E-06	8.98E-06
	AR4M	40	9.06E-07	2.06E-06	4.50E-06	7.75E-06	----
	AR6M	40	1.00E-06	2.06E-06	4.00E-06	7.72E-06	1.34E-05
	AR5M	70	5.86E-06	1.65E-05	2.68E-05	3.56E-05	5.08E-05
	AR9M	70	3.13E-06	8.59E-06	1.51E-05	2.25E-05	3.45E-05
	AR1M	70	4.58E-06	1.04E-05	1.47E-05	1.77E-05	2.25E-05
	AR3M	100	1.04E-05	2.07E-05	2.88E-05	3.65E-05	4.81E-05
	AR10M	100	4.69E-06	1.04E-05	1.47E-05	1.78E-05	2.26E-05
	AR8M	100	1.03E-05	2.22E-05	3.27E-05	4.24E-05	5.64E-05
AR-High	AR1H	40	7.19E-07	1.53E-06	3.42E-06	6.92E-06	1.43E-05
	AR5H	40	6.41E-07	1.44E-06	3.16E-06	6.03E-06	9.84E-06
	AR8H	40	4.38E-07	1.20E-06	2.89E-06	6.17E-06	1.22E-05
	AR3H	70	3.20E-06	8.75E-06	1.69E-05	2.51E-05	3.89E-05
	AR6H	70	4.30E-06	1.05E-05	1.93E-05	3.10E-05	5.00E-05
	AR7H	70	3.05E-06	7.97E-06	1.34E-05	1.76E-05	2.34E-05
	AR2H	100	4.17E-06	9.38E-06	1.31E-05	1.46E-05	2.29E-05
	AR4H	100	9.06E-06	1.77E-05	2.48E-05	3.08E-05	4.00E-05
	AR9H	100	6.15E-06	1.10E-05	1.50E-05	1.69E-05	1.94E-05

*Questionable measurement

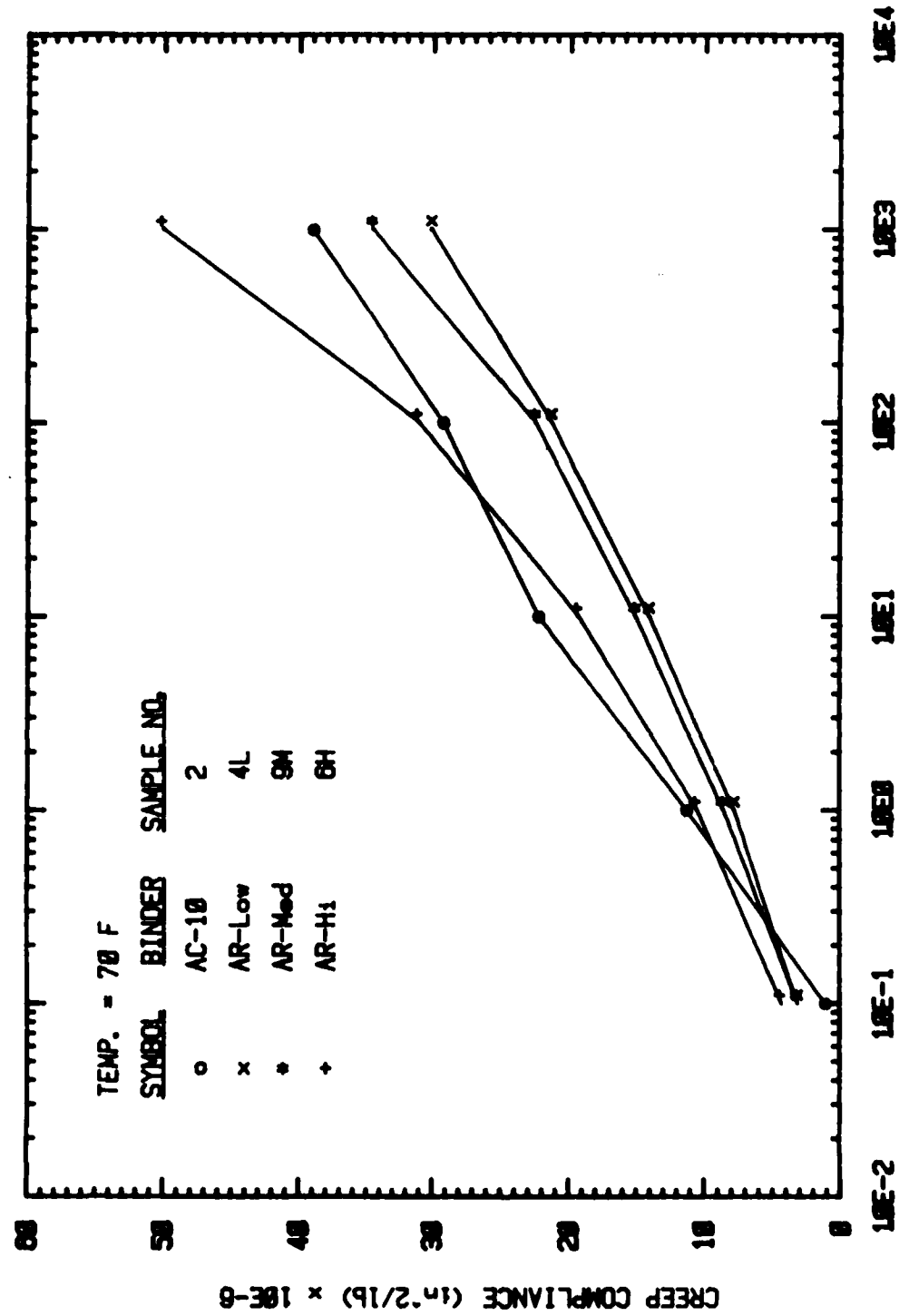

Figure 20. Typical Plot of Creep Compliance Versus Time.

TABLE 11. Creep Compliance Properties of Asphalt-Rubber Concrete and Asphalt Concrete Materials.

Material	Temperature ^{o}F (^{o}C)	D_1	m
AC10 Control	40 (4.4)	1.38×10^{-6}	0.354
	70 (21.1)	7.91×10^{-6}	0.254
	100 (37.8)	1.83×10^{-5}	0.128
AR-Low	40 (4.4)	1.19×10^{-6}	0.290
	70 (21.1)	7.01×10^{-6}	0.247
	100 (37.8)	1.24×10^{-5}	0.177
AR-Medium	40 (4.4)	1.70×10^{-6}	0.289
	70 (21.1)	9.20×10^{-6}	0.211
	100 (37.8)	1.42×10^{-5}	0.164
AR-High	40 (4.4)	1.35×10^{-6}	0.328
	70 (21.1)	7.65×10^{-6}	0.245
	100 (37.8)	1.04×10^{-5}	0.146

The degree to which these values shift with temperature is an indicator of the temperature susceptibility of each material. In order to compare these properties numerically, a time-temperature shift property of each material was determined. The average creep compliance curves for each temperature were shifted horizontally parallel to the time-axis until each lined up with the curve for $70^{o}F$ ($21.1^{o}C$), which was designated as the "master" creep curve. The amount of the shift in time with changing temperature is expressed as a ratio, a_T, which is itself, a function of temperature. The ratio, a_T, is

$$a_T = \frac{t}{t_{To}} \tag{6}$$

where: t_{To} = the time at which a given compliance is reached when the material is at the "master" temperature, T_o. In this case the master temperature is $70^{o}F$ ($21.1^{o}C$).

t = the time at which the same compliance is reached when the material is at some other temperature.

It is more desirable for the value of a_T to change by a small amount over any temperature range. Values of the a_T function for each of the materials are shown in Figure 21, and this indicates that there is some variation of a_T between the four materials.

Two commonly-used functions were fit to the curves in Figure 21 to produce numerical comparisons of the temperature susceptibility of the four materials. The first of these is commonly used in the VESYS-analysis method developed by the Federal Highway Administration (Ref 6). The function is

$$\log a_T = -\beta(T-To) \tag{7}$$

where β = the temperature susceptibility constant

To = the master curve temperature

T = any other temperature

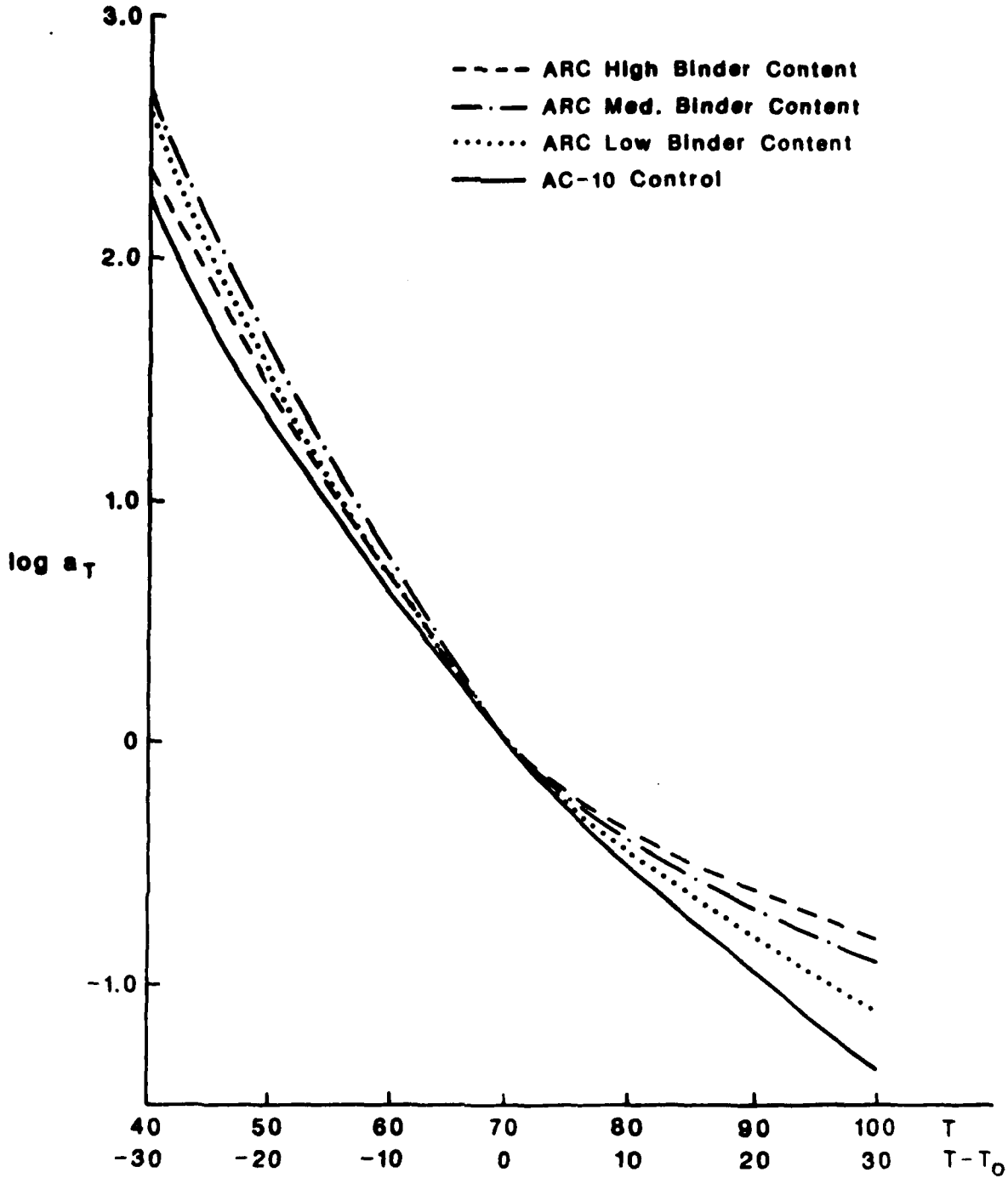

Figure 21. Time-Temperature Shift Function a_T as a Function of Temperature.

The second function is one that is commonly used to describe the time-temperature shift of viscosity in polymers. It is known as the "WLF" equations after its originators, Williams, Landel, and Ferry (Ref 23). The equation is

$$\log a_T = - \frac{C_1(T-To)}{(C_2+T-To)} \qquad (8)$$

in which C_1, C_2 = the material constants. Of the two, the constant C_1 serves as a temperature susceptibility constant.

The values of the temperature shift constants, β, C_1, and C_2 are given in Table 12.

On the basis of the WLF Equation, the materials in this study are ranked in order of ascending temperature susceptibility:

1. Asphalt-rubber concrete, high binder content
2. Asphalt-rubber concrete, medium binder content
3. Asphalt-rubber concrete, low binder content
4. Asphaltic concrete, control

It appears that the addition of rubber helps the material to maintain a more stable compliance (or modulus) during temperature changes. This result agrees reasonably well with the results from the resilient modulus testing described earlier.

Although permanent deformation is not measured directly by the creep test, it is commonly considered that at least a part of the permanent deformation in pavements is due to non-recoverable, time-dependent creep. The other part of permanent deformation is due to plastic deformation when the material follows a different stress-strain curve on loading and unloading.

It is common to estimate the non-recoverable time-dependent creep by subtracting the ordinates of the creep recovery curve after the load has been removed from the ordinates of the creep curve under load. Although the creep reovery curve was not observed in these tests, it usually has the same general shape as the creep curve, and thus the difference between the two has roughly the same shape.

TABLE 12. Time-Temperature Shift Constants.

Material	Temperature °F (°C)	$\log_{10} a_T$	Time-Temperature Shift Constants		
			β	C_1	C_2
AC-10	40 (4.4)	2.25	0.060	6.75	120
(Control)	70 (21.1)	0.0			
	100 (37.8)	-1.35			
AR-Low	40 (4.4)	2.65	0.0625	3.76	72.6
	70 (21.1)	0.0			
	100 (37.8)	-1.10			
AR-Medium	40 (4.4)	2.70	0.060	2.70	60.0
	70 (21.1)	0.0			
	100 (37.8)	-0.90			
AR-High	40 (4.4)	2.40	0.053	2.40	60.0
	70 (21.1)	0.0			
	100 (37.8)	-0.80			

If the non-recoverable strain were equal to the creep curve alone, which it is not, it would be possible to account for that part of the permanent deformation that is due to non-recoverable, time dependent creep by using the creep curve alone. Then, the equation for the time-dependent portion of permanent strain after N repetitions of load pulses would be:

$$\varepsilon(t) = \sigma_o \, D_1 \, (N \, \Delta t)^m \tag{9}$$

The percentage of the resilient strain, ε_r, which is accumulated with each stress pulse is F(N) as given by:

$$F(N) = \left[\frac{\sigma_o D_1 m (\Delta t)^m}{\varepsilon_r}\right]\left(N^{-(1-m)}\right) \tag{10}$$

where:
- σ_o = the stress applied to the sample
- D_1 = the compliance coefficient
- m = the compliance exponent
- ε_r = the resilient strain
- Δt = the time duration of the stress pulse
- N = the total number of load pulses
- F(N) = the percentage of the resilient strain that remains as permanent accumulated strain.

The cluster of terms, $\sigma_o \, D_1 \, m \, (\Delta t)^m / \varepsilon_r$, corresponds to the permanent strain coefficient, GNU, which is explained in the next section of this chapter, and the term (1-m) corresponds to ALPHA, the permanent strain exponent. This exponent has the property that the closer it is to 1.0, the more the material behaves elastically and the closer it is to 0.0, the more the material behaves plastically. On this basis, at 70^oF (21.1^oC), the four materials are ranked in order of increasing plastic behavior, as judged from the m-exponent:

1. Asphalt-rubber concrete, medium binder content
2. Asphalt-rubber concrete, high binder content
3. Asphalt-rubber concrete, low binder content
4. Asphalt concrete, control

This result indicates that the asphalt concrete control material would experience the most time-dependent permanent deformation of the four materials.

The fracture of asphaltic concrete obeys a law of fracture mechanics known as Paris' Law (Ref 21). Although it was originally considered an empirical relation, it has subsequently been derived from first principles of mechanics by Schapery (Ref 22). Paris' Law is stated as follows:

$$\frac{dc}{dn} = A(\Delta K)^n \tag{11}$$

where dc/dn = the rate of growth of a crack with each load cycle, N

ΔK = the change of stress intensity factor, a calculated quantity, with each stress pulse

A,n = the fracture coefficient and exponent which are determined by experiment.

Schapery's derivations showed that the two material properties A and n are, in fact, determined by simpler material properties including the creep compliance and tensile strength (Ref 22). He found that the fracture exponent, n, can be determined simply as

$$n = \frac{2}{m_t} \tag{12}$$

where m_t = the slope of the tensile log-log plot of creep compliance versus time.

The creep compliance tests that are reported here were compressive, not tensile, but their relative size will indicate the way that the fracture exponent varies with binder and with temperature. Table 13

TABLE 13. Calculated Fracture Exponents.

Material	Temperature °F (°C)	Compressive Compliance Slope, mc	Compressive Fracture Exponent $n_c = \frac{2}{mc}$	Volumetric Concentration of Binder C_b	Estimated Tensile Fracture Exponent n_t
AC-10 Control	40 (4.4)	0.354	5.65		0.667
(4.73% Binder)	70 (21.1)	0.254	7.87	0.118	0.929
	100 (37.8)	0.128	15.63		1.844
AR-Low	40 (4.4)	0.290	6.90		0.738
(4.23% Binder)	70 (21.1)	0.247	8.10	0.107	0.867
	100 (37.8)	0.177	11.30		1.209
AR-Medium	40 (4.4)	0.289	6.92		0.817
(4.73% Binder)	70 (21.1)	0.211	9.48	0.118	1.119
	100 (37.8)	0.164	12.20		1.440
AR-High	40 (4.4)	0.328	6.10		0.787
(5.23% Binder)	70 (21.1)	0.245	8.16	0.129	1.053
	100 (37.8)	0.146	13.70		1.767

shows the slope of the compressive creep compliance curve and the fracture exponent derived from it. The fracture exponents are larger than those that were measured at 34°F (1.1°C) and 77°F (25°C) with the overlay tester indicating, correctly, that the compliance of the asphalt-rubber concrete and asphaltic concrete in tension is greater than it is in compression. Typically, the value of tensile m_t is between 0.5 and 1.0, which gives tensile fracture exponents between 1.0 and 2.0.

If the compressive fracture exponent is multiplied by the volumetric concentration of binder, as is suggested by the rule of mixtures, the resulting tensile fracture exponents are shown in the last column of Table 13. These estimated tensile fracture exponents are in the expected range.

The compressive creep test is a simple, quick and valuable test to give not only the creep compliance of a material but also indications of its temperature susceptibility, permanent deformation properties, and fracture exponent.

Repeated Load Testing and Permanent Deformation Parameters

Permanent deformation parameters were used to characterize the materials for rutting susceptibility. Typically, the results of creep or permanent deformation testing are used to plot strain versus number of loading cycles, as shown in Figure 22, and the resulting curve can then be used to predict the rutting life of a pavement. In this study, repeated load tests were performed and an equation with three material parameters was used to describe the accumulated strain versus loading cycles curve. This permanent deformation characterization method was one of the reasons for choosing the modified ILLIPAVE program for analysis instead of the VESYS program initially chosen for use. Typical repeated load test results are plotted in Figure 23, which shows total and accumulated strain.

The VESYS pavement structural analysis program (Ref 6) uses two terms, ALPHA and GNU, to characterize permanent deformation. ALPHA and GNU are calculated from the intercept and the slope of the straight line relationship between the logarithm of the permanent strain and the

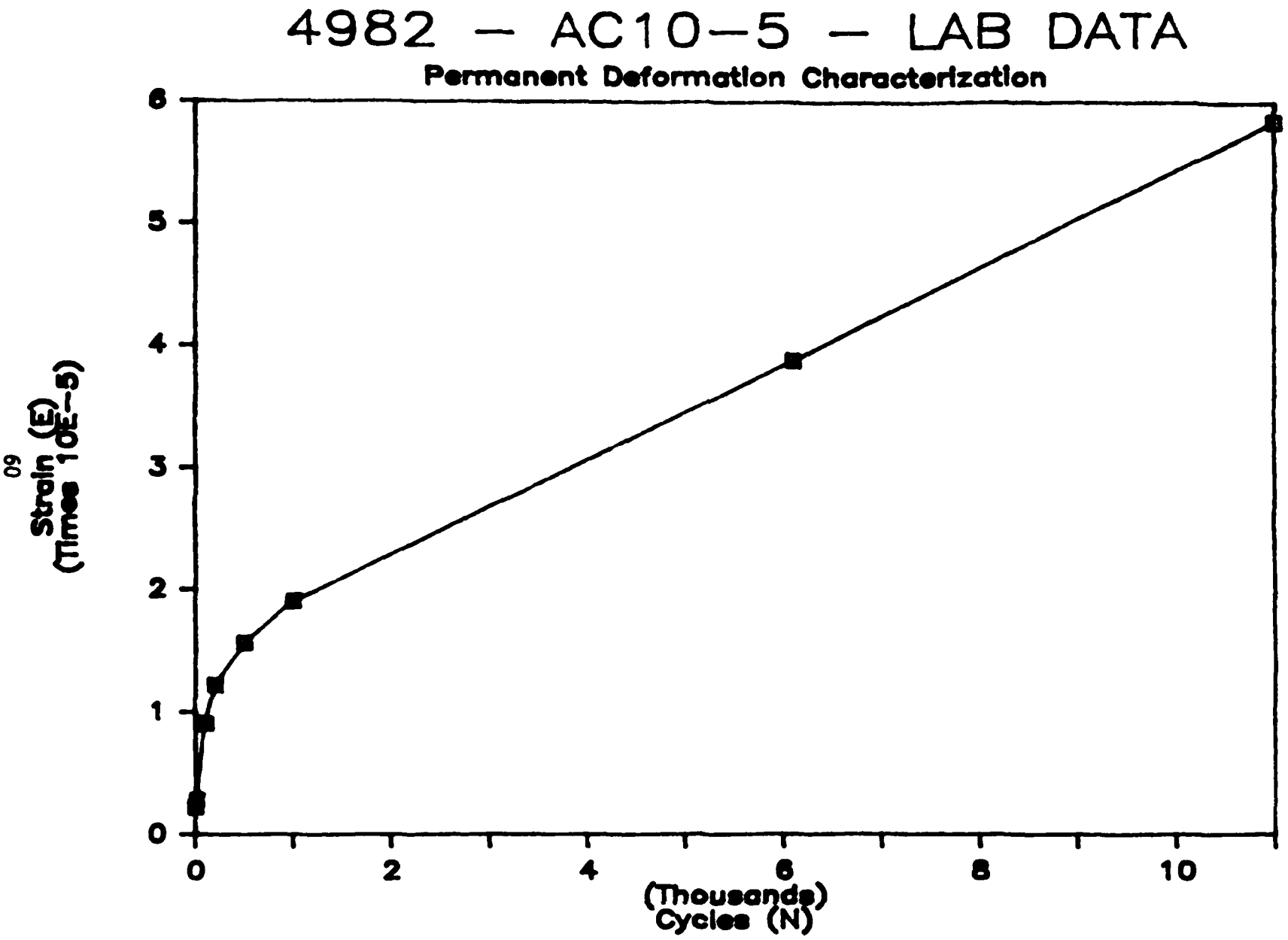

Figure 22. Typical Plot of Strain Versus Number of Loading Cycles.

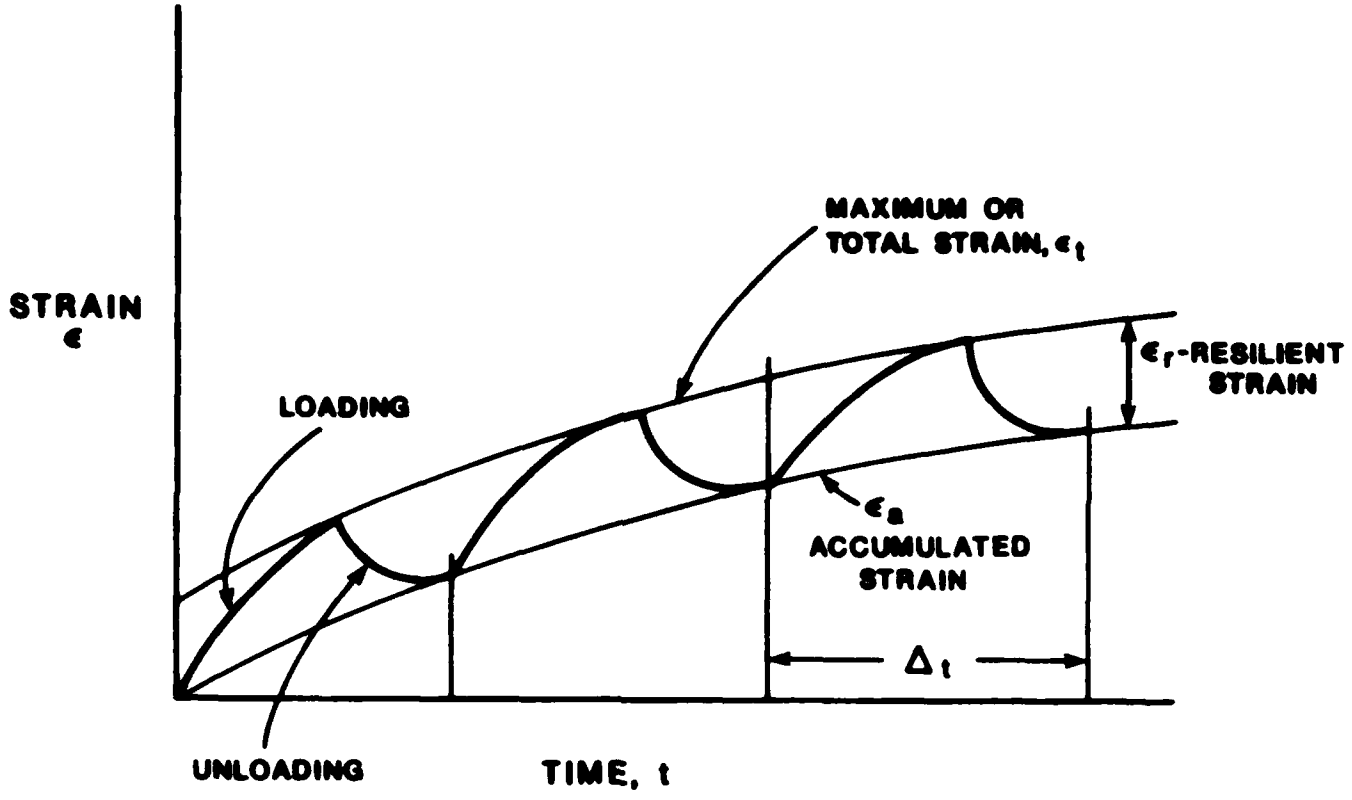

Figure 23. Typical Repeated Load Test Results Showing Total and Accumulated Strains.

logarithm of the number of load applications (Ref 14). They are defined as follows:

$$GNU = I^*S/\varepsilon_r \tag{13}$$

and

$$ALPHA = I-S \tag{14}$$

where I = the arithmetic value of the intercept (not a logarithm)

S = the slope of the linear portion of the logarithmic relationship

ε_r = resilient strain.

However, it has been shown (Ref 8,9,24) that a three-parameter, nonlinear equation more accurately describes the material behavior of asphalt composites due to permanent deformation. The three parameters are developed from the following equation, which is used to describe the same permanent strain versus loading cycles curve:

$$\varepsilon_a = \varepsilon_0 e^{-(\rho/N)^{\beta}} \tag{15}$$

where ε_a = permanent (accumulated) strain

N = loading cycle

ε_0, ρ, and β are calculated parameters

This equation describes an S-shaped curve with the strain at a high number of cycles approaching some horizontal asymptote. The change in direction of the S-shape occurs at $N = \rho$, or where $\varepsilon_a = \varepsilon_0 * e^{-1} = .368\varepsilon_0$. Using this equation, the relationship between strain and cycles never becomes linear and therefore more accurately represents the material behavior.

The procedures for calculating the three parameters, as well as the method of using these parameters for calculating rut depths in the modified ILLIPAVE computer program, are described elsewhere (Ref 8).

In this study, repeated load compression tests were performed to 10,000 or more cycles on cylinders following the VESYS procedures for

direct compression testing (Ref 6). One test was performed for each material at every test temperature (40°F, 70°F and 100°F; or 4.4°C, 21.1°C, 37.8°C). A plot of permanent strain versus cycles was made for each sample tested to determine the shape of the curve and whether the three parameter equation could be used to describe the material behavior (see Appendix C).

Resilient strain was read from the dynamic test output at 200 cycles and the three permanent deformation parameters were calculated. Two methods were used to calculate the three parameters: a linear regression program written at Texas A&M University, and a nonlinear regression program which is part of the S.A.S. statistical analysis package. The linear regression program is based on a method which takes the logarithm of both sides of the S-shaped curve equation and then reduces the result to the linear form $y = mx + b$, where m is the slope of the line and b is the y-intercept. A least squares regression is then applied to the test data and a linear best fit is calculated. Alternatively, the S.A.S. nonlinear regression program uses an iterative process in which an initial guess of each parameter must be input. At least one of these methods produced a good fit for every test, but rarely did both methods produce a good fit for the same test results. Table 14 gives a summary of the calculated permanent deformation parameters and the method of calculation used for each test sample.

The permanent deformation parameters were sensitive to several factors, including stress level and temperature. The laboratory testing had to be performed with an applied load which was much lower than that which would be expected in the field conditions. This was because an axial load was applied to a cyclindrical specimen with a small diameter (4 inches) which had no confining pressure applied, and the specimen failed at much lower stresses than in the field where every element of material is supported by the lateral pressure of surrounding elements. Therefore some adjustment had to be made to the permanent deformation parameters to account for the differences in applied versus field stresses. First, typical field stresses were calculated for each horizontal element (seven elements were defined in the top pavement layer

TABLE 14. Permanent Deformation Parameters from Lab Tests.

Material	T(°F)	Sample	ε_0	RHO	BETA	$\varepsilon_0/\varepsilon_r$	Regression Method
AC-10	40	AC10-5	0.0187E+0	1.1539E16	0.0637	1,662	Nonlinear
	70	AC10-7	0.8232E-3	0.9817E04	0.2070	27.44	Linear
	100	AC10-1	0.9355E+0	6.3750E16	0.0591	31,509	Nonlinear
ARC-Low	40	AR-3L	0.0326E+0	3.4221E16	0.0651	2,219	Nonlinear
	70	AR-4L	0.4379E+0	2.5438E16	0.0670	13,738	Nonlinear
	100	AR-5L	1.1542E-2	0.1917E05	0.1292	94.89	Linear
ARC-Med.	40	AR-4M	0.0181E+0	3.4514E16	0.0645	1,445	Nonlinear
	70	AR-9M	0.0238E+0	2.8904E16	0.0524	544	Nonlinear
	100	AR-8M	0.0588E+0	2.5023E16	0.0560	1,680	Nonlinear
ARC-High	40	AR-5H	0.0357E+0	1.2988E15	0.0709	4,967	Nonlinear
	70	AR-6H	0.7124E-2	0.4716E11	0.0738	165	Linear
	100	AR-9H	0.4829E-3	0.5229E03	0.1528	14.72	Linear

for the finite element mesh used in the modified ILLIPAVE program). These typical stresses were calculated using the modified ILLIPAVE program with typical parameters for asphalt concrete as input values. The typical parameters were derived from other studies and compiled at Texas A&M University and are presented in Ref 9. The calculated typical stresses are tabulated in Tables 15. Using the typical stresses and some regression equations generated from the compiled data base, a ratio of (permanent deformation parameter) at the level of stress expected in the field for a typical asphalt material to the same (permanent deformation parameter) at the level of stress applied in the laboratory for the same typical asphalt material was calculated for every combination of the seven elements of the top pavement layer, each of five aircraft in the traffic distribution, and each of three test temperatures. The following assumption was made:

$$\frac{\text{(permanent deformation parameter)}_{\text{field stress, typical asphalt material}}}{\text{(permanent deformation parameter)}_{\text{lab stress, typical asphalt material}}}$$

$$\frac{\text{(permanent deformation parameter)}_{\text{field stress, test material}}}{\text{(permanent deformation parameter)}_{\text{lab stress, test material}}}$$

The calculated ratio for a typical asphalt material was then multiplied by the permanent deformation parameter calculated from the laboratory test results on a test material to obtain an adjusted (field) value for the permanent deformation parameter for the test material at that temperature, for that aircraft, and in that element of the top pavement layer.

The adjusted values of the permanent deformation parameters were then plotted versus temperature so that the relationship with changing temperature could be determined. The adjusted values of the parameters for all material, aircraft, and temperature combinations are contained in Appendix D along with samples of the plots. For input to the modified ILLIPAVE program, a value for each permanent deformation parameter was read from the plots for each average seasonal temperature chosen. The program used these adjusted parameters to calculate rut depths at specified time increments.

TABLE 15. Stresses in Top Pavement Layer Used to Calculate Permanent Deformation Parameters for the Field Conditions (Aircraft Loads).

Aircraft	Temperature	Element	$Stress_{(Field)}$	$Stress_{(Lab)}$
DC-09	40	2	70.90	20
		3	86.90	20
		4	80.8	20
		5	78.18	20
		6	85.00	20
		7	104.89	20
	70	1	10.8	20
		2	69.60	20
		3	84.79	20
		4	76.90	20
		5	69.55	20
		6	69.80	20
		7	79.06	10
	100	1	69.30	10
		2	117.67	10
		3	113.47	10
		4	89.70	10
		5	70.99	10
		6	59.21	10
		7	51.58	10

TABLE 15. (Continued)

Aircraft	Temperature	Element	Stress(Field)	Stress(Lab)
DC-10	40	2	47.00	20
		3	94.25	20
		4	110.31	20
		5	121.86	20
		6	141.64	20
		7	179.49	20
	70	2	54.60	20
		3	93.63	20
		4	102.40	20
		5	104.67	20
		6	112.70	20
		7	132.04	20
	100	1	67.10	10
		2	124.75	10
		3	138.54	10
		4	123.45	10
		5	105.60	10
		6	92.30	10
		7	83.20	10

TABLE 15. (Continued)

Aircraft	Temperature	Element	Stress(Field)	Stress(Lab)
B-727	40	2	52.40	20
		3	88.07	20
		4	96.06	20
		5	102.04	20
		6	116.36	20
		7	146.30	20
	70	2	56.80	20
		3	86.85	20
		4	89.86	20
		5	88.61	20
		6	93.49	20
		7	108.47	20
	100	1	63.90	10
		2	116.20	10
		3	124.40	10
		4	107.30	10
		5	89.80	10
		6	77.40	10
		7	69.10	10

TABLE 15. (Continued)

Aircraft	Temperature	Element	Stress(Field)	Stress(Lab)
B-737	40	1	8.20	20
		2	61.80	20
		3	74.20	20
		4	70.80	20
		5	69.70	20
		6	76.40	20
		7	94.60	20
	70	1	17.80	20
		2	61.70	20
		3	72.60	20
		4	67.20	20
		5	61.70	20
		6	62.50	20
		7	71.10	20
	100	1	71.34	10
		2	103.60	10
		3	98.10	10
		4	78.80	10
		5	62.90	10
		6	52.80	10
		7	46.20	10

TABLE 15. (Continued)

Aircraft	Temperature	Element	Stress(Field)	Stress(Lab)
B-757	40	1	0.40	20
		2	76.70	20
		3	93.40	20
		4	86.40	20
		5	83.40	20
		6	90.60	20
		7	111.70	20
	70	1	12.30	20
		2	75.20	20
		3	91.10	20
		4	82.30	20
		5	74.20	20
		6	74.40	20
		7	84.22	20
	100	1	74.70	10
		2	126.70	10
		3	121.60	10
		4	96.00	10
		5	75.80	10
		6	63.20	10
		7	55.00	10

CHAPTER III. PERFORMANCE PREDICTION OF ASPHALT-RUBBER CONCRETE AND ASPHALT CONCRETE

In this chapter, the design data and the results of calculations with the modified ILLIPAVE program are presented. In the final section of this chapter a comparison is made of the predicted lives of a typical airport pavement using each of the four mixes under conditions of mixed traffic.

DESIGN DATA

The comparative analysis of this project was accomplished by selecting an airport type, pavement structure, and traffic pattern, and holding these constant. Four environmental zones were simulated by choosing four typical seasonal temperatures for each zone, and the environmental zones and the material in the surface layer were varied in multiple computer runs of the modified ILLIPAVE program.

Airport Type and Traffic

Asphaltic materials are most typically used as surface layer materials at a medium to small civil airport. Asphaltic materials creep under heavy loads of more than a very short duration, and thus are subject to moderate to severe rutting. Therefore, they are generally not considered as suitable materials for larger airports with heavier wheel loads, higher traffic counts and more likelihood of planes standing in line. The Robert Mueller Municipal Airport in Austin, Texas, was selected as an appropriate airport model for this study. This airport uses runways and taxiways made of asphalt concrete. Austin has experienced a tremendous growth in recent years and its airport has experienced the damage problems associated with rapid population and, therefore, traffic growth. The major runway was used as the structural [illegible] for the analyses in this study. Some significant distresses were

expected in the damage analyses, thus providing an actual scenario in which to compare the performance of the materials considered.

Total numbers and types of aircraft using the Austin Airport between 1969 and 1981 were known, and projections were available for the years 1985 and 1990 (Ref 25). Only the air carrier aircraft were considered, because the smaller aircraft (general aviation and air taxi/commuter aircraft) have widely varied taxi patterns. Also, the smaller aircraft individually cause little to no significant pavement damage compared with the larger and heavier air carrier traffic (Ref 25). Five air carriers were included in the traffic: DC-9, DC-10, B-727, B-737, B-757.

Since the major runway of the Austin municipal airport was used as the structural model, it was assumed that all of the traffic logged by the airport used the runway being considered. Therefore, no runway routing percentage factors were applied to the traffic counts. Table 16 gives a summary of the aircraft traffic data. However, not all aircraft follow exactly the same wheel paths. Much more lateral wander from the centerline of the path of travel is exhibited by aircraft over the width of a runway than is exhibited by trucks over the width of a highway. Thus, any one point in the airfield pavement does not experience the same stresses from every aircraft because the airplane gears pass by that point at different distances from the point. Because of this, "wander factors" must be applied to the numbers of aircraft to obtain an estimate of the number of coverages which pass over the area experiencing the maximum or critical strain. It was assumed that the lateral movement of each aircraft type over the width of the runway is normally distributed. Using this assumption and the basic aircraft characteristics, wander factors were computed by Rauhut, et al. (Ref 25), generally following the procedure outlined by Ho Sang (Ref 26). This procedure "was modified somewhat to account for the transverse profile of the critical pavement response parameters of asphalt concrete tensile strain and subgrade vertical compressive strain" (Ref 25, p.IV.5). The wander factors derived by Rauhut, et al. were used in this study and are listed in Table 17. The total traffic counts for each year and each aircraft were multiplied by the wander factors and then divided by 365 to obtain an

TABLE 16. Summary of Aircraft Traffic Data From the Aviation Department, City of Austin, Texas.

	Aircraft Type				
Year	DC-9	DC-10	B-727	B-737	B-757
1969	32,660				
1970	29,482				
1971	17,410		2,176	2,176	
1972	7,520		5,640	5,640	
1973	3,660		7,320	7,320	
1974	2,570		15,430	7,710	
1975	1,680		10,080	5,040	
1976	1,870		11,230	5,610	
1977	2,120		12,740	6,370	
1978	2,940		17,650	8,830	
1979	---		---	---	
1980	4,000		24,000	12,000	
1981	5,200		31,200	15,600	
1985	2,910	580	36,670	17,460	580
1990	3,100	3,100	37,200	15,500	3,100

TABLE 17. Summary of Aircraft Traffic Wander Factors for Each Aircraft Considered in the Pavement Evaluation.

Aircraft	Wander Factor*
B-727	0.77
B-737	0.57
B-757	0.61
DC-9	0.68
DC-10	0.72

*Wander Factor is simply the inverse of the Pass-to-Coverage Ratio

estimate of the maximum or critical number of passes per day for each aircraft. See Table 18 for a summary of the numbers of critical passes per day.

The stress analyses were performed considering only the main landing gear assembly. The nose gear was not considered in the analysis because it is lighter and smaller than the main landing gear, and it does not traverse the same section of pavement as does the heavier main gear assembly. Therefore, the main landing gear assembly was considered as the critical loading condition.

The five carrier aircraft used in the analysis involved a variety of main landing gear configurations, wheel loads and sizes, and tire pressures. The aircraft data used in this study are summarized in Appendix E.

Previous research has confirmed that the tire contact pressures that are experienced by a pavement can in reality be much higher than the "known" tire inflation pressure (Ref 8). This can have significant consequences for the amount of pavement damage caused by heavy vehicles and thus for the design life of a pavement. However, not much previous work has been done in quantifying the tire contact pressures resulting from different load, radius, and inflation pressure combinations. Also, the work which has been done to this point has looked at stationary vehicles (static loads) and not at moving vehicles (dynamic loads with both horizontal and vertical components). There are a great many difficulties in measuring loads due to moving vehicles. However, considering the importance of tire contact pressures versus tire inflation pressures, some estimate was needed for this study of the tire contact pressures of aircraft. Therefore, a known but static contact pressure distribution and the known tire inflation pressures and wheel loads of the five aircraft in this study were used to create an estimate of the tire contact pressure distribution for each of the five aircraft considered. The "known" pressure distribution was a previously calculated pressure distribution for a 32x8.8 Type VII aircraft tire. This was a nose gear tire used in WWII on the Boeing B-52 Stratofortress (Ref 27; see Figure 24). As a starting point, the tire inflation

TABLE 18. Summary of Aircraft Passes Per Day - [Total Yearly Traffic x Wander Factor/365 Days Per Year].

Year #	DC-09	DC-10	B-727	B-737	B-757	Total
1	61					61
2	55					55
3	32		5	3		40
4	14		12	9		35
5	7		15	11		33
6	5		33	12		50
7	3		21	8		32
8	4		24	9		37
9	4		27	10		41
10	6		37	14		57
11	7		44	16		67
12	8		51	19		78
13	10		66	24		100
17	5	1	77	27	1	111
20	6	6	78	24	5	119

AIRCRAFT TIRE CONTACT PRESSURE DISTRIBUTIONS

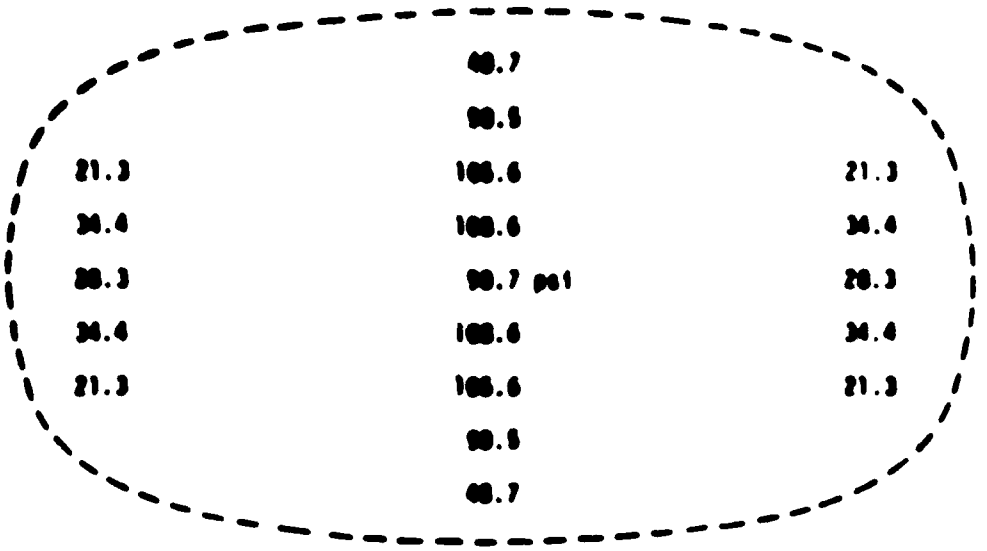

(a) δ = 0.75 in., Fz = 2000 lb

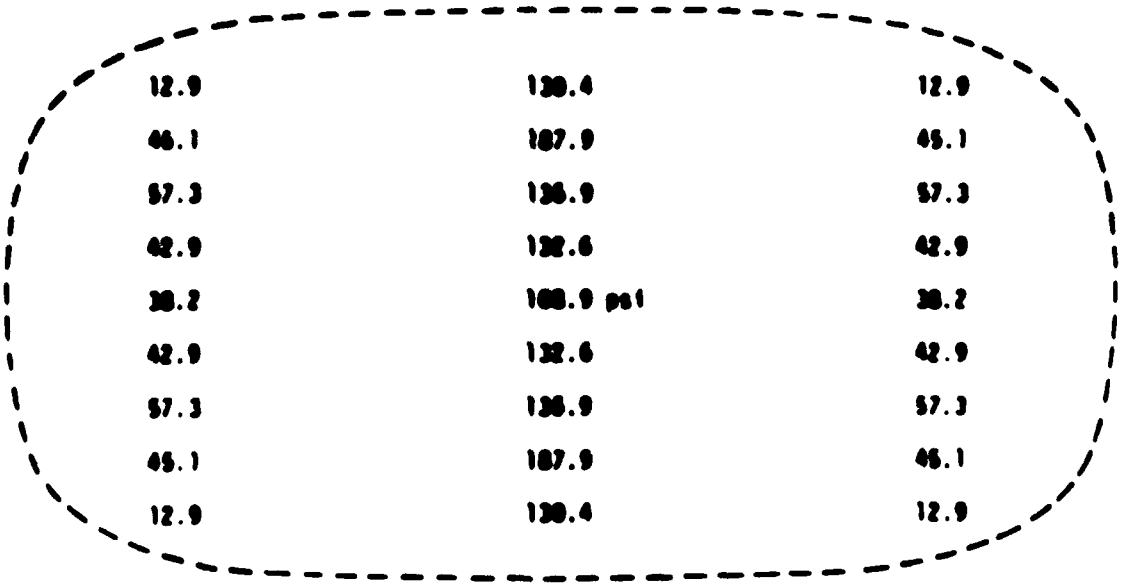

(b) δ = 1.00 in., Fz = 3700 lb

Note: Inflation Pressure: 95 psi (655 kPa).
Tire Type: 32x8.8 TYPE VII Aircraft Tire.
This tire type was used as the nose gear on the Boeing B52 (Stratofortress) in World War II. A high-pressure version is used on the nose gear of the U.S. space shuttle.

Figure 24. Calculated Contact Pressures (psi) for Two Different Tire Loads (Ref 27).

pressure of the aircraft being considered was set at the center of the tire. Then a pressure distribution was created having the same ratios between adjacent points on the tire as were calculated for the "known" model. Then a cylindrical volume of revolution was calculated and the result was compared with the known wheel load for that tire. The newly calculated pressure distribution was then adjusted up or down at the center, and the procedure was repeated, until the cylindrical volume of revolution was approximately equal to the wheel load. The resulting tire pressure distribution was used as input to the ILLIPAVE program. The calculated estimates of tire contact pressures for each of the five aircraft are shown in Appendix E.

Pavement Structure

The thicknesses and materials of the structural layers at the Austin municipal airport vary slightly over the length of the main runway. A typical pavement section was chosen and then was held constant for this analysis. Material properties were then estimated for the underlying structural layers, and laboratory characterizations were used for the top layer, which was variable depending upon the material being analyzed. Figure 25 shows the typical cross section of the runway pavement structure used in this analyis.

Environmental Effects and Seasonal Temperatures

Because asphaltic materials are temperature sensitive, the analysis was performed at different temperatures to determine temperature effects. Four environmental zones which represent typical areas of the U.S. were chosen: wet-freeze, wet-no freeze, dry-freeze, and dry-no freeze. Seasonal average temperatures were used whenever temperatures were needed as input values for the analysis. Table 19 gives a summary of the climatic zones and the seasonal temperatures that were used to represent them.

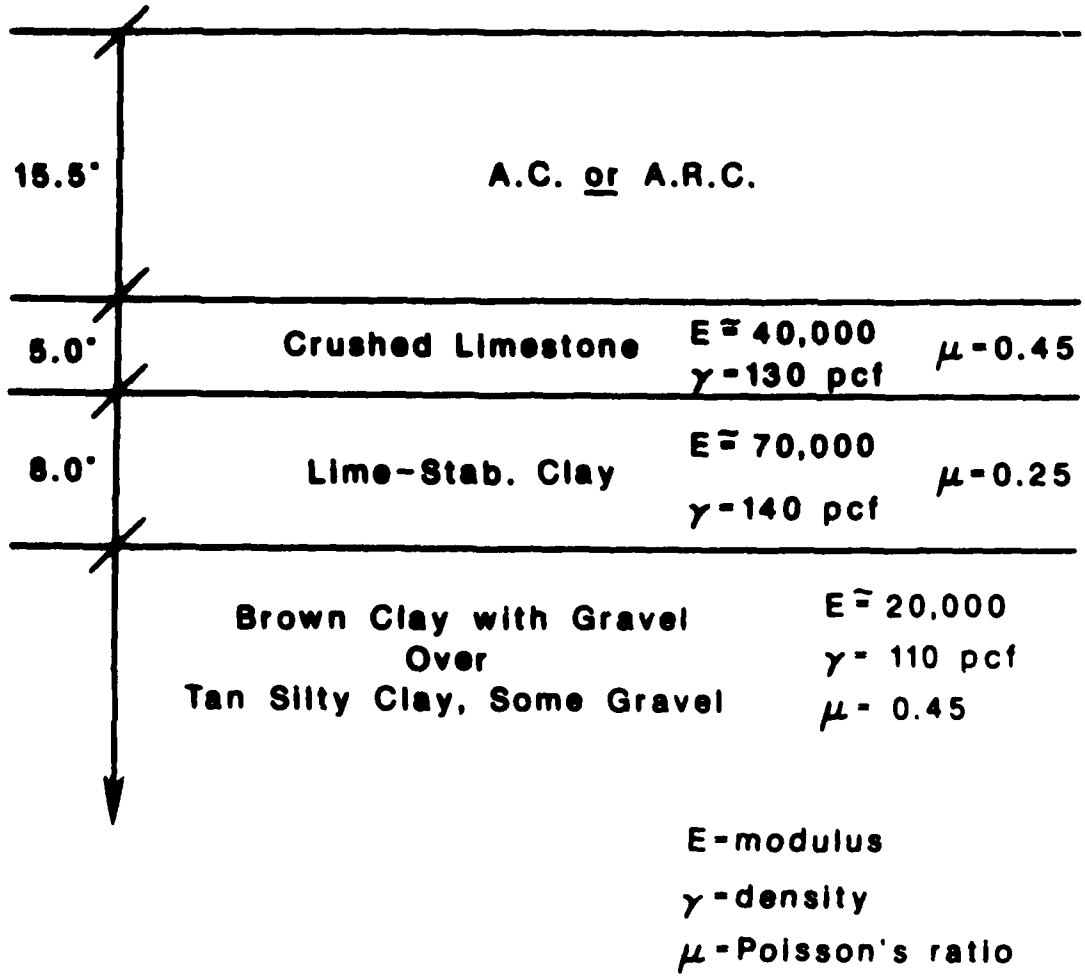

Figure 25. Schematic of the Pavement Structure Used in the ILLIPAVE Analysis.

TABLE 19. Average Seasonal Temperature for Each of Four Seasons for Each Climatic Zone.

Zone	Season	Temperature, °F (°C)
Wet-Freeze	Winter	35 (1.7)
	Spring	65 (18.3)
	Summer	95 (35.0)
	Fall	60 (15.6)
Wet-No Freeze	Winter	75 (23.9)
	Spring	95 (35.0)
	Summer	105 (40.6)
	Fall	95 (35.0)
Dry-Freeze	Winter	35 (1.7)
	Spring	60 (15.6)
	Summer	90 (32.2)
	Fall	50 (10.0)
Dry-No Freeze	Winter	55 (12.8)
	Spring	75 (23.9)
	Summer	95 (35.0)
	Fall	75 (23.9)

EVALUATION OF AIRPORT PAVEMENT PERFORMANCE

In this section of Chapter III, the computer program that was used in the analysis is described and the results of the analysis for individual aircraft are presented.

The Modified ILLIPAVE Program

The modified ILLIPAVE program used in this analysis is the third in a series of finite element computer programs that were developed to analyze the stresses, strains, and displacements in a pavement. The first program in this series was developed by Duncan, et al. (Ref 28), in cylindrical coordinates and provided for one circular load with non-uniform vertical and horizontal contact pressure distributions, multiple layers, and non-linear stress-strain curves for the materials in each layer. The second program was a revision of the first. It provided for one circular load with a uniform vertical pressure distribution and included a variety of methods of estimating the stress-dependent resilient modulus of each element depending upon whether the layer was composed of granular or fine-grained soil. Because this revision was made at the University of Illinois (Ref 7), the program was re-named ILLIPAVE. This second program was obtained by Texas A&M University at which further modifications were made. This third version of the program, referred to as the "modified ILLIPAVE" program, provides for multiple tires on one or two axles, non-uniform vertical and horizontal contact pressure distributions on circular loaded areas, and all of the non-linear stress-strain curve capabilities that were available in the two previous programs. In addition, the program predicts rut depth, variance of rut depth, slope variance, present serviceability index (for highway applications) and fatigue cracking with increasing numbers of load applications. It also has the capability, not present in the previous programs, of using interface elements which permit one layer to slip with respect to another either with or without resistance that is proportional to the slip (Ref 8).

Because it is the only finite element program that has all of these capabilities including the multiple tire - multiple axle ability, the ability to predict distress, the ability to represent actual tire contact pressure distributions, and the ability to consider seasonal variations of material properties, it was chosen for the analysis that is reported below.

Permanent Deformation. The permanent deformation properties that are used in the "modified ILLIPAVE" program are of the three - parameter type that have been developed at Texas Transportation Institute (Ref 8,9). The permanent strain in the vertical direction, ε_a, is assumed to be related to the number of load repetitions by the relation

$$\varepsilon_a = \varepsilon_0 e^{-(\frac{\rho}{N})^{\beta}} \tag{16}$$

where ε_a = the permanent strain in the vertical direction

N = number of load repetitions

$\varepsilon_0, \rho, \beta$ = material parameters

These parameters depend upon the stress level in the material as well as other factors such as asphalt or water content, and others (Ref 9), and must be specified for the material in each layer in order to predict the rutting which is due to the vertical compression of the layers. Rutting also results from the lateral plastic flow of material away from the wheel path, but this component of rutting is not predicted by the modified ILLIPAVE.

Fatigue cracking is predicted in the modified ILLIPAVE program by using a fatigue law applied to the calculated strain at the bottom of the asphaltic layer. The number of cycles of load level i to cause fatigue cracking during the j^{th} season is

$$N_{ij} = K_{1j} (\frac{1}{\varepsilon_{ij}})^{K_{2j}} \tag{17}$$

where ε_{ij} = the strain at the bottom of the asphalt layer due to the i^{th} load level in the j^{th} season

K_{1j}, K_{2j} = fatigue "constants" for the j^{th} season

N_{ij} = the number of load cycles to cause fatigue cracking due to the i^{th} load level in the j^{th} season.

A "cracking index" is derived from these calculated fatigue lives and the actual number of repetitions of the i^{th} load level and the j^{th} season, as follows

$$c_k = \sum_{j=1}^{k} \sum_{j=1}^{m} - \frac{n_{ij}}{N_{ij}} \qquad (18)$$

where c_k = the cracking index after k seasons

n_{ij} = the actual number of repetitions of load level i and season j

N_{ij} = the number of repetitions to cause fatigue cracking of load level i in the j^{th} season

It is assumed that c_k has a normal probability distribution which allows the calculation of an expected area of cracking $E[c_k]$ and a probability that the actual cracking index is greater than 1.0. The percentage of the total area of the pavement that has cracked is assumed to be proportional to the probability that the cracking index is greater than 1.0. A detailed development of the cracking index equations is found in Reference (13).

In this report, the modified ILLIPAVE program was used to calculate the distress that occurs in a standard airport pavement placed in four different climatic zones and carrying the landing gear of five different aircraft. The capability of the program to represent multiple tires on each of two axles, non-uniform vertical and horizontal tire contact pressures, and seasonal material variations made it particularly useful for these analyses. The data used as input to the program is discussed in the preceding sections of this report, and the results of the analyses are in the following sections.

Maximum Stresses and Strains

The structural deterioration of flexible pavements is usually related to two failure criteria, the load-induced cracking of the bituminous surface course and the development of ruts in the wheel paths. Fatigue cracking of an asphaltic material, which generally manifests itself as alligator cracking, is considered to be the result of repeated flexural stresses causing large tensile strains at the bottom of the surface course. Rutting occurs in all layers and results both from permanent vertical strain and lateral plastic flow in each layer. The compressive stresses at the top of the subgrade are a good indication of whether the layers placed above it are sufficiently thick so that only minimal rutting occurs in the subgrade.

In order to locate the point under each aircraft gear assembly where the largest of each of these types of stress or strain is reached, multiple runs of the BISAR pavement structural analysis program were run. BISAR (Bitumen Structures Analysis in Roads) is "a general-purpose program for computing stresses, strains and displacements in an elastic multilayered system subjected to one or more uniform loads, acting uniformly over circular surface areas" (Ref 29). This program was written by Shell Research Laboratory in Amsterdam. The program was run using a pavement structure similar to the one finally used in the materials analysis and comparison in this report, and it was run for a range of surface layer stiffnesses. Stresses and strains were calculated at points under and between the wheels of the main gear assemblies.

In all cases, the largest tensile stresses or strains at the bottom of the asphaltic surface material were found to occur directly under one of the wheels. These stresses or strains increased with increasing wheel load and with increasing surface layer stiffness.

The maximum vertical compressive stresses or strains in the pavement structure occurred directly under the wheels and at the surface. The vertical compressive stresses or strains decreased with depth, so that at the top of the subgrade (at a depth of much less than at the surface of the pavement. At the subgrade, the maximums occurred either directly

AD-A181 433 CRITERIA FOR ASPHALT-RUBBER CONCRETE IN CIVIL AIRPORT PAVEMENTS VOLUME 2.. (U) TEXAS TRANSPORTATION INST COLLEGE STATION D M HOYT ET AL. MAR 87 RF-4982-2 2/3

UNCLASSIFIED DOT/FAA/PM-86/39-VOL-2 DTFA01-83-C-30076 F/G 13/3 NL

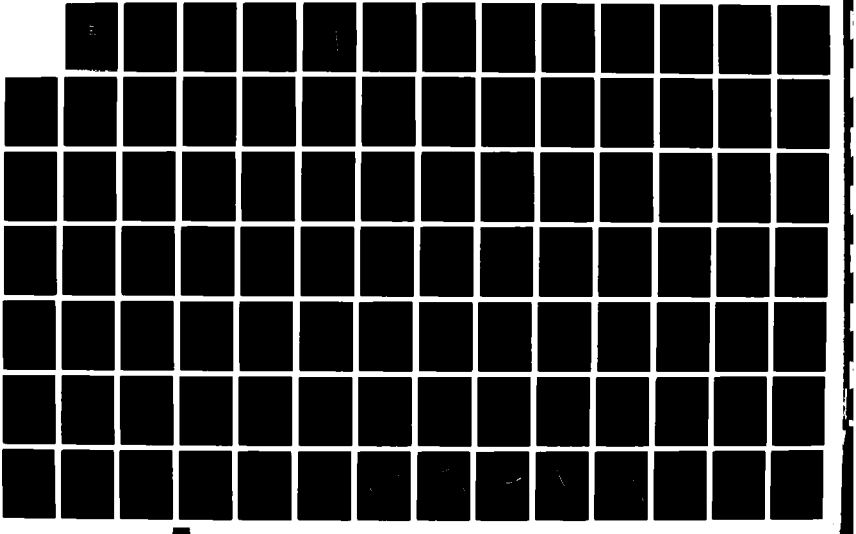

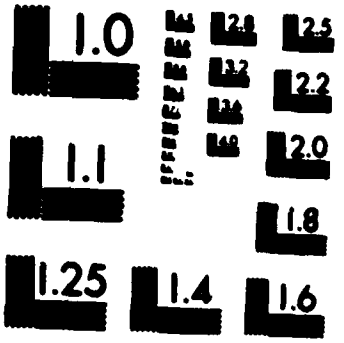

for the DC-10, at all stiffnesses; and for the B-727, at lower stiffnesses) or at the center point of the gear assembly (e.g., for the B-727 at higher stiffnesses). However, at this depth (28.5"), the differences between vertical compressive stresses or strains from point to point under the gear assembly were small. Thus, the vertical compressive stresses or strains at the top of the subgrade may be considered to be the same at every point under the gear assembly. Summaries of the results for the DC-10 (four wheels in the main gear assembly) and the B-727 (two wheels in the main gear assembly) are shown in Table 20.

Cracking Analysis: Comparison by Aircraft

Because the modified ILLIPAVE computer program can handle only one type of load at a time, the computer runs in this study were made initially with the entire traffic count being made up of one aircraft type for each computer run. Therefore, a direct comparison may be made of the relative cracking damage done by each aircraft. For all environmental zones and for all materials, the DC-10 aircraft produced the most cracking damage, followed by the B-727, the B-757, the DC-9, and then the B-737. Figure 26 shows an example plot of the cracking index versus year for the wet-no freeze environment and indicates the relative cracking damage due to each aircraft. It must be emphasized that these cracking indices were obtained using each aircraft as the entire traffic count and so they are only useful here for comparison of damage due to different aircraft. Also, the single-aircraft cracking indices have not been adjusted from laboratory to field fatigue conditions. Cracking indices due to mixed traffic will be discussed in a later section.

The cracking damage ranking of the five aircraft can easily be understood by comparing some of the aircraft characteristics for each of the planes. In Table 21, the aircraft are ranked for each of several variables. It can be seen that the cracking damage rank is directly correlated with the wheel load and with the tire inflation pressure. The sizes and spacing of the tires also affected the damage ranking.

TABLE 20. Stresses Calculated Under the Main Gear Assemblies of the DC-10 and B-727 at Various Depths.

B-727

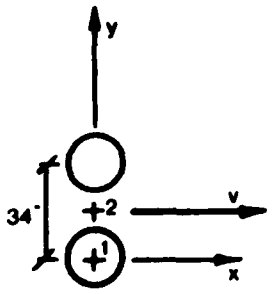

Surface Layer Stiffness psi	Point#	Depth (in.)	$Stress_{xx}$	$Stress_{yy}$	|Resultant|*	$Stress_{zz}$**
200,000	1	8.0	-15.40	-15.40	21.8	-110.00
		15.5	26.10	19.20	32.4	-45.00
		20.5	16.30	10.60	19.4	-28.10
		28.5	7.11	3.80	8.1	-17.40
	2	8.0	-7.95	-29.20	30.3	-12.20
		15.5	17.60	-9.84	20.2	-21.90
		20.5	13.60	-1.30	13.7	-21.00
		28.5	7.27	1.82	7.5	-17.10
880,000	1	8.0	-9.70	-10.60	14.4	-96.80
		15.5	116.0	93.60	149.1	-24.50
		20.5	10.50	6.90	12.6	-16.70
		28.5	4.52	2.60	5.2	-11.50
	2	8.0	-4.06	-24.80	25.1	-9.26
		15.5	89.80	28.00	94.1	-16.70
		20.5	9.80	2.79	10.2	-14.90
		28.5	4.76	2.25	5.3	-12.00

*Maximum Resultant of Stresses in the x and y Directions is Underlined
**Maximum Compressive Stress at the top of the Subgrade is Underlined

TABLE 20. (Continued)

DC-10

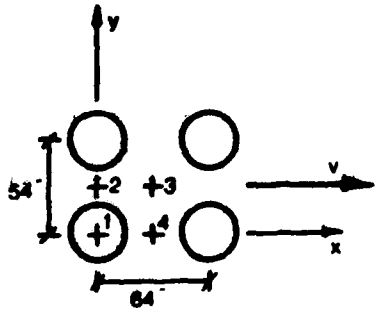

Surface Layer Stiffness psi	Point#	Depth (in.)	$Stress_{xx}$	$Stress_{yy}$	|Resultant|*	$Stress_{zz}$**
200,000	1	8.0	-18.60	-18.60	26.3	-126.0
		15.5	26.60	25.50	36.8	-53.00
		20.5	15.30	14.40	21.0	-32.7
		28.5	5.52	5.05	7.5	-19.80
	2	8.0	-6.92	-13.00	14.7	-3.22
		15.5	4.92	-17.30	18.0	-9.57
		20.5	4.41	-10.50	11.4	-12.00
		28.5	3.17	-3.20	4.5	-13.00
	3	8.0	-5.92	-6.55	8.8	-1.90
		15.5	-10.60	-6.66	12.5	-5.51
		20.5	-8.26	-4.65	9.5	-7.61
		28.5	-3.62	-1.22	3.8	-9.79
	4	8.0	-8.07	-6.12	10.1	-2.21
		15.5	-15.80	1.30	15.8	-6.52
		20.5	-11.30	1.61	11.4	-8.65
		28.5	-4.66	1.89	5.0	-10.30
880,000	1	8.0	-13.10	-13.40	18.7	-110.0
		15.5	117.0	114.0	163.4	-28.50
		20.5	8.70	8.29	12.0	-19.40
		28.5	3.07	2.94	4.3	-13.60
	2	8.0	-7.28	-14.80	16.5	-5.26
		15.5	43.30	-10.30	44.5	-11.80
		20.5	3.92	-2.95	4.9	-12.20
		28.5	2.21	-0.21	2.2	-11.90
	3	8.0	-11.60	-7.65	13.9	-4.48
		15.5	-19.10	28.80	34.6	-9.55
		20.5	-4.61	2.32	5.2	-10.30
		28.5	-1.43	1.69	2.2	-10.50
	4	8.0	-9.99	-9.91	14.1	-4.43
		15.5	-8.78	6.58	11.0	-9.38
		20.5	-3.47	-0.83	3.6	-10.40
		28.5	-1.06	0.51	1.2	-11.00

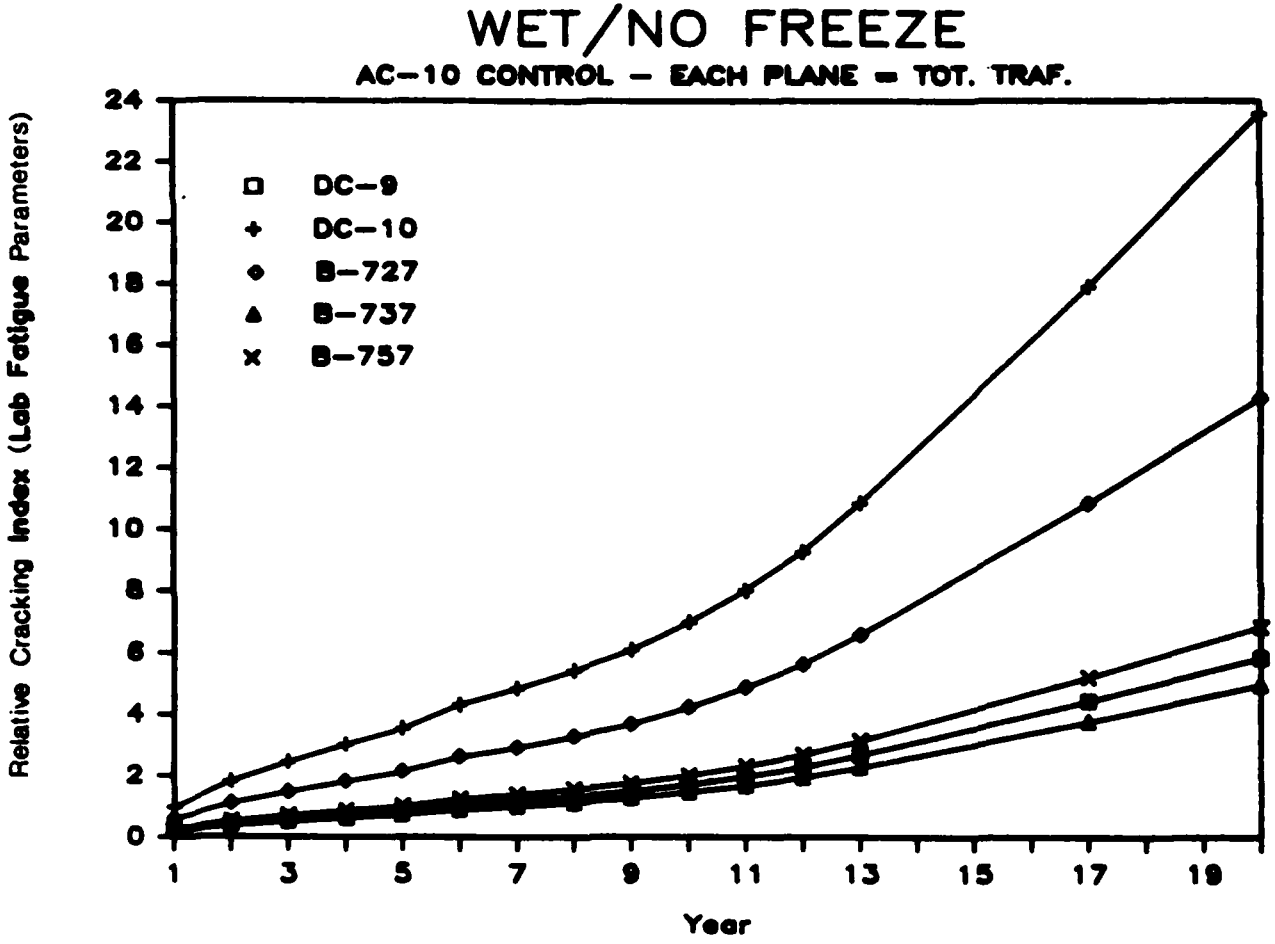

Figure 26. Plot of Relative Cracking Index versus Year, Showing Cracking Damage Comparison of the Five Aircraft in the Mixed Traffic Pattern. (Note: For this Plot, Each Aircraft is Separately Considered as Making Up the Total Traffic).

TABLE 21. Rankings of Each of the Five Aircraft Relating Several Aircraft Characteristics to the Pavement Damage Indicators.

Variable	DC-9		DC-10		B-727		B-737		B-757	
	Rank	Value	Rank	Value	Rank	Value	Rank	Value	Rank	Value
Wheel Load (lbs)	4	26,900	1	50,300	2	39,900	5	25,800	3	28,600
Tire Radius (in)	2	7.25	5	9.30	4	8.69	3	7.45	1	7.21
Tire Inflation Pressure (psi)	4	163	1	185	3	168	5	148	2	175
Diagonal Tire Spacing (in)	1	24	5	83.7	3	34	2	30.5	4	56.4
20-Year Cracking Index*, all 4 Zones, All 4 Materials:	4	var	1	var	2	var	5	var	3	var

*Rankings of Cracking Index are in order of decreasing damage.

Permanent Deformation Analysis: Comparison by Aircraft

Because the modified ILLIPAVE computer runs in this study were made initially with the entire traffic count being made up of the same aircraft for each computer run, a direct comparison could be made of the relative rutting damage done by each aircraft. However, the comparison results were not as simple as they were in the case of the relative cracking damages. In general, the most rutting was produced by the DC-10, followed by the B-727, then the B-757, DC-9, and the B-737. In some cases the B-757 moved either up or down by one place in the ranking of aircraft by the rutting damage produced. As was seen in Table 21, the B-757 has a relatively high tire inflation pressure (ranked second highest of the five aircraft being considered), and higher tire pressures are expected to cause more damage. The B-757 also has the second largest tire spacing of the five aircraft considered, which affects the superposition of the loads caused by the two tires at any point. The interplay between the aircraft characteristics of the B-757 and the permanent deformation calculated in the finite element mesh (as affected by the permanent deformation parameters, which were both temperature and stress dependent) may be the cause of the variable rutting ranking of that aircraft.

The wet-no freeze environmental zone with seasonal average temperatures of 75°F, 95°F, 105°F, and 95°F (23.9°C, 35.0°C, 40.6°C, 35.0°C) experienced the highest rut depths during the twenty-year pavement life considered for all aircraft. For the asphalt concrete control material, the dry/no freeze zone with temperatures of 55°F, 75°F, 95°F, and 75°F (12.8°C, 23.9°C, 35.0°C, 23.9°C) exhibited the lowest rut depths; but for the asphalt-rubber concretes, the dry-freeze zone with temperatures of 35°F, 60°F, 90°F and 50°F (1.7°C, 15.6°C, 32.2°C, 10°C) had the lowest rut depths in the twenty-year life. Thus, the asphalt-rubber concrete appears to be a better material for resisting deformation in cold temperatures than the asphalt concrete.

The analyses were made using one aircraft at a time which permitted an evaluation of the relative amount of damage done by each aircraft. This evaluation, while important, does not reflect the effect of actual mixes of these aircraft on the damage of an airport pavement. In the following section, the effect of mixed traffic will be considered.

Mixed Traffic Damage Evaluation: Comparison of Mixes

Appendix G contains an explanation of how the damage due to mixed traffic was calculated, as well as year by year results for both single and combined aircraft traffic. The mixed traffic damage calculations contain the adjustment from laboratory fatigue to field fatigue which was described in Chapter II of this report under Fatigue Testing.

Rutting was chosen as the critical mode, because the cracking indices for the mixed traffic in the field fatigue condition never got very large. A rut depth of 0.7 inches was considered as the critical level. A rut of this depth on a cross-slope of 2 percent would have a surface depression of approximately 6 feet (1.8 m) wide, which is fairly typical and which would be expected to start collecting water.

A cracking index of 0.2 (adjusted to the field fatigue condition) was used as a basis for comparison, and not as a failure criterion. A pavement with a cracking index of 0.2 would contain low severity level fatigue cracking. Some fine, longitudinal hairline cracks would be detected running parallel to each other in the wheel paths, with very few of the cracks being interconnected and none of the cracks being spalled. Approximately two-tenths of the length of the wheel paths would contain these low severity cracks.

In all cases, the asphalt-rubber concrete performed better (i.e., experienced less damage) than the asphalt concrete control. This was true for all four environmental zones, and for mixed as well as single vehicle traffic.

For all four environmental zones, the field damage index (i.e., laboratory damage index 13, as previously discussed in the section of this report on fatigue testing) was highest for the asphalt concrete control material and lowest for the asphalt-rubber concrete with medium

binder content. This predicted that the asphalt concrete control pavement will fatigue much earlier than will the asphalt-rubber concrete pavement. However, the wet-no freeze environment, with seasonal temperatures of 75°F, 95°F, 105°F and 95°F (23.9°C, 35.0°C, 40.6°C, 35.0°C), displayed the widest difference between the cracking performances of the control and the rubberized materials. Also, the damage indices were the highest for all materials in this zone, which has three seasons with high ($\geq$90°F) temperatures. This result shows that the cracking behavior of all four materials is most susceptible to high temperatures, with the asphalt concrete control being the worst case. Thus, in an area with high temperatures for much of the year, the asphalt-rubber concrete appears to be a better paving material choice for cracking resistance than the asphalt concrete.

The wet-freeze environment, with seasonal temperatures of 35°F, 65°F, 95°F, and 60°F (1.7°C, 18.3°C, 35.0°C, 15.6°C), and the dry-freeze environment, with seasonal temperatures of 35°F, 60°F, 90°F and 50°F (1.7°C, 15.6°C, 32.2°C, 10°C), had the least difference between the cracking performances of the control and the rubberized materials. However, the difference between the two types of materials was still significant. Also, both the asphalt concrete control and the asphalt-rubber concrete performed better in these two zones than they did in the two "no-freeze" environments. It must be emphasized, however, that this analysis did not include consideration of moisture freeze/thaw effects. Only temperature effects on the material properties were accounted for. The two "freeze" environments each had one cold season, two moderate seasons, and one hot season. The cold/moderate seasonal temperature combination seemed to create the better environment for the cracking performances of both materials. Table 22 shows the 20-year field damage indices which illustrate these observations. Figure 27 shows plots of field damage index versus time for all four materials in each environmental zone; these plots provide a graphic comparison of the material performances with respect to cracking.

TABLE 22. Field Cracking Indices for Combined Traffic at 20 Years.

Zone (Temperatures, °F)	Material	Cracking Index (Field, 20 Years)
Wet-Freeze	AC-10 Control	0.21
(35-65-95-60)	Asphalt-Rubber, Low	0.07
	Asphalt-Rubber, Medium	0.04
	Asphalt-Rubber, High	0.05
Dry-Freeze	AC-10 Control	0.16
(35-60-90-50)	Asphalt-Rubber, Low	0.06
	Asphalt-Rubber, Medium	0.03
	Asphalt-Rubber, High	0.04
Wet-No Freeze	AC-10 Control	0.83
(75-95-105-95)	Asphalt-Rubber, Low	0.15
	Asphalt-Rubber, Medium	0.10
	Asphalt-Rubber, High	0.11
Dry-No Freeze	AC-10 Control	0.35
(55-75-95-75)	Asphalt-Rubber, Low	0.13
	Asphalt-Rubber, Medium	0.06
	Asphalt-Rubber, High	0.07

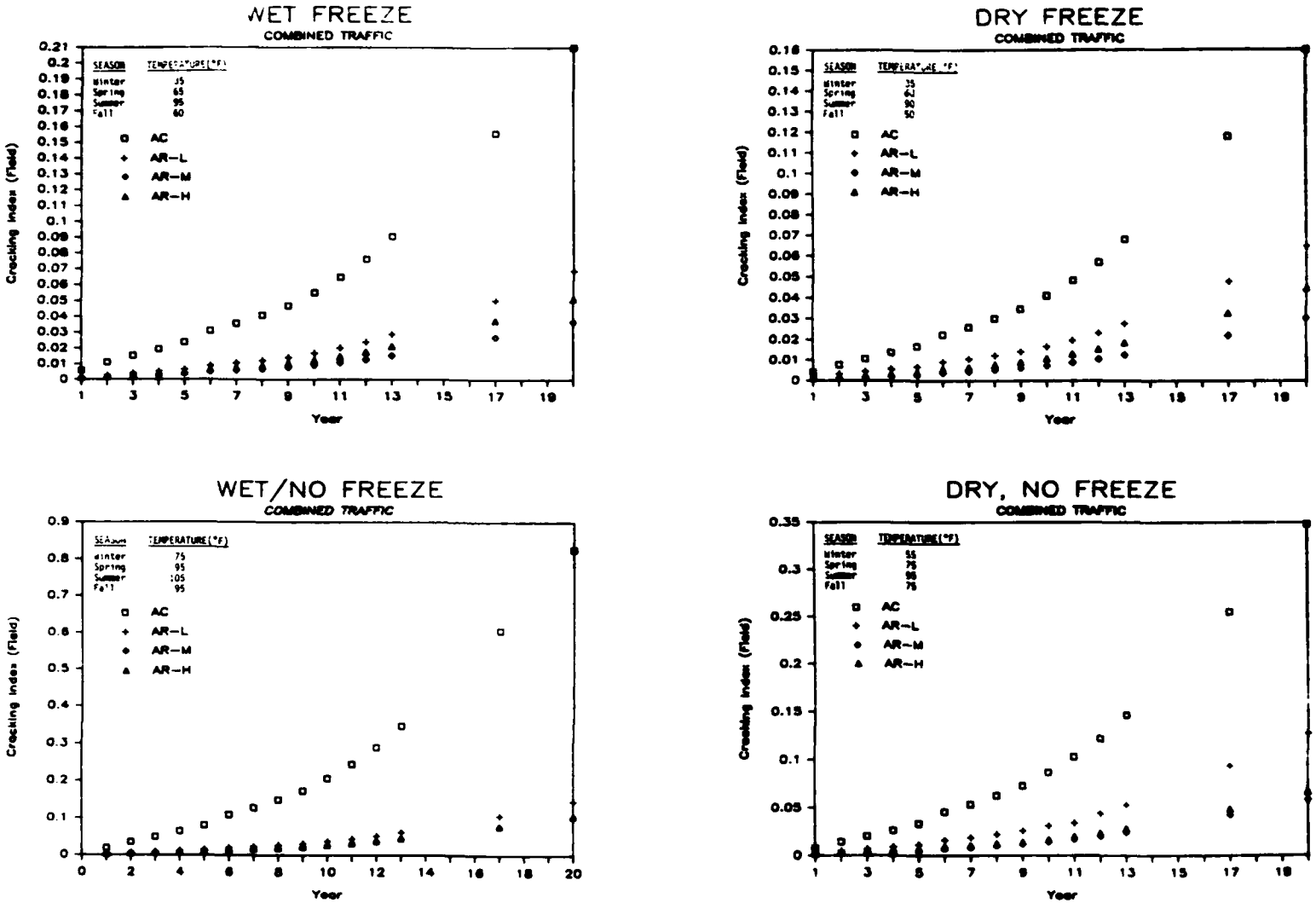

Figure 27. Plots of Cracking Index (Adjusted to Field Fatigue Condition) for Combined Traffic versus Year, Showing Four Materials in Each Climatic Zone.

All of the materials considered reached a rut depth of 0.7 inches or more during the 20-year consideration period. The times to this failure level for all materials in each climatic zone are shown in Table 23.

For all four environmental zones, the asphalt concrete control material experienced the largest rut depths; and the asphalt-rubber concrete, medium binder content, experienced the smallest rut depths. For all zones except the dry-no freeze zone, with seasonal temperatures of 55°F, 75°F, 95°F and 75°F (12.8°C, 23.9°C, 35.0°C, 23.9°C) the rut depths of the asphalt concrete control were much higher than those of the asphalt-rubber materials. For the dry-no freeze climate, the rut depths of all four materials were similar. Therefore, it was evident that, at moderate temperatures and with respect to resistance to permanent deformation, either the asphalt concrete or the asphalt-rubber concrete could be used equally well as a pavement surface material. But at either hot or cold temperatures, the asphalt-rubber concrete appeared to be considerably more resistant to permanent deformation than the asphalt concrete control material. The wet-no freeze environment, with seasonal temperatures of 75°F, 95°F, 105°F, and 95°F (23.9°C, 35.0°C, 40.6°C, 35.0°C), was the harshest zone for the asphalt concrete; this mix was computed to fail in less than a year in the hot temperatures.

The comparisons of rutting behavior discussed above can be visualized by looking at plots of rut depth versus year for each climatic zone, as shown in Figure 28.

In general, the addition of rubber to an asphalt paving mixture seemed to impart increased resistance to both cracking and rutting at high temperatures ($\geq$90°F). At cold/moderate temperature combinations, the addition of rubber imparted some cracking resistance, but the performance difference was not as marked as at high temperatures. At moderate temperatures, the asphalt concrete control material performed almost as well as the asphalt-rubber concrete with respect to rutting (permanent deformation).

TABLE 23. Times to Rut Depths of 0.7" or More for Combined Traffic and for Various Materials and Climatic Zones.

ZONE (Seasonal Temperatures, °F)	MATERIAL	YEAR	RUT DEPTH (First Rut Depth Over 0.70 in.)	DAMAGE INDEX (Field Fatigue Parameters)
Wet/Freeze	AC-10 Control	04	0.71	0.020
(35-65-95-60)	Asphalt-Rubber, Low	17	0.73	0.050
	Asphalt-Rubber, Med.	17	0.70	0.027
	Asphalt-Rubber, High	17	0.76	0.038
Dry/Freeze	AC-10 Control	05	0.73	0.017
(35-60-90-50)	Asphalt-Rubber, Low	18	0.72	0.054
	Asphalt-Rubber, Med.	18	0.72	0.025
	Asphalt-Rubber, High	17	0.72	0.033
Wet/No Freeze	AC-10 Control	1	1.61	0.019
(75-95-105-95)	Asphalt-Rubber, Low	13	0.70	0.062
	Asphalt-Rubber, Med.	15	0.72	0.060
	Asphalt-Rubber, High	13	0.75	0.045
Dry/No Freeze	AC-10 Control	15	0.75	0.201
(55-75-95-75)	Asphalt-Rubber, Low	16	0.73	0.083
	Asphalt-Rubber, Med.	16	0.71	0.038
	Asphalt-Rubber, High	15	0.73	0.038

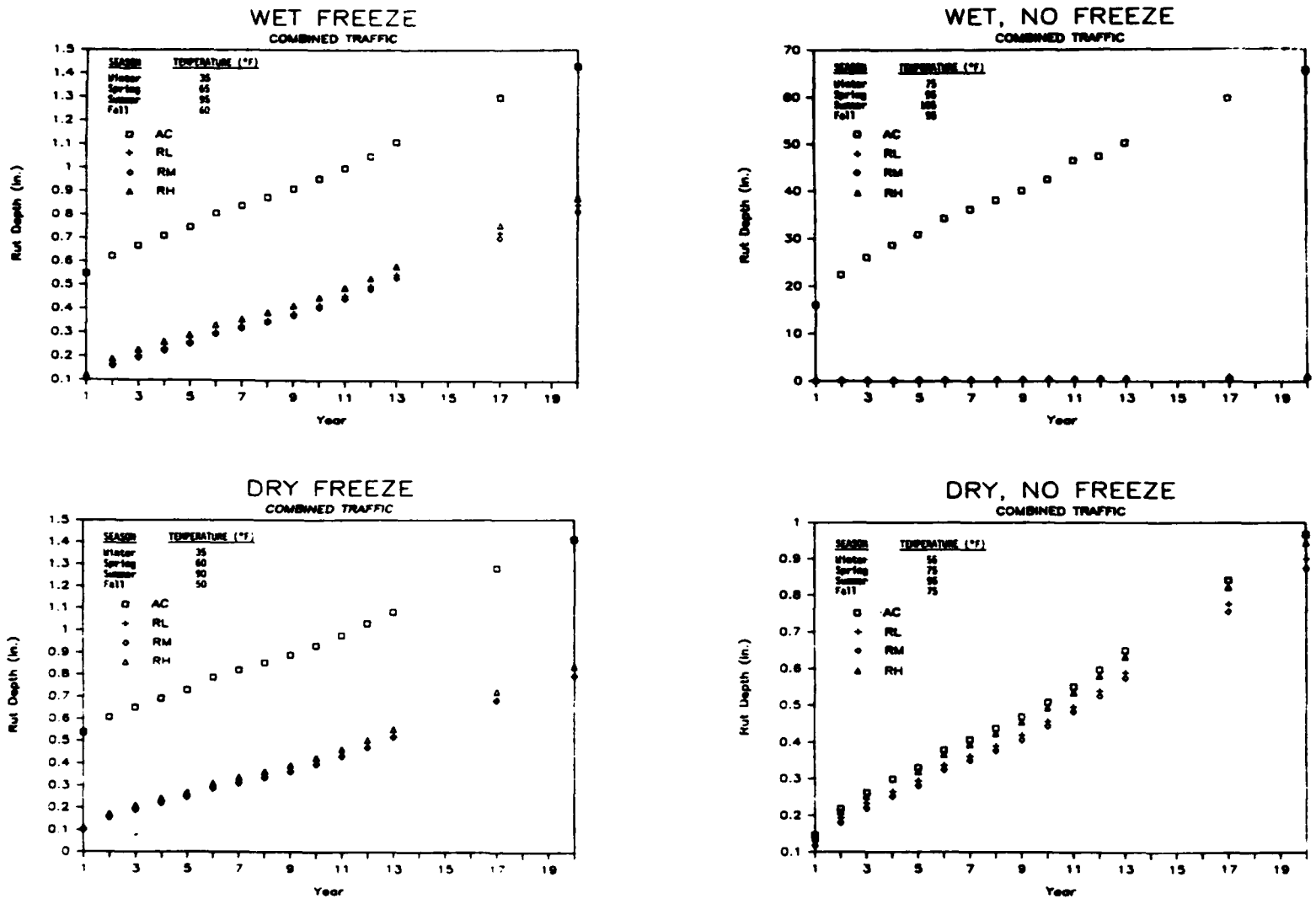

Figure 28. Plots of Rut Depth for Combined Traffic versus Year, Showing Four Materials in Each Climatic Zone.

Relative Lives of Airport Pavements in Different Climatic Zones

A cracking index of 0.2 was chosen as a comparison level for this study. The following are the cracking lives in years to a cracking index of 0.2 for combined traffic acting on the asphalt concrete control and the asphalt-rubber concrete, medium binder content, in each environmental zone:

Environment	AC-10 Control	ARC-Medium
Wet-Freeze	20	>20
Wet-No Freeze	10	>20
Dry-Freeze	>20	>20
Dry-No Freeze	15	>20

The asphalt-rubber concrete passed the entire design period for all environmental zones without reaching the comparison level of 0.2 for cracking index. The asphalt concrete control had a varying cracking life, with the shortest life occurring in the wet-no freeze environment.

A rut depth of 0.7 inches was chosen as the critical level for this study. The following are the rutting lives in years for combined traffic for the two materials in each environmental zone:

Environment	AC-10 Control	ARC-Medium
Wet-Freeze	4	17
Wet-No Freeze	1	15
Dry-Freeze	5	18
Dry-No Freeze	15	16

Comparing the times for cracking to the critical times for rutting shows that rutting is the expected critical failure mode for both materials in all four environmental zones. Because of this, the rutting failure times will be used for the economic evaluation performed in the following section.

CHAPTER IV. COST-EFFECTIVENESS COMPARISON BETWEEN ASPHALT-RUBBER CONCRETE AND ASPHALT CONCRETE

In this chapter, approximate costs of asphalt-rubber concrete and asphalt concrete will be estimated for these materials compacted in place. A cost-effectiveness analysis of each of the four materials that have been analyzed in the previous chapters will be performed. Because the only difference between the pavements analyzed is the materials used in the surface layer, it is the cost-effectiveness of that layer which is analyzed.

COST DATA FOR ASPHALT-RUBBER CONCRETE AND ASPHALT CONCRETE

Estimates for asphalt-rubber concrete are based on (1) the cost of producing the asphalt-rubber binder and (2) substituting the cost of the asphalt-rubber binder for the cost of asphalt cement in asphalt concrete unit prices.

Since the asphalt-rubber binder produced for use in seal coat construction is the same as that to be used in asphalt-rubber concrete, the component prices presented by Shuler, et al. (Ref 30) were updated for current prices and are shown in Table 24.

Representative prices for asphalt-rubber binders, as used in chip seals and interlayers, are given in Table 24. These prices are based on industry-supplied data for asphalt-rubber binder containing 70 percent asphalt, 25 percent rubber and 5 percent petroleum additives. The price per ton was developed from an application rate of 0.60 gal/yd^2. The cost information indicates that the cost of materials represents about one-half of the in-place cost. Blending and reacting the asphalt and rubber and distribution of the asphalt-rubber binder represents about 20 percent of the total in-place cost of the binder.

Approximate in-place component costs for hot mixes made with asphalt cement and asphalt-rubber binders are given in Table 25. Using an asphalt-rubber binder increases the cost of the concrete by about 40

TABLE 24. Representative Prices (1984) for Asphalt-Rubber Binders per Ton, as Used in Chip Seal and Interlayers.*

Component	Cost $/Ton	Cost Percent
A. Materials		
1. Asphalt Cement		
$175 per ton f.o.b. refinery	$122.50	28.0
Transportation - $12 per ton	0.60	0.14
2. Rubber		
$0.18 per lb. f.o.b. plant	90.00	20.5
Transportation - $12 per ton	0.60	0.14
3. Additive		
$0.128 per lb. f.o.b. refinery	10.00	2.3
Transportation - $12 per ton	0.60	0.14
B. Blending and Reacting	30.22	6.9
C. Binder Distribution	53.33	12.2
D. Travel to Job Site	20.00	4.5
E. Profit, Overhead, Taxes, Insurance, Contingencies, etc.	109.28	25.0
TOTAL	$437.13	$100.0

*Based on industry-supplied data with the asphalt-rubber binder containing 70 percent asphalt cement, 25 percent rubber and 5 percent petroleum additive. Application rate 0.60 gal/yd^2 or 4.5 lbs/yd^2.

TABLE 25. Unit Cost Per Ton of Material in Place for Asphalt Concrete and Asphalt-Rubber Concrete.

	Asphalt Cement Binder		Asphalt-Rubber Cement Binder					
			Low Binder Content		Medium Binder Content		High Binder Content	
Component	$/Ton	Percent	$/Ton	Percent	$/Ton	Percent	$/Ton	Percent
Binder*	8.40	25.0	18.61	40.7	20.81	43.1	23.01	45.2
Aggregate	8.85	26.4	8.85	19.4	8.85	18.3	8.85	17.4
Energy Costs	1.20	3.6	1.28	2.8	1.28	2.7	1.28	2.5
Mixing	3.51	10.5	3.51	7.7	3.51	7.3	3.51	6.9
Haul, Laydown, and Compaction	5.92	17.6	5.92	13.0	5.92	12.3	5.92	11.6
Miscellaneous	0.66	2.0	0.66	1.4	0.66	1.4	0.66	1.3
Mark-Up (15%)	5.04	15.0	6.85	15.0	7.24	15.0	7.63	15.0
	33.58	100.0	45.68	100.0	48.27	100.0	50.86	100.0

* 4.8% - Asphalt Cement Binder; 4.23% - Low Asphalt-Rubber Cement Binder; 4.73% - Medium Asphalt-Rubber Cement Binder; 5.23% - High Asphalt-Rubber Cement Binder. Asphalt Cement at $175 per ton and Asphalt-Rubber Cement at $440 per ton at the plant.

percent. Most of this cost difference is directly related to producing the asphalt-rubber binder itself.

COST-EFFECTIVENESS ANALYSIS BASED ON PROJECTED LIVES OF PAVEMENTS

The type of distress which controls the useful life of all pavement surface layers is rutting. In accordance with common practice, a limiting rut depth of 0.50 inches (1.27 cm) was set and annual costs were calculated for each pavement in each climatic zone. However, it was found that the asphaltic concrete control pavement was predicted to reach this level of rut depth within one year. Seeking a more realistic cost comparison between the four materials, a limiting rut depth of 0.70 inches (1.8 cm) was set and new pavement lives were determined.

The cost figures for both limiting rut depths are presented below. The steps in this cost comparison are as follows:

1. Determine the construction cost of each paving material in place per square yard.
2. Determine the equivalent uniform annual cost per square yard of each pavement over its predicted life.
3. Select the most cost-effective material in each climatic zone as the one which provides the least equivalent uniform annual cost per square yard for the life of the pavement.

The equivalent uniform annual cost per square yard is the annual cost per square yard which, if paid annually over the life of the pavement, has a present value equal to the in-place cost per square yard of construction of the asphaltic surface layer. The interest rate that is used in calculating the equivalent uniform annual cost is 4.0 percent and is considered to be a reasonable estimate of the difference between actual interest and actual inflation rates as applied to construction.

Construction Cost Per Square Yard

The determination of the in-place construction cost per square yard for the 15-inch (38 cm) thick asphalt surface layer uses the following steps:

1. Determine the in-place density of each of the four materials. The compaction curves shown in Chapter II were considered to be sufficiently accurate for the purposes of this economic analysis.
2. Determine the tons per square yard of each material.
3. Determine the cost per square yard from the previously determined cost per ton of material in place.

The results of these determinations are contained in Table 26.

Equivalent Uniform Annual Costs per Square Yard of Materials in Place

The equivalent uniform annual cost per square yard of each material in place is similar to a life-cycle cost of each material except that it includes only the cost of construction distributed uniformly over the expected life of the pavement. It does not include the cost of maintenance or rehabilitation of the pavement or the costs to the user while these activities are being carried out. Because these are largely unknown for asphalt-rubber concrete pavements, it is assumed for the purposes of this cost-effectiveness analysis that they will be roughly proportional to the equivalent uniform annual cost of construction and that a comparison of these will provide a rational means of selecting the preferable material in each climatic zone.

The formula for the equivalent uniform annual cost per square yard is

$$\frac{EUAC}{S.Y.} = \frac{(PV/S.Y.)\ (i)}{(1+i)\ [1-(1+i)^{-n}]} \qquad (19)$$

where $\frac{EUAC}{S.Y.}$ = the equivalent uniform annual cost per square yard

$\frac{PV}{SY}$ = the "present value" or construction cost per square yard.

i = the effective interest rate which is assumed to be the difference between the actual interest and actual inflation rate and was set at 4 percent for this analysis. In this case i is the interest rate in percent divided by 100.

n = the useful life of the pavement in years.

TABLE 26. In-Place Costs Per Square Yard for Asphalt Concrete and Asphalt-Rubber Concrete.

Material	Percent Binder %	In-Place Costs per Ton $/Ton	Density, lb/ft^3	Tons per Square Yard T/S.Y.	In-Place Costs per Square Yard $/S.Y.
Asphalt Concrete	4.80	$33.58	151.2	0.851	$28.56
Asphalt-Rubber Concrete					
Low Binder	4.23	45.68	144.8	0.815	37.21
Medium Binder	4.73	48.27	145.3	0.817	39.45
High Binder	5.23	50.86	144.9	0.815	41.46

Two comparisons are made in Table 27, one for a critical rut depth of 0.5 inches (1.27 cm) and the other for a critical rut depth of 0.7 inches (1.8 cm).

The most cost-effective material to use depends, not surprisingly, upon the climatic zone and the level of the critical rut depth. Only in the dry-no freeze zone is the asphaltic concrete more cost effective than the asphalt-rubber concrete. Elsewhere, the most cost-effective materials are either the low or medium (optimum) binder content asphalt-rubber concretes. In the wet-freeze zone, the best material changes from the medium to the low binder content material as the critical rut depth is deepened.

On the basis of this study, it appears to be desirable to perform full scale experiments with asphalt-rubber concrete to determine whether these findings, which are based upon laboratory tests and computer analysis, are borne out in practice.

TABLE 27. Equivalent Uniform Annual Construction Costs per Square Yard of Asphalt Concrete and Asphalt-Rubber Concrete.

Material	Climatic Zone Temperature, °F	0.5 in. Rutting Age, Years	0.5 in. Rutting Cost* per Square Yard per Year	0.7 in. Rutting Age, Years	0.7 in. Rutting Cost* per Square Yard per Year
Asphalt Concrete	Wet-Freeze	1	28.56	4	$7.57
Asphalt-Rubber Concrete	(35-65-95-60)				
Low Binder		12	3.81	17	2.94
Medium Binder		13	3.80	17	3.12
High Binder		12	4.25	17	3.28
Asphalt Concrete	Dry-Freeze	1	28.56	5	6.17
Asphalt-Rubber Concrete	(35-60-90-50)				
Low Binder		13	3.58	18	2.83
Medium Binder		13	3.80	18	3.00
High Binder		12	4.25	17	3.28
Asphalt Concrete	Wet-No Freeze	1	28.56	1	28.56
Asphalt-Rubber Concrete	(75-95-105-95)				
Low Binder		9	4.81	13	3.58
Medium Binder		11	4.33	15	3.41
High Binder		8	5.92	13	3.99
Asphalt Concrete	Dry-No Freeze	10	3.39	15	2.47
Asphalt-Rubber Concrete	(55-75-95-75)				
Low Binder		11	4.08	16	3.07
Medium Binder		12	4.04	16	3.27
High Binder		11	4.55	15	3.59

* Most cost effective choices in each climatic zone are underlined.

CHAPTER V. SUMMARY, CONCLUSIONS, AND RECOMMENDATIONS

This concluding chapter summarizes the changes in the Marshall method of mix design which were necessary to produce a satisfactory mix design for asphalt-rubber concrete. It also presents a brief summary of the results of the laboratory testing, computer analysis, and prediction of field performance, and the study of the cost effectiveness of asphalt concrete as contrasted with asphalt-rubber concrete that have been presented in the three previous chapters.

MODIFICATIONS TO THE MARSHALL METHOD OF MIX DESIGN FOR ASPHALT-RUBBER CONCRETE

The Marshall method of mix design for asphalt concrete (Ref 4) can be used to produce an adequate mix for asphalt-rubber concrete, but several modifications must be made to the design procedure. These modifications were presented in the two volumes of this report, and are summarized below.

Aggregate

An aggregate gradation should be chosen based on the project specifications, and the final aggregate blend combination (mineral aggregate plus rubber particles) must meet the gradation requirements. Before producing the aggregate blend for production, a calculation must be performed which adjusts the aggregate quantities and which treats the rubber as an additional aggregate. The rubber particles may contribute significantly to the total amount of solid particles in the mix, thereby necessitating a reduction in some components of the mineral aggregate blend. If this is the case, then the mineral aggregate blend used in the mix design must be modified to permit space for the rubber particles.

Mixing and Compaction Temperatures

The Marshall method of mix design calls for determination of mixing and compaction temperatures by viscosities. However, the absolute viscosity of asphalt-rubber produced from ground reclaimed rubber and measured with capillary tube viscometers is highly variable. (See Volume I of this report, page 7). Therefore, viscosity as measured by capillary tube viscometer could not be used in the Marshall mix design of asphalt-rubber concrete.

Mixing and compaction temperatures for producing asphalt-rubber concrete for mix design must be higher than those used for asphalt concrete. In this study, temperature and compactive effort experiments showed that mixing and compaction at 375°F (191°C) produced asphalt-rubber concrete with higher stabilities and lower air voids than were attained at lower temperatures. In the materials characterization portion of this study, a mixing temperature of 375°F (191°C) was used. But the beam specimens used in several of the test procedures could not be compacted at this high of a temperature; therefore, a compaction temperature of 325°F (163°C) was adopted for the mix design and specimen production.

Mixing

Mixing must be performed using a high energy mechanical mixer.

Compactive Effort

Compactive effort of 75 blows per face of the specimen has been recommended in this study, regardless of gear load, to obtain desired air voids contents.

Extrusion of Specimens from Molds

Asphalt-rubber concrete specimens must be allowed to cool to room temperature (about 24 hours) before being extruded from the molds. This

prevents the swelling of the specimens which had previously been observed by other researchers, as mentioned in Volume 1 of this report.

Air Void Content

Percent air voids requirements must be raised from those specified in the Marshall method when designing an asphalt-rubber concrete mixture. Difficulty was experienced with the mixes tested in this study in attaining air void contents below about 7% in the laboratory. Therefore, it is recommended that the band on air voids requirement should be between 3% and 8% for the Marshall mix design. However, it may be possible to better compact the asphalt-rubber concrete in the field.

DIFFERENCES IN MATERIAL PROPERTIES

Laboratory testing of asphalt concrete and asphalt-rubber concrete included tests of compaction and air voids, Marshall stability, resilient modulus, creep compliance and temperature susceptibility, beam fatigue, crack propagation and fracture in the Texas Transportation Institute "overlay" test, and permanent deformation. There were four materials tested: an asphalt concrete at the optimum binder content of an AC-10 binder (AC); an asphalt-rubber concrete at the optimum binder content (ARC-Medium Binder Content); and two other asphalt-rubber concretes at binder contents above and below optimum by 0.50 percent by weight (ARC-Low and High Binder Content). The results of the comparisons of these four materials are summarized below.

Compaction and Air Voids

The asphalt-rubber concrete (ARC) had lower density and higher air voids than the asphalt concrete (AC) at the same level of laboratory compaction. The maximum density of the AC was about 6 lb/ft^3 greater than the ARC and the air voids about 4.5 percent less at the optimum binder content which was, in the materials tested, about the same in the AC and the ARC.

Stability

The maximum Marshall stabilities of the AC and the ARC mixes were nearly identical at the same level of compaction, but the maxima occurred at different binder contents: 4.1% for the ARC and 4.8% for the AC. For the binder contents used in the testing program, the Marshall stabilities were approximately 2100 for ARC and 2300 for the AC, both of which are above the minimum required in the Marshall mix design method for heavy traffic.

Resilient Modulus

The resilient moduli of the materials at the same compaction level varied from one temperature to the next. In general, at low temperatures, the resilient modulus of the AC was greater than that of any of the ARC mixes tested, and at high temperatures was lower than that of the ARC mixes. The change of modulus with temperature, which is a measure of temperature susceptibility, was greater in the AC followed by the ARC-High, ARC-Low, and ARC-Medium, in that order.

Creep Compliance and Temperature Susceptibility

Creep tests were made on the four mixes at three different temperatures and the time-temperature shift functions for each were determined. At the 70°F (21.1°C) master temperature and at 10 seconds after loading, the average creep compliances arranged in order of increasing magnitude were as follows: ARC-Low, ARC-High, AC, and ARC-Medium. At the 70°F (21.1°C) master temperature and at 1,000 seconds after loading, the average creep compliances arranged in order of increasing magnitude were as follows: ARC-Low, ARC-Medium, ARC-High, and AC.

The temperature susceptibility, as indicated by the time-temperature shift functions, in decreasing order were: AC, ARC-Low, ARC-Medium, and ARC-High. The addition of the rubber to the binder helps the material to maintain a more stable compliance as temperature changes.

Beam Fatigue Tests

Beam fatigue tests were made at three temperatures to determine how the fatigue properties changed with temperature. Linear relations were found between $\log_{10} K_1$ and K_2 for each mix and the dependence of $\log_{10} K_1$ on temperature was also found for each mix. The fatigue resistance of these materials in the field depends upon these properties as well as the level of strain imposed on the material in the pavement structure. Therefore, it is not strictly correct to compare the fatigue resistance of these materials on the basis of laboratory tests alone. At a temperature of 75°F (24°C) the values of K_1 are arranged in decreasing order as follows: ARC-High, ARC-Medium, AC, and ARC-Low. At a temperature of 35°F (2°C), the values of K_1 in decreasing order are: ARC-High, AC, ARC-Medium, and ARC-Low.

Crack Propagation and Fracture Tests

The Texas Transportation Institute overlay tester was used to determine the fracture properties of each mix at a low temperature, 34°F (1.1°C) and a moderate temperature, 77°F (25°C). By using a "Crack Speed Index", which can be determined from the test results, the materials can be compared in their ability to resist cracking. At the low temperature, the mixes are arranged in the following order of decreasing crack resistance: ARC-Medium, ARC-High, AC, and ARC-Low. At the moderate temperature, the materials were arranged in a different order, again decreasing in crack resistance: AC, ARC-Low, and ARC-Medium.

According to Schapery's theory of crack growth (Ref 22), crack resistance is approximately a function of the square of the ratio of the tensile strength to the modulus. The reversal of the order of crack resistance of the asphalt concrete as compared to the asphalt-rubber concrete, medium binder content, as the temperature decreases from moderate to low temperature is primarily due to the fact that the modulus of the asphalt-rubber concrete decreases relative to that of the control material. See Figure 8 in this report.

Permanent Deformation

Repeated load tests were run on each mix at three different temperatures and material properties were characterized by three parameters which were used to calculate rut depth in the modified ILLIPAVE analyses. At 70°F (21°C), the values of the scale parameter, ρ, which is an indicator of resistance to rutting, are ranked in decreasing order as follows: ARC-Medium, ARC-Low, ARC-High, and AC.

PREDICTED FIELD PERFORMANCE

A typical pavement which was built at Robert Mueller Airport in Austin, Texas was used for all the predictions of field performance.

Four climatic zones, five aircraft, and four materials were analyzed in separate runs using the modified ILLIPAVE computer program for a total of 80 runs. The results were analyzed separately to evaluate the relative effect of different aircraft, different materials, and different climatic zones on the cracking and rutting performance of the typical pavement. Subsequently, the effect of mixed traffic, using a typical mix of the five aircraft, was evaluated to determine the expected useful life of the pavement in each climate using each of the four materials. The aircraft were the DC-9, DC-10, B-727, B-737 and B-757. The most damaging aircraft in both cracking and rutting was the DC-10.

In all climates, the rutting criterion was more critical than the cracking criterion. The materials that lasted longest in each climate were as follows: wet-freeze, ARC-Medium; dry-freeze, ARC-Medium and Low; wet-no freeze, ARC-Low; dry-no freeze, ARC-Medium. The materials that were more resistant to cracking in each climate were as follows: wet-freeze, ARC-Medium; dry-freeze, ARC-Medium; wet-no freeze, ARC-Medium; dry-no freeze, ARC-Medium. The wet-no freeze climate was the most severe in all cases.

LIFE CYCLE COST ANALYSIS

The costs of each of the materials compacted in place were estimated and were used to compute the cost per square yard of pavement surface for the typical pavement that was used in the analyses. The use of the rubber in the asphalt-rubber concrete increases the cost per ton by $12 to $17, increasing with the percent binder that is used. The percentage increase is 36 to 51 percent. The useful life of the pavement, as dictated by the critical rutting criterion, was used to calculate an equivalent uniform annual cost of each material in each climate. An interest rate of four percent, representing the difference between actual interest and actual inflation rates, was used to calculate these annual costs. A comparison of these equivalent uniform annual costs per square yard revealed the most cost effective materials. In each climate, these were as follows: wet-freeze, ARC-Low and Medium; dry-freeze, ARC-Medium; wet-no freeze, ARC-Medium; and dry-no freeze, AC. Thus, according to these analyses, in all climates but the dry-no freeze zone, the additional cost of adding rubber to the binder is justified by the increased life and decreased life cycle costs of the ARC material. There are still questions that remain and these are discussed in the following two sections of this chapter.

RECOMMENDED FUTURE RESEARCH

In view of the promising results of this study of asphalt-rubber concrete, further research is warranted both in the laboratory and in the field.

Laboratory research should investigate the healing, low temperature cracking and moisture susceptibility of asphalt-rubber concrete and a more extensive study of the fracture and permanent deformation properties of ARC should be made with different types of rubber and aggregate. The healing property is particularly important in calculating the lab-to-field fatigue shift factor which was assumed to be 13 in this study. The low temperature cracking should include determination of the thermal coefficient of expansion, glass-transition temperature, and further

studies of the fracture properties of ARC. The possible effect of the increased air void content on an increase in the rate of oxidation and aging is another important study that needs to be conducted. An assessment of the effect of each of these on the predicted useful life and cost effectiveness of the ARC material, as was done in this report, is an essential part of the research evaluation.

Field research with demonstration projects are warranted on the basis of these results. Particularly important is to experiment with laydown and compaction methods to achieve the desired level of compaction, to run tests on cores taken from the completed project, and to make periodic assessments of the condition of the pavement. Because both traffic and climate make a difference in the performance of pavement made with an ARC surface course, it is worthwhile to find sites for demonstration projects in all climatic zones where ARC appears to be cost effective.

RECOMMENDED FUTURE PRACTICE

The use of asphalt-rubber concrete for airport pavement appears to be justified on the basis of its expected cost effectiveness. Production and construction practices must be altered somewhat to account for the different properties and the increased temperatures and increased compactive effort that will be required to mix and place ARC properly. Production and construction practices should be in accordance with the procedures which are outlined in Appendixes A and B.

On the basis of this study, asphalt-rubber cement used as a binder, together with a densely graded aggregate, when properly constructed, should provide a superior cost-effective asphalt-rubber concrete for use on airport pavements in three of the four unique climatic zones in the United States, excluding only the dry-no freeze zone.

REFERENCES

1. Mindess, S. and Young, J. F., Concrete, Prentice-Hall, Inc., Englewood Cliffs, N.J., 1981.

2. "Bituminous Surface Course," STANDARDS FOR SPECIFYING CONSTRUCTION OF AIRPORTS - New Standard for Plant Mix Bituminous Materials, Advisory Circular No. 150/5370-10, Item P-401, Federal Aviation Administration, May, 1977.

3. "Standard Specification for Hot-Mix, Hot-Laid Bituminous Paving Mixtures," 1983 ANNUAL BOOK OF ASTM STANDARDS, Designation D 3515-83, Volume 04.03, Philadelphia, PA., 1983.

4. "Mix Design Methods for Asphalt Concrete and Other Hot-Mix Types," Manual Series No. 2 (MS-2), The Asphalt Institute, College Park, Maryland, May, 1984.

5. Foster, C. R., "The Effect of Voids in Mineral Aggregate on Pavement Performance," Information Series 96/86, National Asphalt Pavement Association, Riverdale, Maryland, 1986.

6. Kenis, W. J., "Predictive Design Procedures, VESYS User's Manual - An Interim Design Method for Flexible Pavement Using the VESYS Structural Subsystem," Final Report No. FHWA-RD-77-154, Federal Highway Administration, January, 1978.

7. "ILLIPAVE User's Manual," Transportation Facilities Group, Department of Civil Engineering, University of Illinois at Urbana-Champaign, May, 1982.

8. Roberts, F. L., Tielking, J. T., Middleton, D., Lytton, R. L. and Tseng, K., "Effects of Tire Pressures on Flexible Pavements," TTI Research Report No. 372-1F, Texas Transportation Institute, Texas A&M University, College Station, Texas, December, 1985.

9. Tseng, K. and Lytton, R. L., "Prediction of Permanent Deformation on Flexible Pavement Materials," Paper prepared for publication at the ASTM Symposium on Implication of Aggregates in the Design, Construction, and Performance of Flexible Pavements, New Orleans, LA., December, 1986.

10. Yoder, E. J. and Witczak, M. W., Principles of Pavement Design, 2nd edition, John Wiley & Sons, Inc., New York, 1975.

11. Schmidt, R. J., "A Practical Method for Measuring the Resilient Modulus of Asphalt-Treated Mixes," HIGHWAY RESEARCH RECORD NO. 404, Highway Research Board, 1972, pp. 22-32.

12. Little, D. N., Al-Balbissi, A. H., Gregory, C. and Richey, B., "Design and Characterization of Paving Mixtures Based on Plasticized Sulfur Binders - Engineering Characterization," TTI Draft Final Report RF 4247, Texas Transportation Institute, Texas A&M University, College Station, Texas, July, 1984.

13. Rauhut, J. B., O'Quin, J. C. and Hudson, W. R., "Sensitivity Analysis of FHWA Structural Model VESYS II," Volume 1 and 2, Federal Highway Administration, Report No. FHWA-RD-76-23, Washington, D.C., March, 1976.

14. Little, D. N., Haxo, H. E. and Saylak, D., "Development of Second Generation Sulphlex Binders for Paving Mixtures," Texas Transportation Institute, Final Report for Federal Highway Administration, May, 1985.

15. Epps, J. A. and Monismith, C. L., "Fatigue of Asphalt Concrete Mixtures - Summary of Existing Information: Fatigue of Compacted Bituminous Aggregate Mixtures," American Society for Testing and Materials, Special Technical Publication No. 508, 1972.

16. Austin Research Engineers, Inc., "Material Properties to Minimize Distress in Zero-Maintenance Pavements," Research Report No. FHWA-RD-80, April, 1980.

17. Adedimila, A. S. and Kennedy, T. W., "Fatigue and Resilient Characteristics of Asphalt Mixtures by Repeated-Load Indirect Tensile Test," Research Report No. 183-5, Center for Highway Research, The University of Texas at Austin, August, 1975.

18. Pell, P. S. and Cooper, K. E., "The Effect of Testing and Mix Variables on the Fatigue Performance of Bituminous Materials," Proceedings, Association of Asphalt Paving Technologists, Volume 44, 1975, pp.

19. Finn, F., Saraf, C., Kulkarni, R., Nair, K., Smith, W. and Abdullah, A., "The Use of Distress Prediction Subsystems for the Design of Pavement Structures," Proceedings, Fourth International Conference - Structural Design of Asphalt Pavements, Volume I, The University of Michigan, Ann Arbor, Michigan, January, 1977, pp. 3-38.

20. Al-Balbissi, A. H., "A Comparative Analysis of the Fracture and Fatigue Properties of Asphalt Concrete and Sulphlex," Ph.D. Dissertation, Texas A&M University, August, 1983.

21. Paris. P .C. and Erdogan, F., "A Critical Analysis of Crack Propagation Laws," Transactions of the ASME, Journal of Basic Engineering, Series D, Volume 85, No. 3, 1963.

22. Schapery, R. A., "A Theory of Crack Growth in Viscoelastic Media," Technical Report No. MM 2764-73-1, Mechanics and Materials Research Center, Texas A&M University, College Station, Texas, March, 1973.

23. Williams, M. L., Landel, R. F. and Ferry, J. D., "Visco-Elastic Properties of Polymers," Journal of American Chemical Society, Vol. 77, p. 3701, 1955.

24. Lytton, R. L., personal communication, Texas Transportation Institute, Texas A&M University, College Station, Texas, 1986.

25. Brent Rauhut Engineering, Inc., "Runway and Taxiway Pavement Evaluations: Robert Mueller Municipal Airport, Austin, Texas," Report Prepared for the City of Austin Aviation Department, January, 1982.

26. Ho Sang, V., "Field Survey and Analysis of Aircraft Distibution on Airport Pavements," Final Report, Federal Aviation Administration, February, 1975.

27. Tielking, J. T., "A Tire Contact Solution Technique," Tire Modeling, NASA Conference Publication 2264, Proceedings of a Workshop held at Langley Research Center, Hampton, Virginia, September, 1982, pp. 95-121.

28. Duncan, J. M., Monismith, C. L. and Wilson, E. L., "Finite Element Analysis of Pavements," Highway Research Record 228, Highway Research Board, 1968, pp. 18-33.

29. "BISAR (Bitumen Structures Analysis in Roads) User's Manual," Abbreviated Version, Koninklijke/Shell-Laboratorium, Shell Research N.V., Amsterdam, July, 1972.

30. Shuler, T. S., Pavlovich, R. D., Epps, J. A. and Adams, C. K., "Investigation of Materials and Structural Properties of Asphalt-Rubber Paving Mixtures," TTI Final Report RF 48711-1F, Texas Transportation Institute, College Station, Texas, September, 1985.

APPENDIX A

Suggested Guide Specification For Production Of Asphalt-Rubber Binder And Its Use In Construction

APPENDIX A. SUGGESTED GUIDE SPECIFICATION FOR PRODUCTION OF ASPHALT-RUBBER BINDER AND ITS USE IN CONSTRUCTION

1. DESCRIPTION

This guide* involves production of asphalt-rubber binders for use in hot asphalt-rubber concrete for pavement surfaces in accordance with the plant and other specifications. The main differences between the use of asphalt-rubber cement and the use of asphalt cement occur in the production of the asphalt-rubber binder. Construction experience has indicated that the same guidelines as those used for other hot-mix types (in particular, for asphalt concrete) will produce an acceptable asphalt-rubber concrete pavement surface. Therefore, construction operations which are not described herein (e.g., mixing, placement, and compaction) should follow the regular FAA Specifications. This specification describes two known proprietary processes for production of the binder hereinafter known as Method A and Method B. Method A uses ground reclaimed "devulcanized" rubber and an extender oil whereas Method B uses ground reclaimed vulcanized rubber and a kerosene diluent. Either method is acceptable based on proper compliance with the specifications and certification of materials.

2. MATERIALS

Asphalt-rubber, as currently used, shall include between 15 and 28 percent by total weight of dry rubber in an asphalt cement matrix. (See Volume I of this report, page 18.)

---

* The bulk of this guide was prepared by Ray Pavlovich.

2.01 ASPHALT CEMENT

Asphalt cement shall meet the requirements of AASHTO M 20-70 (Table 1), M226-80 (Table 1), or M226-80 (Table 3). Acceptable grades for the respective materials will depend on location and circumstances and will require approval of the Supplier of the asphalt rubber. In addition, it shall be fully compatible with the ground rubber proposed for the work as determined by the Supplier.

2.02 RUBBER EXTENDER OIL (METHOD A)

Extender oil shall be a resinous, high flash point aromatic hydrocarbon meeting the following test requirements.

Viscosity, SSU, at 100°F (ASTM D 88)	2500 min.
Flash Point, COC, degrees F (ASTM D 92)	390 min.
Molecular Analysis (ASTM D 2007):	
Asphaltenes, Wt.%	0.1 max.
Aromatics, Wt.%	55.0 min.

2.03 KEROSENE TYPE DILUENT (METHOD B)

The kerosene type diluent used shall be compatible with all materials used and shall have a flash point (ASTM D 92) of not less than 80°F. The Initial Boiling Point shall not be less than 300°F with total distillation (dry point) before 450°F (ASTM D 850). The Contractor is cautioned that a normal kerosene or range oil cut may not be suitable.

2.04 GROUND RUBBER COMPONENTS

A. For Method A. The rubber shall meet the following physical and chemical requirements:

1. Composition. The rubber shall be a dry, free flowing blend of 40 Wt.% powdered devulcanized rubber and 60 Wt.% ground vulcanized rubber scrap specially selected to have a natural

rubber content of at least 40 Wt.% of the rubber. It shall be free from fabric, wire, or other contaminating materials except that up to 4 Wt.% of a mineral powder (such as calcium carbonate) may be included to prevent sticking and caking of the particles.

2. Sieve Analysis (ASTM C 136):

Sieve Number	% Passing
8	100
30	60-80
50	15-40
100	0-15

3. Chemical Analysis (ASTM D 297):

Natural Rubber Content, Wt.% 30 min.

4. Mill Test:

When 40-50 grams of rubber retained on the Number 30 sieve are added to the tight 152.4 mm rubber mill, the material will band on the mill roll in one pass, and will usually be retained on the mill roll. This will indicate the presence of a sufficient quantity of reclaimed devulcanized rubber.

B. For Method B. The rubber shall be a ground tire rubber, 100% vulcanized, recommended by the Contractor for this use and with the approval of the Engineer and meeting the following requirements:

1. Composition. The rubber shall be ground tire rubber, dry and free flowing. The specific gravity of the rubber shall be 1.15 $\pm$ 0.05 and shall be free from fabric, wire, or other contaminating materials except that up to 4 Wt.% of a mineral powder (such as calcium carbonate) may be included to prevent sticking together of the particles.

2. Sieve Analysis (ASTM C 136):

Sieve Number	% Passing
8	100
10	98-100
30	0-10
50	0-2

2.05 AGGREGATES

Aggregates shall be a dry, clean material meeting the requirements of AASHTO M 283-81 and the additional requirements listed below:

A. Only crushed stone or slag will be acceptable (hot or precoated aggregates, if used, will be by special provisions in the contract documents).

B. The aggregate shall not contain more than 5 Wt.% chert or other known stripping material.

C. Gradation shall be according to ASTM D 448-80, Size 7 with the addition that no more than 1 Wt.% shall pass the Number 50 sieve.

D. The aggregate shall be essentially free of deleterious material such as thin, elongated pieces, dirt, dust, and shall contain not more than 1 Wt.% water (ASTM C 566).

2.06 CERTIFICATION AND QUALITY ASSURANCE

Prior to production, the Contractor shall submit certification of specification compliance for all materials to be used in the work. Also certification shall be submitted concerning the design of the asphalt-rubber blend as follows:

A. Method A. The Contractor shall submit certification that the asphalt cement is compatible with the rubber and has been tested to determine the quantity of extender oil (usually 1 to 7 Wt.%) required and that the proposed percentage will produce an absolute viscosity of the blended materials of 600 to 2000 poises at 140°F

when tested in accordance with the requirements of AASHTO T 202-80. New certifications will be required if the asphalt cement lot or source is changed.

B. Method B. The Contractor shall submit certifications that the asphalt cement is compatible with the rubber. New certifications will be required if the asphalt cement lot is changed.

3. EQUIPMENT

3.01 PRE-BLENDING

Rubber and a portion of the asphalt for the asphalt-rubber blend shall be preblended in a master batch prior to introduction of the master batch to the distributor. The master batch can be diluted with additional asphalt and additives in the distributor to the formulation recommended by the Supplier.

4. PRODUCTION DETAILS

4.01 PREPARATION OF BINDER: METHOD A.

A. Preparation of Asphalt-Extender Oil Mix Blend

Blend the preheated asphalt cement (250 to 400^{o}F), and sufficient rubber extender oil (1 to 7 Wt.%) to reduce the viscosity of the asphalt cement-extender oil blend to within the specified viscosity range. Mixing shall be thorough by recirculation, mechanical stirring, air agitation, or other appropriate means. A minimum of 400 gallons of the asphalt cement-extender oil blend shall be prepared before introduction of the rubber.

B. Preparation of Asphalt-Rubber Binder

The asphalt-extender oil blend shall be heated to within the range of 350 to 425^{o}F. The asphalt-rubber blend for the master batch shall be preblended in appropriate preblending equipment as specified by the supplier prior to introduction of the master batch

into the distributor. Addition of asphalt cement into the distributor to provide the specified formula shall be as directed by the supplier. The percentage of rubber shall be 20 to 24 Wt.% of the total blend as specified by the supplier. Recirculation shall continue for a minimum of 30 minutes after all the rubber is incorporated to insure proper mixing and dispersion. Sufficient heat should be applied to maintain the temperature of the blend between 375 and 425°F while mixing. Viscosity of the asphalt-rubber shall be less than 4000 centipoises at the time of application (ASTM D 2994 with the use of a Haake type viscometer in lieu of a Brookfield Model LVF or LVT if desired).

4.02 PREPARATION OF BINDER: METHOD B.

A. Preparation of the Asphalt-Rubber Blend - Mixing

The asphalt cement shall be preheated to within the range of 350 to 450°F. The asphalt-rubber blend for the master batch shall be preblended in appropriate preblending equipment as specified by the supplier prior to introduction of the master batch into the distributor. Addition of asphalt cement and diluent into the distributor to provide the specified formula shall be as directed by the supplier. The percentage of rubber shall be 20 to 24 Wt.% of the total asphalt-rubber mixture (including diluent). Mixing and recirculation shall continue until the consistency of the mixture approaches that of a semi-fluid material (i.e., reaction is complete). At the lower temperature, it will require approximately 30 minutes for the reaction to take place after the start of the addition of rubber. At the higher temperature, the reaction will take place within approximately five minutes; therefore, the temperature used will depend on the type of application and the methods used by the Contractor. Viscosity of the asphalt-rubber shall be less than 4000 centipoises at the time of application (ASTM D 2994 with the use of a Haake type viscometer in lieu of a

Brookfield Model LVF or LVT if desired). After reaching the proper consistency, application shall proceed immediately.

B. Adjustment to Mixing Viscosity with Diluent

After the full reaction described in MIXING (4.02) above has occurred, the mix can be diluted with a kerosene type diluent. The amount of diluent used shall be less than 7.5 percent by volume of the hot asphalt rubber composition as required for adjusting viscosity for better wetting of the aggregate. Temperature of the hot composition shall not exceed the kerosene initial boiling point at the time of adding the diluent.

4.03 JOB DELAYS

Prior to preparation or use of asphalt-rubber (prepared by either Method A or B) maximum holdover times due to job delays (time of application after completion of reaction) to be allowed will be agreed upon between the Contractor, Supplier, and Engineer. However, holdover times in excess of 16 hours will not be allowed at temperatures above 290°F. Retempering including reheating and the addition of asphalt, rubber or diluent (kerosene/extender oil) will be allowed with the approval of the Engineer.

4.04 APPLICATION OF BINDER

The binder material shall be applied at a temperature of 375 to 425°F for Method A and 290 to 350°F for Method B at a rate specified by the Engineer.

5. METHOD OF MEASUREMENT

The asphalt-rubber binder will be measured by the number of tons of material actually used.

6. BASIS OF PAYMENT

The unit price bid per ton shall include the cost of furnishing all material, all labor and equipment necessary to complete the work.

APPENDIX B

Changes To Asphalt Concrete Mix Design Procedures And Construction Guideline For Use Of Asphalt-Rubber Concrete As A Pavement Material

APPENDIX B. CHANGES TO ASPHALT CONCRETE MIX DESIGN PROCEDURES AND CONSTRUCTION GUIDELINES FOR USE OF ASPHALT-RUBBER CONCRETE AS A PAVEMENT MATERIAL

1. DESCRIPTION

This guide involves the mix design for asphalt-rubber concrete and the use of asphalt-rubber concrete as a pavement material. Mix design and construction experience have indicated that the same procedures as those used for other hot-mix types (in particular, for asphalt concrete) will produce an acceptable asphalt-rubber concrete pavement surface. Therefore, mix design procedures not discussed herein should follow the Marshall method of mix design as described in the Asphalt Institute's Manual MS-2 (Ref 4). Construction operations not described herein (for example, methods of mixing, placement, and compaction) should follow the regular FAA specifications for construction with asphalt concrete.

2. MODIFICATIONS TO MARSHALL MIX DESIGN METHOD FOR ASPHALT-RUBBER CONCRETE

To produce an adequate mix for asphalt-rubber concrete, the following modifications must be made to the Marshall mix design method for asphalt concrete (Ref 4):

2.01 AGGREGATE

A calculation must be performed which adjusts the aggregate blend to treat the rubber particles in the binder as an additional aggregate. If this adjusted aggregate blend is significantly different from the original aggregate blend, then the adjusted blend shall be used to combine the aggregate to produce a final blend.

2.02 MIXING AND COMPACTION TEMPERATURES

The Marshall method of mix design calls for determination of mixing and compaction temperatures to be dependent upon viscosity of the material. However, capillary tube viscometers shall not be used to measure viscosity of asphalt-rubber concrete made with ground reclaimed rubber. If viscosity is used to determine mixing and compaction temperatures, then the Schweyer rheometer, the Haake rotational viscometer, or the Brookfield viscometer may be used*.

If specific temperatures are recommended, then the mixing and compaction temperatures for mix design of asphalt-rubber concrete shall be higher than temperatures for asphalt concrete. A mixing temperature of 375°F is suggested by this study; a compaction temperature of above 325°F(163°C) is suggested.

2.03 MIXING

Mixing shall be performed using a high energy mechanical mixer.

2.04 COMPACTIVE EFFORT

A compactive effort of 75 blows per face of the specimen shall be applied, regardless of the gear level.

2.05 EXTRUSION OF SPECIMENS FROM MOLDS

Asphalt-rubber concrete specimens shall be allowed to cool to room temperature before being extruded from the molds. (The project engineer should specify a minimum cooling time; 24 hours is recommended by this study.)

---

*Personal communication with T. S. Shuler, New Mexico Engineering Research Institute, and B. M. Gallaway, Texas A&M University, March, 1987.

2.06 AIR VOID CONTENT

The upper limit on air void content shall be 8%. The lower limit specified by MS-2 (Ref 4) can remain at 3%.

3. MODIFICATIONS TO CONSTRUCTION PROCEDURES WHEN USING ASPHALT-RUBBER CONCRETE

The primary modification to construction procedures involves the temperatures at which the material is mixed, transported, placed, and compacted. Other construction procedures used for asphalt concrete have been successfully used in construction with asphalt-rubber concrete.

3.01 TEMPERATURES

It is recommended that the mixing temperature be in the range of 325-350^{o}F(163-177^{o}C).

It is recommended that compaction be allowed to control the temperatures of the materials during the placement process. The contractor shall construct a test strip which shall be tested for air void content after placement. The suggested temperature range for placement shall be "greater than 300^{o}F(149^{o}C)" and it is recommended that the initial test strip be placed at a temperature of 325^{o}F(163^{o}C) or above, if possible.

If the material cannot be sufficiently compacted at a temperature below 350^{o}F(177^{o}C), then it is recommended that the compactive effort be increased rather than increasing the temperature of the materials above 350^{o}F(177^{o}C). This is due to the high cost of heating the materials.

It is possible that 3 to 5 percent air void contents may be attained in the field, but field verification will be necessary.

3.02 SMOKE CONTROL

At the higher temperatures required for placement of asphalt-rubber concrete, the material may emit smoke. Applicable pollution control measures may need to be taken.

APPENDIX C

Permanent Deformation Analysis:
Strain Versus Cycles To Failure Plots

ASPHALT CONCRETE — AC10—1

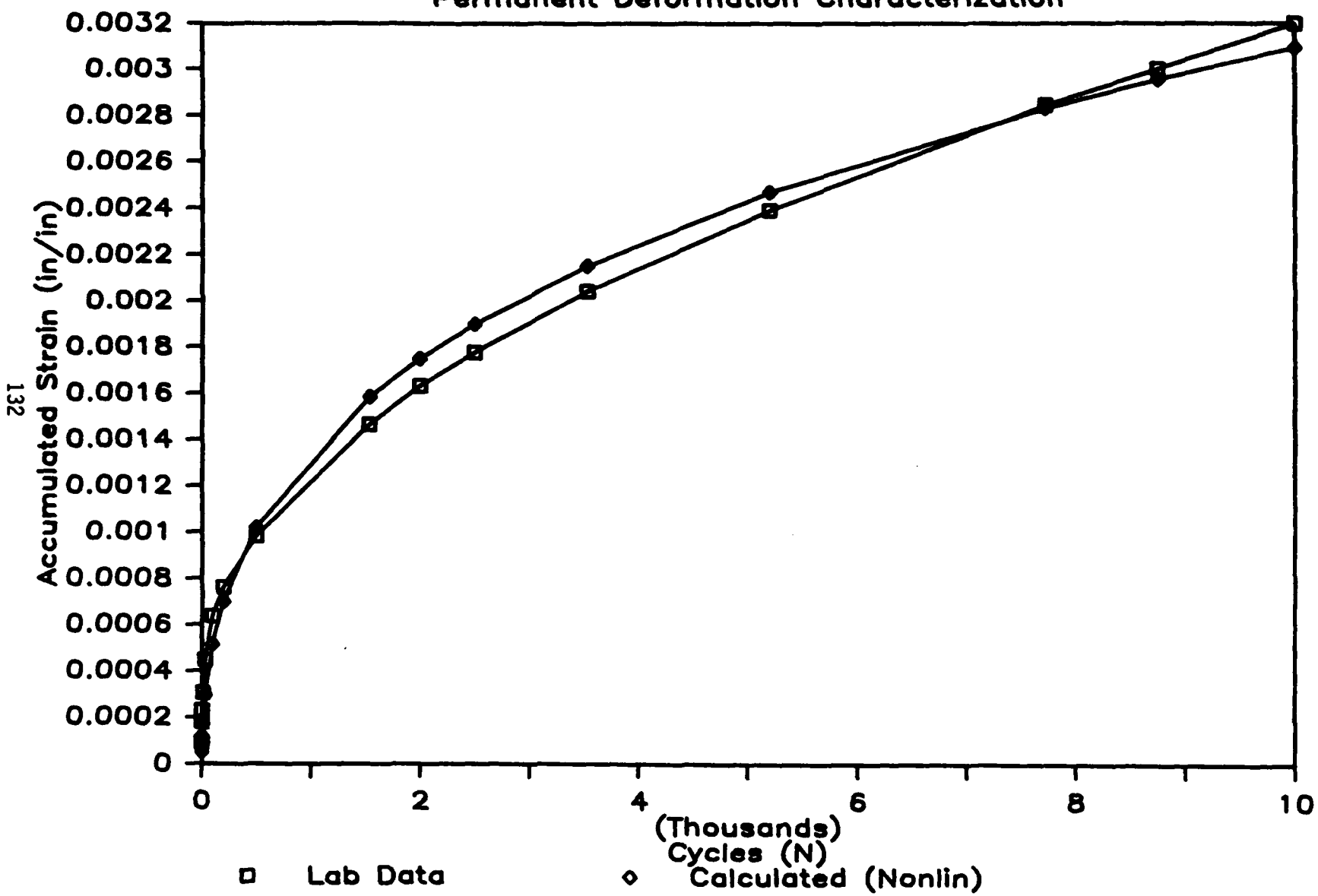

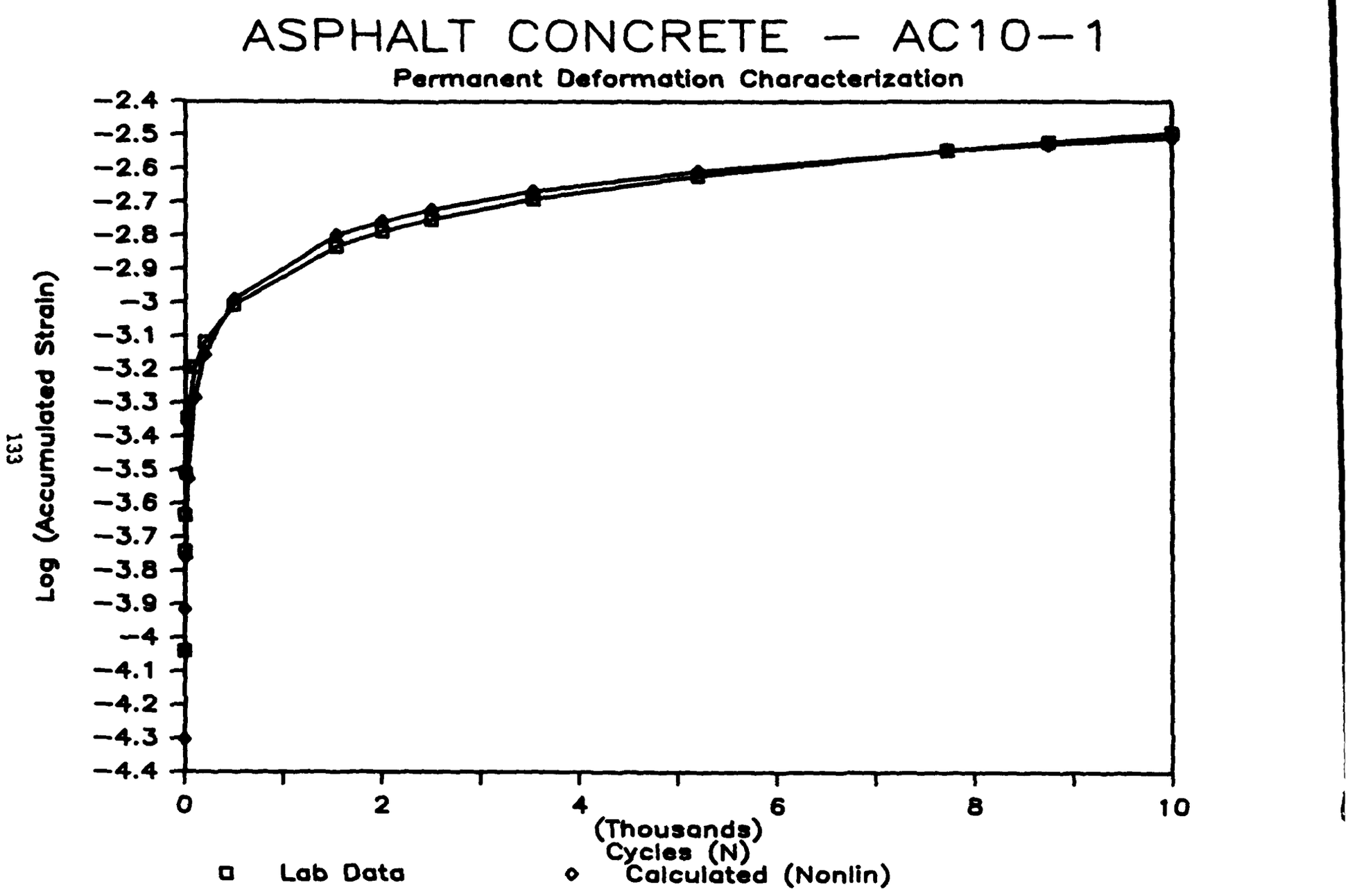
ASPHALT CONCRETE — AC10-1
Permanent Deformation Characterization
Log (Accumulated Strain)
-2.4
-2.5
-2.6
-2.7
-2.8
-2.9
-3
-3.1
-3.2
-3.3
-3.4
-3.5
-3.6
-3.7
-3.8
-3.9
-4
-4.1
-4.2
-4.3
-4.4
0
2
4
6
8
10
(Thousands)
Cycles (N)
Lab Data
Calculated (Nonlin)

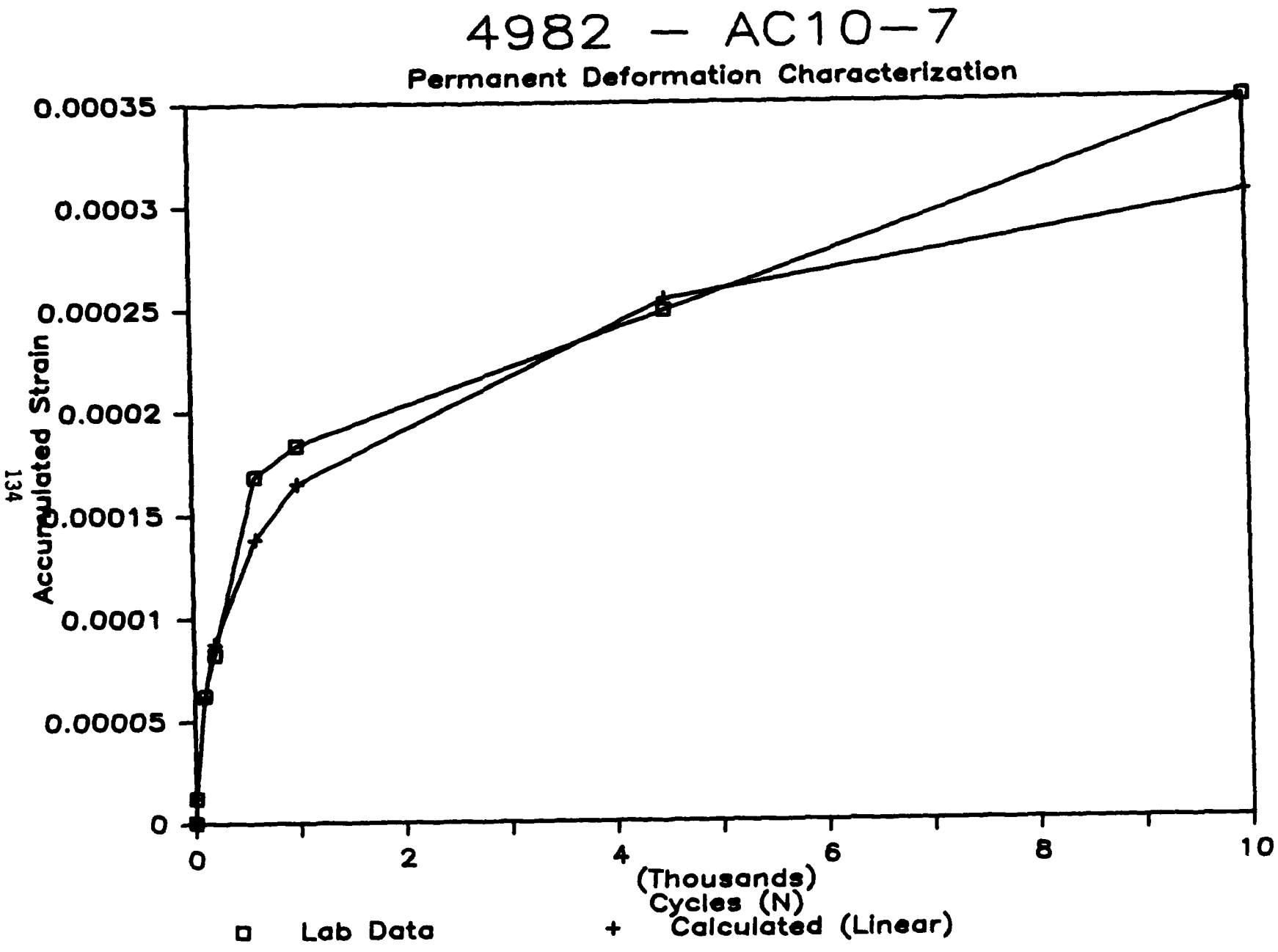
4982 – AC10–7
Permanent Deformation Characterization
0.00035
0.0003
0.00025
0.0002
0.00015
0.0001
0.00005
0
Accumulated Strain
0
2
4
6
8
10
(Thousands)
Cycles (N)
Lab Data
Calculated (Linear)

ASPHALT CONCRETE — AC10-7

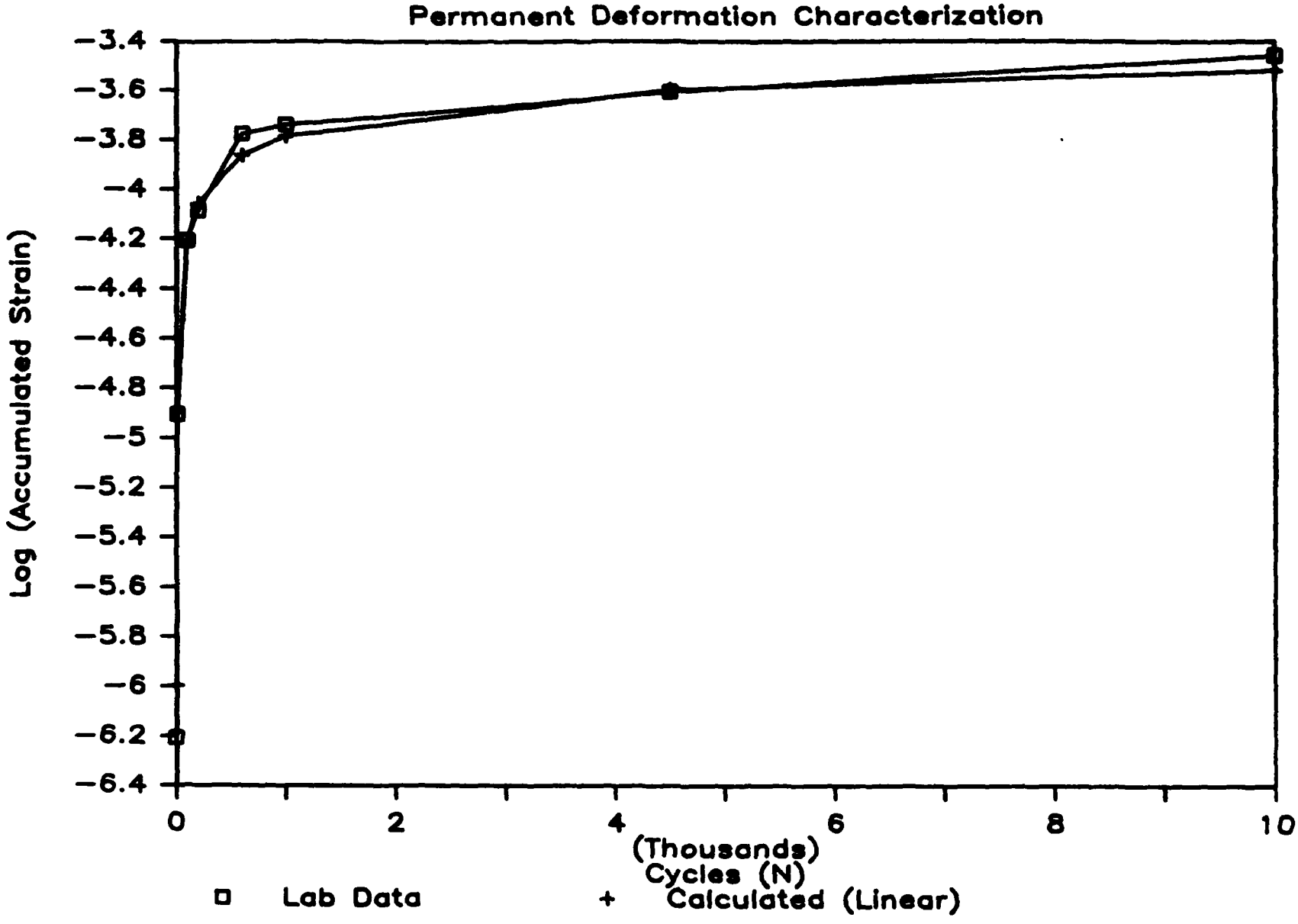

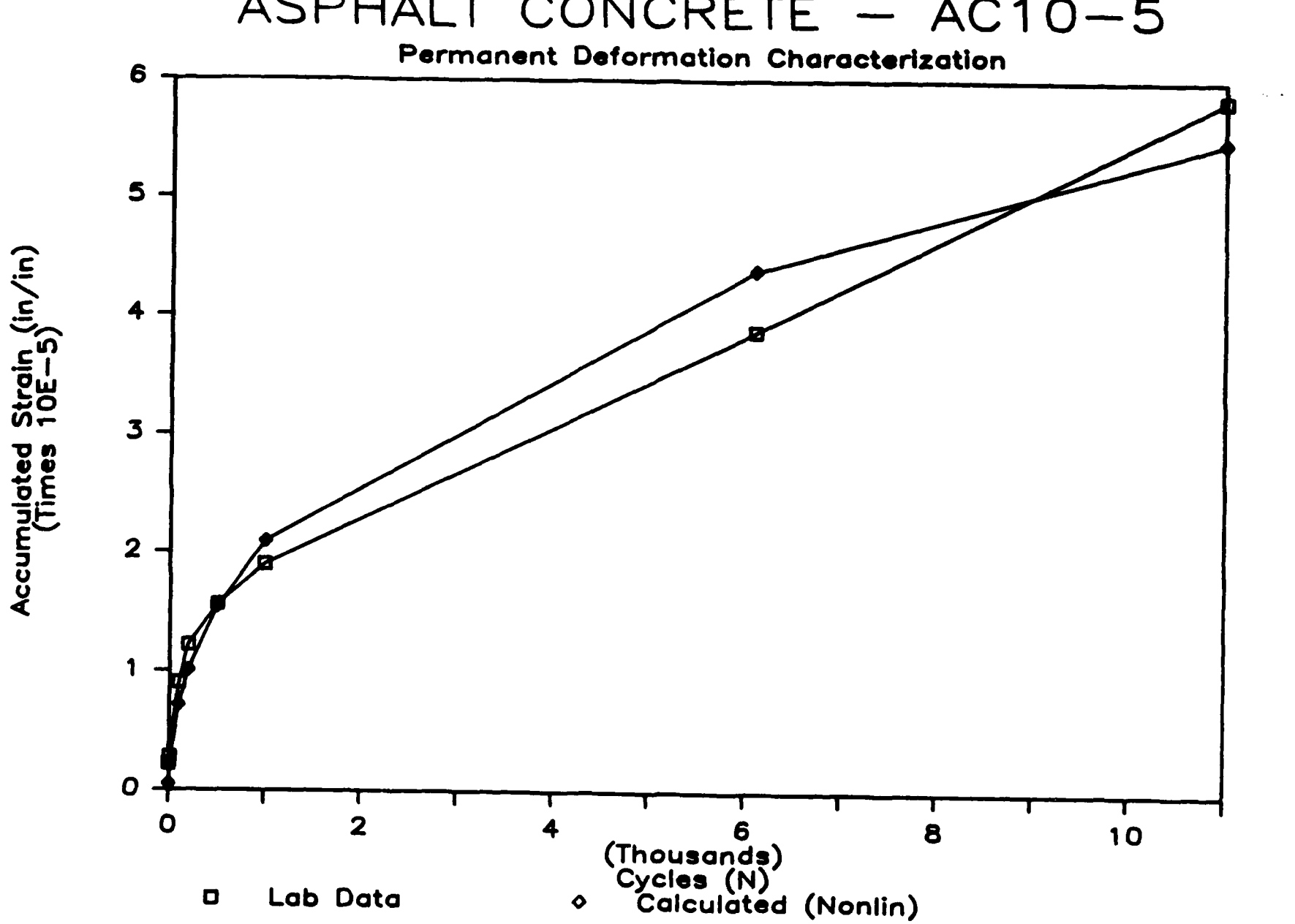
ASPHALT CONCRETE – AC10–5
Permanent Deformation Characterization
Accumulated Strain (in/in)
(Times 10E–5)
0
1
2
3
4
5
6
0
2
4
6
8
10
(Thousands)
Cycles (N)
Lab Data
Calculated (Nonlin)

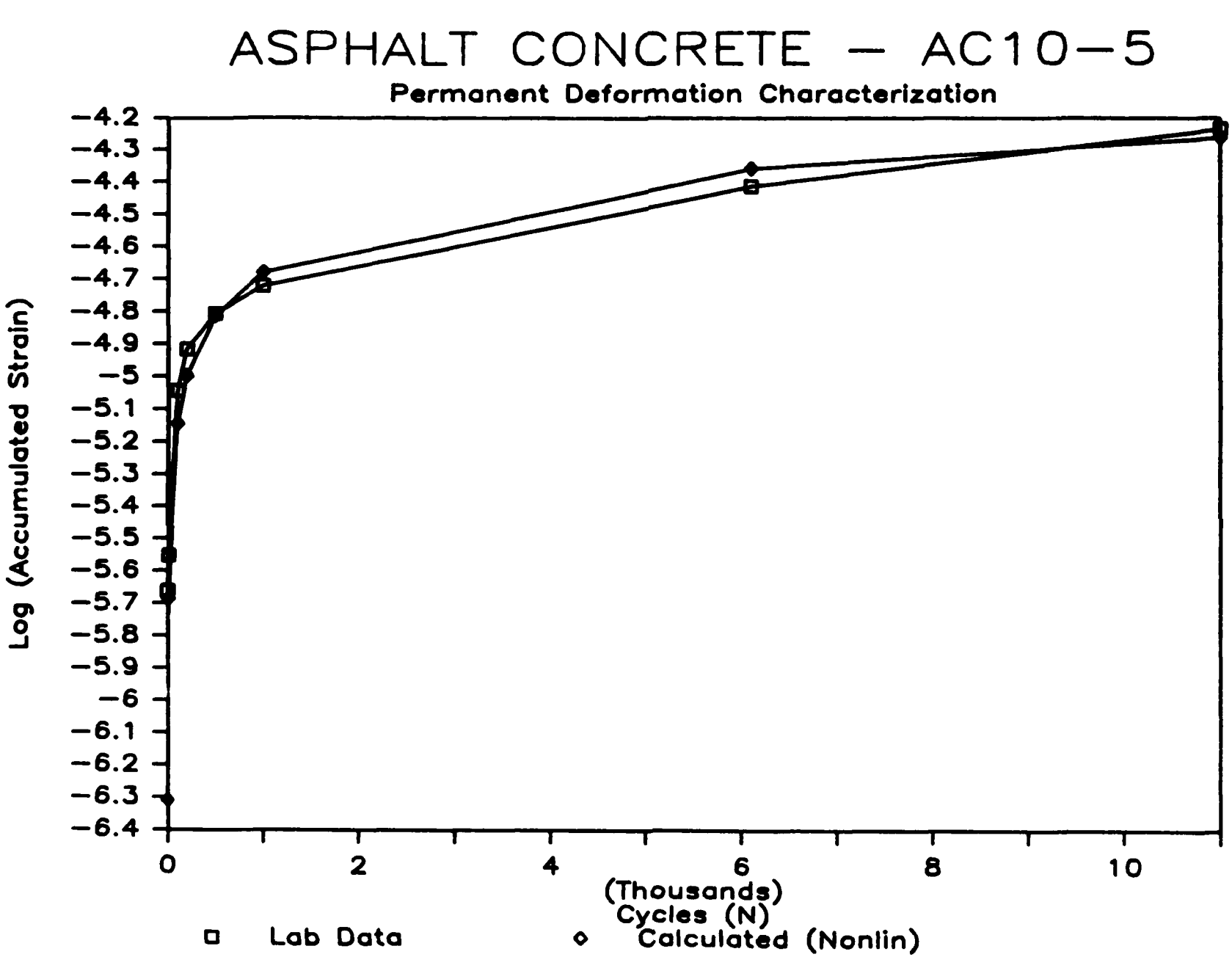
ASPHALT CONCRETE — AC10-5
Permanent Deformation Characterization
Log (Accumulated Strain)
-4.2
-4.3
-4.4
-4.5
-4.6
-4.7
-4.8
-4.9
-5
-5.1
-5.2
-5.3
-5.4
-5.5
-5.6
-5.7
-5.8
-5.9
-6
-6.1
-6.2
-6.3
-6.4
0
2
4
6
8
10
(Thousands)
Cycles (N)
Lab Data
Calculated (Nonlin)

ASPHALT RUBBER CONCRETE — AR4L

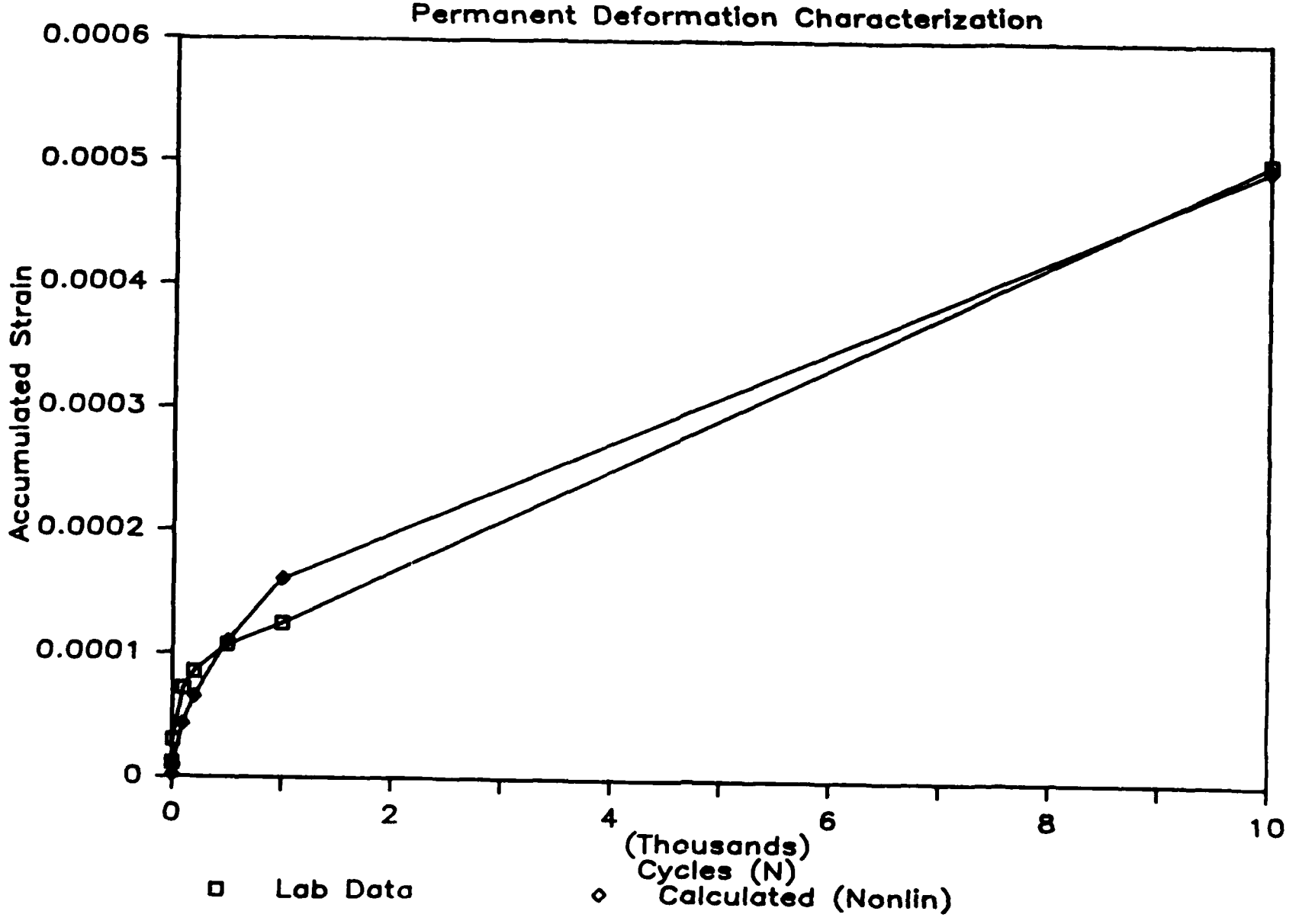

ASPHALT RUBBER — AR4L

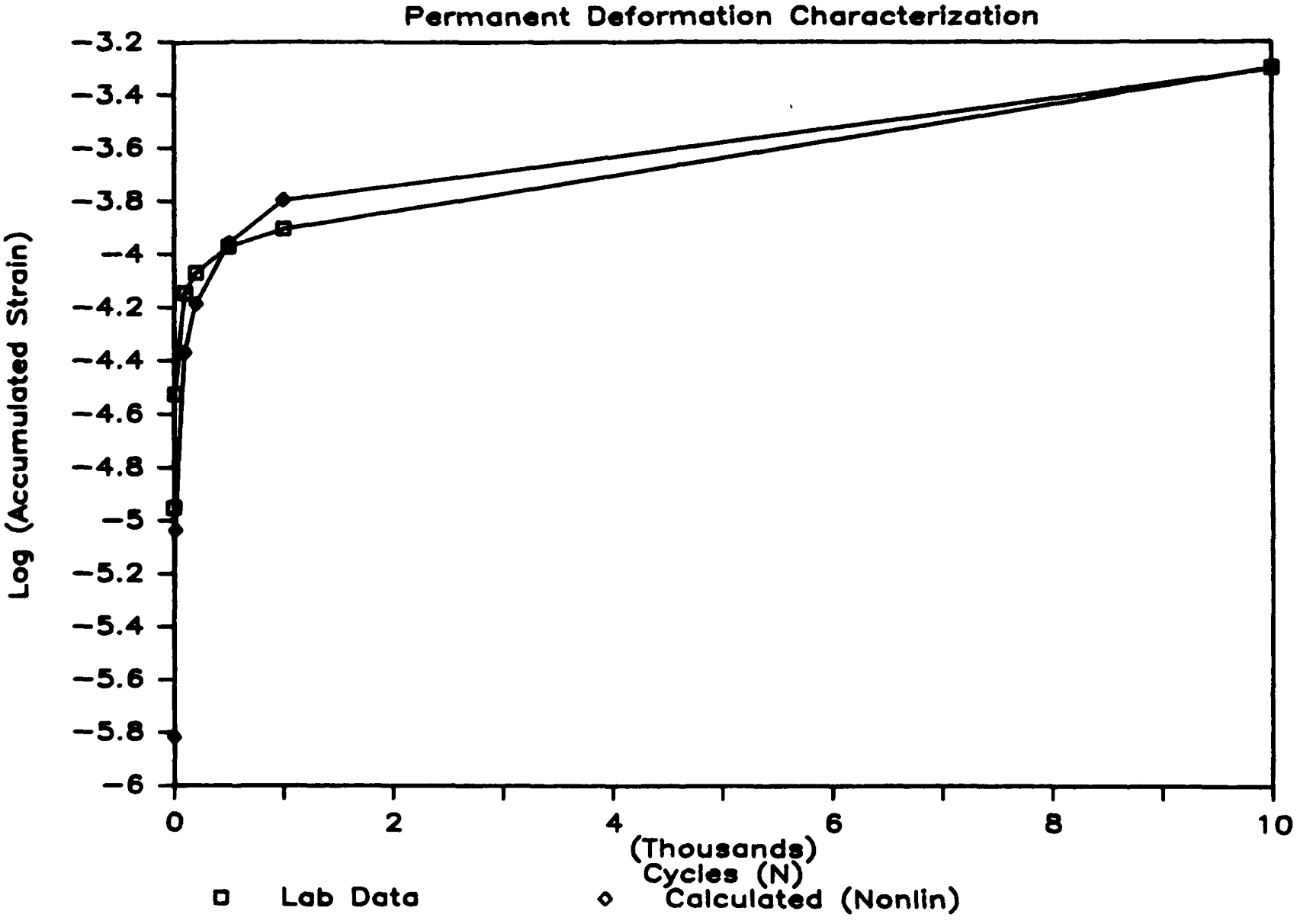

ASPHALT RUBBER CONCRETE — AR5L

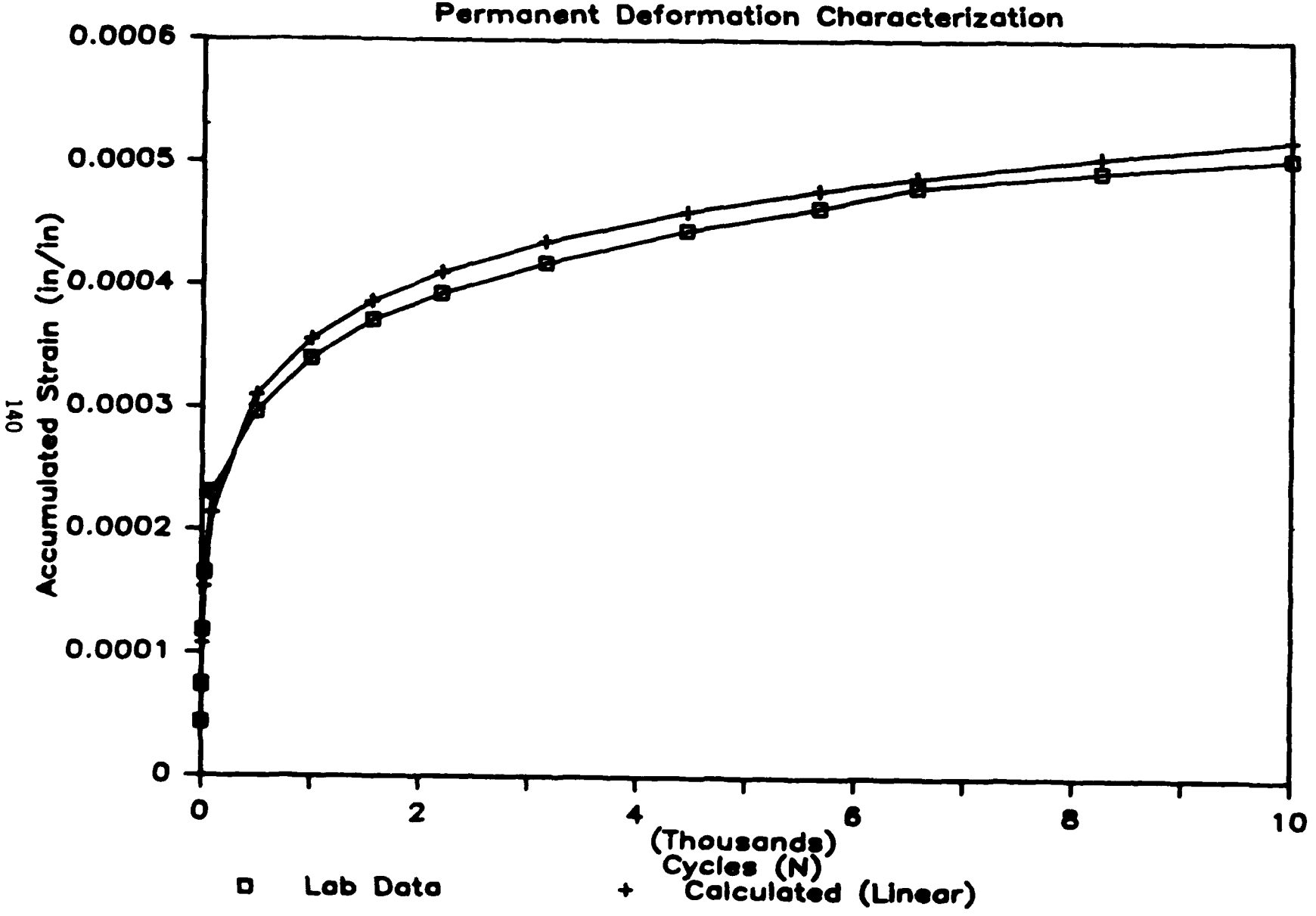

ASPHALT RUBBER CONCRETE — AR5L

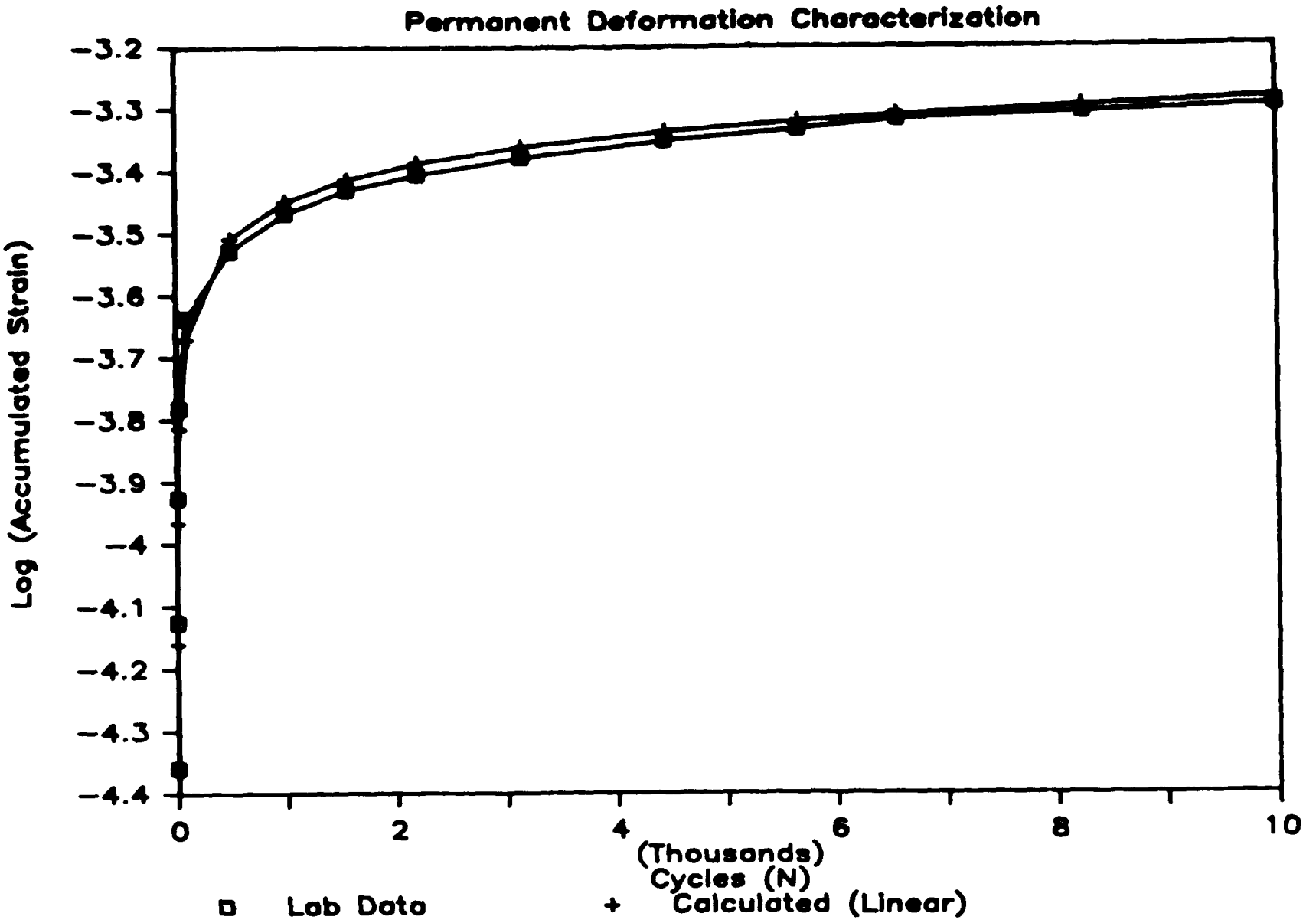

ASPHALT RUBBER CONCRETE — AR3L

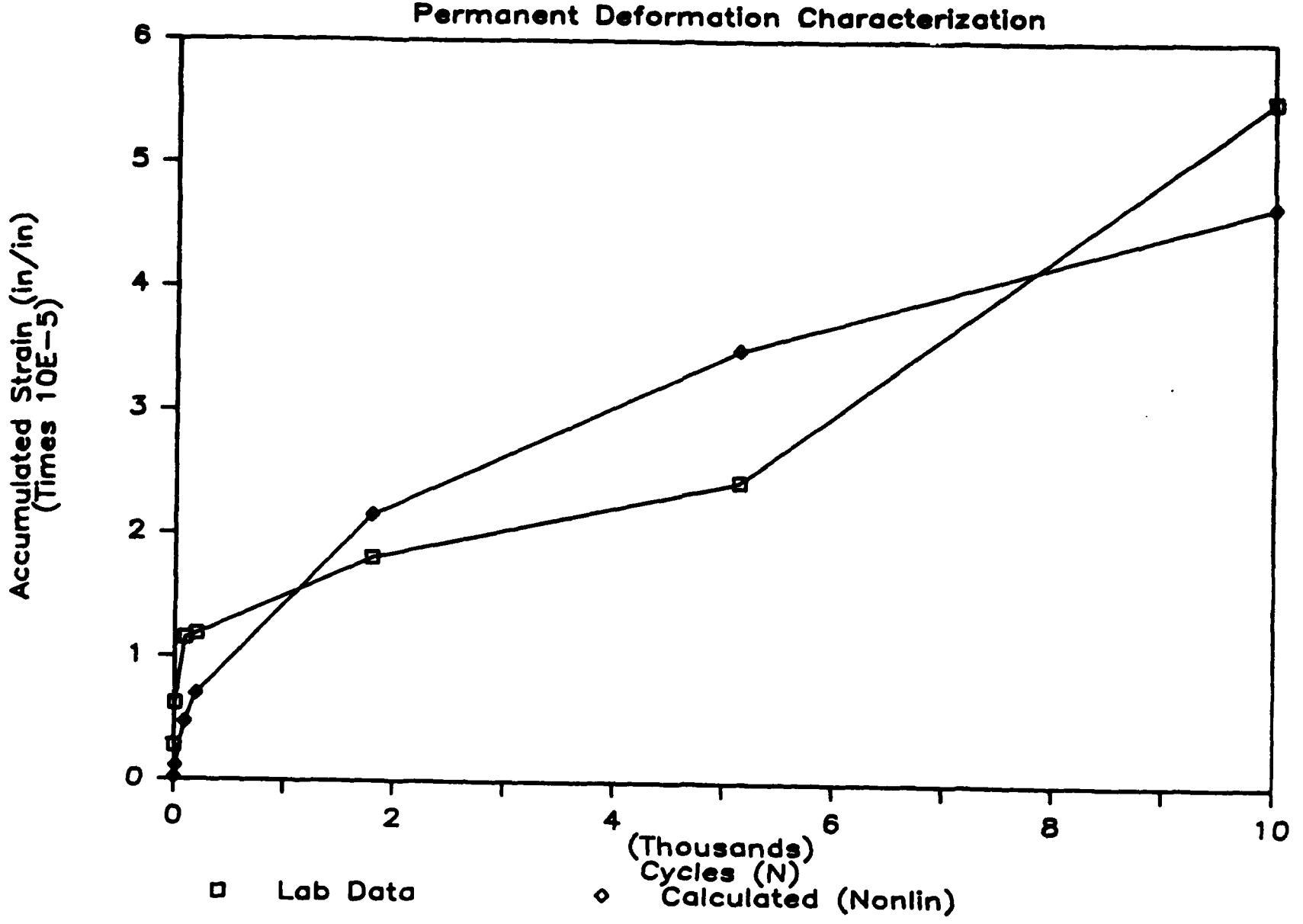

ASPHALT RUBBER CONCRETE — AR3L

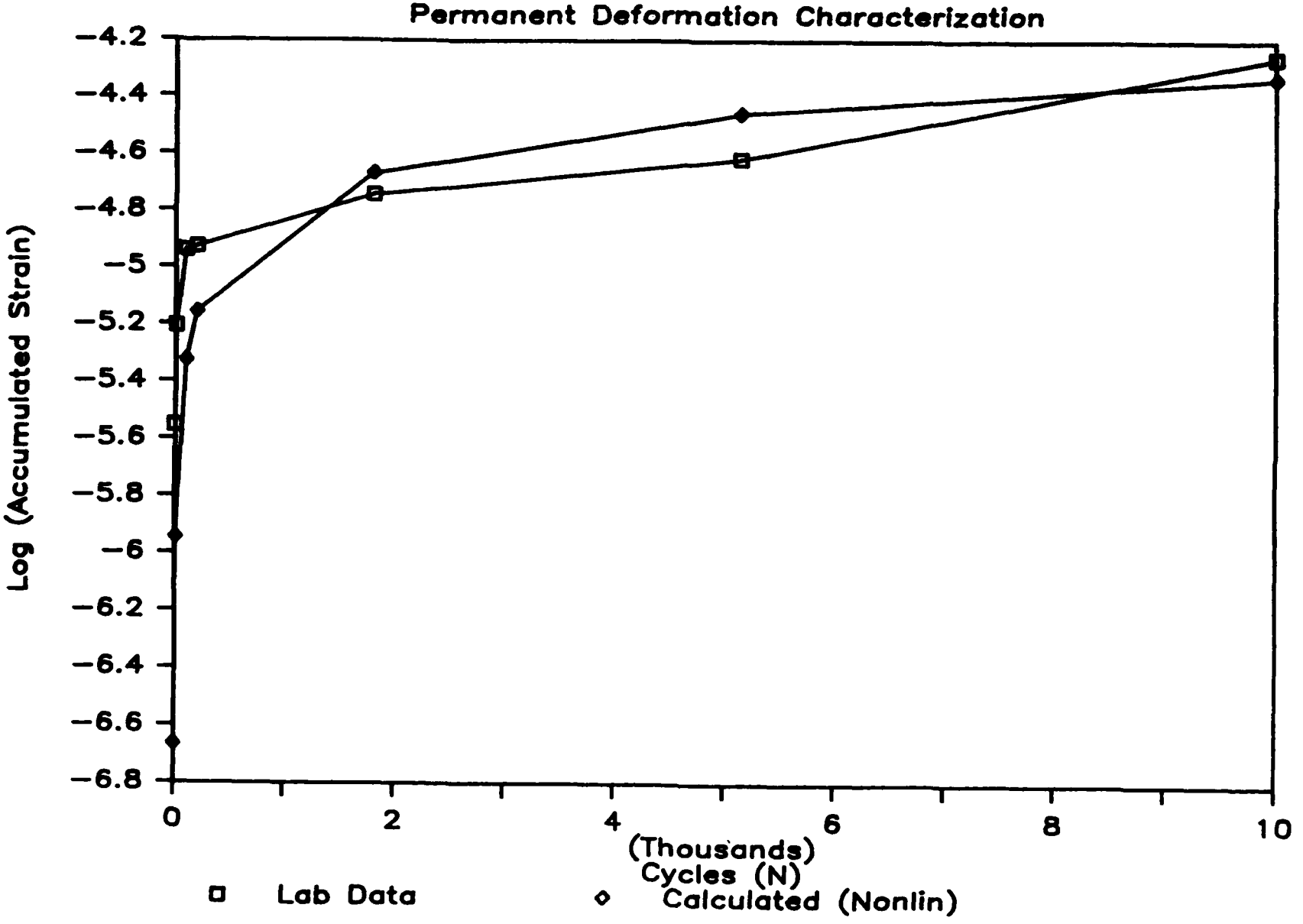

ASPHALT RUBBER CONCRETE — AR4M

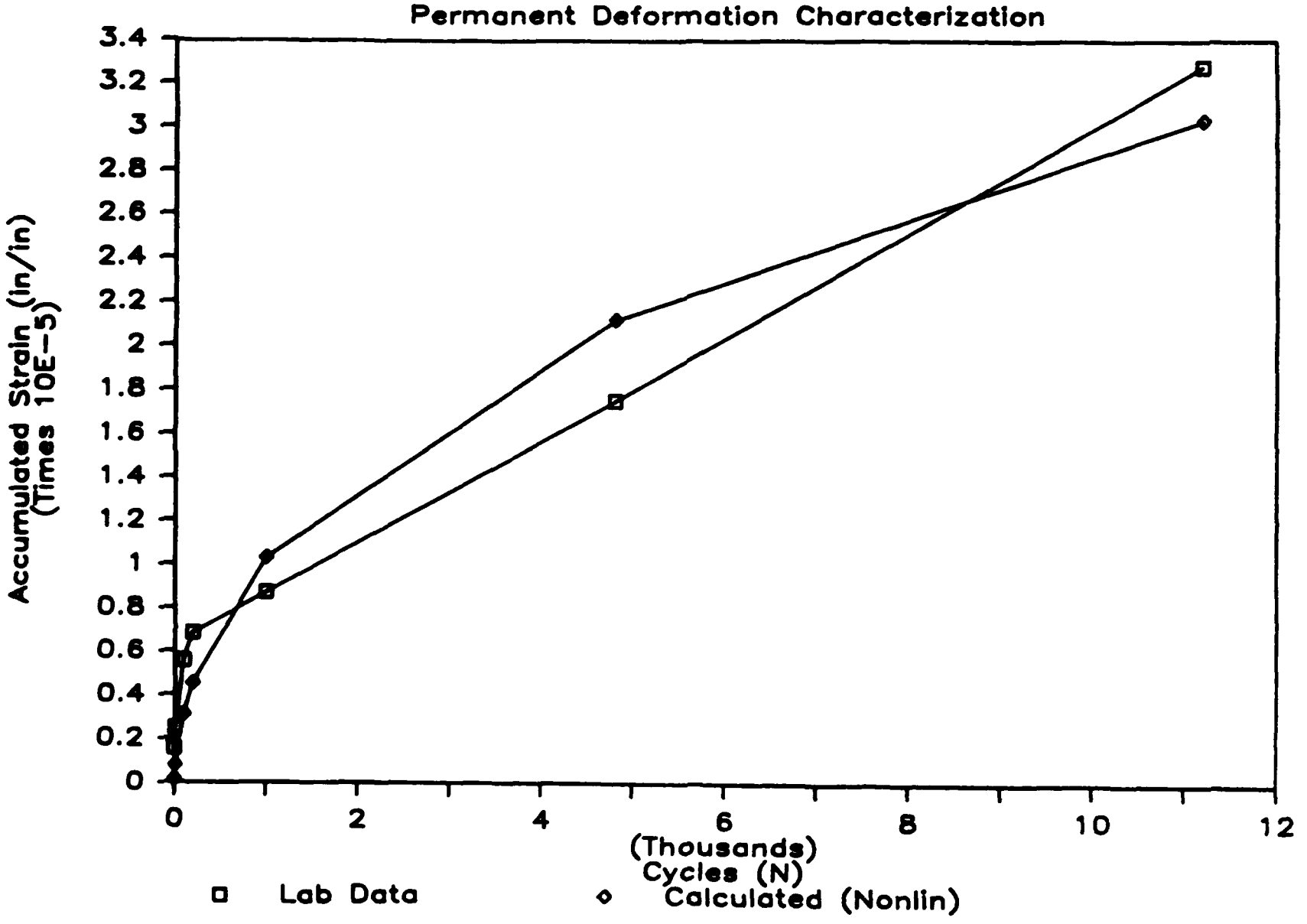

ASPHALT RUBBER CONCRETE — AR4M

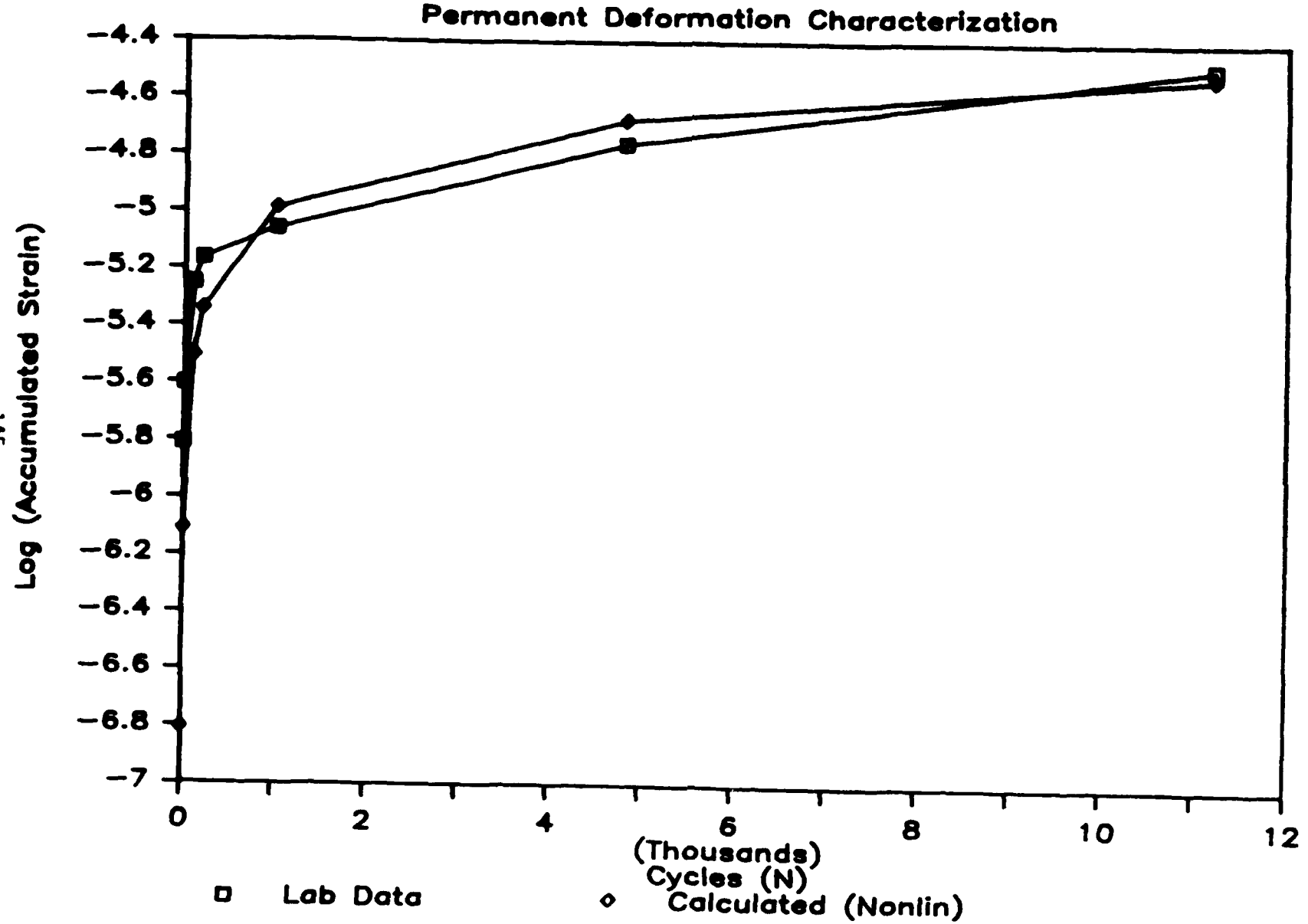

ASPHALT RUBBER CONCRETE — AR8M

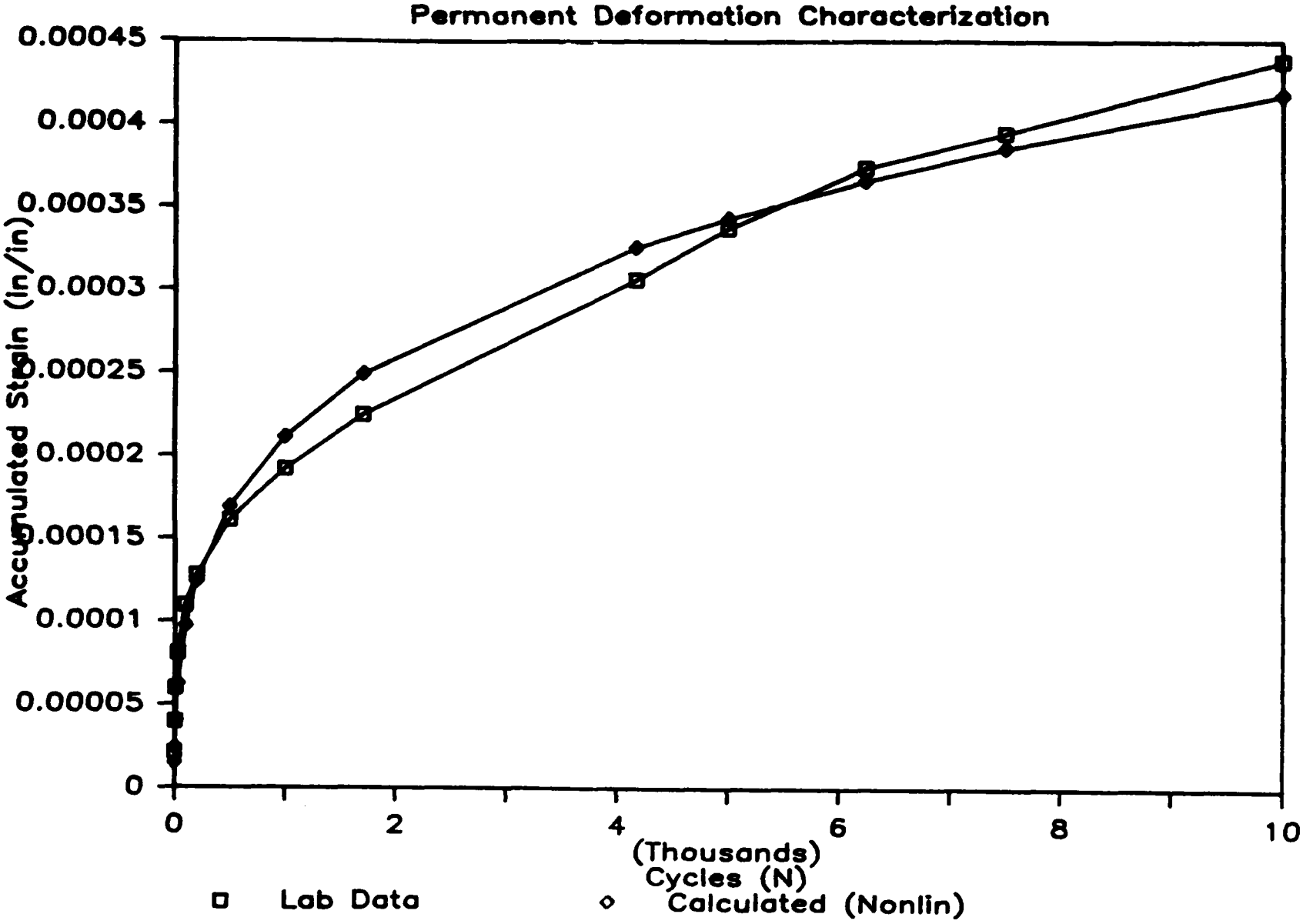

ASPHALT RUBBER CONCRETE — AR8M

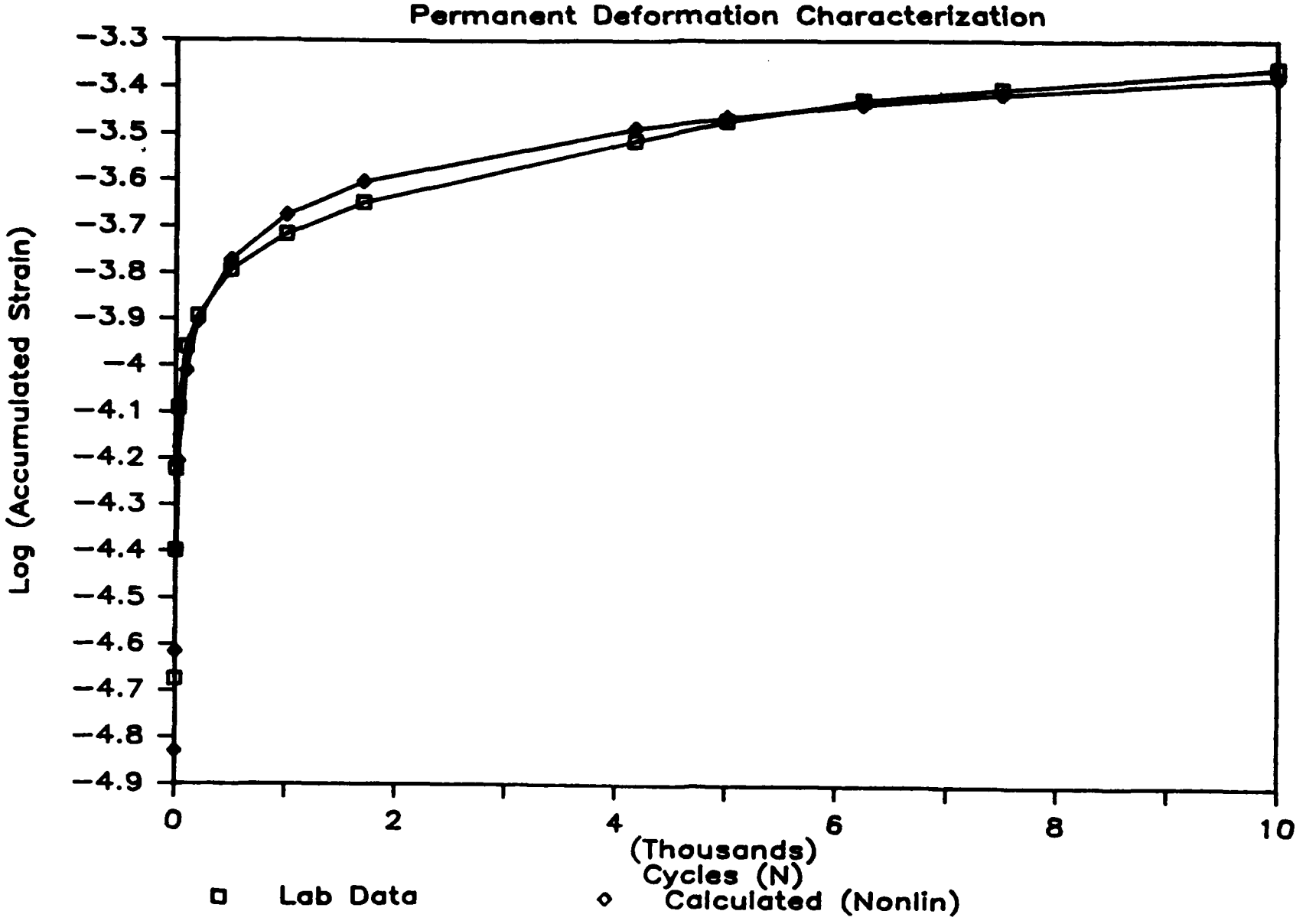

ASPHALT RUBBER CONCRETE — AR9M

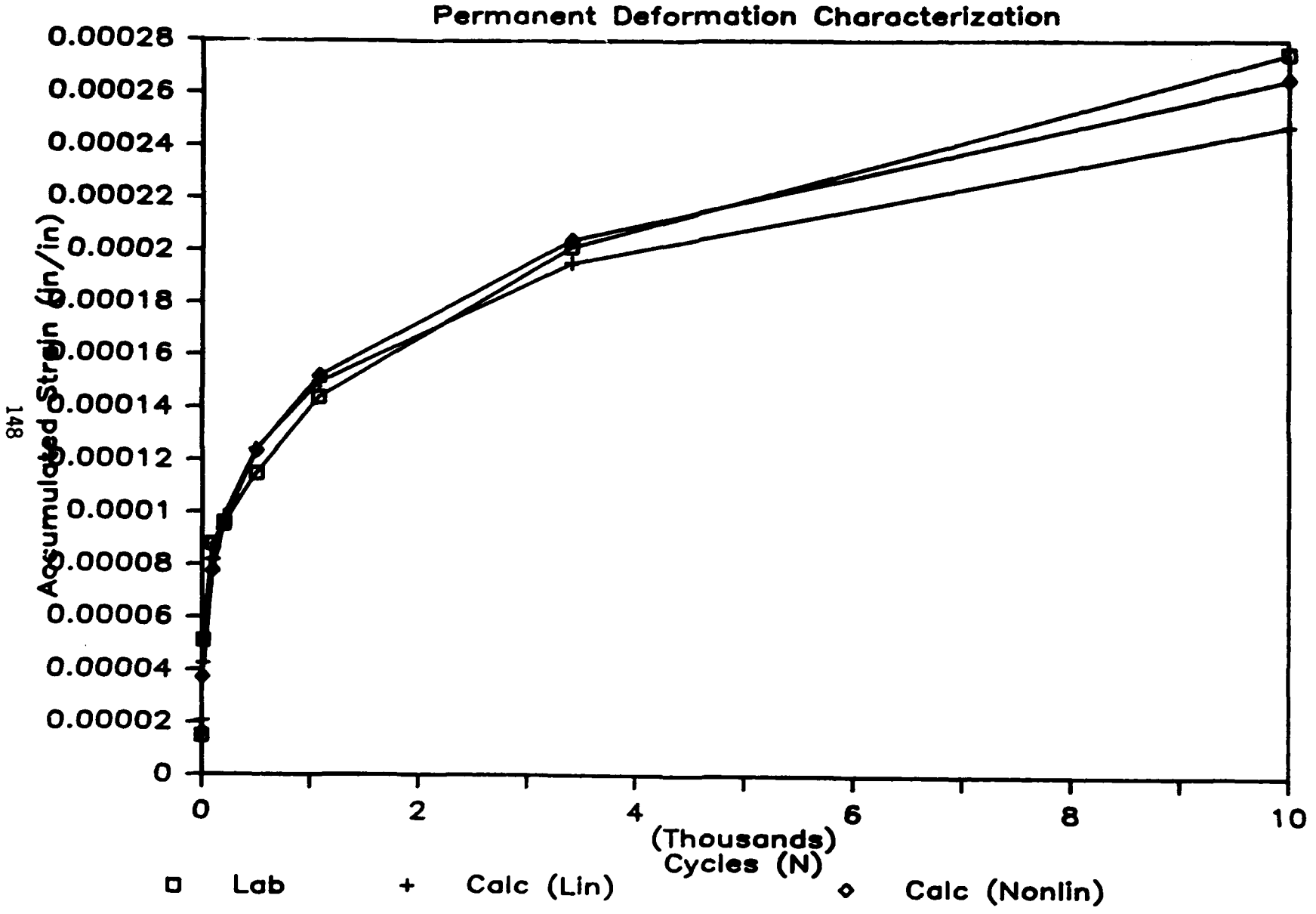

ASPHALT RUBBER CONCRETE — AR9M

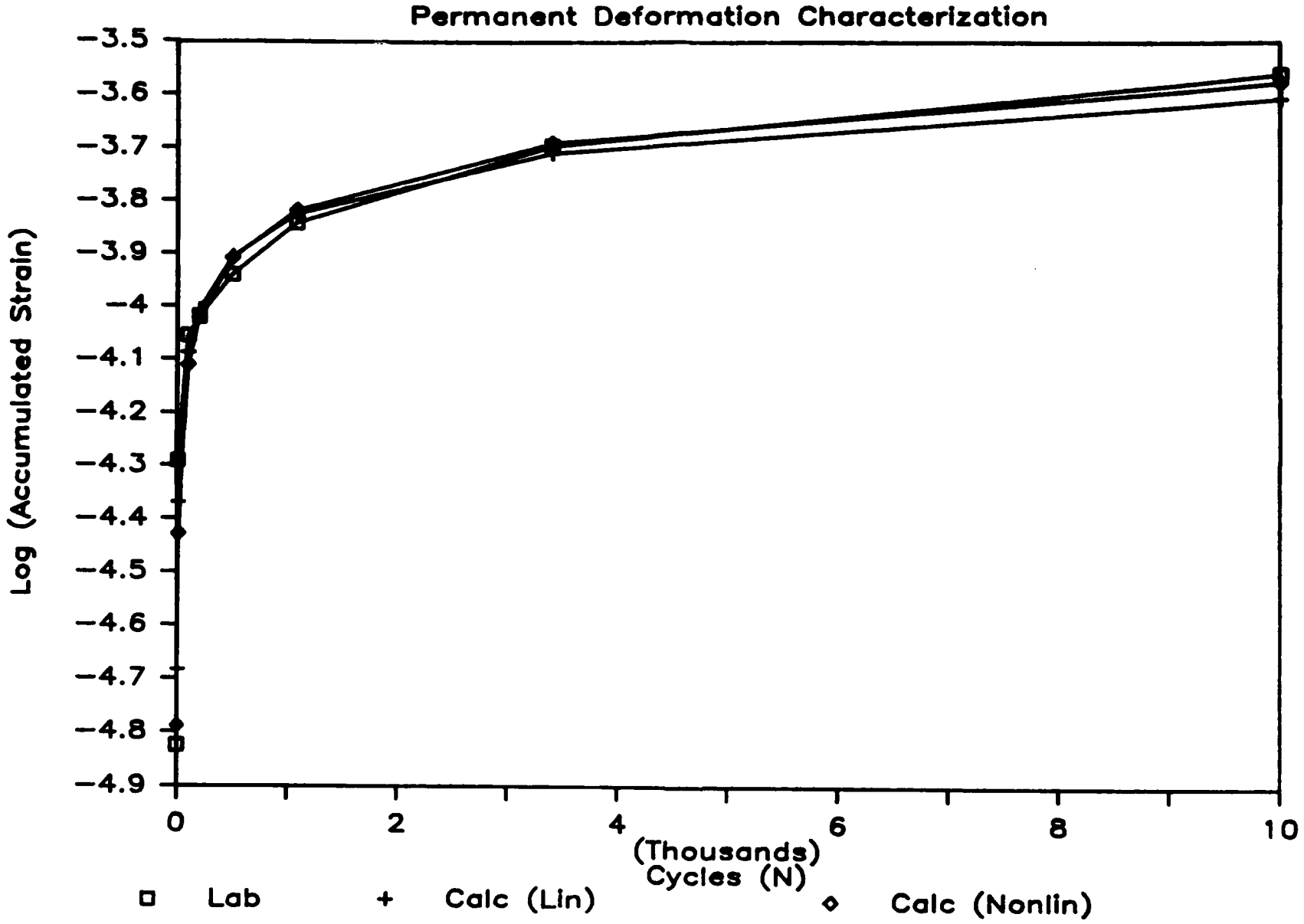

ASPHALT RUBBER CONCRETE — AR9H

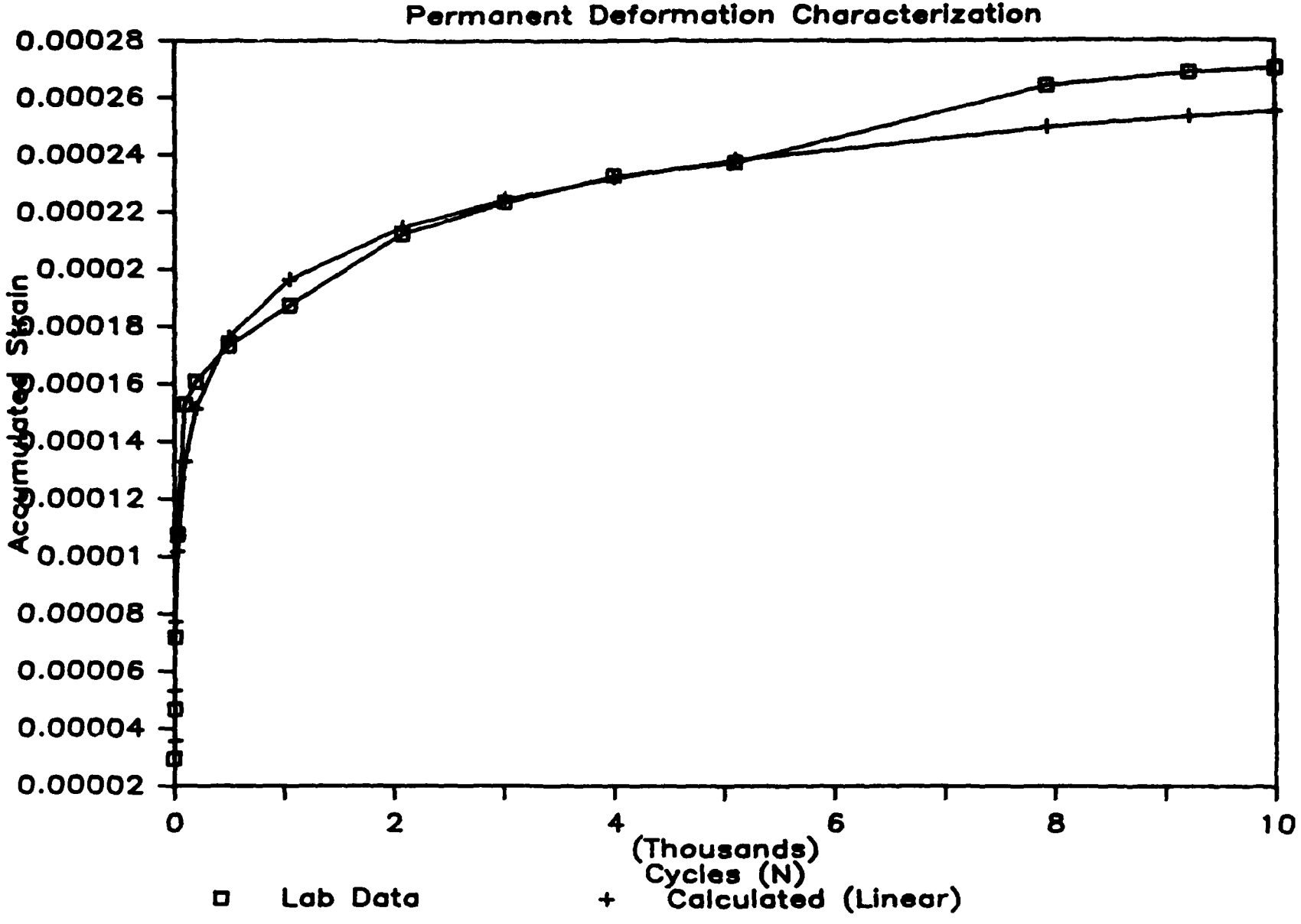

ASPHALT RUBBER CONCRETE — AR9H

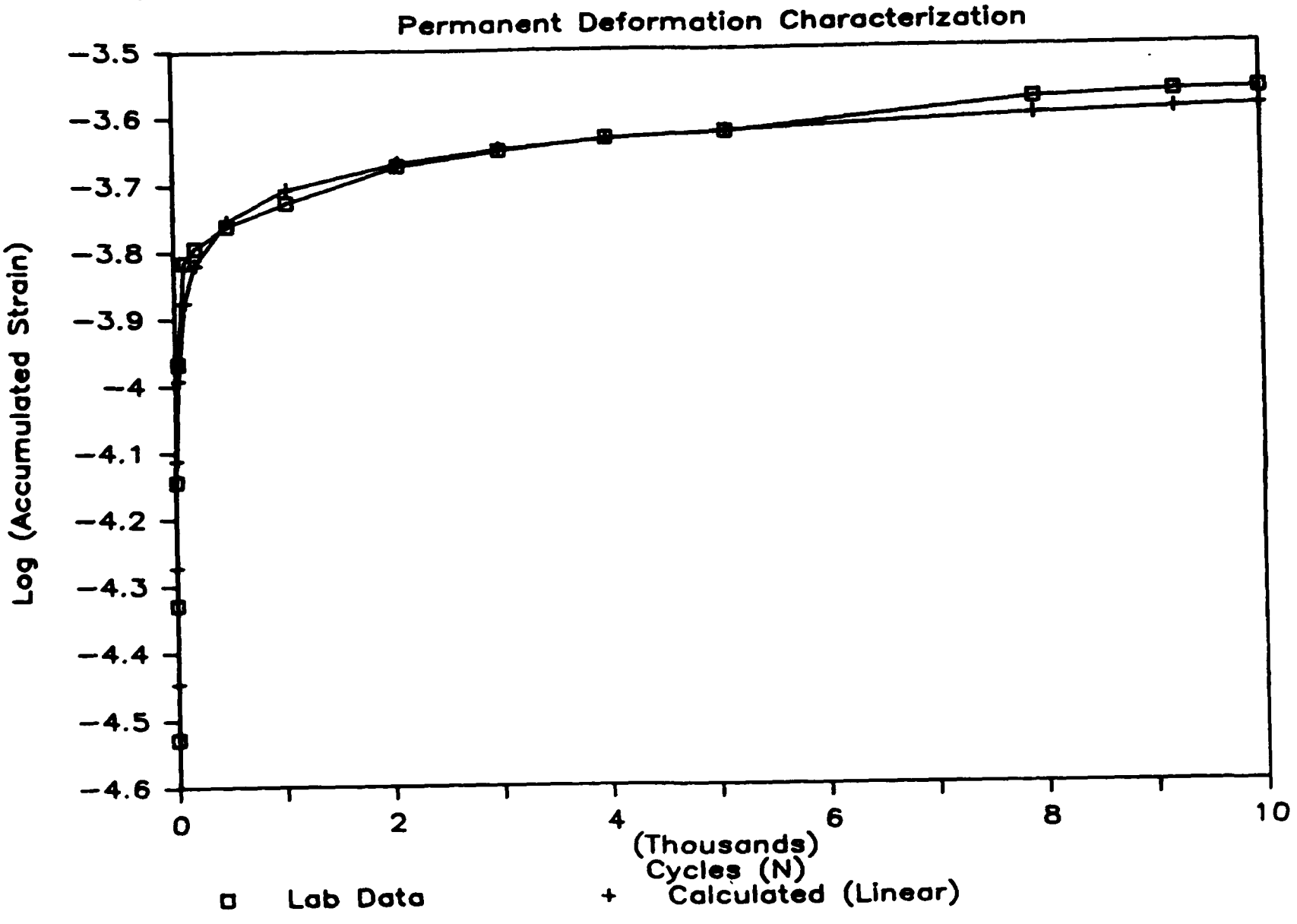

ASPHALT RUBBER CONCRETE — AR6H

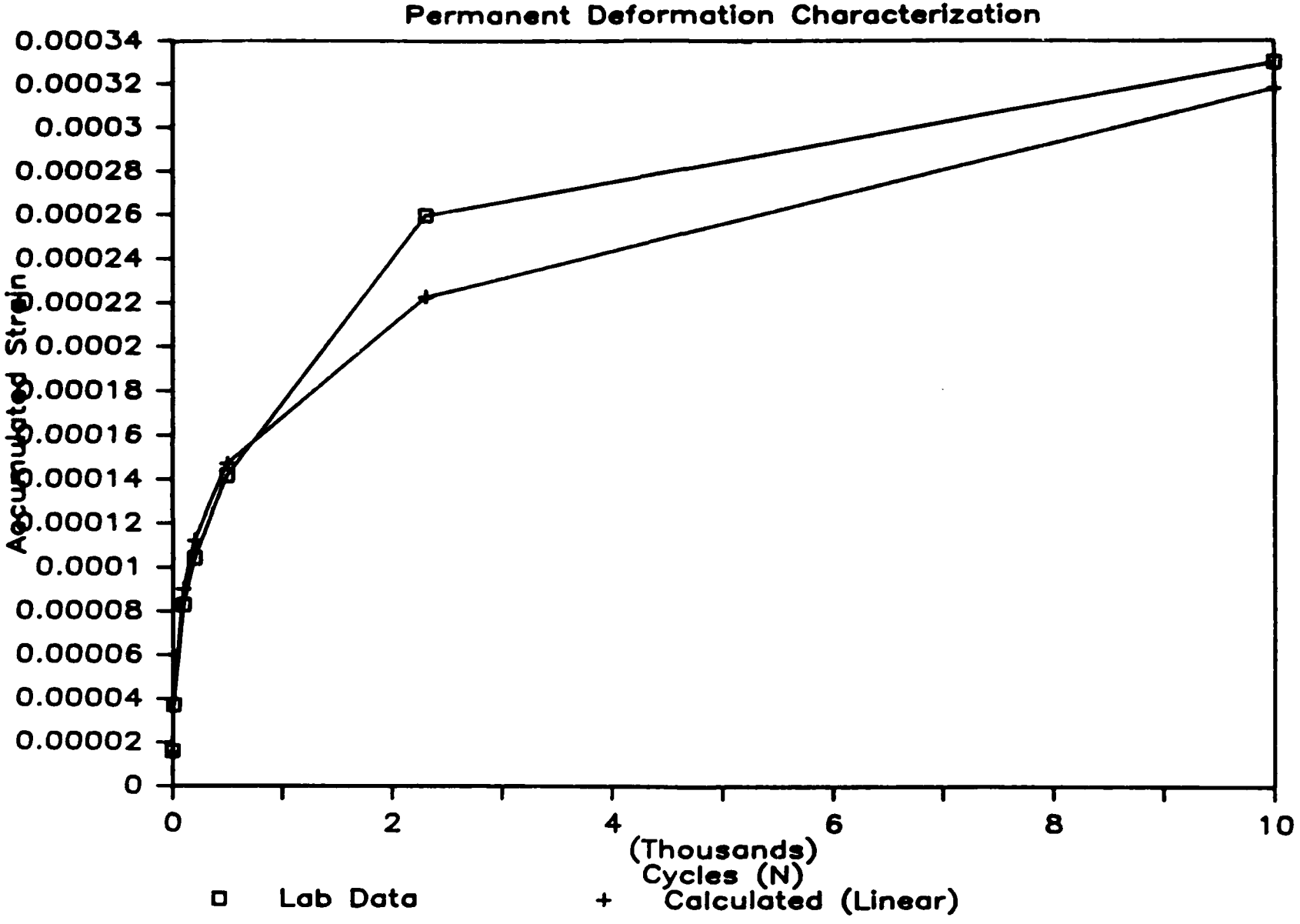

ASPHALT RUBBER CONCRETE — AR6H

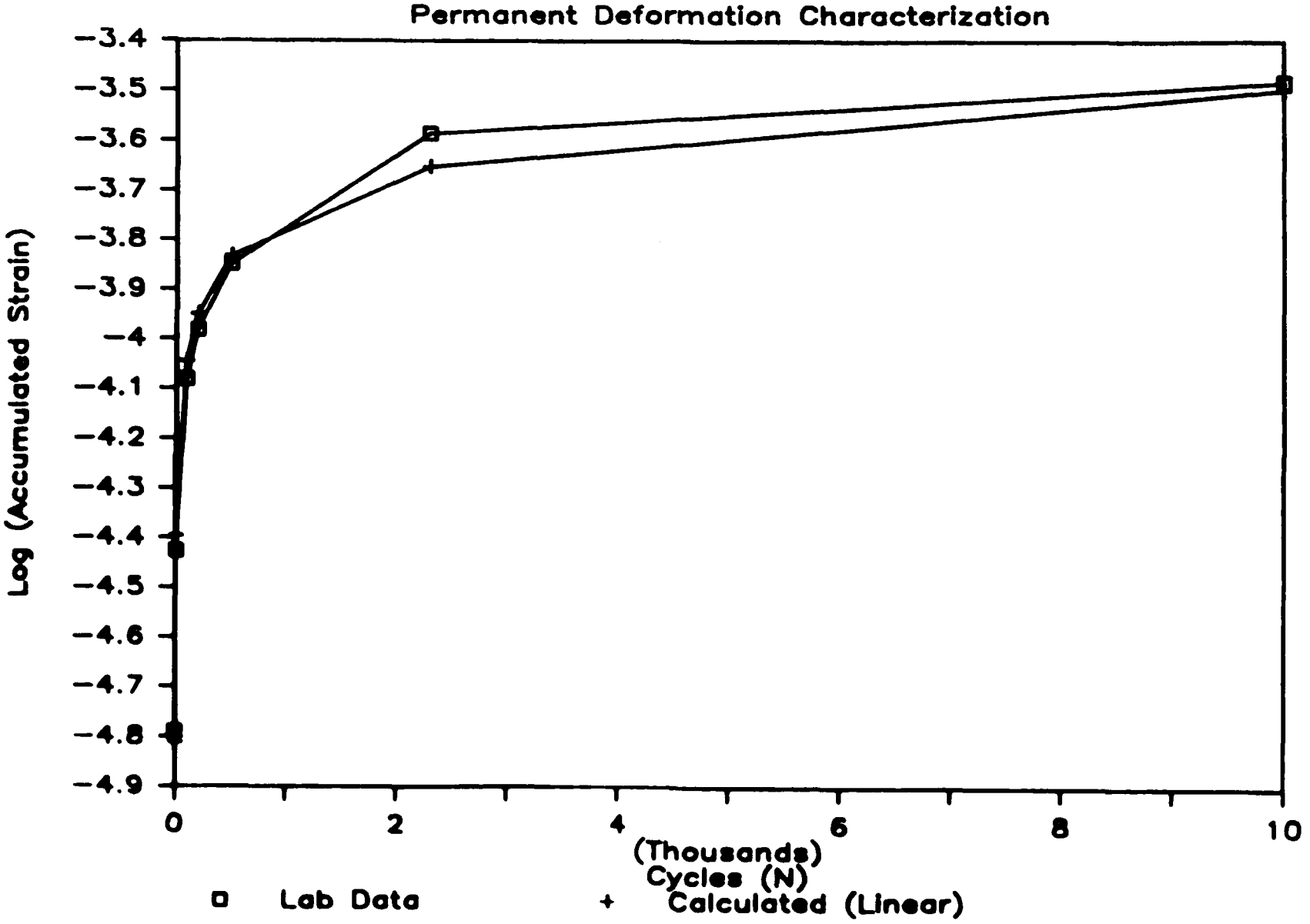

ASPHALT RUBBER CONCRETE — AR5H

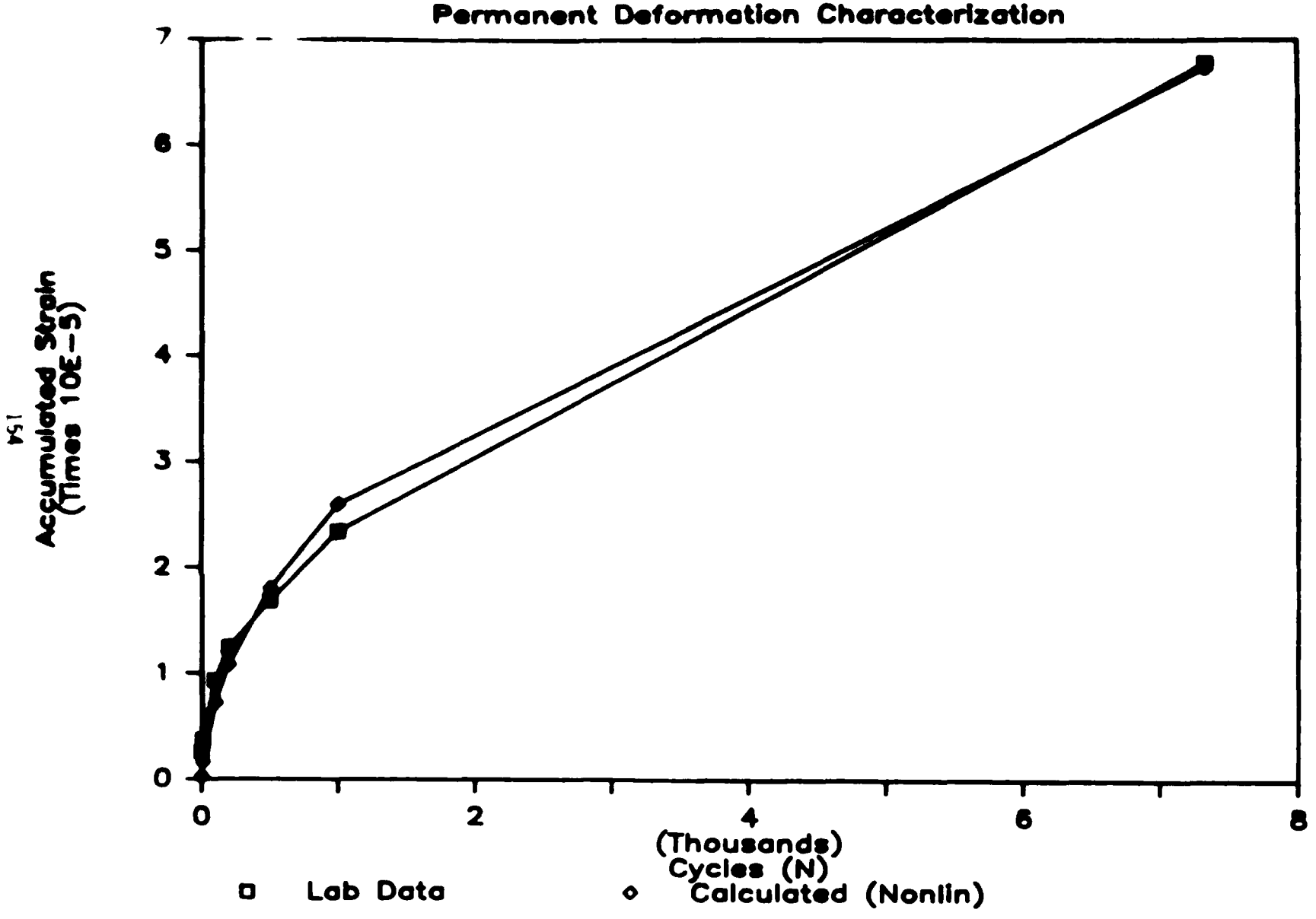

ASPHALT RUBBER CONCRETE — AR5H

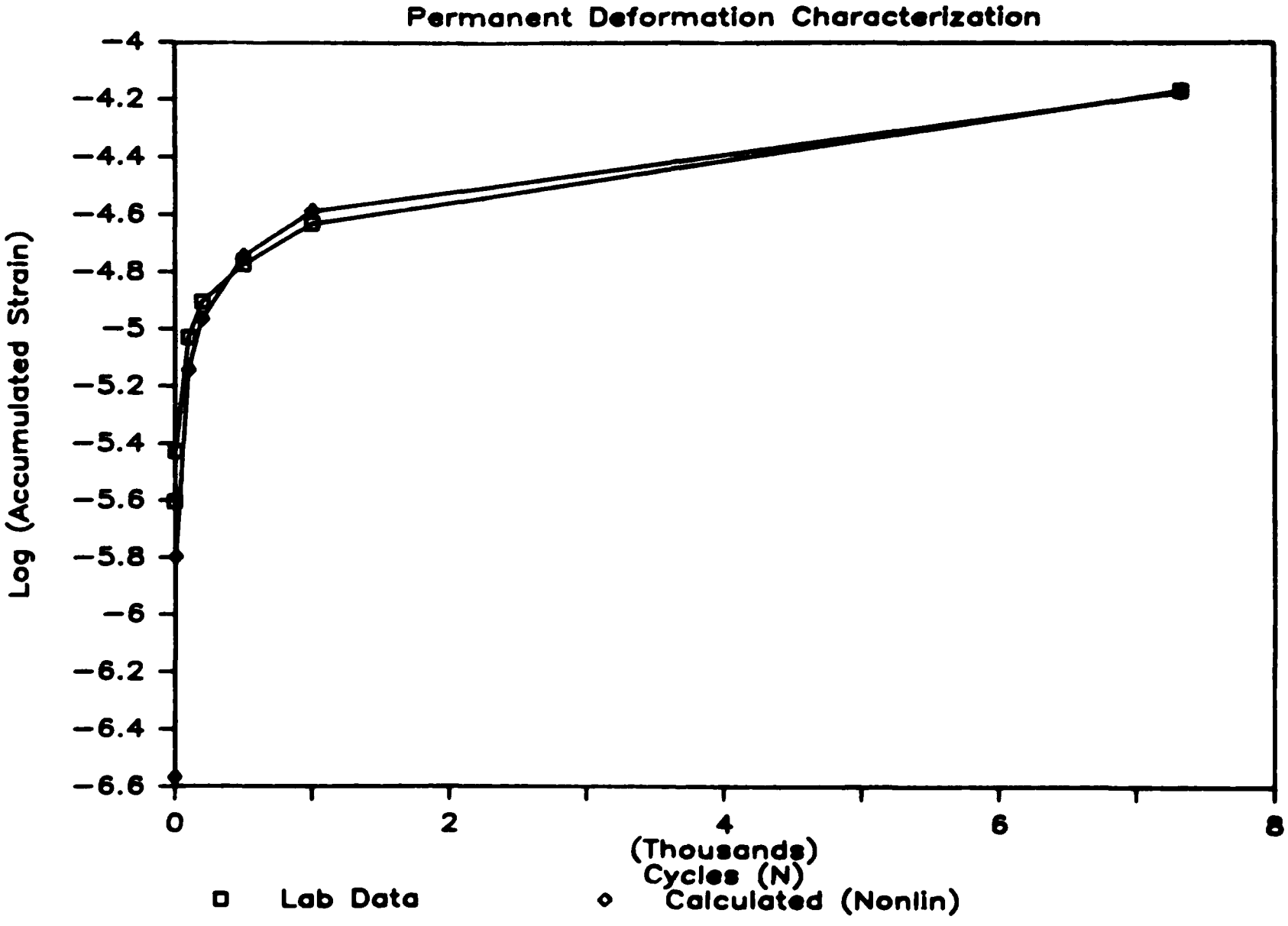

APPENDIX D

Permanent Deformation Parameters For All Material, Aircraft, And Temperature Combinations; And Sample Plots, Permanent Deformation Parameters Versus Temperature

APPENDIX D. PERMANENT DEFORMATION PARAMETERS FOR ALL MATERIAL, AIRCRAFT, AND TEMPERATURE COMBINATIONS; AND SAMPLE PLOTS, PERMANENT DEFORMATION PARAMETERS VERSUS TEMPERATURE

This appendix contains the permanent deformation parameters for each material and each aircraft after the parameters have been adjusted to the field stress level. Also in this appendix are samples of the plots of the adjusted permanent deformation parameters versus temperature. The plots for the DC-10 aircraft are included here.

In this appendix, the element numbers are the horizontal finite element mesh rows, with element number 1 being at the top of the asphalt layer and element number 7 being at the bottom. When no data are shown for element number 1, the typical stress calculated for that aircraft load in the top of the asphalt layer was negative. In that case, no ratio (of permanent deformation parameter at field stress to permanent deformation parameter at laboratory stress for the typical asphalt concrete material) could be calculated. This ratio was necessary for calculating the parameter at field stress for the test material. Thus, when no ratio could be calculated, the parameter from element number 2 was input in the computer program for element number 1 as well.

Note that the parameter does not change with element number, or with increasing depth. This is because the parameter is not sensitive to stress. It is, however, sensitive to temperature and to material.

PERMANENT DEFORMATION PARAMETER: ρ

AIRCRAFT: All

		Temperature, ^{o}F (^{o}C)		
Material	Element	40 (4.4)	70 (21.1)	100 (37.7)
AC-10 Control	all	1.15×10^{16}	9.82×10^{3}	6.38×10^{16}
ARC-Low	all	3.42×10^{16}	2.54×10^{16}	1.92×10^{4}
ARC-Medium	all	3.45×10^{16}	2.89×10^{16}	2.50×10^{16}
ARC-High	all	1.30×10^{15}	4.72×10^{10}	5.23×10^{2}

PERMANENT DEFORMATION PARAMETER: $\varepsilon_o/\varepsilon_r$

AIRCRAFT: DC-9

Material	Element	Temperature, °F (°C) 40 (4.4)	70 (21.1)	00 (37.7)
AC-10 Control	1	-	2.46×10^{1}	6.43×10^{4}
	2	3.07×10^{3}	4.99×10^{1}	1.15×10^{5}
	3	3.72×10^{3}	5.99×10^{1}	1.09×10^{5}
	4	3.46×10^{3}	5.44×10^{1}	8.22×10^{4}
	5	3.35×10^{3}	4.98×10^{1}	6.57×10^{4}
	6	3.63×10^{3}	5.00×10^{1}	5.70×10^{4}
	7	4.62×10^{3}	5.59×10^{1}	5.20×10^{4}
ARC-Low	1	-	1.23×10^{4}	1.94×10^{2}
	2	4.10×10^{3}	2.50×10^{4}	3.47×10^{2}
	3	4.96×10^{3}	3.00×10^{4}	3.30×10^{2}
	4	4.61×10^{3}	2.73×10^{4}	2.48×10^{2}
	5	4.47×10^{3}	2.49×10^{4}	1.98×10^{2}
	6	4.85×10^{3}	2.50×10^{4}	1.72×10^{2}
	7	6.17×10^{3}	2.80×10^{4}	1.57×10^{2}
ARC-Medium	1	-	4.87×10^{2}	[illegible]
	2	2.67×10^{3}	9.88×10^{2}	[illegible]
	3	3.23×10^{3}	1.19×10^{3}	5.84×10^{3}
	4	3.00×10^{3}	1.08×10^{3}	4.39×10^{3}
	5	2.91×10^{3}	9.88×10^{2}	3.50×10^{3}
	6	3.16×10^{3}	9.91×10^{2}	3.04×10^{3}
	7	4.01×10^{3}	1.11×10^{3}	2.77×10^{3}
ARC-High	1	-	1.48×10^{2}	3.01×10^{1}
	2	9.17×10^{3}	3.00×10^{2}	5.38×10^{1}
	3	1.11×10^{4}	3.60×10^{2}	5.12×10^{1}
	4	1.03×10^{4}	3.27×10^{2}	1.84×10^{1}
	5	1.00×10^{4}	3.00×10^{2}	3.07×10^{1}
	6	1.09×10^{4}	3.00×10^{2}	2.66×10^{1}
	7	1.38×10^{4}	3.36×10^{2}	2.43×10^{1}

PERMANENT DEFORMATION PARAMETER: β

AIRCRAFT: DC-9

Material	Element	Temperature, °F (°C) 40 (4.4)	70 (21.1)	100 (37.7)
AC-10 Control	1	-	0.1870	0.0819
	2	0.0789	0.2550	0.0896
	3	0.0816	0.2640	0.0891
	4	0.0806	0.2600	0.0856
	5	0.0802	0.2550	0.0823
	6	0.0813	0.2560	0.0798
	7	0.0843	0.2610	0.0780
ARC-Low	1	-	0.0604	0.1790
	2	0.0806	0.0827	0.1960
	3	0.0834	0.0855	0.1950
	4	0.0824	0.0841	0.1870
	5	0.0819	0.0827	0.1800
	6	0.0831	0.0827	0.1740
	7	0.0861	0.0845	0.1700
ARC-Medium	1	-	0.0472	0.0776
	2	0.0799	0.0647	0.0849
	3	0.0827	0.0669	0.0844
	4	0.0816	0.0658	0.0811
	5	0.0812	0.0647	0.0780
	6	0.0823	0.0647	0.0780
	7	0.0853	0.0661	0.0739
ARC-High	1	-	0.0665	0.2120
	2	0.0878	0.0911	0.2320
	3	0.0909	0.0942	0.2300
	4	0.0897	0.0926	0.2210
	5	0.0892	0.0911	0.2130
	6	0.0905	0.0911	0.2060
	7	0.0938	0.0931	0.2020

PERMANENT DEFORMATION PARAMETER: $\varepsilon_o/\varepsilon_r$

AIRCRAFT: DC-10

Material	Element	Temperature, °F (°C) 40 (4.4)	70 (21.1)	100 (37.7)
AC-10 Control	1	-	-	6.27×10^4
	2	2.30×10^3	4.16×10^1	1.25×10^5
	3	4.06×10^3	6.66×10^1	1.48×10^5
	4	4.93×10^3	7.40×10^1	1.23×10^5
	5	5.66×10^3	7.60×10^1	9.96×10^4
	6	7.19×10^3	8.38×10^1	8.49×10^4
	7	1.13×10^4	1.06×10^2	7.61×10^4
ARC-Low	1	-	-	1.89×10^2
	2	3.07×10^3	2.08×10^4	3.78×10^2
	3	5.42×10^3	3.33×10^4	4.46×10^2
	4	6.58×10^3	3.70×10^4	3.72×10^2
	5	7.56×10^3	3.81×10^4	3.00×10^2
	6	9.60×10^3	4.19×10^4	2.56×10^2
	7	1.51×10^4	5.29×10^4	2.29×10^2
ARC-Medium	1	-	-	3.34×10^3
	2	2.00×10^3	8.25×10^2	6.69×10^3
	3	3.53×10^3	1.32×10^3	7.89×10^3
	4	4.29×10^3	1.47×10^3	6.58×10^3
	5	4.92×10^3	1.51×10^3	5.31×10^3
	6	6.25×10^3	1.66×10^3	4.52×10^3
	7	9.86×10^3	2.10×10^3	4.06×10^3
ARC-High	1	-	-	0.293×10^2
	2	0.68×10^4	0.250×10^3	0.586×10^2
	3	0.121×10^5	0.400×10^3	0.692×10^2
	4	0.147×10^5	0.445×10^3	0.577×10^2
	5	0.164×10^5	0.457×10^3	0.465×10^2
	6	0.215×10^5	0.504×10^3	0.396×10^2
	7	0.339×10^5	0.636×10^3	0.355×10^2

PERMANENT DEFORMATION PARAMETER: β

AIRCRAFT: DC-10

Material	Element	Temperature, ^{o}F (^{o}C) 40 (4.4)	70 (21.1)	100 (37.7)
AC-10 Control	1	-	-	0.0815
	2	0.0736	0.2450	0.0905
	3	0.0828	0.2690	0.0921
	4	0.0850	0.2730	0.0903
	5	0.0864	0.2740	0.0880
	6	0.0886	0.2770	0.0860
	7	0.0923	0.2850	0.0845
ARC-Low	1	-	-	0.1780
	2	0.0752	0.0794	0.1980
	3	0.0846	0.0869	0.2010
	4	0.0868	0.0883	0.1970
	5	0.0883	0.0886	0.1920
	6	0.0906	0.0897	0.1880
	7	0.0943	0.0921	0.1850
ARC-Medium	1	-	-	0.0772
	2	0.0745	0.0621	0.0857
	3	0.0838	0.0680	0.0873
	4	0.0860	0.0690	0.0856
	5	0.0875	0.0693	0.0834
	6	0.0898	0.0702	0.0815
	7	0.0934	0.0721	0.0801
ARC-High	1	-	-	0.2110
	2	0.0819	0.0874	0.2340
	3	0.0921	0.0958	0.2380
	4	0.0946	0.0972	0.2340
	5	0.0962	0.0976	0.2270
	6	0.0987	0.0988	0.2220
	7	0.1030	0.1010	0.2180

PERMANENT DEFORMATION PARAMETER: $\varepsilon_o/\varepsilon_r$

AIRCRAFT: B-727

Material	Element	Temperature, °F (°C) 40 (4.4)	70 (21.1)	100 (37.7)
AC-10 Control	1	-	-	6.03×10^4
	2	2.45×10^3	4.27×10^1	1.13×10^5
	3	3.77×10^3	6.14×10^1	1.25×10^5
	4	4.15×10^3	6.36×10^1	1.02×10^5
	5	4.46×10^3	6.27×10^1	8.23×10^4
	6	5.30×10^3	6.65×10^1	7.09×10^4
	7	7.60×10^3	7.96×10^1	6.42×10^4
ARC-Low	1	-	-	1.82×10^2
	2	3.28×10^3	2.14×10^4	3.41×10^2
	3	5.04×10^3	3.07×10^4	3.76×10^2
	4	5.55×10^3	3.19×10^4	3.06×10^2
	5	5.96×10^3	3.14×10^4	2.48×10^2
	6	7.08×10^3	3.33×10^4	2.14×10^2
	7	1.02×10^4	3.99×10^4	1.93×10^2
ARC-Medium	1	-	-	3.21×10^3
	2	2.13×10^3	8.47×10^2	6.03×10^3
	3	3.28×10^3	1.22×10^3	6.66×10^3
	4	3.61×10^3	1.26×10^3	5.42×10^3
	5	3.88×10^3	1.24×10^3	4.39×10^3
	6	4.61×10^3	1.32×10^3	3.78×10^3
	7	6.61×10^3	1.58×10^3	3.42×10^3
ARC-High	1	-	-	2.80×10^1
	2	7.34×10^3	2.57×10^2	5.30×10^1
	3	1.13×10^4	3.69×10^2	5.80×10^1
	4	1.24×10^4	3.83×10^2	4.70×10^1
	5	1.33×10^4	3.77×10^2	3.80×10^1
	6	1.58×10^4	4.00×10^2	3.30×10^1
	7	2.27×10^4	4.79×10^2	3.00×10^1

PERMANENT DEFORMATION PARAMETER: β

AIRCRAFT: B-727

Material	Element	Temperature, °F (°C) 40 (4.4)	70 (21.1)	100 (37.7)
AC-10 Control	1	-	-	0.0808
	2	0.0749	0.2470	0.0894
	3	0.818	0.2650	0.0904
	4	0.0830	0.2670	0.0882
	5	0.0839	0.2660	0.0856
	6	0.0857	0.2690	0.0835
	7	0.0891	0.2750	0.0819
ARC-Low	1	-	-	0.1767
	2	0.0766	0.0799	0.1955
	3	0.0836	0.0858	0.1977
	4	0.0848	0.0864	0.1929
	5	0.0857	0.0862	0.1871
	6	0.0876	0.0869	0.1829
	7	0.911	0.0891	0.1791
ARC-Medium	1	-	-	0.0766
	2	0.0759	0.0625	0.0847
	3	0.0828	0.0671	0.0857
	4	0.0841	0.0675	0.0836
	5	0.0849	0.0674	0.0811
	6	0.0868	0.0680	0.0791
	7	0.0902	0.0697	0.0776
ARC-High	1	-	-	0.2090
	2	0.0834	0.0880	0.2312
	3	0.0910	0.0945	0.2338
	4	0.0924	0.0951	0.2281
	5	0.0934	0.0949	0.2213
	6	0.0954	0.0957	0.2159
	7	0.0992	0.0992	0.2118

PERMANENT DEFORMATION PARAMETER: ϵ_{o/ϵ_r}

AIRCRAFT: B-737

		Temperature, °F (°C)		
Material	Element	40 (4.4)	70 (21.1)	100 (37.7)
AC-10 Control	1	1.44×10^{3}	2.67×10^{1}	6.59×10^{4}
	2	2.75×10^{3}	4.53×10^{1}	9.72×10^{4}
	3	3.19×10^{3}	5.17×10^{1}	9.10×10^{4}
	4	3.06×10^{3}	4.84×10^{1}	7.21×10^{4}
	5	3.02×10^{3}	4.53×10^{1}	5.96×10^{4}
	6	3.28×10^{3}	4.58×10^{1}	5.27×10^{4}
	7	4.08×10^{3}	5.08×10^{1}	4.87×10^{4}
ARC-Low	1	1.93×10^{3}	1.34×10^{4}	1.99×10^{2}
	2	3.67×10^{3}	2.27×10^{4}	2.93×10^{2}
	3	4.26×10^{3}	2.59×10^{4}	2.74×10^{2}
	4	4.09×10^{3}	2.42×10^{4}	2.17×10^{2}
	5	4.04×10^{3}	2.27×10^{4}	$1.[illegible] \times 10^{2}$
	6	4.38×10^{3}	2.29×10^{4}	$1.[illegible] \times 10^{2}$
	7	5.45×10^{3}	2.54×10^{4}	$1.[illegible] \times 10^{2}$
ARC-Medium	1	1.25×10^{3}	5.30×10^{3}	[illegible]
	2	2.39×10^{3}	8.99×10^{3}	[illegible]
	3	2.77×10^{3}	$1.[illegible] \times 10^{4}$	[illegible]
	4	2.66×10^{3}	[illegible]	[illegible]
	5	2.63×10^{3}	[illegible]	[illegible]
	6	2.85×10^{3}	[illegible]	[illegible]
	7	3.55×10^{3}	[illegible]	[illegible]
ARC-High	1	[illegible]	[illegible]	[illegible]
	2	[illegible]	[illegible]	[illegible]
	3	[illegible]	[illegible]	[illegible]
	4	[illegible]	[illegible]	[illegible]
	5	[illegible]	[illegible]	[illegible]
	6	[illegible]	[illegible]	[illegible]
	7	[illegible]	[illegible]	[illegible]

PERMANENT DEFORMATION PARAMETER: β

AIRCRAFT: B-737

Material	Element	Temperature, ^{o}F (^{o}C) 40 (4.4)	70 (21.1)	100 (37.7)
AC-10 Control	1	0.0548	0.2030	0.0823
	2	0.0771	0.2500	0.0877
	3	0.0795	0.2570	0.0869
	4	0.0789	0.2540	0.0837
	5	0.0786	0.2500	0.0806
	6	0.0799	0.2510	0.0783
	7	0.0828	0.2560	0.0765
ARC-Low	1	0.0560	0.0657	0.1800
	2	0.0788	0.0810	0.1917
	3	0.0812	0.0833	0.1899
	4	0.0806	0.0822	0.1831
	5	0.0804	0.0810	0.1762
	6	0.0816	0.0812	0.1711
	7	0.0846	0.0830	0.1673
ARC-Medium	1	0.0555	0.0514	0.0780
	2	0.0780	0.0634	0.0831
	3	0.0805	0.0651	0.0823
	4	0.0798	0.0643	0.0793
	5	0.0796	0.0634	0.0764
	6	0.0809	0.0635	0.0742
	7	0.0838	0.0649	0.0725
ARC-High	1	0.0610	0.0724	0.2129
	2	0.0858	0.0892	0.2268
	3	0.0885	0.0917	0.2246
	4	0.0878	0.0906	0.2165
	5	0.0876	0.0892	0.2084
	6	0.0889	0.0894	0.2023
	7	0.0922	0.0914	0.1979

PERMANENT DEFORMATION PARAMETER: $\varepsilon_o/\varepsilon_r$

AIRCRAFT: B-757

Material	Element	Temperature, °F (°C) 40 (4.4)	70 (21.1)	100 (37.7)
AC-10 Control	1	1.31×10^{3}	2.50×10^{1}	6.87×10^{4}
	2	3.29×10^{3}	5.33×10^{1}	1.28×10^{5}
	3	4.02×10^{3}	6.46×10^{1}	1.21×10^{5}
	4	3.70×10^{3}	5.81×10^{1}	8.87×10^{4}
	5	3.57×10^{3}	5.27×10^{1}	6.96×10^{4}
	6	3.89×10^{3}	5.28×10^{1}	5.98×10^{4}
	7	5.01×10^{3}	5.94×10^{1}	5.42×10^{4}
ARC-Low	1	1.75×10^{3}	1.25×10^{4}	2.07×10^{2}
	2	4.39×10^{3}	2.67×10^{4}	3.87×10^{2}
	3	5.37×10^{3}	3.23×10^{4}	3.64×10^{2}
	4	4.94×10^{3}	2.91×10^{4}	2.67×10^{2}
	5	4.76×10^{3}	2.64×10^{4}	2.10×10^{2}
	6	5.19×10^{3}	2.64×10^{4}	1.80×10^{2}
	7	6.69×10^{3}	2.98×10^{4}	1.63×10^{2}
ARC-Medium	1	1.14×10^{3}	4.96×10^{2}	3.66×10^{2}
	2	2.86×10^{3}	1.06×10^{3}	6.85×10^{3}
	3	3.50×10^{3}	1.28×10^{3}	6.44×10^{3}
	4	1.21×10^{3}	1.15×10^{3}	4.73×10^{3}
	5	3.10×10^{3}	1.04×10^{3}	3.71×10^{3}
	6	3.38×10^{3}	1.05×10^{3}	3.19×10^{3}
	7	4.36×10^{3}	1.18×10^{3}	2.89×10^{3}
ARC-High	1	3.92×10^{3}	1.50×10^{2}	3.20×10^{1}
	2	9.83×10^{3}	3.21×10^{2}	6.00×10^{1}
	3	1.20×10^{4}	3.89×10^{2}	5.60×10^{1}
	4	1.10×10^{4}	3.50×10^{2}	4.10×10^{1}
	5	1.07×10^{4}	3.17×10^{2}	3.30×10^{1}
	6	1.16×10^{4}	3.18×10^{2}	2.80×10^{1}
	7	1.50×10^{4}	3.58×10^{2}	2.50×10^{1}

PERMANENT DEFORMATION PARAMETER: β

AIRCRAFT: B-757

Material	Element	Temperature, °F (°C) 40 (4.4)	70 (21.1)	100 (37.7)
AC-10 Control	1	0.0329	0.1910	0.0830
	2	0.0799	0.2590	0.0907
	3	0.0826	0.2670	0.0901
	4	0.0815	0.2630	0.0866
	5	0.0811	0.2580	0.0832
	6	0.0822	0.2580	0.0807
	7	0.0852	0.2640	0.0788
ARC-Low	1	0.0337	0.0617	0.1814
	2	0.0817	0.0838	0.1983
	3	0.0844	0.0866	0.1970
	4	0.0833	0.0851	0.1893
	5	0.0829	0.0836	0.1819
	6	0.0840	0.0836	0.1764
	7	0.0870	0.0854	0.1722
ARC-Medium	1	0.0333	0.0483	0.0786
	2	0.0809	0.0655	0.0860
	3	0.0837	0.0677	0.0854
	4	0.0826	0.0665	0.0820
	5	0.0821	0.0654	0.0788
	6	0.0832	0.0654	0.0764
	7	0.0862	0.0668	0.0747
ARC-High	1	0.0367	0.0680	0.2145
	2	0.0890	0.0923	0.2345
	3	0.0920	0.0953	0.2330
	4	0.0908	0.0937	0.2239
	5	0.0903	0.0921	0.2151
	6	0.0915	0.0921	0.2086
	7	0.0948	0.0941	0.2037

Aircraft: DC-10

Material: AC-10 Control

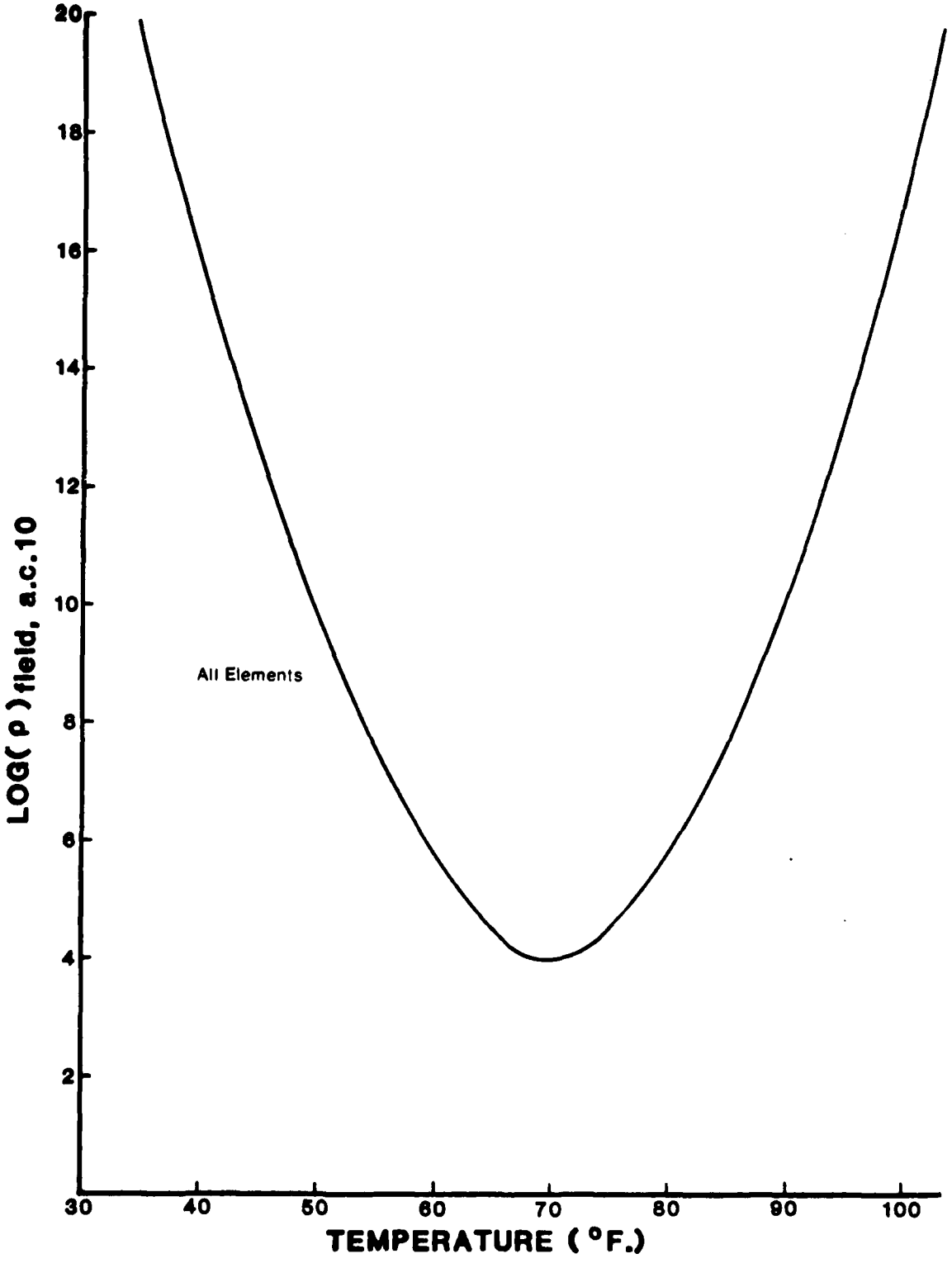

Aircraft: DC-10

Material: ARC-Low

Parameter: ρ

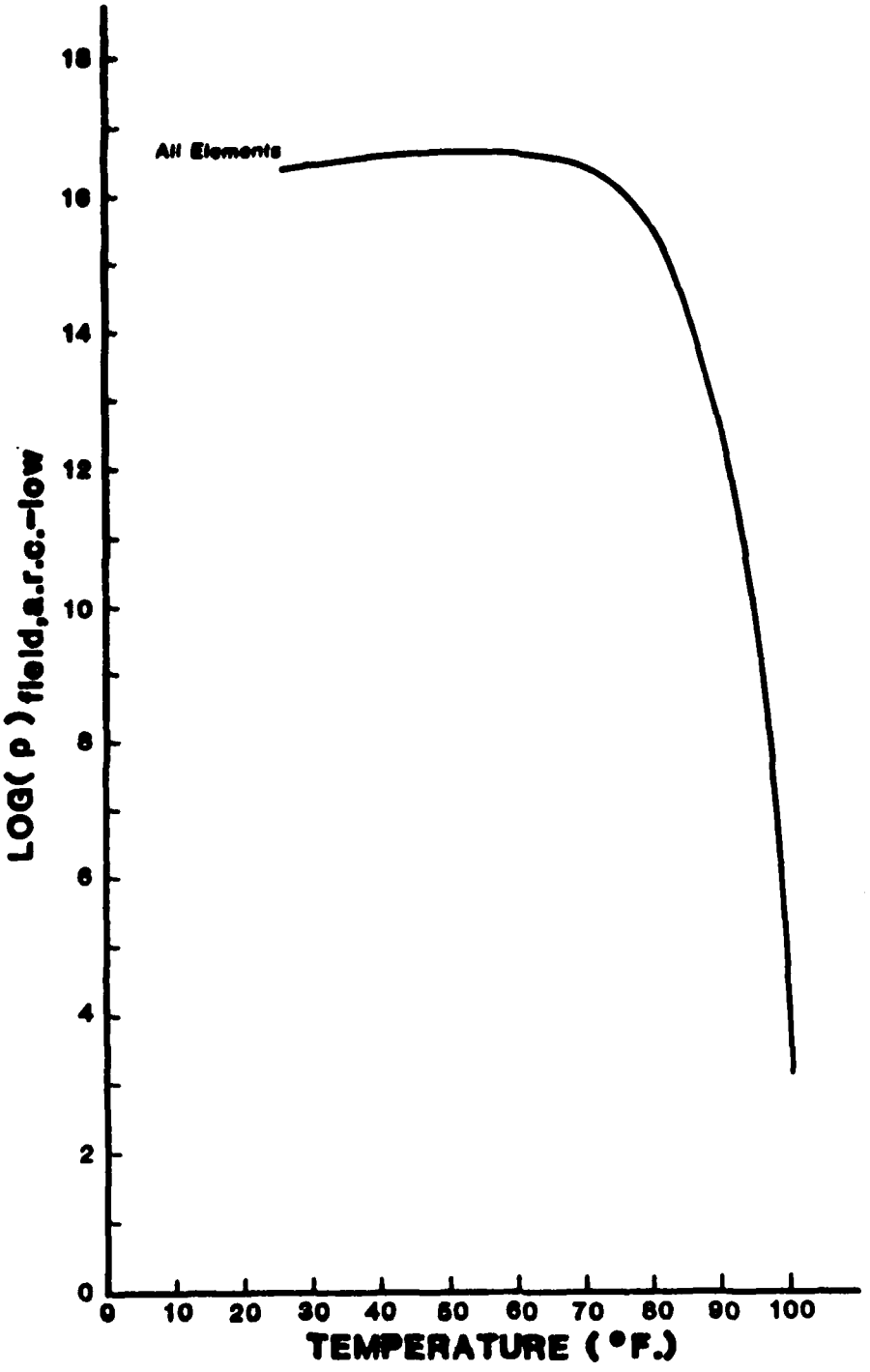

Aircraft: DC-10

Material: ARC-Medium

Parameter: ρ

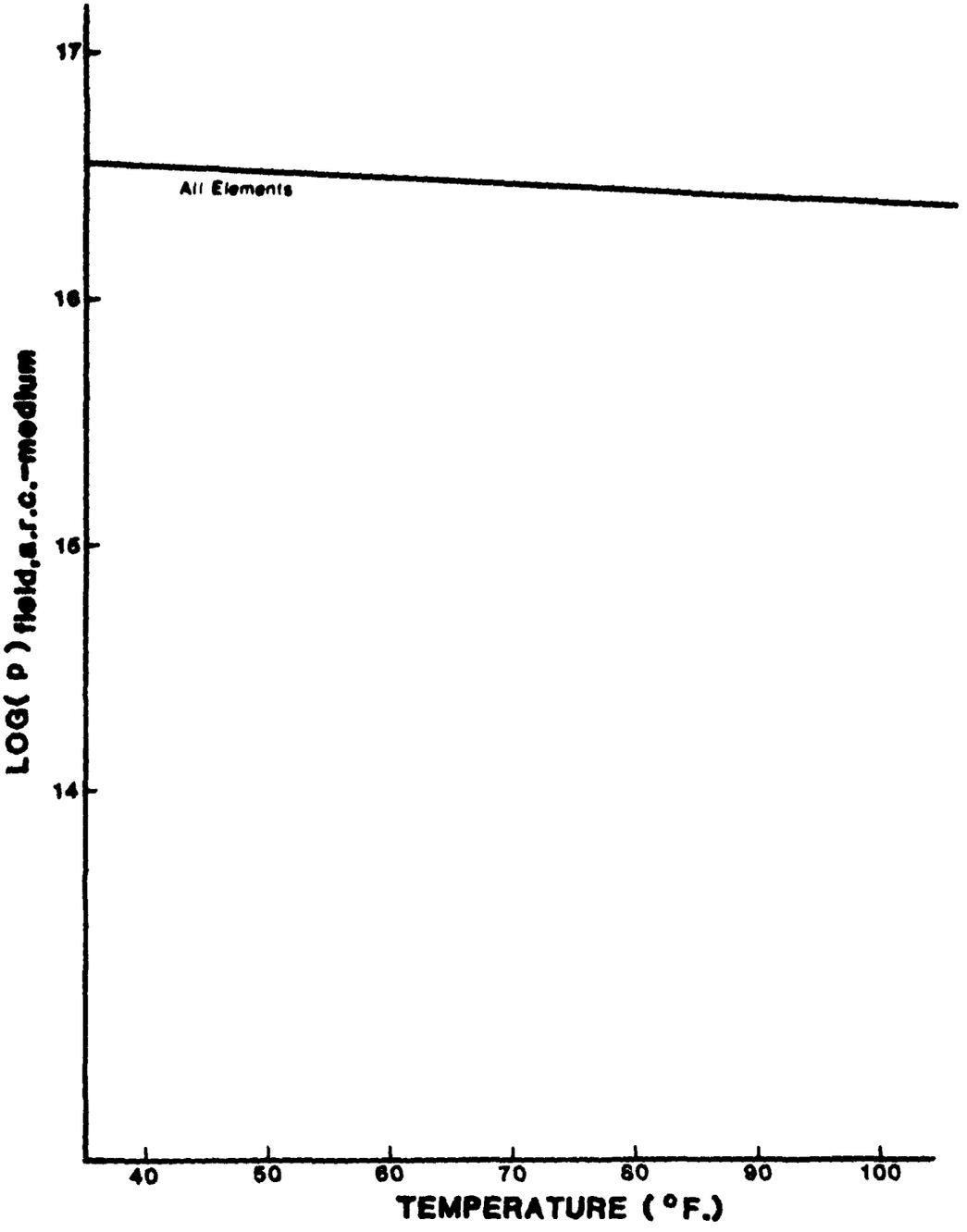

Aircraft: DC-10

Material: ARC-High

Parameter: ρ

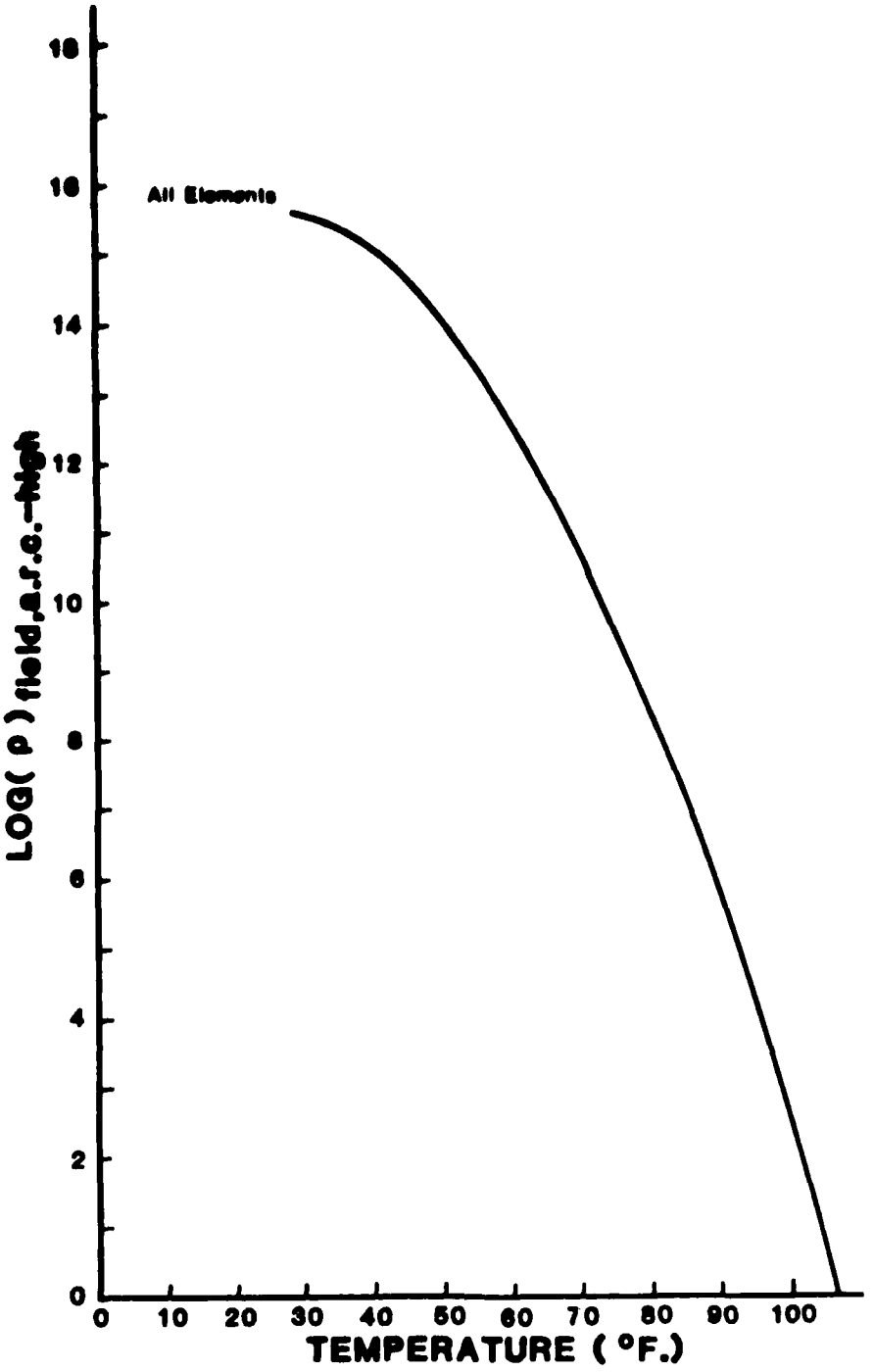

Aircraft: DC-10

Material: AC-10 Control

Parameter: ϵ_o/ϵ_r

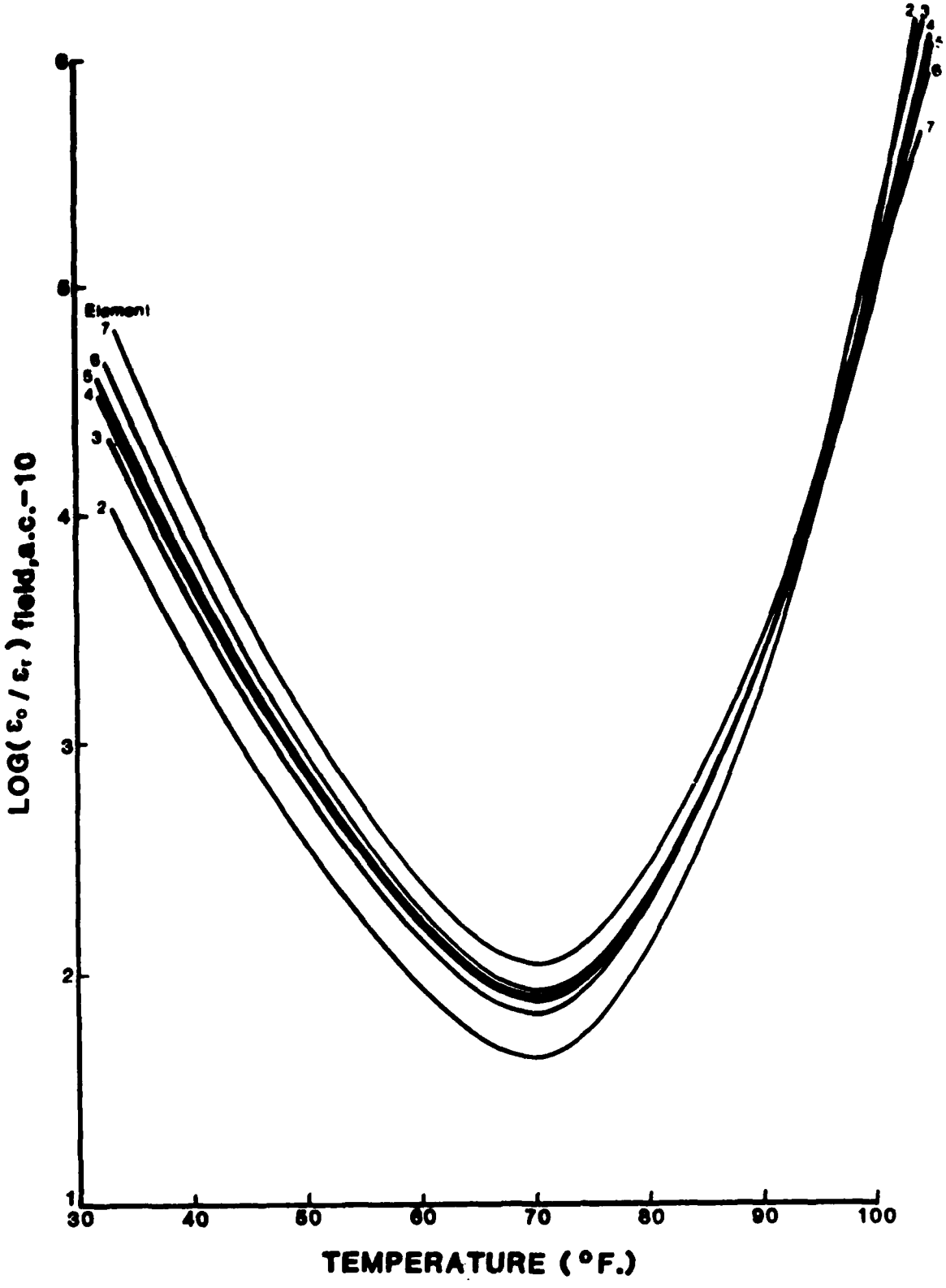

Aircraft: DC-10

Material: ARC-Low

Parameter: ϵ_0/ϵ_r

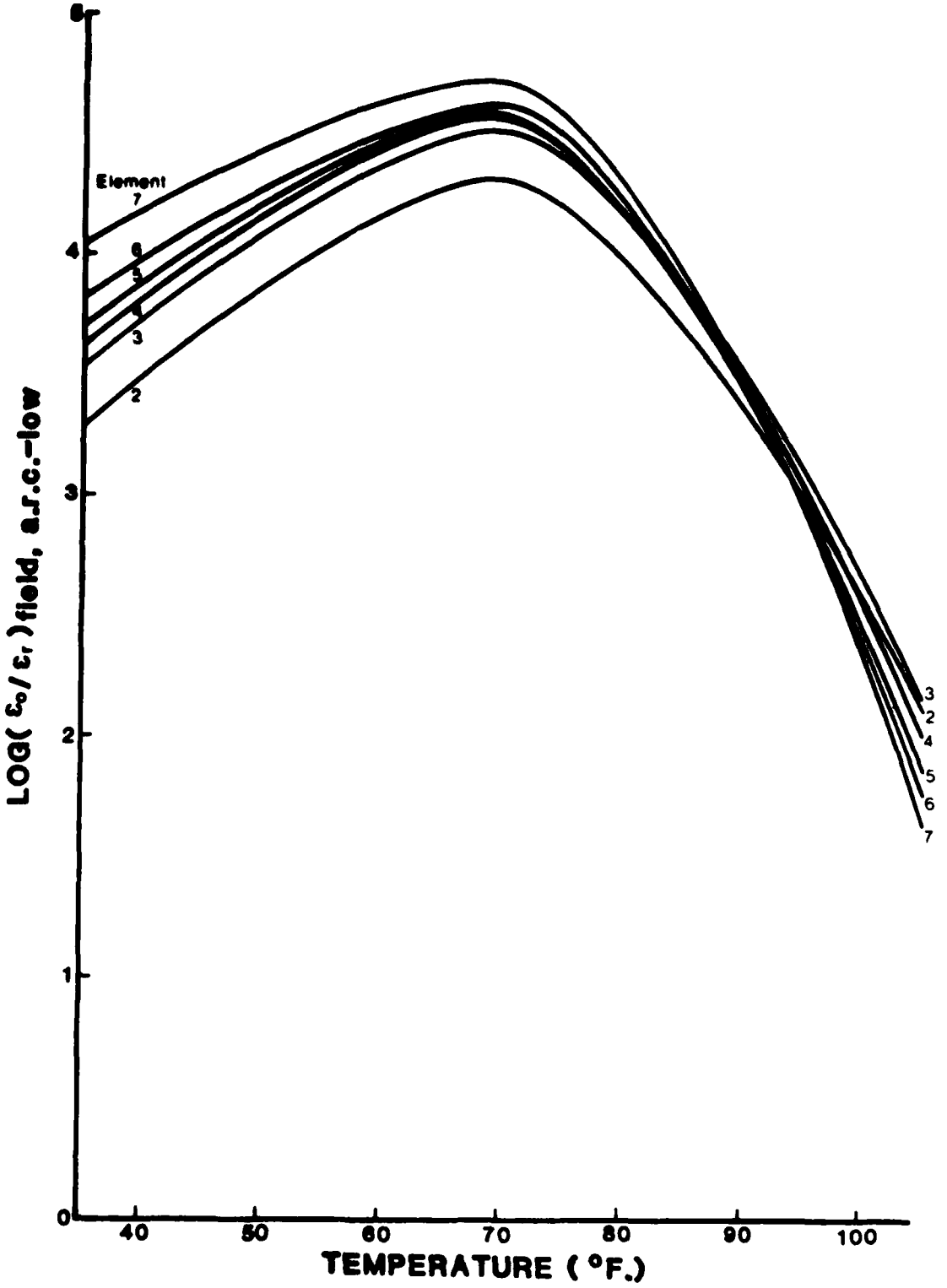

Aircraft: DC-10

Material: ARC-Medium

Parameter: $\varepsilon_o/\varepsilon_r$

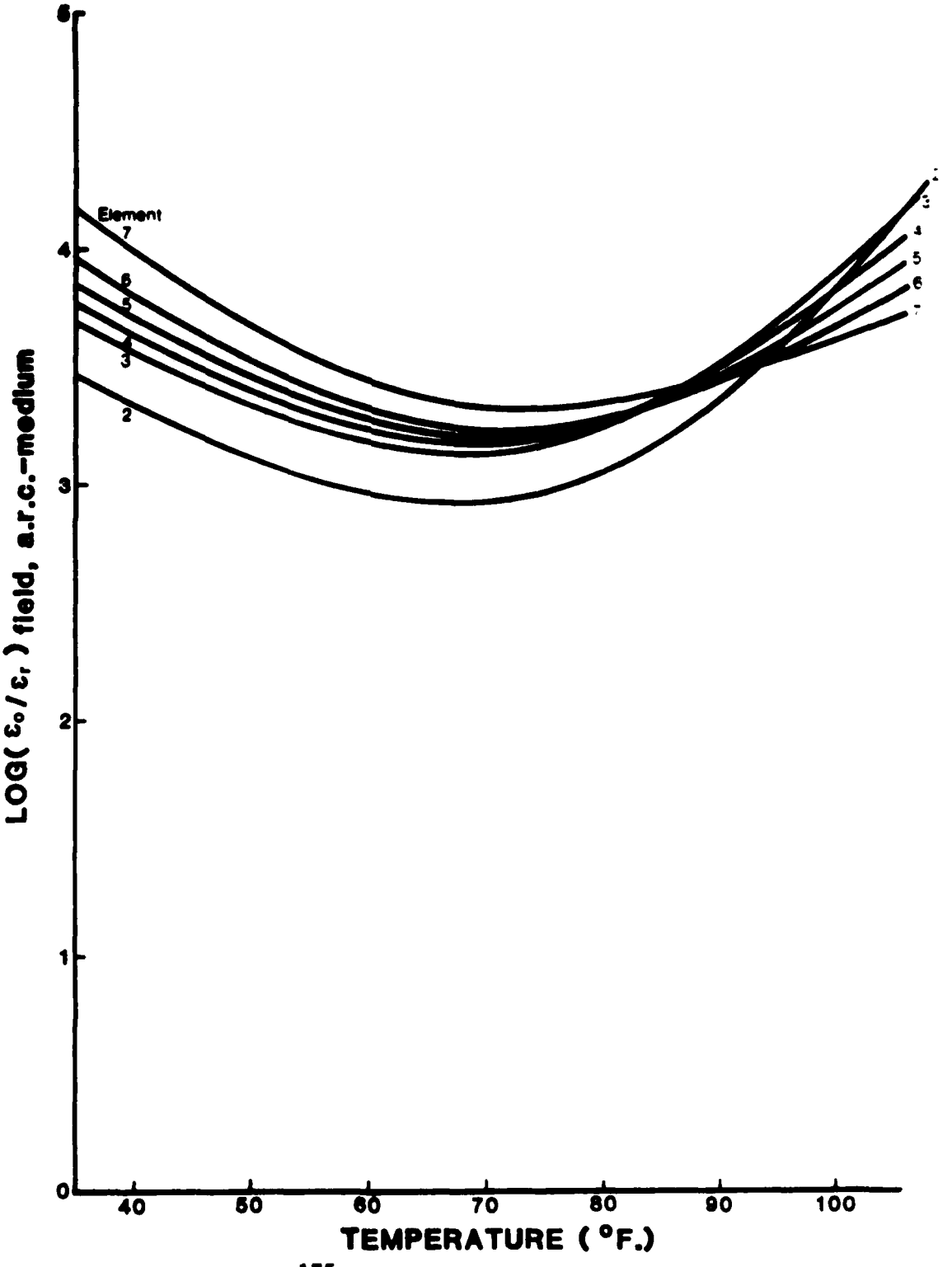

Aircraft: DC-10

Material: ARC-High

Parameter: $\varepsilon_o/\varepsilon_r$

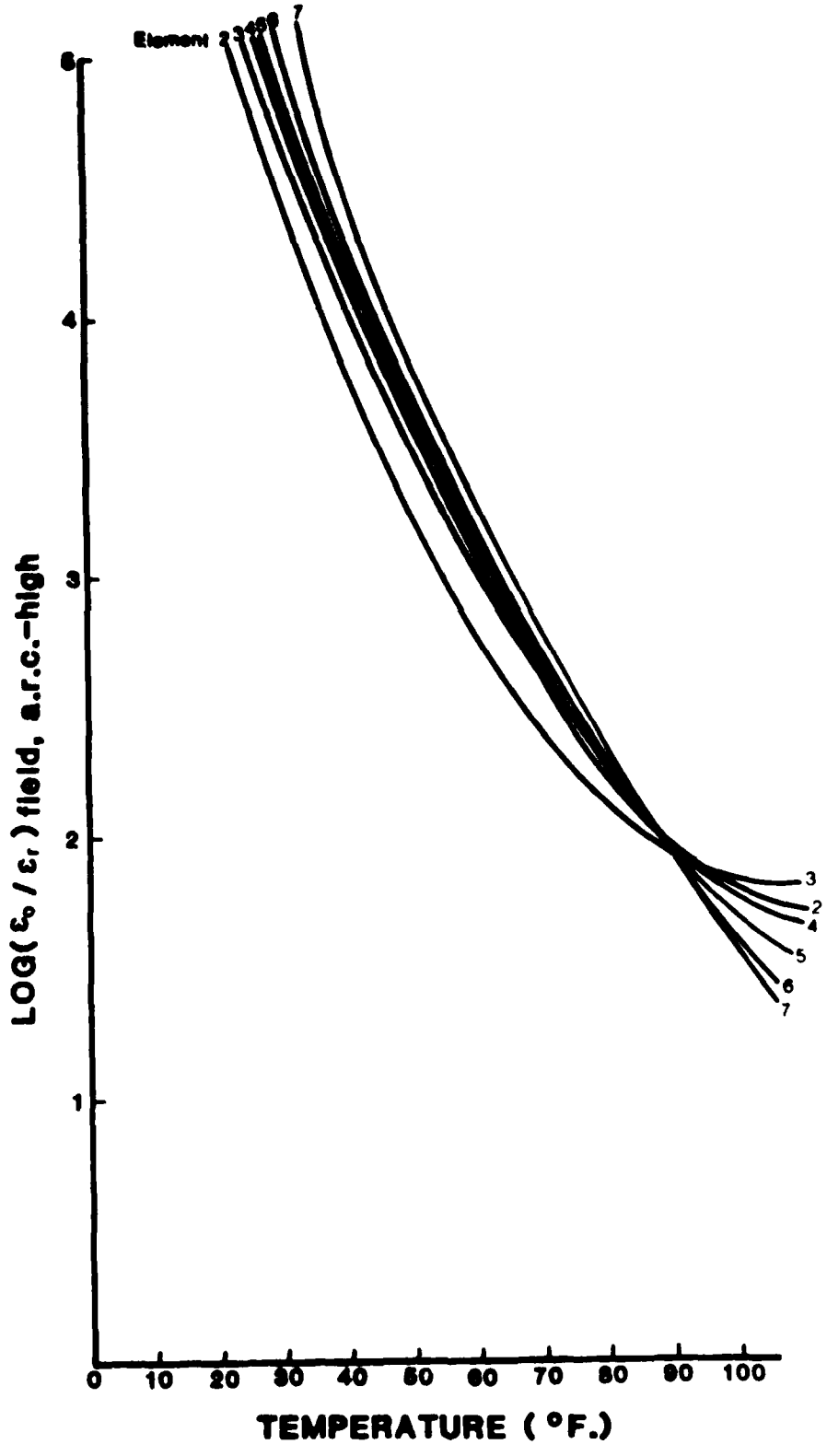

Aircraft: DC-10

Material: AC-10 Control

Parameter: β

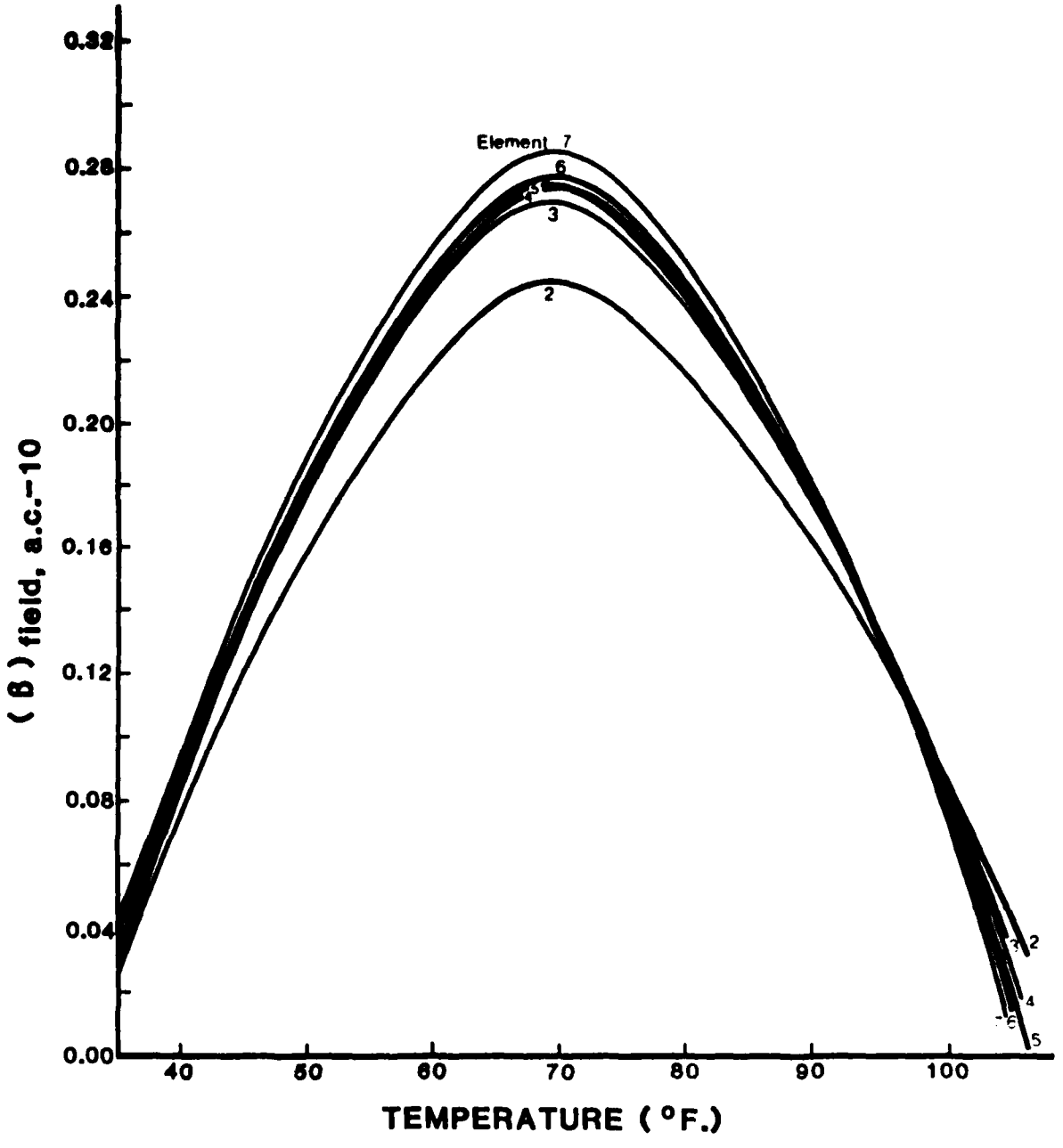

Aircraft: DC-10

Material: ARC-Low

Parameter: β

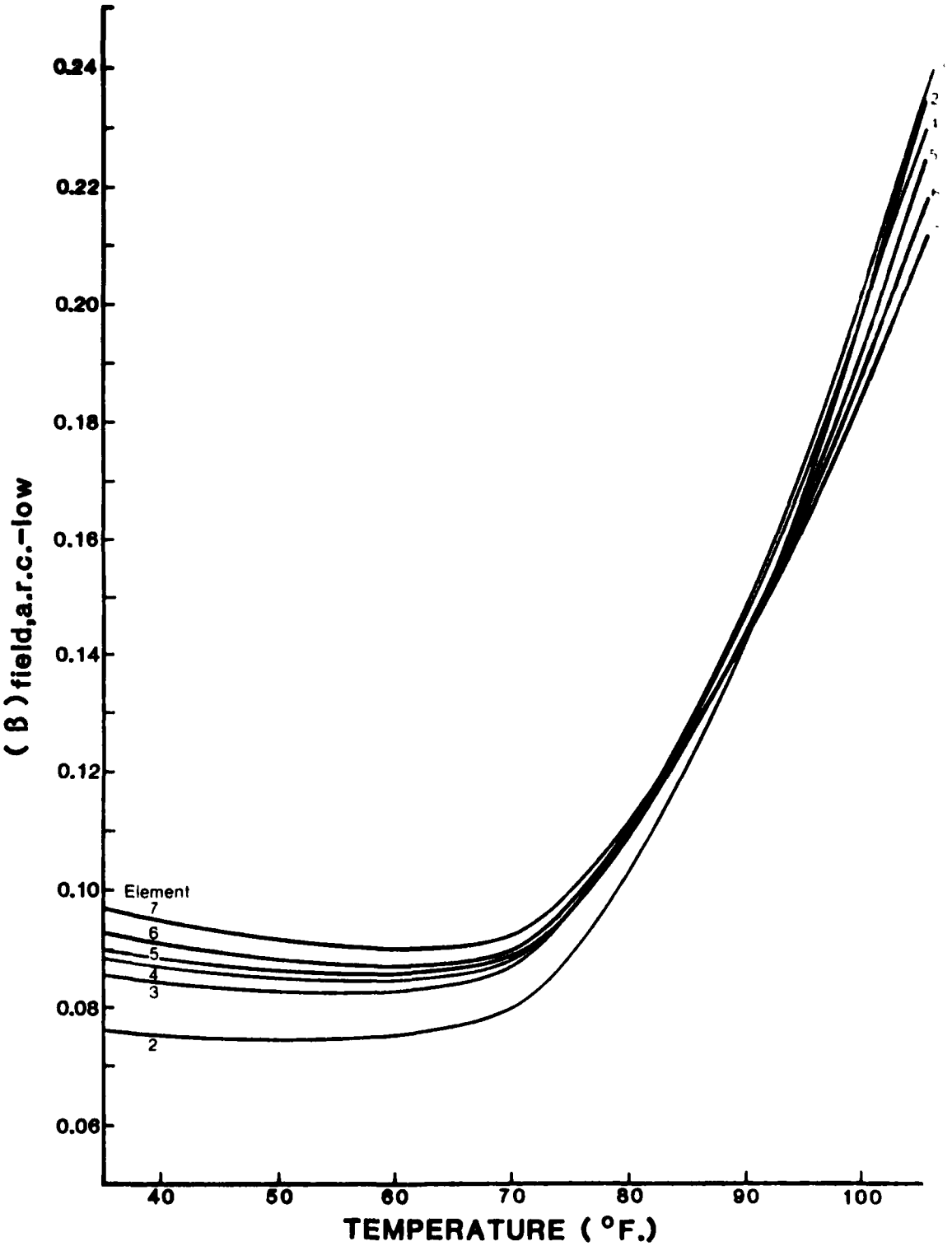

Aircraft: DC-10

Material: ARC-Medium

Parameter: β

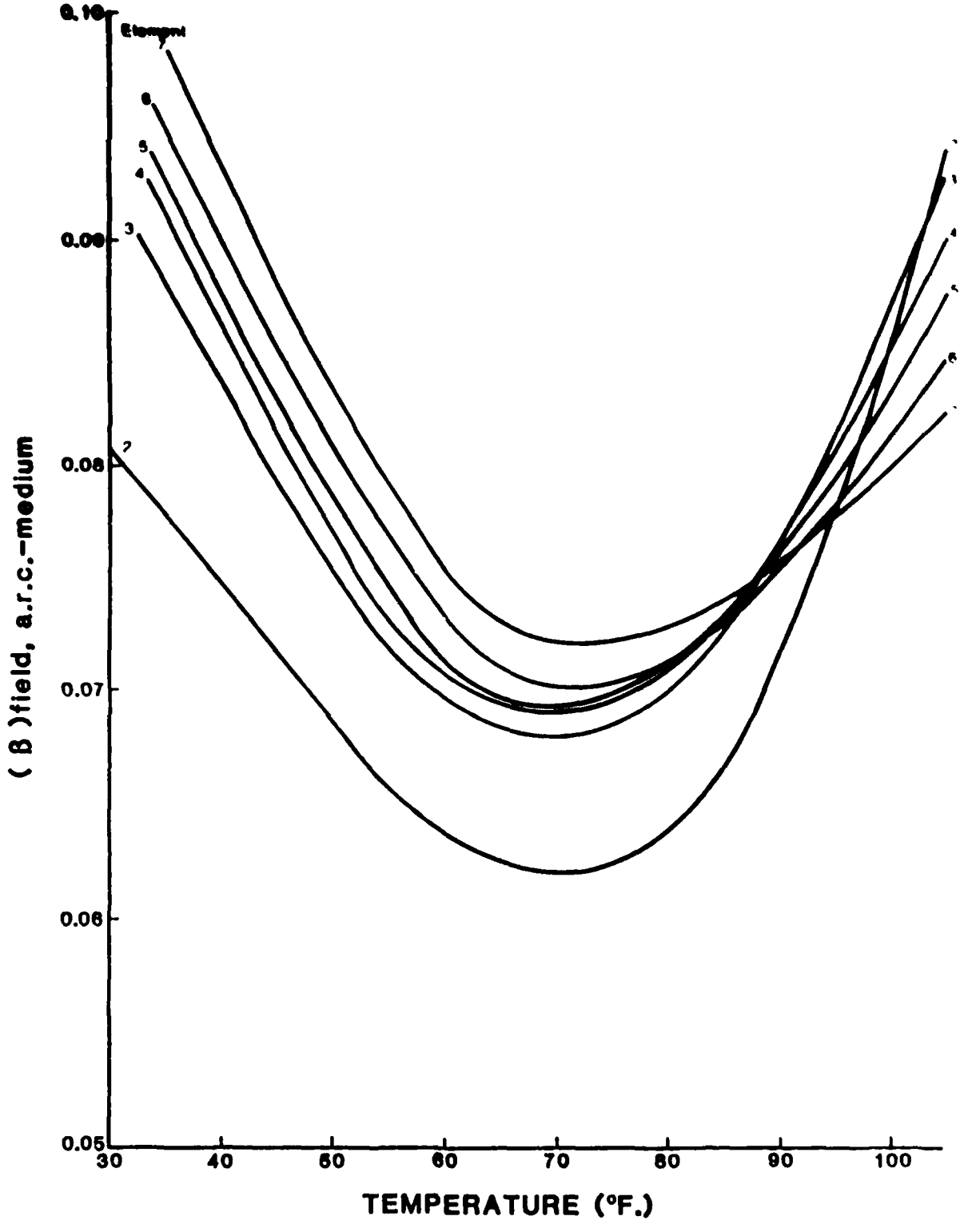

Aircraft: DC-10

Material: ARC-High

Parameter: β

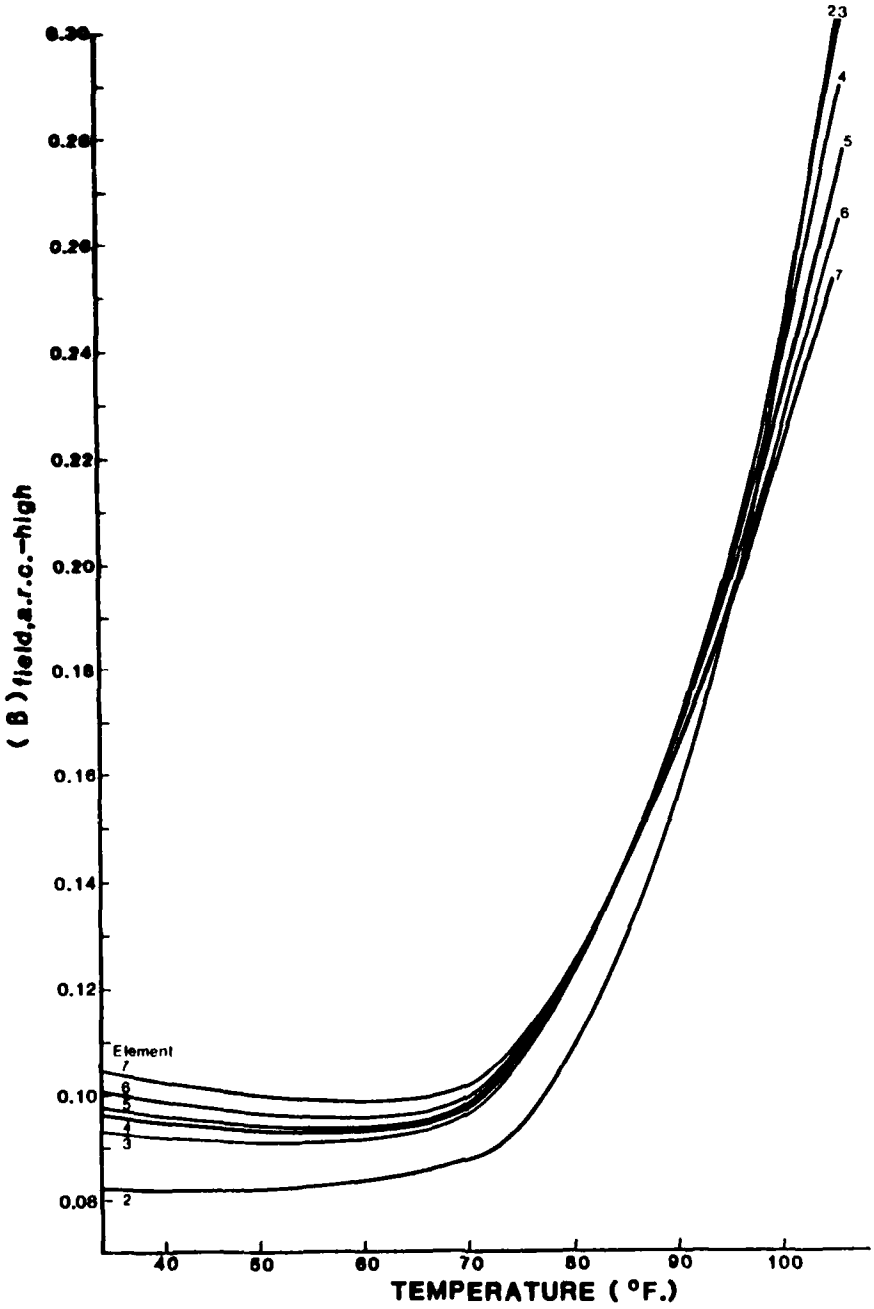

AD-A181 433 CRITERIA FOR ASPHALT-RUBBER CONCRETE IN CIVIL AIRPORT PAVEMENTS VOLUME 2.. (U) TEXAS TRANSPORTATION INST COLLEGE STATION D M HOYT ET AL. MAR 87 RF-4902-2 3/3

UNCLASSIFIED DOT/FAA/PM-86/39-VOL-2 DTFA01-83-C-30076 F/G 13/3 NL

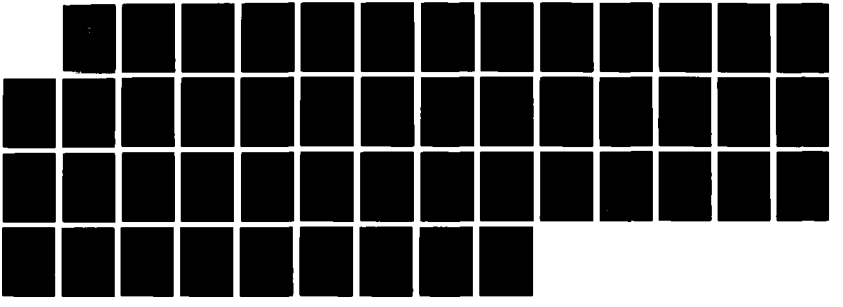

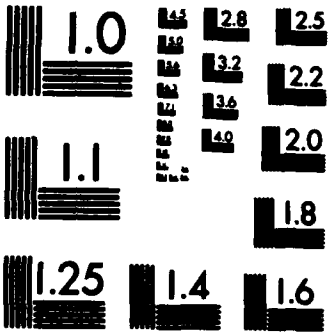

MICROCOPY RESOLUTION TEST CHART
NATIONAL BUREAU OF STANDARDS-1963-A

APPENDIX E

Summary Of Aircraft Data; And Calculated Estimates For Tire Contact Pressure Distributions

Aircraft: DC-9-41

Main Gear:

Type of Gear: Twin

Main Gear Dimension (in.): 24

Circular Imprint, Tire Radius (in.): 7.25

Tire Inflation Pressure (psi): 163

Max Load Per Tire ($lbx10^3$): 26.9

(Approximate)

Tire Contact Pressure Distribution:

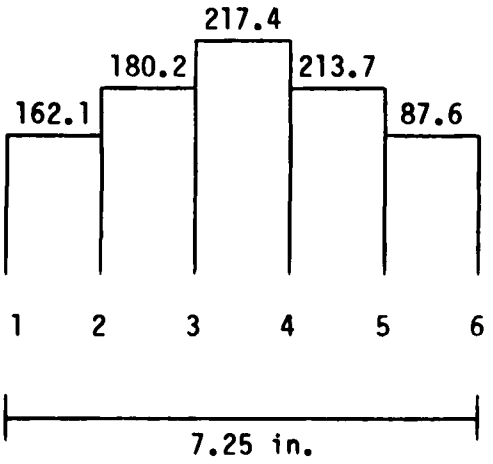

Finite Element Node Number:

Aircraft: DC-10-30 CF

Main Gear:

Type of Gear: Twin-Tandem

Main Gear Dimension (in.): 54x64

Circular Imprint, Tire Radius (in.): 9.30

Tire Inflation Pressure (psi): 185

Max Load Per Tire ($lbx10^3$): 50.3

(Approximate)
Tire Contact
Pressure
Distribution:

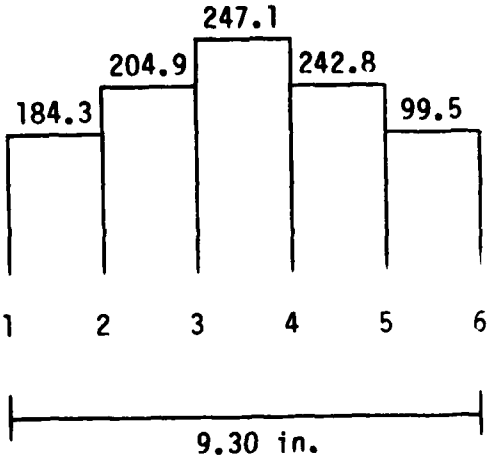

Finite Element
Node Number:

Aircraft: B-727-200

Main Gear:

Type of Gear: Twin

Main Gear Dimension (in.): 34

Circular Imprint, Tire Radius (in.): 8.69

Tire Inflation Pressure (psi): 168

Max Load Per Tire ($lbx10^3$): 39.9

(Approximate)

Tire Contact Pressure Distribution:

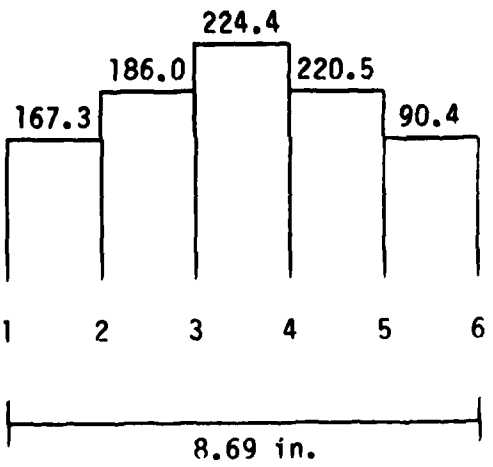

Finite Element Node Number:

Aircraft: B-737-200C

Main Gear:

Type of Gear: Twin

Main Gear Dimension (in.): 30.5

Circular Imprint, Tire Radius (in.): 7.45

Tire Inflation Pressure (psi): 148

Max Load Per Tire ($lbx10^3$): 25.8

(Approximate)
Tire Contact
Pressure
Distribution:

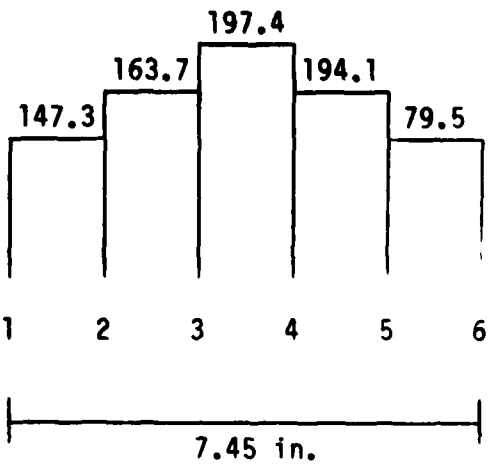

Finite Element
Node Number:

Aircraft: B-757

Main Gear:

Type of Gear: Twin-Tandem

Main Gear Dimension (in.): 34x45

Circular Imprint, Tire Radius (in.): 7.21

Tire Inflation Pressure (psi): 175

Max Load Per Tire ($lbx10^3$): 28.6

(Approximate)

Tire Contact Pressure Distribution:

Finite Element Node Number:

APPENDIX F

Beam Fatigue Laboratory Data For Asphalt Concrete And Asphalt-Rubber Concrete

APPENDIX F. BEAM FATIGUE DATA

Asphalt-Rubber Low at 34°F

Test Date: 11-85

Beam Number	E Modulus	Bending Strain	Actual Cycles to Failure	Predicted Cycles to Failure
F19L	589400	.0001525	604510	542690
F23L	552600	.0001627	607140	406520
F24L	982300	.0001525	1003590	542690
F26L	468700	.0006394	4440	890
F27L	1171700	.0002557	15490	53670
F28L	901300	.0003325	12740	16590
F30L	937400	.0005115	700	2410

K_1 = 4.466 E-12 K_2 = 4.476

Correlation Coefficient R=- .93

Asphalt-Rubber Low at 68°F

Test Date: 7-85

Beam Number	E Modulus	Bending Strain	Actual Cycles to Failure	Predicted Cycles to Failure
F8L	124900	.0007196	9080	9100
F4L	153300	.0005864	19950	17400
F1L	146600	.000613	9410	15120
F3L	150100	.0003865	139250	65120
F9L	146500	.0004092	25730	54330
F2L	136800	.0004731	54270	34320
F6L	205000	.0002339	114670	319190
F7L	144200	.0003325	163660	104830
F5L	327400	.000183	1084220	693430

K_1 = 1.026 E-6 K_2 = 3.165

Correlation Coefficient R=- .91

BEAM FATIGUE DATA

Asphalt-Rubber Low at 104°F

Test Date: 9-85

Beam Number	E Modulus	Bending Strain	Actual Cycles to Failure	Predicted Cycles to Failure
F10L	26500	.0018125	2500	5140
F11L	13500	.0026656	1990	1390
F13L	291000	.0007996	130370	81950
F14L	44600	.0005371	211740	314970
F15L	32100	.0011195	14380	26250
F17L	28400	.000144	18530	68250
F20L	15300	.0023458	2830	2150
F21L	19700	.0018125	8870	5140
F22L	241000	.00143933	4570	11220
F27L	9800	.0042628	270	280

K_1 = 2.718 E-6 K_2 = 3.383

Correlation Coefficient R=- .95

Asphalt-Rubber Medium at 34°F

Test Date: 11-85

Beam Number	E Modulus	Bending Strain	Actual Cycles to Failure	Predicted Cycles to Failure
F11M	328200	.0002029	529760	7882100
F12M	199500	.0005565	19320	13450
F15M	398900	.0002782	211120	220430
F17M	455900	.0002434	868600	377810
F21M	389200	.0005704	24680	12170
F26M	375900	.0005906	55590	10580
F24M	409100	.0005425	168100	14890
F25M	693800	.0003199	39760	125420
F28M	5041000	.0007033	640	5230

K_1 = 9.913 E-10 K_2 = 4.035

Correlation Coefficient R=- .85

BEAM FATIGUE DATA

Asphalt-Rubber Medium at 68°F

Test Date: 6-85

Beam Number	E Modulus	Bending Strain	Actual Cycles to Failure	Predicted Cycles to Failure
F8M	221000	.0030919	680	380
F1M	731000	.0009002	7340	12460
F5M	39500	.001688	1780	2110
F9M	46000	.0010128	8030	8940
F2M	75800	.0003515	140350	177110
F7M	145700	.0001828	1766120	1121570
F6M	87600	.0003547	92720	172630
F4M	67200	.0003965	130000	126120
F3M	85100	.000313	449560	245780

K_1 = 3.156 E-5 K_2 = 2.822

Correlation Coefficient R=- .98

Asphalt-Rubber Medium at 104°F

Test Date: 9-85

Beam Number	E Modulus	Bending Strain	Actual Cycles to Failure	Predicted Cycles to Failure
F10M	35500	.00225081	4190	4340
F13M	17100	.0010406	15460	63010
F14M	14300	.0018568	13780	8450
F16M	26300	.0008437	37990	130440
F18M	18000	.0009843	413700	76410
F19M	18900	.001688	6770	11760
F20M	10500	.0025322	3070	2880
F22M	22500	.0007875	358790	165720
F23M	28200	.0007875	81470	165720
F25M	26300	.0008437	327930	130440

K_1 = 2.823 E-6 K_2 = 3.469

Correlation Coefficient R=- .85

BEAM FATIGUE DATA

Asphalt-Rubber High at 34°F

Test Date: 12-85

Beam Number	E Modulus	Bending Strain	Actual Cycles to Failure	Predicted Cycles to Failure
F11H	585900	.0008184	240	2740
F14H	585900	.0005115	1660	12280
F16H	585900	.0005115	11900	12280
F17H	701700	.0002135	85400	199640
F18H	701700	.0002135	357970	199640
F21H	294700	.000305	763400	63940
F23H	208200	.0014393	1790	450
F25H	293300	.0012261	1820	750

K_1 = 3.824 E-7 K_2 = 3.192

Correlation Coefficient R=- .81

Asphalt-Rubber High at 68°F

Test Date: 7-85

Beam Number	E Modulus	Bending Strain	Actual Cycles to Failure	Predicted Cycles to Failure
F5H	116000	.0002295	770870	705580
F2H	1061000	.0002573	504090	529050
F9H	73600	.0003617	267030	224660
F3H	56400	.0011812	6430	11430
F8H	184100	.0003617	139820	224660
F1H	36300	.0020819	2130	2755
F6H	35100	.0025297	1940	1680
F4H	80800	.0005495	117700	78420
F7H	166500	.0003199	342230	305860
F10H	52200	.0019131	5210	33100

K_1 = 4.895 E-4 K_2 = 2.516

Correlation Coefficient R=- .98

BEAM FATIGUE DATA

Asphalt-Rubber High at 104°F

Test Date: 10-85

Beam Number	E Modulus	Bending Strain	Actual Cycles to Failure	Predicted Cycles to Failure
F12H	21800	.0016526	22080	16290
F13H	20400	.0023456	6760	5800
F15H	16500	.0021857	5430	7140
F19H	9400	.005177	510	580
F20H	24600	.0019458	2450	10060
F22H	15200	.0015726	11650	18860
F25H	41000	.005331	620	520
F26H	16500	.0021857	27220	7140
F27H	15200	.0010487	111050	62280
F24H	17300	.001386	21050	27360

K_1 = 1.020 E-4 K_2 = 2.948

Correlation Coefficient R=- .90

Asphalt Concrete Control at 34°F

Test Date: 12-85

Beam Number	E Modulus	Bending Strain	Actual Cycles to Failure	Predicted Cycles to Failure
F20C	435500	.0008156	470	1490
F21C	638300	.0003478	97130	17990
F22C	531900	.0004173	127640	10560
F23C	569900	.0001947	469280	97770
F25C	1314100	.0002365	6590	55470
F26C	1489300	.0002086	15510	79940
F27C	785600	.0004521	3700	8360

K_1 = 1.428 E-6 K_2 = 2.920

Correlation Coefficient R=- .62

BEAM FATIGUE DATA

Asphalt Concrete Control at 68°F

Test Date: 8-85

Beam Number	E Modulus	Bending Strain	Actual Cycles to Failure	Predicted Cycles to Failure
F6C	133900	.0004476	32530	47350
F9C	170400	.0002813	710110	417330
F4C	151200	.0003964	56200	83630
F5C	187500	.0003836	181800	97520
F8C	119700	.000601	9120	11890
F2C	104200	.0006906	11100	6200
F7C	117200	.0005115	17950	25320
F3C	171500	.0002796	301300	429280

K_1 = 9.475 E-12 K_2 = 4.687

Correlation Coefficient R=- .95

Asphalt Concrete Control at 104°F

Test Date: 10-85

Beam Number	E Modulus	Bending Strain	Actual Cycles to Failure	Predicted Cycles to Failure
F10C	4500	.0079965	1080	270
F11C	7000	.0037946	520	1550
F12C	8200	.0032325	1050	2260
F13C	7700	.0023069	6970	49100
F14C	10900	.0016317	9940	11270
F16C	7200	.0024757	3040	4240
F17C	6600	.003373	16100	2050
F19C	11700	.0007593	148900	67940

K_1 = 3.209 E3 K_2 = 2.348

Correlation Coefficient R=- .89

APPENDIX G

ILLIPAVE Damage Results, With Descriptions Of Calculations For Combined Traffic Damage

APPENDIX G. ILLIPAVE DAMAGE RESULTS, WITH DESCRIPTION OF CALCULATIONS FOR COMBINED TRAFFIC DAMAGE

The printouts in this Appendix summarize the damage results of the ILLIPAVE analyses performed for this study. There are 16 printouts, one for each combination of the four climatic zones and the four materials tested. Each printout shows the resulting damage when each plane was considered as making up the total traffic number, and the resulting damage after the combined traffic pattern containing five aircraft was accounted for.

Table 18 in the text summarizes the numbers of aircraft passes per day at the critical point in the pavement for each aircraft type during each year. In order to calculate the damage due to the combined traffic, the numbers of each aircraft had to be made cumulative for each year. Then, for each year, the percentage of the total cumulative traffic which each aircraft represented was calculated. This percentage appears in the printouts in Column A labeled "% of Total Traffic". The traffic data in this form are shown in the table preceding the damage printouts.

The ILLIPAVE program calculated the damage index based on laboratory fatigue conditions and the rut depth which could be expected every year if all of the traffic had been made up of the same aircraft. These are shown in the printouts in Columns B and D, which are labeled "Damage Index - Total" and "Rut Depth - Total". Multiplying Column A times Column B gives Column C, which indicates the amount of damage index, which that aircraft contributed in that year to the combined traffic damage index. Multiplying Column A times Column D gives Column E, which indicates the amount of rut depth which that aircraft contributes in that year to the combined traffic rut depth. Summing Column C for each aircraft for any year and dividing by 13 gives the damage index due to the combined traffic for that year and adjusted from laboratory to field fatigue conditions. Summing Column E for each aircraft for any year gives the rut depth due to the combined traffic for that year. These sums are shown on the second page of each printout next to "All Traffic".

Cumulative Critical Passes Per Day of Combined Aircraft Traffic.

	DC-9		DC-10		B-727		B-737		B-757		Total	
Year	Number	%	Number	%	Number	%	Number	%	Number	%	Number	%
1	61	100.0	-		-		-		-		61	100.0
2	116	100.0	-		-		-		-		116	100.0
3	148	94.9	-		5	3.2	3	1.9	-		156	100.0
4	162	84.8	-		17	8.9	12	6.3	-		191	100.0
5	169	75.4	-		32	14.3	23	10.3	-		224	100.0
6	174	63.5	-		65	23.7	35	12.8	-		274	100.0
7	177	57.8	-		86	28.1	43	14.1	-		306	100.0
8	181	52.8	-		110	32.1	52	15.2	-		343	100.0
9	185	48.2	-		137	35.7	62	16.1	-		384	100.0
10	191	43.3	-		174	39.5	76	17.2	-		441	100.0
11	198	39.0	-		218	42.9	92	18.1	-		508	100.0
12	206	35.2	-		269	45.9	111	18.9	-		586	100.0
13	216	31.5	-		335	48.8	135	19.7	-		686	100.0
17	251	22.9	1	0.1	610	55.6	234	21.3	1	0.1	1097	100.0
20	267	18.6	9	0.6	842	58.6	312	21.7	8	0.5	1438	100.0

ZONE: Wet Freeze
MATERIAL: AC-10 Control

		A	B	C	D	E
		% of	DAMAGE	INDEX	RUT	DEPTH
PLANE	YEAR	TOT.TRAF.	total	total*%	total	total*%
DC-09	1	1.000	7.62E-02	7.62E-02	5.49E-01	5.49E-01
	2	1.000	1.45E-01	1.45E-01	6.22E-01	6.22E-01
	3	0.949	1.95E-01	1.85E-01	6.63E-01	6.30E-01
	4	0.848	2.39E-01	2.02E-01	6.95E-01	5.89E-01
	5	0.754	2.80E-01	2.11E-01	7.21E-01	5.44E-01
	6	0.635	3.43E-01	2.17E-01	7.58E-01	4.81E-01
	7	0.578	3.83E-01	2.21E-01	7.80E-01	4.51E-01
	8	0.527	4.29E-01	2.26E-01	8.03E-01	4.23E-01
	9	0.482	4.80E-01	2.31E-01	8.27E-01	3.99E-01
	10	0.433	5.51E-01	2.39E-01	8.58E-01	3.72E-01
	11	0.390	6.35E-01	2.48E-01	8.92E-01	3.48E-01
	12	0.352	7.32E-01	2.58E-01	9.28E-01	3.27E-01
	13	0.315	8.57E-01	2.70E-01	9.70E-01	3.06E-01
	17	0.229	1.41E+00	3.23E-01	1.12E+00	2.57E-01
	20	0.186	1.86E+00	3.46E-01	1.22E+00	2.27E-01
		% of	DAMAGE	INDEX	RUT	DEPTH
	YEAR	TOT.TRAF.	total	total*%	total	total*%
DC-10	1	0.000		0.00E+00		0.00E+00
	2	0.000		0.00E+00		0.00E+00
	3	0.000		0.00E+00		0.00E+00
	4	0.000		0.00E+00		0.00E+00
	5	0.000		0.00E+00		0.00E+00
	6	0.000		0.00E+00		0.00E+00
	7	0.000		0.00E+00		0.00E+00
	8	0.000		0.00E+00		0.00E+00
	9	0.000		0.00E+00		0.00E+00
	10	0.000		0.00E+00		0.00E+00
	11	0.000		0.00E+00		0.00E+00
	12	0.000		0.00E+00		0.00E+00
	13	0.000		0.00E+00		0.00E+00
	17	0.001	4.31E+00	4.31E-03	2.28E+00	2.28E-03
	20	0.006	5.67E+00	3.40E-02	2.42E+00	1.45E-02
		% of	DAMAGE	INDEX	RUT	DEPTH
		TOT.TRAF.	total	total*%	total	total*%
B-727	1	0.000		0.00E+00		0.00E+00
	2	0.000		0.00E+00		0.00E+00
	3	0.032	3.57E-01	1.14E-02	8.91E-01	2.85E-02
	4	0.089	4.37E-01	3.89E-02	9.33E-01	8.30E-02
	5	0.143	5.12E-01	7.32E-02	9.68E-01	1.38E-01
	6	0.237	6.27E-01	1.49E-01	1.02E+00	2.41E-01
	7	0.281	7.00E-01	1.97E-01	1.04E+00	2.93E-01
	8	0.321	7.84E-01	2.52E-01	1.08E+00	3.45E-01
	9	0.357	8.78E-01	3.13E-01	1.11E+00	3.95E-01
	10	0.395	1.01E+00	3.98E-01	1.15E+00	4.53E-01
	11	0.429	1.16E+00	4.98E-01	1.19E+00	5.11E-01
	12	0.459	1.34E+00	6.15E-01	1.24E+00	5.69E-01
	13	0.488	1.57E+00	7.66E-01	1.29E+00	6.31E-01
	17	0.556	2.58E+00	1.44E+00	1.49E+00	8.30E-01
	20	0.586	3.40E+00	1.99E+00	1.62E+00	9.48E-01

		A	B	C	D	E
		% of	DAMAGE	INDEX	RUT	DEPTH
PLANE	YEAR	TOT.TRAF.	total	total*%	total	total*%
B-737	1	0.000	6.49E-02	0.00E+00	4.89E-01	0.00E+00
	2	0.000	1.23E-01	0.00E+00	5.52E-01	0.00E+00
	3	0.019	1.66E-01	3.15E-03	5.88E-01	1.12E-02
	4	0.063	2.03E-01	1.28E-02	6.16E-01	3.88E-02
	5	0.103	2.38E-01	2.45E-02	6.39E-01	6.58E-02
	6	0.128	2.91E-01	3.73E-02	6.71E-01	8.59E-02
	7	0.141	3.25E-01	4.59E-02	6.90E-01	9.72E-02
	8	0.152	3.65E-01	5.54E-02	7.10E-01	1.08E-01
	9	0.161	4.08E-01	6.57E-02	7.31E-01	1.18E-01
	10	0.172	4.69E-01	8.07E-02	7.59E-01	1.31E-01
	11	0.181	5.40E-01	9.78E-02	7.89E-01	1.43E-01
	12	0.189	6.23E-01	1.18E-01	8.21E-01	1.55E-01
	13	0.197	7.29E-01	1.44E-01	8.58E-01	1.69E-01
	17	0.213	1.20E+00	2.56E-01	9.94E-01	2.12E-01
	20	0.217	1.58E+00	3.43E-01	1.08E+00	2.35E-01
		% of	DAMAGE	INDEX	RUT	DEPTH
	YEAR	TOT.TRAF.	total	total*%	total	total*%
B-757	1	0.000		0.00E+00		0.00E+00
	2	0.000		0.00E+00		0.00E+00
	3	0.000		0.00E+00		0.00E+00
	4	0.000		0.00E+00		0.00E+00
	5	0.000		0.00E+00		0.00E+00
	6	0.000		0.00E+00		0.00E+00
	7	0.000		0.00E+00		0.00E+00
	8	0.000		0.00E+00		0.00E+00
	9	0.000		0.00E+00		0.00E+00
	10	0.000		0.00E+00		0.00E+00
	11	0.000		0.00E+00		0.00E+00
	12	0.000		0.00E+00		0.00E+00
	13	0.000		0.00E+00		0.00E+00
	17	0.001	1.67E+00	1.67E-03	1.26E+00	1.26E-03
	20	0.005	2.20E+00	1.10E-02	1.36E+00	6.80E-03
		% of	DAMAGE	INDEX	RUT	DEPTH
	YEAR	TOT.TRAF.		tot.*%/13		total*%
All Traf.	1	1.000		5.86E-03		5.49E-01
	2	1.000		1.12E-02		6.22E-01
	3	1.000		1.54E-02		6.69E-01
	4	1.000		1.95E-02		7.11E-01
	5	1.000		2.38E-02		7.48E-01
	6	1.000		3.10E-02		8.08E-01
	7	1.000		3.57E-02		8.41E-01
	8	1.000		4.10E-02		8.76E-01
	9	1.000		4.70E-02		9.11E-01
	10	1.000		5.52E-02		9.55E-01
	11	1.000		6.49E-02		1.00E+00
	12	1.000		7.62E-02		1.05E+00
	13	1.000		9.07E-02		1.11E+00
	17	1.000		1.56E-01		1.30E+00
	20	1.000		2.10E-01		1.43E+00

ZONE: Wet Freeze
MATERIAL:RL

PLANE	YEAR	% of TOT.TRAF.	DAMAGE INDEX total	total*%	RUT DEPTH total	total*%
DC-09	1	1.000	2.02E-02	2.02E-02	1.06E-01	1.06E-01
	2	1.000	3.84E-02	3.84E-02	1.66E-01	1.66E-01
	3	0.949	5.17E-02	4.90E-02	2.02E-01	1.91E-01
	4	0.848	6.33E-02	5.37E-02	2.30E-01	1.95E-01
	5	0.754	7.42E-02	5.60E-02	2.54E-01	1.92E-01
	6	0.635	9.08E-02	5.76E-02	2.88E-01	1.83E-01
	7	0.578	1.01E-01	5.86E-02	3.08E-01	1.78E-01
	8	0.527	1.14E-01	5.99E-02	3.30E-01	1.74E-01
	9	0.482	1.27E-01	6.13E-02	3.52E-01	1.70E-01
	10	0.433	1.46E-01	6.33E-02	3.82E-01	1.65E-01
	11	0.390	1.68E-01	6.56E-02	4.15E-01	1.62E-01
	12	0.352	1.94E-01	6.83E-02	4.50E-01	1.58E-01
	13	0.315	2.27E-01	7.16E-02	4.91E-01	1.55E-01
	17	0.229	3.74E-01	8.57E-02	6.43E-01	1.47E-01
	20	0.186	4.93E-01	9.16E-02	7.42E-01	1.38E-01
	YEAR	% of TOT.TRAF.	DAMAGE INDEX total	total*%	RUT DEPTH total	total*%
DC-10	1	0.000	1.12E-01	0.00E+00	2.11E-01	0.00E+00
	2	0.000	2.14E-01	0.00E+00	3.22E-01	0.00E+00
	3	0.000	2.87E-01	0.00E+00	3.87E-01	0.00E+00
	4	0.000	3.52E-01	0.00E+00	4.39E-01	0.00E+00
	5	0.000	4.13E-01	0.00E+00	4.83E-01	0.00E+00
	6	0.000	5.05E-01	0.00E+00	5.44E-01	0.00E+00
	7	0.000	5.64E-01	0.00E+00	5.80E-01	0.00E+00
	8	0.000	6.32E-01	0.00E+00	6.20E-01	0.00E+00
	9	0.000	7.07E-01	0.00E+00	6.61E-01	0.00E+00
	10	0.000	8.12E-01	0.00E+00	7.14E-01	0.00E+00
	11	0.000	9.35E-01	0.00E+00	7.72E-01	0.00E+00
	12	0.000	1.08E+00	0.00E+00	8.35E-01	0.00E+00
	13	0.000	1.26E+00	0.00E+00	9.09E-01	0.00E+00
	17	0.001	2.08E+00	2.08E-03	1.18E+00	1.18E-03
	20	0.006	2.74E+00	1.64E-02	1.35E+00	8.09E-03
		% of TOT.TRAF.	DAMAGE INDEX total	total*%	RUT DEPTH total	total*%
B-727	1	0.000	4.97E-02	0.00E+00	1.39E-01	0.00E+00
	2	0.000	9.45E-02	0.00E+00	2.16E-01	0.00E+00
	3	0.032	1.27E-01	4.06E-03	2.62E-01	8.37E-03
	4	0.089	1.56E-01	1.38E-02	2.97E-01	2.65E-02
	5	0.143	1.82E-01	2.61E-02	3.28E-01	4.69E-02
	6	0.237	2.23E-01	5.29E-02	3.71E-01	8.79E-02
	7	0.281	2.49E-01	7.00E-02	3.96E-01	1.11E-01
	8	0.321	2.79E-01	8.97E-02	4.24E-01	1.36E-01
	9	0.357	3.13E-01	1.12E-01	4.53E-01	1.62E-01
	10	0.395	3.59E-01	1.42E-01	4.90E-01	1.94E-01
	11	0.429	4.14E-01	1.77E-01	5.31E-01	2.28E-01
	12	0.459	4.77E-01	2.19E-01	5.75E-01	2.64E-01
	13	0.488	5.59E-01	2.73E-01	6.27E-01	3.06E-01
	17	0.556	9.20E-01	5.12E-01	8.18E-01	4.55E-01
	20	0.586	1.21E+00	7.10E-01	9.41E-01	5.51E-01

PLANE	YEAR	% of TOT.TRAF.	DAMAGE INDEX total	total*%	RUT DEPTH total	total*%
B-737	1	0.000	1.40E-02	0.00E+00	9.22E-02	0.00E+00
	2	0.000	2.67E-02	0.00E+00	1.45E-01	0.00E+00
	3	0.019	3.59E-02	6.82E-04	1.77E-01	3.36E-03
	4	0.063	4.40E-02	2.77E-03	2.01E-01	1.27E-02
	5	0.103	5.16E-02	5.31E-03	2.23E-01	2.30E-02
	6	0.128	6.31E-02	8.07E-03	2.53E-01	3.24E-02
	7	0.141	7.04E-02	9.93E-03	2.71E-01	3.82E-02
	8	0.152	7.89E-02	1.20E-02	2.90E-01	4.41E-02
	9	0.161	8.84E-02	1.42E-02	3.11E-01	5.00E-02
	10	0.172	1.02E-01	1.75E-02	3.37E-01	5.80E-02
	11	0.181	1.17E-01	2.12E-02	3.66E-01	6.63E-02
	12	0.189	1.35E-01	2.55E-02	3.97E-01	7.51E-02
	13	0.197	1.58E-01	3.11E-02	4.35E-01	8.56E-02
	17	0.213	2.60E-01	5.54E-02	5.71E-01	1.22E-01
	20	0.217	3.42E-01	7.43E-02	6.59E-01	1.43E-01
	YEAR	% of TOT.TRAF.	DAMAGE INDEX total	total*%	RUT DEPTH total	total*%
B-757	1	0.000	3.11E-02	0.00E+00	1.83E-01	0.00E+00
	2	0.000	5.92E-02	0.00E+00	2.59E-01	0.00E+00
	3	0.000	7.96E-02	0.00E+00	3.03E-01	0.00E+00
	4	0.000	9.75E-02	0.00E+00	3.37E-01	0.00E+00
	5	0.000	1.14E-01	0.00E+00	3.67E-01	0.00E+00
	6	0.000	1.40E-01	0.00E+00	4.07E-01	0.00E+00
	7	0.000	1.56E-01	0.00E+00	4.31E-01	0.00E+00
	8	0.000	1.75E-01	0.00E+00	4.57E-01	0.00E+00
	9	0.000	1.96E-01	0.00E+00	4.84E-01	0.00E+00
	10	0.000	2.25E-01	0.00E+00	5.19E-01	0.00E+00
	11	0.000	2.59E-01	0.00E+00	5.57E-01	0.00E+00
	12	0.000	2.99E-01	0.00E+00	5.98E-01	0.00E+00
	13	0.000	3.50E-01	0.00E+00	6.46E-01	0.00E+00
	17	0.001	5.77E-01	5.77E-04	8.21E-01	8.21E-04
	20	0.005	7.59E-01	3.79E-03	9.33E-01	4.66E-03
	YEAR	% of TOT.TRAF.	DAMAGE INDEX tot.*%/13		RUT DEPTH total*%	
All Traf.	1	1.000	1.55E-03		1.06E-01	
	2	1.000	2.96E-03		1.66E-01	
	3	1.000	4.14E-03		2.03E-01	
	4	1.000	5.40E-03		2.34E-01	
	5	1.000	6.72E-03		2.61E-01	
	6	1.000	9.12E-03		3.03E-01	
	7	1.000	1.07E-02		3.27E-01	
	8	1.000	1.24E-02		3.54E-01	
	9	1.000	1.44E-02		3.81E-01	
	10	1.000	1.71E-02		4.17E-01	
	11	1.000	2.03E-02		4.56E-01	
	12	1.000	2.41E-02		4.97E-01	
	13	1.000	2.89E-02		5.46E-01	
	17	1.000	5.04E-02		7.26E-01	
	20	1.000	6.89E-02		8.45E-01	

ZONE: Wet Freeze
MATERIAL:RM

PLANE	YEAR	% of TOT.TRAF.	DAMAGE INDEX total	total*%	RUT DEPTH total	total*%
DC-09	1	1.000	1.18E-02	1.18E-02	1.03E-01	1.03E-01
	2	1.000	2.24E-02	2.24E-02	1.60E-01	1.60E-01
	3	0.949	3.01E-02	2.86E-02	1.94E-01	1.84E-01
	4	0.848	3.69E-02	3.13E-02	2.21E-01	1.88E-01
	5	0.754	4.32E-02	3.26E-02	2.44E-01	1.84E-01
	6	0.635	5.29E-02	3.36E-02	2.76E-01	1.75E-01
	7	0.578	5.91E-02	3.41E-02	2.95E-01	1.71E-01
	8	0.527	6.62E-02	3.49E-02	3.16E-01	1.66E-01
	9	0.482	7.41E-02	3.57E-02	3.38E-01	1.63E-01
	10	0.433	8.51E-02	3.69E-02	3.66E-01	1.58E-01
	11	0.390	9.81E-02	3.82E-02	3.96E-01	1.55E-01
	12	0.352	1.13E-01	3.98E-02	4.29E-01	1.51E-01
	13	0.315	1.32E-01	4.17E-02	4.68E-01	1.47E-01
	17	0.229	2.18E-01	4.99E-02	6.10E-01	1.40E-01
	20	0.186	2.87E-01	5.34E-02	7.01E-01	1.30E-01
	YEAR	% of TOT.TRAF.	DAMAGE INDEX total	total*%	RUT DEPTH total	total*%
DC-10	1	0.000	5.53E-02	0.00E+00	1.82E-01	0.00E+00
	2	0.000	1.05E-01	0.00E+00	2.68E-01	0.00E+00
	3	0.000	1.42E-01	0.00E+00	3.17E-01	0.00E+00
	4	0.000	1.73E-01	0.00E+00	3.55E-01	0.00E+00
	5	0.000	2.03E-01	0.00E+00	3.87E-01	0.00E+00
	6	0.000	2.49E-01	0.00E+00	4.31E-01	0.00E+00
	7	0.000	2.78E-01	0.00E+00	4.57E-01	0.00E+00
	8	0.000	3.11E-01	0.00E+00	4.85E-01	0.00E+00
	9	0.000	3.48E-01	0.00E+00	5.14E-01	0.00E+00
	10	0.000	4.00E-01	0.00E+00	5.51E-01	0.00E+00
	11	0.000	4.61E-01	0.00E+00	5.91E-01	0.00E+00
	12	0.000	5.32E-01	0.00E+00	6.34E-01	0.00E+00
	13	0.000	6.22E-01	0.00E+00	6.84E-01	0.00E+00
	17	0.001	1.02E+00	1.02E-03	8.63E-01	8.63E-04
	20	0.006	1.35E+00	8.09E-03	9.75E-01	5.85E-03
		% of TOT.TRAF.	DAMAGE INDEX total	total*%	RUT DEPTH total	total*%
B-727	1	0.000	2.59E-02	0.00E+00	1.41E-01	0.00E+00
	2	0.000	4.92E-02	0.00E+00	2.17E-01	0.00E+00
	3	0.032	6.62E-02	2.12E-03	2.62E-01	8.39E-03
	4	0.089	8.10E-02	7.21E-03	2.97E-01	2.65E-02
	5	0.143	9.50E-02	1.36E-02	3.28E-01	4.68E-02
	6	0.237	1.16E-01	2.75E-02	3.69E-01	8.75E-02
	7	0.281	1.30E-01	3.65E-02	3.94E-01	1.11E-01
	8	0.321	1.46E-01	4.67E-02	4.21E-01	1.35E-01
	9	0.357	1.63E-01	5.82E-02	4.49E-01	1.60E-01
	10	0.395	1.87E-01	7.39E-02	4.86E-01	1.92E-01
	11	0.429	2.16E-01	9.24E-02	5.26E-01	2.25E-01
	12	0.459	2.49E-01	1.14E-01	5.68E-01	2.61E-01
	13	0.488	2.91E-01	1.42E-01	6.18E-01	3.02E-01
	17	0.556	4.79E-01	2.67E-01	8.01E-01	4.46E-01
	20	0.586	6.31E-01	3.70E-01	9.19E-01	5.38E-01

PLANE	YEAR	% of TOT.TRAF.	DAMAGE INDEX total	DAMAGE INDEX total*%	RUT DEPTH total	RUT DEPTH total*%
B-737	1	0.000	8.29E-03	0.00E+00	9.17E-02	0.00E+00
	2	0.000	1.58E-02	0.00E+00	1.43E-01	0.00E+00
	3	0.019	2.12E-02	4.03E-04	1.74E-01	3.30E-03
	4	0.063	2.60E-02	1.64E-03	1.98E-01	1.25E-02
	5	0.103	3.05E-02	3.14E-03	2.18E-01	2.25E-02
	6	0.128	3.72E-02	4.77E-03	2.47E-01	3.16E-02
	7	0.141	4.16E-02	5.86E-03	2.64E-01	3.73E-02
	8	0.152	4.66E-02	7.09E-03	2.83E-01	4.30E-02
	9	0.161	5.22E-02	8.40E-03	3.02E-01	4.87E-02
	10	0.172	5.99E-02	1.03E-02	3.28E-01	5.63E-02
	11	0.181	6.91E-02	1.25E-02	3.55E-01	6.43E-02
	12	0.189	7.97E-02	1.51E-02	3.85E-01	7.27E-02
	13	0.197	9.32E-02	1.84E-02	4.20E-01	8.27E-02
	17	0.213	1.54E-01	3.27E-02	5.48E-01	1.17E-01
	20	0.217	2.02E-01	4.39E-02	6.30E-01	1.37E-01
	YEAR	% of TOT.TRAF.	DAMAGE INDEX total	DAMAGE INDEX total*%	RUT DEPTH total	RUT DEPTH total*%
B-757	1	0.000	1.41E-02	0.00E+00	1.52E-01	0.00E+00
	2	0.000	2.68E-02	0.00E+00	2.06E-01	0.00E+00
	3	0.000	3.61E-02	0.00E+00	2.37E-01	0.00E+00
	4	0.000	4.42E-02	0.00E+00	2.61E-01	0.00E+00
	5	0.000	5.18E-02	0.00E+00	2.82E-01	0.00E+00
	6	0.000	6.34E-02	0.00E+00	3.10E-01	0.00E+00
	7	0.000	7.08E-02	0.00E+00	3.27E-01	0.00E+00
	8	0.000	7.94E-02	0.00E+00	3.45E-01	0.00E+00
	9	0.000	8.89E-02	0.00E+00	3.63E-01	0.00E+00
	10	0.000	1.02E-01	0.00E+00	3.87E-01	0.00E+00
	11	0.000	1.18E-01	0.00E+00	4.13E-01	0.00E+00
	12	0.000	1.36E-01	0.00E+00	4.41E-01	0.00E+00
	13	0.000	1.59E-01	0.00E+00	4.73E-01	0.00E+00
	17	0.001	2.62E-01	2.62E-04	5.90E-01	5.90E-04
	20	0.005	3.44E-01	1.72E-03	6.63E-01	3.32E-03
	YEAR	% of TOT.TRAF.	DAMAGE	INDEX tot.*%/13	RUT	DEPTH total*%
All Traf.	1	1.000		9.06E-04		1.03E-01
	2	1.000		1.72E-03		1.60E-01
	3	1.000		2.39E-03		1.96E-01
	4	1.000		3.09E-03		2.26E-01
	5	1.000		3.79E-03		2.54E-01
	6	1.000		5.07E-03		2.95E-01
	7	1.000		5.88E-03		3.19E-01
	8	1.000		6.82E-03		3.45E-01
	9	1.000		7.87E-03		3.72E-01
	10	1.000		9.31E-03		4.07E-01
	11	1.000		1.10E-02		4.44E-01
	12	1.000		1.30E-02		4.85E-01
	13	1.000		1.55E-02		5.32E-01
	17	1.000		2.70E-02		7.03E-01
	20	1.000		3.67E-02		8.15E-01

ZONE: Wet Freeze
MATERIAL:RH

PLANE	YEAR	% of TOT.TRAF.	DAMAGE INDEX total	DAMAGE INDEX total*%	RUT DEPTH total	RUT DEPTH total*%
DC-09	1	1.000	1.33E-02	1.33E-02	1.24E-01	1.24E-01
	2	1.000	2.53E-02	2.53E-02	1.89E-01	1.89E-01
	3	0.949	3.40E-02	3.23E-02	2.27E-01	2.16E-01
	4	0.848	4.17E-02	3.53E-02	2.57E-01	2.18E-01
	5	0.754	4.89E-02	3.68E-02	2.82E-01	2.12E-01
	6	0.635	5.98E-02	3.79E-02	3.16E-01	2.01E-01
	7	0.578	6.67E-02	3.86E-02	3.36E-01	1.94E-01
	8	0.527	7.48E-02	3.94E-02	3.58E-01	1.89E-01
	9	0.482	8.37E-02	4.04E-02	3.81E-01	1.84E-01
	10	0.433	9.62E-02	4.16E-02	4.11E-01	1.78E-01
	11	0.390	1.11E-01	4.32E-02	4.43E-01	1.73E-01
	12	0.352	1.28E-01	4.50E-02	4.78E-01	1.68E-01
	13	0.315	1.50E-01	4.71E-02	5.18E-01	1.63E-01
	17	0.229	2.46E-01	5.64E-02	6.65E-01	1.52E-01
	20	0.186	3.24E-01	6.03E-02	7.59E-01	1.41E-01
	YEAR	% of TOT.TRAF.	DAMAGE INDEX total	INDEX total*%	RUT total	DEPTH total*%
DC-10	1	0.000		0.00E+00		0.00E+00
	2	0.000		0.00E+00		0.00E+00
	3	0.000		0.00E+00		0.00E+00
	4	0.000		0.00E+00		0.00E+00
	5	0.000		0.00E+00		0.00E+00
	6	0.000		0.00E+00		0.00E+00
	7	0.000		0.00E+00		0.00E+00
	8	0.000		0.00E+00		0.00E+00
	9	0.000		0.00E+00		0.00E+00
	10	0.000		0.00E+00		0.00E+00
	11	0.000		0.00E+00		0.00E+00
	12	0.000		0.00E+00		0.00E+00
	13	0.000		0.00E+00		0.00E+00
	17	0.001	9.58E-01	9.58E-04	1.05E+00	1.05E-03
	20	0.006	1.26E+00	7.57E-03	1.17E+00	7.04E-03
		% of TOT.TRAF.	DAMAGE INDEX total	INDEX total*%	RUT total	DEPTH total*%
B-727	1	0.000		0.00E+00		0.00E+00
	2	0.000		0.00E+00		0.00E+00
	3	0.032	9.57E-02	3.06E-03	2.96E-01	9.46E-03
	4	0.089	1.17E-01	1.04E-02	3.33E-01	2.97E-02
	5	0.143	1.37E-01	1.96E-02	3.66E-01	5.23E-02
	6	0.237	1.68E-01	3.98E-02	4.10E-01	9.71E-02
	7	0.281	1.88E-01	5.27E-02	4.36E-01	1.23E-01
	8	0.321	2.10E-01	6.75E-02	4.64E-01	1.49E-01
	9	0.357	2.36E-01	8.41E-02	4.94E-01	1.76E-01
	10	0.395	2.70E-01	1.07E-01	5.32E-01	2.10E-01
	11	0.429	3.12E-01	1.34E-01	5.73E-01	2.46E-01
	12	0.459	3.59E-01	1.65E-01	6.18E-01	2.84E-01
	13	0.488	4.21E-01	2.05E-01	6.70E-01	3.27E-01
	17	0.556	6.93E-01	3.85E-01	8.58E-01	4.77E-01
	20	0.586	9.12E-01	5.34E-01	9.78E-01	5.73E-01

PLANE	YEAR	% of TOT.TRAF.	DAMAGE INDEX total	total*%	RUT DEPTH total	total*%
B-737	1	0.000		0.00E+00		0.00E+00
	2	0.000		0.00E+00		0.00E+00
	3	0.019	2.94E-02	5.59E-04	2.04E-01	3.88E-03
	4	0.063	3.60E-02	2.27E-03	2.30E-01	1.45E-02
	5	0.103	4.23E-02	4.35E-03	2.53E-01	2.60E-02
	6	0.128	5.17E-02	6.62E-03	2.83E-01	3.63E-02
	7	0.141	5.77E-02	8.14E-03	3.02E-01	4.25E-02
	8	0.152	6.47E-02	9.84E-03	3.21E-01	4.88E-02
	9	0.161	7.25E-02	1.17E-02	3.42E-01	5.50E-02
	10	0.172	8.32E-02	1.43E-02	3.68E-01	6.33E-02
	11	0.181	9.59E-02	1.74E-02	3.97E-01	7.18E-02
	12	0.189	1.11E-01	2.09E-02	4.28E-01	8.08E-02
	13	0.197	1.30E-01	2.55E-02	4.64E-01	9.14E-02
	17	0.213	2.13E-01	4.54E-02	5.95E-01	1.27E-01
	20	0.217	2.81E-01	6.09E-02	6.79E-01	1.47E-01
	YEAR	% of TOT.TRAF.	DAMAGE INDEX total	total*%	RUT DEPTH total	total*%
B-757	1	0.000		0.00E+00		0.00E+00
	2	0.000		0.00E+00		0.00E+00
	3	0.000		0.00E+00		0.00E+00
	4	0.000		0.00E+00		0.00E+00
	5	0.000		0.00E+00		0.00E+00
	6	0.000		0.00E+00		0.00E+00
	7	0.000		0.00E+00		0.00E+00
	8	0.000		0.00E+00		0.00E+00
	9	0.000		0.00E+00		0.00E+00
	10	0.000		0.00E+00		0.00E+00
	11	0.000		0.00E+00		0.00E+00
	12	0.000		0.00E+00		0.00E+00
	13	0.000		0.00E+00		0.00E+00
	17	0.001	3.44E-01	3.44E-04	9.47E-01	9.47E-04
	20	0.005	4.53E-01	2.26E-03	1.03E+00	5.14E-03
	YEAR	% of TOT.TRAF.	DAMAGE	INDEX tot.*%/13	RUT	DEPTH total*%
All Traf.	1	1.000		1.02E-03		1.24E-01
	2	1.000		1.95E-03		1.89E-01
	3	1.000		2.76E-03		2.29E-01
	4	1.000		3.69E-03		2.62E-01
	5	1.000		4.68E-03		2.91E-01
	6	1.000		6.49E-03		3.34E-01
	7	1.000		7.65E-03		3.59E-01
	8	1.000		8.98E-03		3.87E-01
	9	1.000		1.05E-02		4.15E-01
	10	1.000		1.25E-02		4.51E-01
	11	1.000		1.49E-02		4.91E-01
	12	1.000		1.78E-02		5.32E-01
	13	1.000		2.14E-02		5.81E-01
	17	1.000		3.76E-02		7.58E-01
	20	1.000		5.12E-02		8.74E-01

ZONE: Dry Freeze
MATERIAL:AC-10 Control

PLANE	YEAR	A % of TOT.TRAF.	B DAMAGE total	C INDEX total*%	D RUT total	E DEPTH total*%
DC-09	1	1.000	5.26E-02	5.26E-02	5.38E-01	5.38E-01
	2	1.000	1.00E-01	1.00E-01	6.07E-01	6.07E-01
	3	0.949	1.35E-01	1.28E-01	6.46E-01	6.13E-01
	4	0.848	1.65E-01	1.40E-01	6.76E-01	5.74E-01
	5	0.754	1.93E-01	1.46E-01	7.02E-01	5.30E-01
	6	0.635	2.36E-01	1.50E-01	7.38E-01	4.69E-01
	7	0.578	2.64E-01	1.53E-01	7.59E-01	4.39E-01
	8	0.527	2.96E-01	1.56E-01	7.81E-01	4.12E-01
	9	0.482	3.31E-01	1.60E-01	8.05E-01	3.88E-01
	10	0.433	3.80E-01	1.65E-01	8.36E-01	3.62E-01
	11	0.390	4.38E-01	1.71E-01	8.69E-01	3.39E-01
	12	0.352	5.05E-01	1.78E-01	9.05E-01	3.19E-01
	13	0.315	5.92E-01	1.86E-01	9.47E-01	2.98E-01
	17	0.229	9.75E-01	2.23E-01	1.10E+00	2.52E-01
	20	0.186	1.28E+00	2.38E-01	1.20E+00	2.23E-01
	YEAR	% of TOT.TRAF.	DAMAGE total	INDEX total*%	RUT total	DEPTH total*%
DC-10	1	0.000		0.00E+00		0.00E+00
	2	0.000		0.00E+00		0.00E+00
	3	0.000		0.00E+00		0.00E+00
	4	0.000		0.00E+00		0.00E+00
	5	0.000		0.00E+00		0.00E+00
	6	0.000		0.00E+00		0.00E+00
	7	0.000		0.00E+00		0.00E+00
	8	0.000		0.00E+00		0.00E+00
	9	0.000		0.00E+00		0.00E+00
	10	0.000		0.00E+00		0.00E+00
	11	0.000		0.00E+00		0.00E+00
	12	0.000		0.00E+00		0.00E+00
	13	0.000		0.00E+00		0.00E+00
	17	0.001	3.42E+00	3.42E-03	2.31E+00	2.31E-03
	20	0.006	4.51E+00	2.70E-02	2.46E+00	1.48E-02
		% of TOT.TRAF.	DAMAGE total	INDEX total*%	RUT total	DEPTH total*%
B-727	1	0.000		0.00E+00		0.00E+00
	2	0.000		0.00E+00		0.00E+00
	3	0.032	2.80E-01	8.96E-03	8.68E-01	2.78E-02
	4	0.089	3.43E-01	3.05E-02	9.09E-01	8.09E-02
	5	0.143	4.02E-01	5.75E-02	9.43E-01	1.35E-01
	6	0.237	4.92E-01	1.17E-01	9.90E-01	2.35E-01
	7	0.281	5.49E-01	1.54E-01	1.02E+00	2.86E-01
	8	0.321	6.16E-01	1.98E-01	1.05E+00	3.36E-01
	9	0.357	6.89E-01	2.46E-01	1.08E+00	3.85E-01
	10	0.395	7.92E-01	3.13E-01	1.12E+00	4.42E-01
	11	0.429	9.12E-01	3.91E-01	1.16E+00	4.99E-01
	12	0.459	1.05E+00	4.83E-01	1.21E+00	5.55E-01
	13	0.488	1.23E+00	6.01E-01	1.27E+00	6.18E-01
	17	0.556	2.03E+00	1.13E+00	1.47E+00	8.16E-01
	20	0.586	2.67E+00	1.56E+00	1.60E+00	9.35E-01

		A	B	C	D	E
		% of	DAMAGE	INDEX	RUT	DEPTH
PLANE	YEAR	TOT.TRAF.	total	total*%	total	total*%
B-737	1	0.000		0.00E+00		0.00E+00
	2	0.000		0.00E+00		0.00E+00
	3	0.019	1.15E-01	2.18E-03	5.75E-01	1.09E-02
	4	0.063	1.40E-01	8.83E-03	6.01E-01	3.79E-02
	5	0.103	1.64E-01	1.69E-02	6.24E-01	6.43E-02
	6	0.128	2.01E-01	2.57E-02	6.55E-01	8.39E-02
	7	0.141	2.25E-01	3.17E-02	6.74E-01	9.50E-02
	8	0.152	2.52E-01	3.83E-02	6.94E-01	1.05E-01
	9	0.161	2.82E-01	4.54E-02	7.14E-01	1.15E-01
	10	0.172	3.24E-01	5.57E-02	7.42E-01	1.28E-01
	11	0.181	3.73E-01	6.75E-02	7.71E-01	1.40E-01
	12	0.189	4.30E-01	8.13E-02	8.03E-01	1.52E-01
	13	0.197	5.03E-01	9.92E-02	8.40E-01	1.66E-01
	17	0.213	8.29E-01	1.77E-01	9.77E-01	2.08E-01
	20	0.217	1.09E+00	2.37E-01	1.06E+00	2.31E-01
		% of	DAMAGE	INDEX	RUT	DEPTH
	YEAR	TOT.TRAF.	total	total*%	total	total*%
B-757	1	0.000		0.00E+00		0.00E+00
	2	0.000		0.00E+00		0.00E+00
	3	0.000		0.00E+00		0.00E+00
	4	0.000		0.00E+00		0.00E+00
	5	0.000		0.00E+00		0.00E+00
	6	0.000		0.00E+00		0.00E+00
	7	0.000		0.00E+00		0.00E+00
	8	0.000		0.00E+00		0.00E+00
	9	0.000		0.00E+00		0.00E+00
	10	0.000		0.00E+00		0.00E+00
	11	0.000		0.00E+00		0.00E+00
	12	0.000		0.00E+00		0.00E+00
	13	0.000		0.00E+00		0.00E+00
	17	0.001	1.16E+00	1.16E-03	1.37E+00	1.37E-03
	20	0.005	1.53E+00	7.64E-03	1.48E+00	7.42E-03
		% of	DAMAGE	INDEX	RUT	DEPTH
	YEAR	TOT.TRAF.		tot.*%/13		total*%
All Traf.	1	1.000		4.05E-03		5.38E-01
	2	1.000		7.69E-03		6.07E-01
	3	1.000		1.07E-02		6.52E-01
	4	1.000		1.38E-02		6.92E-01
	5	1.000		1.69E-02		7.29E-01
	6	1.000		2.25E-02		7.87E-01
	7	1.000		2.60E-02		8.20E-01
	8	1.000		3.01E-02		8.54E-01
	9	1.000		3.47E-02		8.88E-01
	10	1.000		4.10E-02		9.31E-01
	11	1.000		4.84E-02		9.77E-01
	12	1.000		5.71E-02		1.03E+00
	13	1.000		6.82E-02		1.08E+00
	17	1.000		1.18E-01		1.28E+00
	20	1.000		1.60E-01		1.41E+00

ZONE: Dry Freeze
MATERIAL:RL

PLANE	YEAR	% of TOT.TRAF.	DAMAGE INDEX total	total*%	RUT DEPTH total	total*%
DC-09	1	1.000	2.22E-02	2.22E-02	1.05E-01	1.05E-01
	2	1.000	4.22E-02	4.22E-02	1.62E-01	1.62E-01
	3	0.949	5.67E-02	5.38E-02	1.96E-01	1.86E-01
	4	0.848	6.95E-02	5.89E-02	2.22E-01	1.89E-01
	5	0.754	8.15E-02	6.14E-02	2.45E-01	1.85E-01
	6	0.635	9.96E-02	6.33E-02	2.77E-01	1.76E-01
	7	0.578	1.11E-01	6.43E-02	2.96E-01	1.71E-01
	8	0.527	1.25E-01	6.57E-02	3.17E-01	1.67E-01
	9	0.482	1.40E-01	6.73E-02	3.38E-01	1.63E-01
	10	0.433	1.60E-01	6.95E-02	3.66E-01	1.58E-01
	11	0.390	1.85E-01	7.20E-02	3.96E-01	1.55E-01
	12	0.352	2.13E-01	7.50E-02	4.29E-01	1.51E-01
	13	0.315	2.50E-01	7.86E-02	4.68E-01	1.47E-01
	17	0.229	4.11E-01	9.41E-02	6.09E-01	1.39E-01
	20	0.186	5.41E-01	1.01E-01	7.00E-01	1.30E-01
	YEAR	% of TOT.TRAF.	DAMAGE INDEX total	total*%	RUT DEPTH total	total*%
DC-10	1	0.000		0.00E+00		0.00E+00
	2	0.000		0.00E+00		0.00E+00
	3	0.000		0.00E+00		0.00E+00
	4	0.000		0.00E+00		0.00E+00
	5	0.000		0.00E+00		0.00E+00
	6	0.000		0.00E+00		0.00E+00
	7	0.000		0.00E+00		0.00E+00
	8	0.000		0.00E+00		0.00E+00
	9	0.000		0.00E+00		0.00E+00
	10	0.000		0.00E+00		0.00E+00
	11	0.000		0.00E+00		0.00E+00
	12	0.000		0.00E+00		0.00E+00
	13	0.000		0.00E+00		0.00E+00
	17	0.001	1.92E+00	1.92E-03	8.15E-01	8.15E-04
	20	0.006	2.53E+00	1.52E-02	9.23E-01	5.54E-03
		% of TOT.TRAF.	DAMAGE INDEX total	total*%	RUT DEPTH total	total*%
B-727	1	0.000		0.00E+00		0.00E+00
	2	0.000		0.00E+00		0.00E+00
	3	0.032	1.15E-01	3.68E-03	2.50E-01	8.00E-03
	4	0.089	1.41E-01	1.25E-02	2.84E-01	2.52E-02
	5	0.143	1.65E-01	2.36E-02	3.13E-01	4.47E-02
	6	0.237	2.02E-01	4.79E-02	3.53E-01	8.37E-02
	7	0.281	2.26E-01	6.34E-02	3.77E-01	1.06E-01
	8	0.321	2.53E-01	8.12E-02	4.03E-01	1.29E-01
	9	0.357	2.83E-01	1.01E-01	4.29E-01	1.53E-01
	10	0.395	3.25E-01	1.29E-01	4.65E-01	1.84E-01
	11	0.429	3.75E-01	1.61E-01	5.03E-01	2.16E-01
	12	0.459	4.32E-01	1.98E-01	5.45E-01	2.50E-01
	13	0.488	5.06E-01	2.47E-01	5.93E-01	2.89E-01
	17	0.556	8.34E-01	4.64E-01	7.70E-01	4.28E-01
	20	0.586	1.10E+00	6.43E-01	8.84E-01	5.18E-01

PLANE	YEAR	% of TOT.TRAF.	DAMAGE INDEX total	total*%	RUT DEPTH total	total*%
B-737	1	0.000		0.00E+00		0.00E+00
	2	0.000		0.00E+00		0.00E+00
	3	0.019	3.95E-02	7.50E-04	1.74E-01	3.30E-03
	4	0.063	4.84E-02	3.05E-03	1.98E-01	1.24E-02
	5	0.103	5.67E-02	5.84E-03	2.18E-01	2.25E-02
	6	0.128	6.94E-02	8.88E-03	2.47E-01	3.16E-02
	7	0.141	7.75E-02	1.09E-02	2.64E-01	3.72E-02
	8	0.152	8.68E-02	1.32E-02	2.82E-01	4.29E-02
	9	0.161	9.72E-02	1.57E-02	3.01E-01	4.85E-02
	10	0.172	1.12E-01	1.92E-02	3.26E-01	5.61E-02
	11	0.181	1.29E-01	2.33E-02	3.54E-01	6.40E-02
	12	0.189	1.48E-01	2.80E-02	3.83E-01	7.24E-02
	13	0.197	1.74E-01	3.42E-02	4.18E-01	8.23E-02
	17	0.213	2.86E-01	6.09E-02	5.45E-01	1.16E-01
	20	0.217	3.76E-01	8.17E-02	6.27E-01	1.36E-01
	YEAR	% of TOT.TRAF.	DAMAGE INDEX total	total*%	RUT DEPTH total	total*%
B-757	1	0.000		0.00E+00		0.00E+00
	2	0.000		0.00E+00		0.00E+00
	3	0.000		0.00E+00		0.00E+00
	4	0.000		0.00E+00		0.00E+00
	5	0.000		0.00E+00		0.00E+00
	6	0.000		0.00E+00		0.00E+00
	7	0.000		0.00E+00		0.00E+00
	8	0.000		0.00E+00		0.00E+00
	9	0.000		0.00E+00		0.00E+00
	10	0.000		0.00E+00		0.00E+00
	11	0.000		0.00E+00		0.00E+00
	12	0.000		0.00E+00		0.00E+00
	13	0.000		0.00E+00		0.00E+00
	17	0.001	5.06E-01	5.06E-04	6.48E-01	6.48E-04
	20	0.005	6.66E-01	3.33E-03	7.29E-01	3.65E-03
	YEAR	% of TOT.TRAF.	DAMAGE	INDEX tot.*%/13	RUT	DEPTH total*%
All Traf.	1	1.000		1.71E-03		1.05E-01
	2	1.000		3.24E-03		1.62E-01
	3	1.000		4.48E-03		1.97E-01
	4	1.000		5.73E-03		2.26E-01
	5	1.000		6.99E-03		2.52E-01
	6	1.000		9.24E-03		2.91E-01
	7	1.000		1.07E-02		3.14E-01
	8	1.000		1.23E-02		3.39E-01
	9	1.000		1.42E-02		3.65E-01
	10	1.000		1.67E-02		3.98E-01
	11	1.000		1.97E-02		4.34E-01
	12	1.000		2.32E-02		4.73E-01
	13	1.000		2.77E-02		5.19E-01
	17	1.000		4.78E-02		6.85E-01
	20	1.000		6.49E-02		7.93E-01

ZONE: Dry Freeze
MATERIAL: RM

PLANE	YEAR	% of TOT. TRAF.	DAMAGE INDEX total	total*%	RUT DEPTH total	total*%
DC-09	1	1.000	7.99E-03	7.99E-03	9.94E-02	9.94E-02
	2	1.000	1.52E-02	1.52E-02	1.55E-01	1.55E-01
	3	0.949	2.04E-02	1.94E-02	1.88E-01	1.79E-01
	4	0.848	2.50E-02	2.12E-02	2.14E-01	1.82E-01
	5	0.754	2.93E-02	2.21E-02	2.37E-01	1.78E-01
	6	0.635	3.59E-02	2.28E-02	2.68E-01	1.70E-01
	7	0.578	4.01E-02	2.32E-02	2.86E-01	1.65E-01
	8	0.527	4.49E-02	2.37E-02	3.06E-01	1.61E-01
	9	0.482	5.03E-02	2.42E-02	3.27E-01	1.58E-01
	10	0.433	5.78E-02	2.50E-02	3.55E-01	1.53E-01
	11	0.390	6.65E-02	2.59E-02	3.84E-01	1.50E-01
	12	0.352	7.67E-02	2.70E-02	4.16E-01	1.47E-01
	13	0.315	8.98E-02	2.83E-02	4.54E-01	1.43E-01
	17	0.229	1.48E-01	3.39E-02	5.92E-01	1.36E-01
	20	0.186	1.95E-01	3.62E-02	6.81E-01	1.27E-01
	YEAR	% of TOT. TRAF.	DAMAGE INDEX total	total*%	RUT DEPTH total	total*%
DC-10	1	0.000		0.00E+00		0.00E+00
	2	0.000		0.00E+00		0.00E+00
	3	0.000		0.00E+00		0.00E+00
	4	0.000		0.00E+00		0.00E+00
	5	0.000		0.00E+00		0.00E+00
	6	0.000		0.00E+00		0.00E+00
	7	0.000		0.00E+00		0.00E+00
	8	0.000		0.00E+00		0.00E+00
	9	0.000		0.00E+00		0.00E+00
	10	0.000		0.00E+00		0.00E+00
	11	0.000		0.00E+00		0.00E+00
	12	0.000		0.00E+00		0.00E+00
	13	0.000		0.00E+00		0.00E+00
	17	0.001	7.03E-01	7.03E-04	8.45E-01	8.45E-04
	20	0.006	9.26E-01	5.55E-03	9.55E-01	5.73E-03
		% of TOT. TRAF.	DAMAGE INDEX total	total*%	RUT DEPTH total	total*%
B-727	1	0.000		0.00E+00		0.00E+00
	2	0.000		0.00E+00		0.00E+00
	3	0.032	5.49E-02	1.76E-03	2.54E-01	8.14E-03
	4	0.089	6.72E-02	5.98E-03	2.89E-01	2.57E-02
	5	0.143	7.89E-02	1.13E-02	3.18E-01	4.55E-02
	6	0.237	9.65E-02	2.29E-02	3.59E-01	8.50E-02
	7	0.281	1.08E-01	3.03E-02	3.83E-01	1.08E-01
	8	0.321	1.21E-01	3.88E-02	4.09E-01	1.31E-01
	9	0.357	1.35E-01	4.83E-02	4.37E-01	1.56E-01
	10	0.395	1.55E-01	6.13E-02	4.72E-01	1.86E-01
	11	0.429	1.79E-01	7.67E-02	5.11E-01	2.19E-01
	12	0.459	2.06E-01	9.47E-02	5.52E-01	2.54E-01
	13	0.488	2.42E-01	1.18E-01	6.01E-01	2.93E-01
	17	0.556	3.98E-01	2.21E-01	7.80E-01	4.33E-01
	20	0.586	5.24E-01	3.07E-01	8.94E-01	5.24E-01

PLANE	YEAR	% of TOT.TRAF.	DAMAGE total	INDEX total*%	RUT total	DEPTH total*%
B-737	1	0.000		0.00E+00		0.00E+00
	2	0.000		0.00E+00		0.00E+00
	3	0.019	1.98E-02	3.77E-04	1.68E-01	3.19E-03
	4	0.063	2.43E-02	1.53E-03	1.91E-01	1.20E-02
	5	0.103	2.85E-02	2.93E-03	2.11E-01	2.17E-02
	6	0.128	3.49E-02	4.46E-03	2.38E-01	3.05E-02
	7	0.141	3.89E-02	5.49E-03	2.55E-01	3.59E-02
	8	0.152	4.36E-02	6.63E-03	2.73E-01	4.14E-02
	9	0.161	4.88E-02	7.86E-03	2.91E-01	4.69E-02
	10	0.172	5.61E-02	9.65E-03	3.16E-01	5.43E-02
	11	0.181	6.46E-02	1.17E-02	3.42E-01	6.19E-02
	12	0.189	7.45E-02	1.41E-02	3.71E-01	7.00E-02
	13	0.197	8.73E-02	1.72E-02	4.04E-01	7.96E-02
	17	0.213	1.44E-01	3.06E-02	5.27E-01	1.12E-01
	20	0.217	1.89E-01	4.10E-02	6.07E-01	1.32E-01
	YEAR	% of TOT.TRAF.	DAMAGE total	INDEX total*%	RUT total	DEPTH total*%
B-757	1	0.000		0.00E+00		0.00E+00
	2	0.000		0.00E+00		0.00E+00
	3	0.000		0.00E+00		0.00E+00
	4	0.000		0.00E+00		0.00E+00
	5	0.000		0.00E+00		0.00E+00
	6	0.000		0.00E+00		0.00E+00
	7	0.000		0.00E+00		0.00E+00
	8	0.000		0.00E+00		0.00E+00
	9	0.000		0.00E+00		0.00E+00
	10	0.000		0.00E+00		0.00E+00
	11	0.000		0.00E+00		0.00E+00
	12	0.000		0.00E+00		0.00E+00
	13	0.000		0.00E+00		0.00E+00
	17	0.001	2.04E-01	2.04E-04	5.68E-01	5.68E-04
	20	0.005	2.69E-01	1.34E-03	6.39E-01	3.19E-03
	YEAR	% of TOT.TRAF.	DAMAGE	INDEX tot.*%/13	RUT	DEPTH total*%
All Traf.	1	1.000		6.14E-04		9.94E-02
	2	1.000		1.17E-03		1.55E-01
	3	1.000		1.66E-03		1.90E-01
	4	1.000		2.21E-03		2.19E-01
	5	1.000		2.79E-03		2.46E-01
	6	1.000		3.85E-03		2.86E-01
	7	1.000		4.53E-03		3.09E-01
	8	1.000		5.31E-03		3.34E-01
	9	1.000		6.18E-03		3.60E-01
	10	1.000		7.38E-03		3.94E-01
	11	1.000		8.80E-03		4.31E-01
	12	1.000		1.04E-02		4.70E-01
	13	1.000		1.26E-02		5.16E-01
	17	1.000		2.20E-02		6.83E-01
	20	1.000		3.01E-02		7.91E-01

ZONE: Dry Freeze
MATERIAL:RH

PLANE	YEAR	% of TOT.TRAF.	DAMAGE INDEX total	total*%	RUT DEPTH total	total*%
DC-09	1	1.000	1.15E-02	1.15E-02	1.12E-01	1.12E-01
	2	1.000	2.19E-02	2.19E-02	1.72E-01	1.72E-01
	3	0.949	2.95E-02	2.80E-02	2.08E-01	1.97E-01
	4	0.848	3.61E-02	3.06E-02	2.35E-01	1.99E-01
	5	0.754	4.24E-02	3.19E-02	2.59E-01	1.95E-01
	6	0.635	5.18E-02	3.29E-02	2.92E-01	1.85E-01
	7	0.578	5.79E-02	3.34E-02	3.11E-01	1.80E-01
	8	0.527	6.49E-02	3.42E-02	3.32E-01	1.75E-01
	9	0.482	7.26E-02	3.50E-02	3.54E-01	1.70E-01
	10	0.433	8.34E-02	3.61E-02	3.82E-01	1.65E-01
	11	0.390	9.61E-02	3.75E-02	4.13E-01	1.61E-01
	12	0.352	1.11E-01	3.90E-02	4.46E-01	1.57E-01
	13	0.315	1.30E-01	4.09E-02	4.85E-01	1.53E-01
	17	0.229	2.14E-01	4.89E-02	6.26E-01	1.43E-01
	20	0.186	2.81E-01	5.23E-02	7.17E-01	1.33E-01
	YEAR	% of TOT.TRAF.	DAMAGE INDEX total	total*%	RUT DEPTH total	total*%
DC-10	1	0.000		0.00E+00		0.00E+00
	2	0.000		0.00E+00		0.00E+00
	3	0.000		0.00E+00		0.00E+00
	4	0.000		0.00E+00		0.00E+00
	5	0.000		0.00E+00		0.00E+00
	6	0.000		0.00E+00		0.00E+00
	7	0.000		0.00E+00		0.00E+00
	8	0.000		0.00E+00		0.00E+00
	9	0.000		0.00E+00		0.00E+00
	10	0.000		0.00E+00		0.00E+00
	11	0.000		0.00E+00		0.00E+00
	12	0.000		0.00E+00		0.00E+00
	13	0.000		0.00E+00		0.00E+00
	17	0.001	9.97E-01	9.97E-04	9.72E-01	9.72E-04
	20	0.006	1.31E+00	7.87E-03	1.09E+00	6.54E-03
		% of TOT.TRAF.	DAMAGE INDEX total	total*%	RUT DEPTH total	total*%
B-727	1	0.000		0.00E+00		0.00E+00
	2	0.000		0.00E+00		0.00E+00
	3	0.032	8.20E-02	2.62E-03	2.78E-01	8.89E-03
	4	0.089	1.00E-01	8.93E-03	3.14E-01	2.79E-02
	5	0.143	1.18E-01	1.68E-02	3.45E-01	4.93E-02
	6	0.237	1.44E-01	3.41E-02	3.88E-01	9.19E-02
	7	0.281	1.61E-01	4.52E-02	4.13E-01	1.16E-01
	8	0.321	1.80E-01	5.78E-02	4.40E-01	1.41E-01
	9	0.357	2.02E-01	7.20E-02	4.69E-01	1.67E-01
	10	0.395	2.32E-01	9.15E-02	5.06E-01	2.00E-01
	11	0.429	2.67E-01	1.15E-01	5.46E-01	2.34E-01
	12	0.459	3.08E-01	1.41E-01	5.89E-01	2.70E-01
	13	0.488	3.60E-01	1.76E-01	6.39E-01	3.12E-01
	17	0.556	5.94E-01	3.30E-01	8.23E-01	4.57E-01
	20	0.586	7.81E-01	4.58E-01	9.40E-01	5.51E-01

PLANE	YEAR	% of TOT.TRAF.	DAMAGE INDEX total	total*%	RUT DEPTH total	total*%
B-737	1	0.000		0.00E+00		0.00E+00
	2	0.000		0.00E+00		0.00E+00
	3	0.019	2.94E-02	5.59E-04	1.92E-01	3.65E-03
	4	0.063	3.60E-02	2.27E-03	2.17E-01	1.37E-02
	5	0.103	4.23E-02	4.35E-03	2.38E-01	2.45E-02
	6	0.128	5.17E-02	6.62E-03	2.67E-01	3.42E-02
	7	0.141	5.77E-02	8.14E-03	2.84E-01	4.01E-02
	8	0.152	6.47E-02	9.84E-03	3.03E-01	4.60E-02
	9	0.161	7.24E-02	1.17E-02	3.22E-01	5.19E-02
	10	0.172	8.32E-02	1.43E-02	3.48E-01	5.98E-02
	11	0.181	9.58E-02	1.73E-02	3.75E-01	6.79E-02
	12	0.189	1.11E-01	2.09E-02	4.05E-01	7.65E-02
	13	0.197	1.29E-01	2.55E-02	4.40E-01	8.66E-02
	17	0.213	2.13E-01	4.54E-02	5.67E-01	1.21E-01
	20	0.217	2.81E-01	6.09E-02	6.48E-01	1.41E-01
	YEAR	% of TOT.TRAF.	DAMAGE INDEX total	total*%	RUT DEPTH total	total*%
B-757	1	0.000		0.00E+00		0.00E+00
	2	0.000		0.00E+00		0.00E+00
	3	0.000		0.00E+00		0.00E+00
	4	0.000		0.00E+00		0.00E+00
	5	0.000		0.00E+00		0.00E+00
	6	0.000		0.00E+00		0.00E+00
	7	0.000		0.00E+00		0.00E+00
	8	0.000		0.00E+00		0.00E+00
	9	0.000		0.00E+00		0.00E+00
	10	0.000		0.00E+00		0.00E+00
	11	0.000		0.00E+00		0.00E+00
	12	0.000		0.00E+00		0.00E+00
	13	0.000		0.00E+00		0.00E+00
	17	0.001	2.91E-01	2.91E-04	9.11E-01	9.11E-04
	20	0.005	3.82E-01	1.91E-03	9.89E-01	4.95E-03
	YEAR	% of TOT.TRAF.	DAMAGE	INDEX tot.*%/13	RUT	DEPTH total*%
All Traf.	1	1.000		8.87E-04		1.12E-01
	2	1.000		1.69E-03		1.72E-01
	3	1.000		2.40E-03		2.10E-01
	4	1.000		3.22E-03		2.41E-01
	5	1.000		4.09E-03		2.69E-01
	6	1.000		5.66E-03		3.11E-01
	7	1.000		6.67E-03		3.36E-01
	8	1.000		7.84E-03		3.62E-01
	9	1.000		9.13E-03		3.90E-01
	10	1.000		1.09E-02		4.25E-01
	11	1.000		1.30E-02		4.63E-01
	12	1.000		1.55E-02		5.04E-01
	13	1.000		1.86E-02		5.51E-01
	17	1.000		3.27E-02		7.23E-01
	20	1.000		4.47E-02		8.36E-01

ZONE: Wet-No Freeze
MATERIAL: ASPHALT CONCRETE CONTROL

		A	B	C	D	E
		% of	DAMAGE	INDEX	RUT	DEPTH
PLANE	YEAR	TOT.TRAF.	total	total*%	total	total*%
DC-09	1	1.000	2.41E-01	2.41E-01	1.61E+01	1.61E+01
	2	1.000	4.58E-01	4.58E-01	2.25E+01	2.25E+01
	3	0.949	6.15E-01	5.84E-01	2.58E+01	2.45E+01
	4	0.848	7.53E-01	6.39E-01	2.82E+01	2.39E+01
	5	0.754	8.84E-01	6.66E-01	3.01E+01	2.27E+01
	6	0.635	1.08E+00	6.86E-01	3.26E+01	2.07E+01
	7	0.578	1.21E+00	6.98E-01	3.40E+01	1.97E+01
	8	0.527	1.35E+00	7.13E-01	3.55E+01	1.87E+01
	9	0.482	1.52E+00	7.30E-01	3.69E+01	1.78E+01
	10	0.433	1.74E+00	7.53E-01	3.88E+01	1.68E+01
	11	0.390	2.00E+00	7.82E-01	4.07E+01	1.59E+01
	12	0.352	2.31E+00	8.13E-01	4.26E+01	1.50E+01
	13	0.315	2.71E+00	8.52E-01	4.48E+01	1.41E+01
	17	0.229	4.46E+00	1.02E+00	5.21E+01	1.19E+01
	20	0.186	5.87E+00	1.09E+00	5.63E+01	1.05E+01
		% of	DAMAGE	INDEX	RUT	DEPTH
	YEAR	TOT.TRAF.	total	total*%	total	total*%
DC-10	1	0.000		0.00E+00		0.00E+00
	2	0.000		0.00E+00		0.00E+00
	3	0.000		0.00E+00		0.00E+00
	4	0.000		0.00E+00		0.00E+00
	5	0.000		0.00E+00		0.00E+00
	6	0.000		0.00E+00		0.00E+00
	7	0.000		0.00E+00		0.00E+00
	8	0.000		0.00E+00		0.00E+00
	9	0.000		0.00E+00		0.00E+00
	10	0.000		0.00E+00		0.00E+00
	11	0.000		0.00E+00		0.00E+00
	12	0.000		0.00E+00		0.00E+00
	13	0.000		0.00E+00		0.00E+00
	17	0.001	1.79E+01	1.79E-02	1.88E+02	1.88E-01
	20	0.006	2.36E+01	1.41E-01	2.03E+02	1.22E+00
		% of	DAMAGE	INDEX	RUT	DEPTH
		TOT.TRAF.	total	total*%	total	total*%
B-727	1	0.000		0.00E+00		0.00E+00
	2	0.000		0.00E+00		0.00E+00
	3	0.032	1.50E+00	4.81E-02	3.42E+01	1.09E+00
	4	0.089	1.84E+00	1.64E-01	3.73E+01	3.32E+00
	5	0.143	2.16E+00	3.08E-01	3.98E+01	5.69E+00
	6	0.237	2.64E+00	6.25E-01	4.30E+01	1.02E+01
	7	0.281	2.95E+00	8.28E-01	4.49E+01	1.26E+01
	8	0.321	3.30E+00	1.06E+00	4.68E+01	1.50E+01
	9	0.357	3.70E+00	1.32E+00	4.87E+01	1.74E+01
	10	0.395	4.25E+00	1.68E+00	5.11E+01	2.02E+01
	11	0.429	4.89E+00	2.10E+00	5.36E+01	2.30E+01
	12	0.459	5.64E+00	2.59E+00	5.61E+01	2.57E+01
	13	0.488	6.60E+00	3.22E+00	5.90E+01	2.88E+01
	17	0.556	1.09E+01	6.05E+00	6.87E+01	3.82E+01
	20	0.586	1.43E+01	8.39E+00	7.38E+01	4.33E+01

		A	B	C	D	E
		% of	DAMAGE	INDEX	RUT	DEPTH
PLANE	YEAR	TOT.TRAF.	total	total*%	total	total*%
B-737	1	0.000		0.00E+00		0.00E+00
	2	0.000		0.00E+00		0.00E+00
	3	0.019	5.24E-01	9.95E-03	2.20E+01	4.18E-01
	4	0.063	6.41E-01	4.04E-02	2.40E+01	1.51E+00
	5	0.103	7.52E-01	7.74E-02	2.56E+01	2.63E+00
	6	0.128	9.19E-01	1.18E-01	2.76E+01	3.54E+00
	7	0.141	1.03E+00	1.45E-01	2.88E+01	4.06E+00
	8	0.152	1.15E+00	1.75E-01	3.00E+01	4.56E+00
	9	0.161	1.29E+00	2.08E-01	3.12E+01	5.03E+00
	10	0.172	1.48E+00	2.55E-01	3.27E+01	5.63E+00
	11	0.181	1.71E+00	3.09E-01	4.33E+01	7.84E+00
	12	0.189	1.97E+00	3.72E-01	3.59E+01	6.78E+00
	13	0.197	2.30E+00	4.53E-01	3.77E+01	7.42E+00
	17	0.213	3.79E+00	8.08E-01	4.36E+01	9.29E+00
	20	0.217	4.99E+00	1.08E+00	4.70E+01	1.02E+01
		% of	DAMAGE	INDEX	RUT	DEPTH
	YEAR	TOT.TRAF.	total	total*%	total	total*%
B-757	1	0.000		0.00E+00		0.00E+00
	2	0.000		0.00E+00		0.00E+00
	3	0.000		0.00E+00		0.00E+00
	4	0.000		0.00E+00		0.00E+00
	5	0.000		0.00E+00		0.00E+00
	6	0.000		0.00E+00		0.00E+00
	7	0.000		0.00E+00		0.00E+00
	8	0.000		0.00E+00		0.00E+00
	9	0.000		0.00E+00		0.00E+00
	10	0.000		0.00E+00		0.00E+00
	11	0.000		0.00E+00		0.00E+00
	12	0.000		0.00E+00		0.00E+00
	13	0.000		0.00E+00		0.00E+00
	17	0.001	5.23E+00	5.23E-03	3.31E+01	3.31E-02
	20	0.005	6.88E+00	3.44E-02	3.63E+01	1.81E-01
		% of	DAMAGE	INDEX	RUT	DEPTH
	YEAR	TOT.TRAF.		tot.*%/13		total*%
All Traf.	1	1.000		1.85E-02		1.61E+01
	2	1.000		3.52E-02		2.25E+01
	3	1.000		4.94E-02		2.60E+01
	4	1.000		6.48E-02		2.87E+01
	5	1.000		8.09E-02		3.10E+01
	6	1.000		1.10E-01		3.44E+01
	7	1.000		1.28E-01		3.63E+01
	8	1.000		1.50E-01		3.83E+01
	9	1.000		1.74E-01		4.02E+01
	10	1.000		2.07E-01		4.26E+01
	11	1.000		2.45E-01		4.67E+01
	12	1.000		2.90E-01		4.75E+01
	13	1.000		3.48E-01		5.03E+01
	17	1.000		6.08E-01		5.96E+01
	20	1.000		8.26E-01		6.53E+01

ZONE: Wet-No Freeze
MATERIAL:ASPHALT RUBBER LOW

PLANE	YEAR	% of TOT.TRAF.	DAMAGE total	INDEX total*%	RUT total	DEPTH total*%
DC-09	1	1.000	4.68E-02	4.68E-02	1.64E-01	1.64E-01
	2	1.000	8.90E-02	8.90E-02	2.42E-01	2.42E-01
	3	0.949	1.20E-01	1.14E-01	2.87E-01	2.72E-01
	4	0.848	1.47E-01	1.24E-01	3.22E-01	2.73E-01
	5	0.754	1.72E-01	1.30E-01	3.51E-01	2.65E-01
	6	0.635	2.10E-01	1.33E-01	3.92E-01	2.49E-01
	7	0.578	2.35E-01	1.36E-01	4.16E-01	2.41E-01
	8	0.527	2.63E-01	1.39E-01	4.43E-01	2.33E-01
	9	0.482	2.95E-01	1.42E-01	4.70E-01	2.26E-01
	10	0.433	3.39E-01	1.47E-01	5.05E-01	2.19E-01
	11	0.390	3.90E-01	1.52E-01	5.44E-01	2.12E-01
	12	0.352	4.49E-01	1.58E-01	5.85E-01	2.06E-01
	13	0.315	5.26E-01	1.66E-01	6.33E-01	2.00E-01
	17	0.229	8.67E-01	1.98E-01	8.10E-01	1.85E-01
	20	0.186	1.14E+00	2.12E-01	9.23E-01	1.72E-01
	YEAR	% of TOT.TRAF.	DAMAGE total	INDEX total*%	RUT total	DEPTH total*%
DC-10	1	0.000		0.00E+00		0.00E+00
	2	0.000		0.00E+00		0.00E+00
	3	0.000		0.00E+00		0.00E+00
	4	0.000		0.00E+00		0.00E+00
	5	0.000		0.00E+00		0.00E+00
	6	0.000		0.00E+00		0.00E+00
	7	0.000		0.00E+00		0.00E+00
	8	0.000		0.00E+00		0.00E+00
	9	0.000		0.00E+00		0.00E+00
	10	0.000		0.00E+00		0.00E+00
	11	0.000		0.00E+00		0.00E+00
	12	0.000		0.00E+00		0.00E+00
	13	0.000		0.00E+00		0.00E+00
	17	0.001	3.83E+00	3.83E-03	1.28E+00	1.28E-03
	20	0.006	5.04E+00	3.03E-02	1.43E+00	8.60E-03
		% of TOT.TRAF.	DAMAGE total	INDEX total*%	RUT total	DEPTH total*%
B-727	1	0.000		0.00E+00		0.00E+00
	2	0.000		0.00E+00		0.00E+00
	3	0.032	2.64E-01	8.46E-03	3.63E-01	1.16E-02
	4	0.089	3.24E-01	2.88E-02	4.07E-01	3.62E-02
	5	0.143	3.80E-01	5.43E-02	4.45E-01	6.36E-02
	6	0.237	4.64E-01	1.10E-01	4.97E-01	1.18E-01
	7	0.281	5.19E-01	1.46E-01	5.27E-01	1.48E-01
	8	0.321	5.81E-01	1.87E-01	5.60E-01	1.80E-01
	9	0.357	6.51E-01	2.32E-01	5.95E-01	2.12E-01
	10	0.395	7.47E-01	2.95E-01	6.39E-01	2.53E-01
	11	0.429	8.61E-01	3.69E-01	6.88E-01	2.95E-01
	12	0.459	9.93E-01	4.56E-01	7.40E-01	3.40E-01
	13	0.488	1.16E+00	5.68E-01	8.01E-01	3.91E-01
	17	0.556	1.92E+00	1.06E+00	1.02E+00	5.69E-01
	20	0.586	2.52E+00	1.48E+00	1.17E+00	6.84E-01

PLANE	YEAR	% of TOT.TRAF.	DAMAGE total	INDEX total*%	RUT total	DEPTH total*%
B-737	1	0.000		0.00E+00		0.00E+00
	2	0.000		0.00E+00		0.00E+00
	3	0.019	8.61E-02	1.63E-03	2.45E-01	4.66E-03
	4	0.063	1.05E-01	6.64E-03	2.76E-01	1.74E-02
	5	0.103	1.24E-01	1.27E-02	3.03E-01	3.12E-02
	6	0.128	1.51E-01	1.93E-02	3.39E-01	4.34E-02
	7	0.141	1.69E-01	2.38E-02	3.61E-01	5.09E-02
	8	0.152	1.89E-01	2.88E-02	3.84E-01	5.84E-02
	9	0.161	2.12E-01	3.41E-02	4.09E-01	6.58E-02
	10	0.172	2.43E-01	4.18E-02	4.40E-01	7.57E-02
	11	0.181	2.80E-01	5.07E-02	4.75E-01	8.59E-02
	12	0.189	3.23E-01	6.11E-02	5.12E-01	9.67E-02
	13	0.197	3.78E-01	7.45E-02	5.55E-01	1.09E-01
	17	0.213	6.23E-01	1.33E-01	7.14E-01	1.52E-01
	20	0.217	8.20E-01	1.78E-01	8.16E-01	1.77E-01
	YEAR	% of TOT.TRAF.	DAMAGE total	INDEX total*%	RUT total	DEPTH total*%
B-757	1	0.000		0.00E+00		0.00E+00
	2	0.000		0.00E+00		0.00E+00
	3	0.000		0.00E+00		0.00E+00
	4	0.000		0.00E+00		0.00E+00
	5	0.000		0.00E+00		0.00E+00
	6	0.000		0.00E+00		0.00E+00
	7	0.000		0.00E+00		0.00E+00
	8	0.000		0.00E+00		0.00E+00
	9	0.000		0.00E+00		0.00E+00
	10	0.000		0.00E+00		0.00E+00
	11	0.000		0.00E+00		0.00E+00
	12	0.000		0.00E+00		0.00E+00
	13	0.000		0.00E+00		0.00E+00
	17	0.001	1.03E+00	1.03E-03	1.05E+00	1.05E-03
	20	0.005	1.35E+00	6.77E-03	1.19E+00	5.96E-03
	YEAR	% of TOT.TRAF.	DAMAGE	INDEX tot.*%/13	RUT	DEPTH total*%
All Traf.	1	1.000		3.60E-03		1.64E-01
	2	1.000		6.84E-03		2.42E-01
	3	1.000		9.51E-03		2.88E-01
	4	1.000		1.23E-02		3.26E-01
	5	1.000		1.51E-02		3.60E-01
	6	1.000		2.02E-02		4.10E-01
	7	1.000		2.35E-02		4.40E-01
	8	1.000		2.72E-02		4.72E-01
	9	1.000		3.14E-02		5.05E-01
	10	1.000		3.72E-02		5.47E-01
	11	1.000		4.40E-02		5.93E-01
	12	1.000		5.19E-02		6.42E-01
	13	1.000		6.21E-02		7.00E-01
	17	1.000		1.08E-01		9.09E-01
	20	1.000		1.46E-01		1.05E+00

ZONE: Wet-No Freeze
MATERIAL: ASPHALT RUBBER MEDIUM

PLANE	YEAR	% of TOT.TRAF.	DAMAGE INDEX total	DAMAGE INDEX total*%	RUT DEPTH total	RUT DEPTH total*%
DC-09	1	1.000	2.98E-02	2.98E-02	1.38E-01	1.38E-01
	2	1.000	5.66E-02	5.66E-02	2.07E-01	2.07E-01
	3	0.949	7.61E-02	7.22E-02	2.48E-01	2.35E-01
	4	0.848	9.32E-02	7.90E-02	2.80E-01	2.37E-01
	5	0.754	1.09E-01	8.24E-02	3.07E-01	2.31E-01
	6	0.635	1.34E-01	8.48E-02	3.45E-01	2.19E-01
	7	0.578	1.49E-01	8.63E-02	3.67E-01	2.12E-01
	8	0.527	1.67E-01	8.82E-02	3.91E-01	2.06E-01
	9	0.482	1.87E-01	9.03E-02	4.16E-01	2.01E-01
	10	0.433	2.15E-01	9.31E-02	4.49E-01	1.95E-01
	11	0.390	2.48E-01	9.66E-02	4.85E-01	1.89E-01
	12	0.352	2.86E-01	1.01E-01	5.23E-01	1.84E-01
	13	0.315	3.35E-01	1.05E-01	5.69E-01	1.79E-01
	17	0.229	5.51E-01	1.26E-01	7.34E-01	1.68E-01
	20	0.186	7.25E-01	1.35E-01	8.39E-01	1.56E-01
	YEAR	% of TOT.TRAF.	DAMAGE INDEX total	DAMAGE INDEX total*%	RUT DEPTH total	RUT DEPTH total*%
DC-10	1	0.000		0.00E+00		0.00E+00
	2	0.000		0.00E+00		0.00E+00
	3	0.000		0.00E+00		0.00E+00
	4	0.000		0.00E+00		0.00E+00
	5	0.000		0.00E+00		0.00E+00
	6	0.000		0.00E+00		0.00E+00
	7	0.000		0.00E+00		0.00E+00
	8	0.000		0.00E+00		0.00E+00
	9	0.000		0.00E+00		0.00E+00
	10	0.000		0.00E+00		0.00E+00
	11	0.000		0.00E+00		0.00E+00
	12	0.000		0.00E+00		0.00E+00
	13	0.000		0.00E+00		0.00E+00
	17	0.001	2.33E+00	2.33E-03	1.05E+00	1.05E-03
	20	0.006	3.06E+00	1.84E-02	1.18E+00	7.08E-03
		% of TOT.TRAF.	DAMAGE INDEX total	DAMAGE INDEX total*%	RUT DEPTH total	RUT DEPTH total*%
B-727	1	0.000		0.00E+00		0.00E+00
	2	0.000		0.00E+00		0.00E+00
	3	0.032	1.91E-01	6.10E-03	3.15E-01	1.01E-02
	4	0.089	2.33E-01	2.08E-02	3.55E-01	3.16E-02
	5	0.143	2.74E-01	3.91E-02	3.89E-01	5.56E-02
	6	0.237	3.35E-01	7.93E-02	4.36E-01	1.03E-01
	7	0.281	3.74E-01	1.05E-01	4.64E-01	1.30E-01
	8	0.321	4.19E-01	1.34E-01	4.94E-01	1.59E-01
	9	0.357	4.69E-01	1.67E-01	5.26E-01	1.88E-01
	10	0.395	5.39E-01	2.13E-01	5.66E-01	2.24E-01
	11	0.429	6.20E-01	2.66E-01	6.11E-01	2.62E-01
	12	0.459	7.16E-01	3.28E-01	6.58E-01	3.02E-01
	13	0.488	8.38E-01	4.09E-01	7.14E-01	3.49E-01
	17	0.556	1.38E+00	7.67E-01	9.18E-01	5.10E-01
	20	0.586	1.82E+00	1.06E+00	1.05E+00	6.14E-01

PLANE	YEAR	% of TOT.TRAF.	DAMAGE total	INDEX total*%	RUT total	DEPTH total*%
B-737	1	0.000		0.00E+00		0.00E+00
	2	0.000		0.00E+00		0.00E+00
	3	0.019	6.49E-02	1.23E-03	2.21E-01	4.20E-03
	4	0.063	7.95E-02	5.01E-03	2.49E-01	1.57E-02
	5	0.103	9.32E-02	9.60E-03	2.74E-01	2.82E-02
	6	0.128	1.14E-01	1.46E-02	3.08E-01	3.94E-02
	7	0.141	1.27E-01	1.79E-02	3.28E-01	4.62E-02
	8	0.152	1.43E-01	2.17E-02	3.50E-01	5.32E-02
	9	0.161	1.60E-01	2.57E-02	3.73E-01	6.00E-02
	10	0.172	1.84E-01	3.16E-02	4.02E-01	6.92E-02
	11	0.181	2.11E-01	3.83E-02	4.35E-01	7.86E-02
	12	0.189	2.44E-01	4.61E-02	4.69E-01	8.87E-02
	13	0.197	2.85E-01	5.62E-02	5.10E-01	1.00E-01
	17	0.213	4.70E-01	1.00E-01	6.59E-01	1.40E-01
	20	0.217	6.19E-01	1.34E-01	7.55E-01	1.64E-01
	YEAR	% of TOT.TRAF.	DAMAGE total	INDEX total*%	RUT total	DEPTH total*%
B-757	1	0.000		0.00E+00		0.00E+00
	2	0.000		0.00E+00		0.00E+00
	3	0.000		0.00E+00		0.00E+00
	4	0.000		0.00E+00		0.00E+00
	5	0.000		0.00E+00		0.00E+00
	6	0.000		0.00E+00		0.00E+00
	7	0.000		0.00E+00		0.00E+00
	8	0.000		0.00E+00		0.00E+00
	9	0.000		0.00E+00		0.00E+00
	10	0.000		0.00E+00		0.00E+00
	11	0.000		0.00E+00		0.00E+00
	12	0.000		0.00E+00		0.00E+00
	13	0.000		0.00E+00		0.00E+00
	17	0.001	6.51E-01	6.51E-04	6.96E-01	6.96E-04
	20	0.005	8.57E-01	4.28E-03	7.86E-01	3.93E-03
	YEAR	% of TOT.TRAF.	DAMAGE	INDEX tot.*%/13	RUT	DEPTH total*%
All Traf.	1	1.000		2.29E-03		1.38E-01
	2	1.000		4.35E-03		2.07E-01
	3	1.000		6.12E-03		2.49E-01
	4	1.000		8.06E-03		2.84E-01
	5	1.000		1.01E-02		3.15E-01
	6	1.000		1.37E-02		3.61E-01
	7	1.000		1.61E-02		3.89E-01
	8	1.000		1.88E-02		4.18E-01
	9	1.000		2.18E-02		4.48E-01
	10	1.000		2.60E-02		4.87E-01
	11	1.000		3.09E-02		5.30E-01
	12	1.000		3.65E-02		5.75E-01
	13	1.000		4.39E-02		6.28E-01
	17	1.000		7.67E-02		8.20E-01
	20	1.000		1.04E-01		9.45E-01

ZONE: Wet-No Freeze
MATERIAL:ASPHALT RUBBER HIGH

PLANE	YEAR	% of TOT.TRAF.	DAMAGE total	INDEX total*%	RUT total	DEPTH total*%
DC-09	1	1.000	3.33E-02	3.33E-02	1.94E-01	1.94E-01
	2	1.000	6.34E-02	6.34E-02	2.76E-01	2.76E-01
	3	0.949	8.52E-02	8.09E-02	3.22E-01	3.06E-01
	4	0.848	1.04E-01	8.84E-02	3.58E-01	3.03E-01
	5	0.754	1.22E-01	9.22E-02	3.88E-01	2.92E-01
	6	0.635	1.50E-01	9.50E-02	4.29E-01	2.72E-01
	7	0.578	1.67E-01	9.66E-02	4.53E-01	2.62E-01
	8	0.527	1.87E-01	9.87E-02	4.79E-01	2.52E-01
	9	0.482	2.10E-01	1.01E-01	5.06E-01	2.44E-01
	10	0.433	2.41E-01	1.04E-01	5.41E-01	2.34E-01
	11	0.390	2.78E-01	1.08E-01	5.79E-01	2.26E-01
	12	0.352	3.20E-01	1.13E-01	6.19E-01	2.18E-01
	13	0.315	3.75E-01	1.18E-01	6.66E-01	2.10E-01
	17	0.229	6.17E-01	1.41E-01	8.36E-01	1.91E-01
	20	0.186	8.12E-01	1.51E-01	9.43E-01	1.75E-01
	YEAR	% of TOT.TRAF.	DAMAGE total	INDEX total*%	RUT total	DEPTH total*%
DC-10	1	0.000		0.00E+00		0.00E+00
	2	0.000		0.00E+00		0.00E+00
	3	0.000		0.00E+00		0.00E+00
	4	0.000		0.00E+00		0.00E+00
	5	0.000		0.00E+00		0.00E+00
	6	0.000		0.00E+00		0.00E+00
	7	0.000		0.00E+00		0.00E+00
	8	0.000		0.00E+00		0.00E+00
	9	0.000		0.00E+00		0.00E+00
	10	0.000		0.00E+00		0.00E+00
	11	0.000		0.00E+00		0.00E+00
	12	0.000		0.00E+00		0.00E+00
	13	0.000		0.00E+00		0.00E+00
	17	0.001	2.17E+00	2.17E-03	1.41E+00	1.41E-03
	20	0.006	2.85E+00	1.71E-02	1.55E+00	9.29E-03
		% of TOT.TRAF.	DAMAGE total	INDEX total*%	RUT total	DEPTH total*%
B-727	1	0.000		0.00E+00		0.00E+00
	2	0.000		0.00E+00		0.00E+00
	3	0.032	1.90E-01	6.07E-03	4.29E-01	1.37E-02
	4	0.089	2.32E-01	2.07E-02	4 74E-01	4.22E-02
	5	0.143	2.73E-01	3.90E-02	5.12E-01	7.32E-02
	6	0.237	3.33E-01	7.90E-02	5.64E-01	1.34E-01
	7	0.281	3.72E-01	1.05E-01	5.95E-01	1.67E-01
	8	0.321	4.17E-01	1.34E-01	6.28E-01	2.01E-01
	9	0.357	4.67E-01	1.67E-01	6.62E-01	2.36E-01
	10	0.395	5.36E-01	2.12E-01	7.06E-01	2.79E-01
	11	0.429	6.18E-01	2.65E-01	7.53E-01	3.23E-01
	12	0.459	7.13E-01	3.27E-01	8.04E-01	3.69E-01
	13	0.488	8.34E-01	4.07E-01	8.63E-01	4.21E-01
	17	0.556	1.38E+00	7.67E-01	1.07E+00	5.97E-01
	20	0.586	1.81E+00	1.06E+00	1.21E+00	7.08E-01

PLANE	YEAR	% of TOT.TRAF.	DAMAGE total	INDEX total*%	RUT total	DEPTH total*%
B-737	1	0.000		0.00E+00		0.00E+00
	2	0.000		0.00E+00		0.00E+00
	3	0.019	7.41E-02	1.41E-03	2.80E-01	5.33E-03
	4	0.063	9.07E-02	5.71E-03	3.12E-01	1.96E-02
	5	0.103	1.06E-01	1.10E-02	3.39E-01	3.49E-02
	6	0.128	1.30E-01	1.67E-02	3.75E-01	4.80E-02
	7	0.141	1.45E-01	2.05E-02	3.96E-01	5.59E-02
	8	0.152	1.63E-01	2.48E-02	4.20E-01	6.38E-02
	9	0.161	1.82E-01	2.94E-02	4.44E-01	7.14E-02
	10	0.172	2.09E-01	3.60E-02	4.75E-01	8.16E-02
	11	0.181	2.41E-01	4.37E-02	5.08E-01	9.20E-02
	12	0.189	2.78E-01	5.26E-02	5.44E-01	1.03E-01
	13	0.197	3.26E-01	6.42E-02	5.86E-01	1.15E-01
	17	0.213	5.37E-01	1.14E-01	7.38E-01	1.57E-01
	20	0.217	7.06E-01	1.53E-01	8.34E-01	1.81E-01
	YEAR	% of TOT.TRAF.	DAMAGE total	INDEX total*%	RUT total	DEPTH total*%
B-757	1	0.000		0.00E+00		0.00E+00
	2	0.000		0.00E+00		0.00E+00
	3	0.000		0.00E+00		0.00E+00
	4	0.000		0.00E+00		0.00E+00
	5	0.000		0.00E+00		0.00E+00
	6	0.000		0.00E+00		0.00E+00
	7	0.000		0.00E+00		0.00E+00
	8	0.000		0.00E+00		0.00E+00
	9	0.000		0.00E+00		0.00E+00
	10	0.000		0.00E+00		0.00E+00
	11	0.000		0.00E+00		0.00E+00
	12	0.000		0.00E+00		0.00E+00
	13	0.000		0.00E+00		0.00E+00
	17	0.001	7.14E-01	7.14E-04	9.33E-01	9.33E-04
	20	0.005	9.39E-01	4.69E-03	1.03E+00	5.13E-03
	YEAR	% of TOT.TRAF.	DAMAGE	INDEX tot.*%/13	RUT	DEPTH total*%
All Traf.	1	1.000		2.56E-03		1.94E-01
	2	1.000		4.87E-03		2.76E-01
	3	1.000		6.80E-03		3.25E-01
	4	1.000		8.83E-03		3.65E-01
	5	1.000		1.09E-02		4.00E-01
	6	1.000		1.47E-02		4.54E-01
	7	1.000		1.71E-02		4.85E-01
	8	1.000		1.98E-02		5.18E-01
	9	1.000		2.29E-02		5.52E-01
	10	1.000		2.71E-02		5.95E-01
	11	1.000		3.21E-02		6.41E-01
	12	1.000		3.79E-02		6.90E-01
	13	1.000		4.53E-02		7.46E-01
	17	1.000		7.89E-02		9.48E-01
	20	1.000		1.07E-01		1.08E+00

ZONE: Dry-No Freeze
MATERIAL:ASPHALT CONCRETE CONTROL

		A	B	C	D	E
		% of	DAMAGE	INDEX	RUT	DEPTH
PLANE	YEAR	TOT. TRAF.	total	total*%	total	total*%
DC-09	1	1.000	9.80E-01	9.80E-01	1.46E-01	1.46E-01
	2	1.000	1.86E-01	1.86E-01	2.18E-01	2.18E-01
	3	0.949	2.51E-01	2.38E-01	2.60E-01	2.47E-01
	4	0.848	3.07E-01	2.60E-01	2.92E-01	2.48E-01
	5	0.754	3.60E-01	2.71E-01	3.20E-01	2.41E-01
	6	0.635	4.40E-01	2.79E-01	3.58E-01	2.27E-01
	7	0.578	4.91E-01	2.84E-01	3.80E-01	2.19E-01
	8	0.527	5.51E-01	2.90E-01	4.04E-01	2.13E-01
	9	0.482	6.17E-01	2.97E-01	4.29E-01	2.07E-01
	10	0.433	7.08E-01	3.07E-01	4.61E-01	2.00E-01
	11	0.390	8.16E-01	3.18E-01	4.96E-01	1.94E-01
	12	0.352	9.41E-01	3.31E-01	5.34E-01	1.88E-01
	13	0.315	1.10E+00	3.47E-01	5.78E-01	1.82E-01
	17	0.229	1.82E+00	4.16E-01	7.38E-01	1.69E-01
	20	0.186	2.39E+00	4.44E-01	8.40E-01	1.56E-01
		% of	DAMAGE	INDEX	RUT	DEPTH
	YEAR	TOT. TRAF.	total	total*%	total	total*%
DC-10	1	0.000		0.00E+00		0.00E+00
	2	0.000		0.00E+00		0.00E+00
	3	0.000		0.00E+00		0.00E+00
	4	0.000		0.00E+00		0.00E+00
	5	0.000		0.00E+00		0.00E+00
	6	0.000		0.00E+00		0.00E+00
	7	0.000		0.00E+00		0.00E+00
	8	0.000		0.00E+00		0.00E+00
	9	0.000		0.00E+00		0.00E+00
	10	0.000		0.00E+00		0.00E+00
	11	0.000		0.00E+00		0.00E+00
	12	0.000		0.00E+00		0.00E+00
	13	0.000		0.00E+00		0.00E+00
	17	0.001	7.89E+00	7.89E-03	1.20E+00	1.20E-03
	20	0.006	1.04E+01	6.23E-02	1.34E+00	8.01E-03
		% of	DAMAGE	INDEX	RUT	DEPTH
		TOT. TRAF.	total	total*%	total	total*%
B-727	1	0.000		0.00E+00		0.00E+00
	2	0.000		0.00E+00		0.00E+00
	3	0.032	6.39E-01	2.04E-02	3.48E-01	1.11E-02
	4	0.089	7.82E-01	6.96E-02	3.89E-01	3.47E-02
	5	0.143	9.17E-01	1.31E-01	4.25E-01	6.08E-02
	6	0.237	1.12E+00	2.66E-01	4.74E-01	1.12E-01
	7	0.281	1.25E+00	3.52E-01	5.02E-01	1.41E-01
	8	0.321	1.40E+00	4.51E-01	5.33E-01	1.71E-01
	9	0.357	1.57E+00	5.61E-01	5.66E-01	2.02E-01
	10	0.395	1.81E+00	7.13E-01	6.07E-01	2.40E-01
	11	0.429	2.08E+00	8.92E-01	6.52E-01	2.80E-01
	12	0.459	2.40E+00	1.10E+00	7.00E-01	3.21E-01
	13	0.488	2.81E+00	1.37E+00	7.56E-01	3.69E-01
	17	0.556	4.63E+00	2.57E+00	9.58E-01	5.33E-01
	20	0.586	6.09E+00	3.57E+00	1.09E+00	6.37E-01

		A	B	C	D	E
		% of	DAMAGE	INDEX	RUT	DEPTH
PLANE	YEAR	TOT. TRAF.	total	total*%	total	total*%
B-737	1	0.000		0.00E+00		0.00E+00
	2	0.000		0.00E+00		0.00E+00
	3	0.019	2.13E-01	4.05E-03	2.26E-01	4.30E-03
	4	0.063	2.61E-01	1.64E-02	2.55E-01	1.61E-02
	5	0.103	3.06E-01	3.15E-02	2.79E-01	2.88E-02
	6	0.128	3.75E-01	4.79E-02	3.13E-01	4.00E-02
	7	0.141	4.18E-01	5.90E-02	3.32E-01	4.69E-02
	8	0.152	4.69E-01	7.13E-02	3.54E-01	5.38E-02
	9	0.161	5.25E-01	8.45E-02	3.76E-01	6.05E-02
	10	0.172	6.03E-01	1.04E-01	4.05E-01	6.96E-02
	11	0.181	6.94E-01	1.26E-01	4.36E-01	7.89E-02
	12	0.189	8.01E-01	1.51E-01	4.70E-01	8.88E-02
	13	0.197	9.38E-01	1.85E-01	5.09E-01	1.00E-01
	17	0.213	1.55E+00	3.29E-01	6.52E-01	1.39E-01
	20	0.217	2.03E+00	4.41E-01	7.44E-01	1.61E-01
		% of	DAMAGE	INDEX	RUT	DEPTH
	YEAR	TOT. TRAF.	total	total*%	total	total*%
B-757	1	0.000		0.00E+00		0.00E+00
	2	0.000		0.00E+00		0.00E+00
	3	0.000		0.00E+00		0.00E+00
	4	0.000		0.00E+00		0.00E+00
	5	0.000		0.00E+00		0.00E+00
	6	0.000		0.00E+00		0.00E+00
	7	0.000		0.00E+00		0.00E+00
	8	0.000		0.00E+00		0.00E+00
	9	0.000		0.00E+00		0.00E+00
	10	0.000		0.00E+00		0.00E+00
	11	0.000		0.00E+00		0.00E+00
	12	0.000		0.00E+00		0.00E+00
	13	0.000		0.00E+00		0.00E+00
	17	0.001	2.15E+00	2.15E-03	7.95E-01	7.95E-04
	20	0.005	2.83E+00	1.42E-02	8.93E-01	4.47E-03
		% of	DAMAGE	INDEX	RUT	DEPTH
	YEAR	TOT. TRAF.		tot.*%/13		total*%
All Traf.	1	1.000		7.54E-03		1.46E-01
	2	1.000		1.43E-02		2.18E-01
	3	1.000		2.02E-02		2.62E-01
	4	1.000		2.66E-02		2.98E-01
	5	1.000		3.34E-02		3.31E-01
	6	1.000		4.56E-02		3.79E-01
	7	1.000		5.34E-02		4.07E-01
	8	1.000		6.25E-02		4.38E-01
	9	1.000		7.25E-02		4.69E-01
	10	1.000		8.64E-02		5.09E-01
	11	1.000		1.03E-01		5.52E-01
	12	1.000		1.22E-01		5.98E-01
	13	1.000		1.46E-01		6.51E-01
	17	1.000		2.56E-01		8.43E-01
	20	1.000		3.48E-01		9.67E-01

ZONE: Dry-No Freeze
MATERIAL:ASPHALT RUBBER LOW

PLANE	YEAR	% of TOT. TRAF.	DAMAGE INDEX total	total*%	RUT DEPTH total	total*%
DC-09	1	1.000	3.31E-02	3.31E-02	1.28E-01	1.28E-01
	2	1.000	6.29E-02	6.29E-02	1.94E-01	1.94E-01
	3	0.949	8.45E-02	8.02E-02	2.32E-01	2.21E-01
	4	0.848	1.04E-01	8.78E-02	2.63E-01	2.23E-01
	5	0.754	1.21E-01	9.15E-02	2.89E-01	2.18E-01
	6	0.635	1.49E-01	9.43E-02	3.25E-01	2.06E-01
	7	0.578	1.66E-01	9.58E-02	3.46E-01	2.00E-01
	8	0.527	1.86E-01	9.80E-02	3.70E-01	1.95E-01
	9	0.482	2.08E-01	1.00E-01	3.94E-01	1.90E-01
	10	0.433	2.39E-01	1.03E-01	4.26E-01	1.84E-01
	11	0.390	2.75E-01	1.07E-01	4.61E-01	1.80E-01
	12	0.352	3.18E-01	1.12E-01	4.98E-01	1.75E-01
	13	0.315	3.72E-01	1.17E-01	5.42E-01	1.71E-01
	17	0.229	6.12E-01	1.40E-01	7.03E-01	1.61E-01
	20	0.186	8.06E-01	1.50E-01	8.07E-01	1.50E-01
	YEAR	% of TOT. TRAF.	DAMAGE INDEX total	total*%	RUT DEPTH total	total*%
DC-10	1	0.000		0.00E+00		0.00E+00
	2	0.000		0.00E+00		0.00E+00
	3	0.000		0.00E+00		0.00E+00
	4	0.000		0.00E+00		0.00E+00
	5	0.000		0.00E+00		0.00E+00
	6	0.000		0.00E+00		0.00E+00
	7	0.000		0.00E+00		0.00E+00
	8	0.000		0.00E+00		0.00E+00
	9	0.000		0.00E+00		0.00E+00
	10	0.000		0.00E+00		0.00E+00
	11	0.000		0.00E+00		0.00E+00
	12	0.000		0.00E+00		0.00E+00
	13	0.000		0.00E+00		0.00E+00
	17	0.001	3.13E+00	3.13E-03	9.75E-01	9.75E-04
	20	0.006	4.12E+00	2.47E-02	1.11E+00	6.65E-03
		% of TOT. TRAF.	DAMAGE INDEX total	total*%	RUT DEPTH total	total*%
B-727	1	0.000		0.00E+00		0.00E+00
	2	0.000		0.00E+00		0.00E+00
	3	0.032	2.38E-01	7.60E-03	2.86E-01	9.16E-03
	4	0.089	2.91E-01	2.59E-02	3.24E-01	2.88E-02
	5	0.143	3.41E-01	4.88E-02	3.56E-01	5.10E-02
	6	0.237	4.17E-01	9.89E-02	4.01E-01	9.51E-02
	7	0.281	4.66E-01	1.31E-01	4.28E-01	1.20E-01
	8	0.321	5.22E-01	1.68E-01	4.57E-01	1.47E-01
	9	0.357	5.85E-01	2.09E-01	4.87E-01	1.74E-01
	10	0.395	6.72E-01	2.65E-01	5.26E-01	2.08E-01
	11	0.429	7.74E-01	3.32E-01	5.69E-01	2.44E-01
	12	0.459	8.92E-01	4.10E-01	6.15E-01	2.82E-01
	13	0.488	1.05E+00	5.10E-01	6.69E-01	3.27E-01
	17	0.556	1.72E+00	9.57E-01	8.67E-01	4.82E-01
	20	0.586	2.27E+00	1.33E+00	9.95E-01	5.83E-01

PLANE	YEAR	% of TOT. TRAF.	DAMAGE total	INDEX total*%	RUT total	DEPTH total*%
B-737	1	0.000		0.00E+00		0.00E+00
	2	0.000		0.00E+00		0.00E+00
	3	0.019	7.12E-02	1.35E-03	2.01E-01	3.82E-03
	4	0.063	8.72E-02	5.49E-03	2.28E-01	1.44E-02
	5	0.103	1.02E-01	1.05E-02	2.51E-01	2.59E-02
	6	0.128	1.25E-01	1.60E-02	2.84E-01	3.63E-02
	7	0.141	1.40E-01	1.97E-02	3.03E-01	4.27E-02
	8	0.152	1.57E-01	2.38E-02	3.24E-01	4.92E-02
	9	0.161	1.75E-01	2.82E-02	3.45E-01	5.56E-02
	10	0.172	2.01E-01	3.46E-02	3.74E-01	6.43E-02
	11	0.181	2.32E-02	4.20E-03	4.05E-01	7.33E-02
	12	0.189	2.68E-01	5.06E-02	4.38E-01	8.28E-02
	13	0.197	3.13E-01	6.17E-02	4.78E-01	9.41E-02
	17	0.213	5.16E-01	1.10E-01	6.22E-01	1.33E-01
	20	0.217	6.79E-01	1.47E-01	7.16E-01	1.55E-01
	YEAR	% of TOT. TRAF.	DAMAGE total	INDEX total*%	RUT total	DEPTH total*%
B-757	1	0.000		0.00E+00		0.00E+00
	2	0.000		0.00E+00		0.00E+00
	3	0.000		0.00E+00		0.00E+00
	4	0.000		0.00E+00		0.00E+00
	5	0.000		0.00E+00		0.00E+00
	6	0.000		0.00E+00		0.00E+00
	7	0.000		0.00E+00		0.00E+00
	8	0.000		0.00E+00		0.00E+00
	9	0.000		0.00E+00		0.00E+00
	10	0.000		0.00E+00		0.00E+00
	11	0.000		0.00E+00		0.00E+00
	12	0.000		0.00E+00		0.00E+00
	13	0.000		0.00E+00		0.00E+00
	17	0.001	7.42E-01	7.42E-04	9.61E-01	9.61E-04
	20	0.005	9.76E-01	4.88E-03	1.08E+00	5.39E-03
	YEAR	% of TOT. TRAF.	DAMAGE	INDEX tot.*%/13	RUT	DEPTH total*%
All Traf.	1	1.000		2.54E-03		1.28E-01
	2	1.000		4.84E-03		1.94E-01
	3	1.000		6.86E-03		2.34E-01
	4	1.000		9.17E-03		2.66E-01
	5	1.000		1.16E-02		2.95E-01
	6	1.000		1.61E-02		3.38E-01
	7	1.000		1.90E-02		3.63E-01
	8	1.000		2.23E-02		3.91E-01
	9	1.000		2.59E-02		4.19E-01
	10	1.000		3.10E-02		4.57E-01
	11	1.000		3.41E-02		4.97E-01
	12	1.000		4.40E-02		5.40E-01
	13	1.000		5.30E-02		5.91E-01
	17	1.000		9.31E-02		7.78E-01
	20	1.000		1.27E-01		9.00E-01

ZONE: Dry-No Freeze
MATERIAL:ASPHALT RUBBER MEDIUM

PLANE	YEAR	% of TOT. TRAF.	DAMAGE total	INDEX total*%	RUT total	DEPTH total*%
DC-09	1	1.000	1.57E-02	1.57E-02	1.17E-01	1.17E-01
	2	1.000	2.98E-02	2.98E-02	1.80E-01	1.80E-01
	3	0.949	4.01E-02	3.81E-02	2.18E-01	2.06E-01
	4	0.848	4.91E-02	4.16E-02	2.47E-01	2.09E-01
	5	0.754	5.76E-02	4.34E-02	2.72E-01	2.05E-01
	6	0.635	7.05E-02	4.47E-02	3.06E-01	1.95E-01
	7	0.578	7.87E-02	4.55E-02	3.27E-01	1.89E-01
	8	0.527	8.82E-02	4.65E-02	3.49E-01	1.84E-01
	9	0.482	9.87E-02	4.76E-02	3.73E-01	1.80E-01
	10	0.433	1.13E-01	4.91E-02	4.03E-01	1.74E-01
	11	0.390	1.31E-01	5.09E-02	4.36E-01	1.70E-01
	12	0.352	1.51E-01	5.30E-02	4.71E-01	1.66E-01
	13	0.315	1.76E-01	5.56E-02	5.13E-01	1.62E-01
	17	0.229	2.91E-01	6.65E-02	6.65E-01	1.52E-01
	20	0.186	3.82E-01	7.11E-02	7.63E-01	1.42E-01
	YEAR	% of TOT. TRAF.	DAMAGE total	INDEX total*%	RUT total	DEPTH total*%
DC-10	1	0.000		0.00E+00		0.00E+00
	2	0.000		0.00E+00		0.00E+00
	3	0.000		0.00E+00		0.00E+00
	4	0.000		0.00E+00		0.00E+00
	5	0.000		0.00E+00		0.00E+00
	6	0.000		0.00E+00		0.00E+00
	7	0.000		0.00E+00		0.00E+00
	8	0.000		0.00E+00		0.00E+00
	9	0.000		0.00E+00		0.00E+00
	10	0.000		0.00E+00		0.00E+00
	11	0.000		0.00E+00		0.00E+00
	12	0.000		0.00E+00		0.00E+00
	13	0.000		0.00E+00		0.00E+00
	17	0.001	1.36E+00	1.36E-03	9.50E-01	9.50E-04
	20	0.006	1.78E+00	1.07E-02	1.07E+00	6.43E-03
		% of TOT. TRAF.	DAMAGE total	INDEX total*%	RUT total	DEPTH total*%
B-727	1	0.000		0.00E+00		0.00E+00
	2	0.000		0.00E+00		0.00E+00
	3	0.032	1.06E-01	3.40E-03	2.87E-01	9.18E-03
	4	0.089	1.30E-01	1.16E-02	3.24E-01	2.89E-02
	5	0.143	1.53E-01	2.18E-02	3.57E-01	5.10E-02
	6	0.237	1.87E-01	4.43E-02	4.01E-01	9.51E-02
	7	0.281	2.09E-01	5.86E-02	4.27E-01	1.20E-01
	8	0.321	2.34E-01	7.51E-02	4.56E-01	1.46E-01
	9	0.357	2.62E-01	9.35E-02	4.86E-01	1.73E-01
	10	0.395	3.01E-01	1.19E-01	5.24E-01	2.07E-01
	11	0.429	3.46E-01	1.49E-01	5.66E-01	2.43E-01
	12	0.459	4.00E-01	1.83E-01	6.11E-01	2.81E-01
	13	0.488	4.68E-01	2.28E-01	6.64E-01	3.24E-01
	17	0.556	7.71E-01	4.28E-01	8.57E-01	4.76E-01
	20	0.586	1.01E+00	5.94E-01	9.80E-01	5.74E-01

PLANE	YEAR	% of TOT. TRAF.	DAMAGE total	INDEX total*%	RUT total	DEPTH total*%
B-737	1	0.000		0.00E+00		0.00E+00
	2	0.000		0.00E+00		0.00E+00
	3	0.019	3.41E-02	6.48E-04	1.94E-01	3.68E-03
	4	0.063	4.18E-02	2.63E-03	2.20E-01	1.38E-02
	5	0.103	4.90E-02	5.05E-03	2.42E-01	2.49E-02
	6	0.128	6.00E-02	7.67E-03	2.73E-01	3.49E-02
	7	0.141	6.70E-02	9.44E-03	2.91E-01	4.11E-02
	8	0.152	7.50E-02	1.14E-02	3.11E-01	4.73E-02
	9	0.161	8.40E-02	1.35E-02	3.32E-01	5.35E-02
	10	0.172	9.65E-02	1.66E-02	3.59E-01	6.18E-02
	11	0.181	1.11E-01	2.01E-02	3.89E-01	7.04E-02
	12	0.189	1.28E-01	2.42E-02	4.21E-01	7.95E-02
	13	0.197	1.50E-01	2.96E-02	4.58E-01	9.02E-02
	17	0.213	2.47E-01	5.27E-02	5.95E-01	1.27E-01
	20	0.217	3.25E-01	7.06E-02	6.82E-01	1.48E-01
	YEAR	% of TOT. TRAF.	DAMAGE total	INDEX total*%	RUT total	DEPTH total*%
B-757	1	0.000		0.00E+00		0.00E+00
	2	0.000		0.00E+00		0.00E+00
	3	0.000		0.00E+00		0.00E+00
	4	0.000		0.00E+00		0.00E+00
	5	0.000		0.00E+00		0.00E+00
	6	0.000		0.00E+00		0.00E+00
	7	0.000		0.00E+00		0.00E+00
	8	0.000		0.00E+00		0.00E+00
	9	0.000		0.00E+00		0.00E+00
	10	0.000		0.00E+00		0.00E+00
	11	0.000		0.00E+00		0.00E+00
	12	0.000		0.00E+00		0.00E+00
	13	0.000		0.00E+00		0.00E+00
	17	0.001	3.48E-01	3.48E-04	6.25E-01	6.25E-04
	20	0.005	4.58E-01	2.29E-03	7.05E-01	3.52E-03
	YEAR	% of TOT. TRAF.	DAMAGE	INDEX tot.*%/13	RUT	DEPTH total*%
All traf.	1	1.000		1.21E-03		1.17E-01
	2	1.000		2.29E-03		1.80E-01
	3	1.000		3.24E-03		2.19E-01
	4	1.000		4.30E-03		2.52E-01
	5	1.000		5.41E-03		2.81E-01
	6	1.000		7.44E-03		3.25E-01
	7	1.000		8.74E-03		3.50E-01
	8	1.000		1.02E-02		3.78E-01
	9	1.000		1.19E-02		4.06E-01
	10	1.000		1.42E-02		4.43E-01
	11	1.000		1.69E-02		4.83E-01
	12	1.000		2.01E-02		5.26E-01
	13	1.000		2.41E-02		5.76E-01
	17	1.000		4.23E-02		7.57E-01
	20	1.000		5.76E-02		8.74E-01

ZONE: Dry-No Freeze
MATERIAL:ASPHALT RUBBER HIGH

PLANE	YEAR	% of TOT. TRAF.	DAMAGE INDEX total	total*%	RUT DEPTH total	total*%
DC-09	1	1.000	1.99E-02	1.99E-02	1.40E-01	1.40E-01
	2	1.000	3.79E-02	3.79E-02	2.10E-01	2.10E-01
	3	0.949	5.09E-02	4.83E-02	2.50E-01	2.38E-01
	4	0.848	6.24E-02	5.29E-02	2.82E-01	2.39E-01
	5	0.754	7.32E-02	5.52E-02	3.09E-01	2.33E-01
	6	0.635	8.95E-02	5.68E-02	3.46E-01	2.19E-01
	7	0.578	9.99E-02	5.78E-02	3.67E-01	2.12E-01
	8	0.527	1.12E-01	5.90E-02	3.91E-01	2.06E-01
	9	0.482	1.25E-01	6.04E-02	4.16E-01	2.00E-01
	10	0.433	1.44E-01	6.24E-02	4.47E-01	1.94E-01
	11	0.390	1.68E-01	6.47E-02	4.82E-01	1.88E-01
	12	0.352	1.91E-01	6.74E-02	5.19E-01	1.83E-01
	13	0.315	2.24E-01	7.06E-02	5.62E-01	1.77E-01
	17	0.229	3.69E-01	8.45E-02	7.19E-01	1.65E-01
	20	0.186	4.86E-01	9.03E-02	8.19E-01	1.52E-01
	YEAR	% of TOT. TRAF.	DAMAGE INDEX total	total*%	RUT DEPTH total	total*%
DC-10	1	0.000		0.00E+00		0.00E+00
	2	0.000		0.00E+00		0.00E+00
	3	0.000		0.00E+00		0.00E+00
	4	0.000		0.00E+00		0.00E+00
	5	0.000		0.00E+00		0.00E+00
	6	0.000		0.00E+00		0.00E+00
	7	0.000		0.00E+00		0.00E+00
	8	0.000		0.00E+00		0.00E+00
	9	0.000		0.00E+00		0.00E+00
	10	0.000		0.00E+00		0.00E+00
	11	0.000		0.00E+00		0.00E+00
	12	0.000		0.00E+00		0.00E+00
	13	0.000		0.00E+00		0.00E+00
	17	0.001	1.41E+00	1.41E-03	1.16E+00	1.16E-03
	20	0.006	1.85E+00	1.11E-02	1.29E+00	7.72E-03
		% of TOT. TRAF.	DAMAGE INDEX total	total*%	RUT DEPTH total	total*%
B-727	1	0.000		0.00E+00		0.00E+00
	2	0.000		0.00E+00		0.00E+00
	3	0.032	1.19E-01	3.81E-03	3.32E-01	1.06E-02
	4	0.089	1.46E-01	1.30E-02	3.73E-02	3.32E-03
	5	0.143	1.71E-01	2.44E-02	4.08E-01	5.84E-02
	6	0.237	2.09E-01	4.95E-02	4.56E-01	1.08E-01
	7	0.281	2.33E-01	6.56E-02	4.84E-01	1.36E-01
	8	0.321	2.62E-01	8.40E-02	5.15E-01	1.65E-01
	9	0.357	2.93E-01	1.05E-01	5.47E-01	1.95E-01
	10	0.395	3.36E-01	1.33E-01	5.88E-01	2.32E-01
	11	0.429	3.88E-01	1.66E-01	6.32E-01	2.71E-01
	12	0.459	4.47E-01	2.05E-01	6.79E-01	3.12E-01
	13	0.488	5.23E-01	2.55E-01	7.35E-01	3.59E-01
	17	0.556	8.62E-01	4.79E-01	9.35E-01	5.20E-01
	20	0.586	1.13E+00	6.65E-01	1.06E+00	6.22E-01

PLANE	YEAR	% of TOT. TRAF.	DAMAGE total	INDEX total*%	RUT total	DEPTH total*%
B-737	1	0.000		0.00E+00		0.00E+00
	2	0.000		0.00E+00		0.00E+00
	3	0.019	4.43E-02	8.42E-04	2.22E-01	4.21E-03
	4	0.063	5.42E-02	3.42E-03	2.50E-01	1.57E-02
	5	0.103	6.36E-02	6.55E-03	2.74E-01	2.82E-02
	6	0.128	7.78E-02	9.96E-03	3.06E-01	3.92E-02
	7	0.141	8.69E-02	1.23E-02	3.26E-01	4.59E-02
	8	0.152	9.74E-02	1.48E-02	3.47E-01	5.27E-02
	9	0.161	1.09E-01	1.75E-02	3.68E-01	5.93E-02
	10	0.172	1.25E-01	2.15E-02	3.97E-01	6.82E-02
	11	0.181	1.44E-01	2.61E-02	4.27E-01	7.74E-02
	12	0.189	1.66E-01	3.14E-02	4.60E-01	8.70E-02
	13	0.197	1.95E-01	3.84E-02	4.99E-01	9.83E-02
	17	0.213	3.21E-01	6.84E-02	6.39E-01	1.36E-01
	20	0.217	4.22E-01	9.16E-02	7.29E-01	1.58E-01
	YEAR	% of TOT. TRAF.	DAMAGE total	INDEX total*%	RUT total	DEPTH total*%
B-757	1	0.000		0.00E+00		0.00E+00
	2	0.000		0.00E+00		0.00E+00
	3	0.000		0.00E+00		0.00E+00
	4	0.000		0.00E+00		0.00E+00
	5	0.000		0.00E+00		0.00E+00
	6	0.000		0.00E+00		0.00E+00
	7	0.000		0.00E+00		0.00E+00
	8	0.000		0.00E+00		0.00E+00
	9	0.000		0.00E+00		0.00E+00
	10	0.000		0.00E+00		0.00E+00
	11	0.000		0.00E+00		0.00E+00
	12	0.000		0.00E+00		0.00E+00
	13	0.000		0.00E+00		0.00E+00
	17	0.001	4.32E-01	4.32E-04	7.54E-01	7.54E-04
	20	0.005	5.69E-01	2.84E-03	8.39E-01	4.20E-03
	YEAR	% of TOT. TRAF.	DAMAGE	INDEX tot.*%/13	RUT	DEPTH total*%
All Traf.	1	1.000		1.53E-03		1.40E-01
	2	1.000		2.91E-03		2.10E-01
	3	1.000		4.08E-03		2.52E-01
	4	1.000		5.33E-03		2.58E-01
	5	1.000		6.63E-03		3.19E-01
	6	1.000		8.95E-03		3.67E-01
	7	1.000		1.04E-02		3.94E-01
	8	1.000		1.21E-02		4.24E-01
	9	1.000		1.40E-02		4.55E-01
	10	1.000		1.67E-02		4.94E-01
	11	1.000		1.98E-02		5.36E-01
	12	1.000		2.34E-02		5.81E-01
	13	1.000		2.80E-02		6.34E-01
	17	1.000		4.88E-02		8.22E-01
	20	1.000		6.62E-02		9.45E-01

END

7-87

DTIC